frontiers | Research Topics

Epidemiology of antimicrobial resistance and virulence factors of emerging and re-emerging bacteria

Edited by
Rosa Del Carmen Rocha-Gracia, Gerardo Cortés Cortés, Manuel Gerardo Ballesteros Monrreal and Margarita María De La Paz Arenas-Hernandez

Coordinated by
Edwin Barrios-Villa

Published in
Frontiers in Cellular and Infection Microbiology

ISSN 1664-8714
ISBN 978-2-8325-4618-5
DOI 10.3389/978-2-8325-4618-5

About Frontiers

Frontiers is more than just an open access publisher of scholarly articles: it is a pioneering approach to the world of academia, radically improving the way scholarly research is managed. The grand vision of Frontiers is a world where all people have an equal opportunity to seek, share and generate knowledge. Frontiers provides immediate and permanent online open access to all its publications, but this alone is not enough to realize our grand goals.

Frontiers journal series

The Frontiers journal series is a multi-tier and interdisciplinary set of open-access, online journals, promising a paradigm shift from the current review, selection and dissemination processes in academic publishing. All Frontiers journals are driven by researchers for researchers; therefore, they constitute a service to the scholarly community. At the same time, the *Frontiers journal series* operates on a revolutionary invention, the tiered publishing system, initially addressing specific communities of scholars, and gradually climbing up to broader public understanding, thus serving the interests of the lay society, too.

Dedication to quality

Each Frontiers article is a landmark of the highest quality, thanks to genuinely collaborative interactions between authors and review editors, who include some of the world's best academicians. Research must be certified by peers before entering a stream of knowledge that may eventually reach the public - and shape society; therefore, Frontiers only applies the most rigorous and unbiased reviews. Frontiers revolutionizes research publishing by freely delivering the most outstanding research, evaluated with no bias from both the academic and social point of view. By applying the most advanced information technologies, Frontiers is catapulting scholarly publishing into a new generation.

What are Frontiers Research Topics?

Frontiers Research Topics are very popular trademarks of the *Frontiers journals series*: they are collections of at least ten articles, all centered on a particular subject. With their unique mix of varied contributions from Original Research to Review Articles, Frontiers Research Topics unify the most influential researchers, the latest key findings and historical advances in a hot research area.

Find out more on how to host your own Frontiers Research Topic or contribute to one as an author by contacting the Frontiers editorial office: frontiersin.org/about/contact

Epidemiology of antimicrobial resistance and virulence factors of emerging and re-emerging bacteria

Topic editors

Rosa Del Carmen Rocha-Gracia — Benemérita Universidad Autónoma de Puebla, Mexico

Gerardo Cortés Cortés — University of California, Santa Cruz, United States

Manuel Gerardo Ballesteros Monrreal — University of Sonora, Mexico

Margarita María De La Paz Arenas-Hernandez — Benemérita Universidad Autónoma de Puebla, Mexico

Topic coordinator

Edwin Barrios-Villa — Universidad de Sonora, Mexico

Citation

Rocha-Gracia, R. D. C., Cortés Cortés, G., Ballesteros Monrreal, M. G., Arenas-Hernandez, M. M. D. L. P., Barrios-Villa, E., eds. (2025). *Epidemiology of antimicrobial resistance and virulence factors of emerging and re-emerging bacteria*. Lausanne: Frontiers Media SA. doi: 10.3389/978-2-8325-4618-5

Table of contents

frontiers | Frontiers in Cellular and Infection Microbiology

TYPE Editorial
PUBLISHED 06 March 2024
DOI 10.3389/fcimb.2024.1387087

OPEN ACCESS

EDITED AND REVIEWED BY
Alain Filloux,
Imperial College London, United Kingdom

*CORRESPONDENCE
Edwin Barrios-Villa
edwin.barrios@unison.mx

RECEIVED 16 February 2024
ACCEPTED 26 February 2024
PUBLISHED 06 March 2024

CITATION
Cortés-Cortés G, Arenas-Hernández MMP, Ballesteros-Monrreal MG, Rocha-Gracia RC and Barrios-Villa E (2024) Editorial: Epidemiology of antimicrobial resistance and virulence factors of emerging and re-emerging bacteria. *Front. Cell. Infect. Microbiol.* 14:1387087. doi: 10.3389/fcimb.2024.1387087

Editorial: Epidemiology of antimicrobial resistance and virulence factors of emerging and re-emerging bacteria

Gerardo Cortés-Cortés[1,2], Margarita M. P. Arenas-Hernández[1], Manuel G. Ballesteros-Monrreal[3], Rosa del Carmen Rocha-Gracia[1] and Edwin Barrios-Villa[3]*

[1]Posgrado en Microbiología, Centro de Investigaciones en Ciencias Microbiológicas, Instituto de Ciencias, Benemérita Universidad Autónoma de Puebla, Puebla, Mexico, [2]Department of Microbiology and Environmental Toxicology, University of California at Santa Cruz, Santa Cruz, CA, United States, [3]Departamento de Ciencias Químico-Biológicas y Agropecuarias, Universidad de Sonora, H. Caborca, Sonora, Mexico

KEYWORDS

antimicrobial resistance (AMR), virulence factors, mobilizable genetic elements, emerging pathogens, virulence-resistance co-occurrence

Editorial on the Research Topic
Epidemiology of antimicrobial resistance and virulence factors of emerging and re-emerging bacteria

The World Health Organization has declared antimicrobial resistance (AMR) a concerning top global public health issue that is estimated to result in significant additional healthcare costs, hospitalizations, and deaths, affecting millions of people by 2050 (Antimicrobial Resistance Collaborators, 2022). AMR is a phenomenon that has been evolving through time due to the participation of mobilizable genetic elements (MGEs), including plasmids, transposons, and integrons, which accelerate the horizontal spread of antibiotic resistance genes (Sultan et al., 2018). This Research Topic compiled information about the prevalence of virulence and resistance determinants in clinically important bacteria such as *Escherichia coli*, *Klebsiella pneumoniae*, *Staphylococcus aureus*, *Salmonella*, *Acinetobacter baumannii*, and *Streptococcus pneumoniae*, as well as emerging pathogens such as *Staphylococcus epidermidis*, *Staphylococcus warneri*, *Mycobacterium fortuitum*, and *Parvimonas micra*.

AMR represents a public health concern affecting whole living beings that needs to be analyzed from the one health approach, in which comprehensive human activities influence animal and environmental health and *vice versa*. Based on this perspective, Gonzales-Zubiate et al. observed the occurrence of $bla_{\text{CTX-M}}$ resistance genes from the variants CTX-M-55 and -65 in *E. coli*, and CTX-M-14 and -27 in *K. pneumoniae* in companion animals from Ecuador; this study highlights the identification of sequence types that might be clonally expanded. The tracking of bacterial clones has been improved by implementing novel tools such as whole-genome sequencing (WGS), which also highly contribute to the study of MGEs. Using this technology, Neidhöfer et al. obtained important data on the distribution of the AMR genes and sequence types of bacteria implicated in bloodstream infections; they predominantly identified

Enterococcus faecalis, Enterococcus faecium, S. aureus, S. pneumoniae, Streptococcus pyogenes, Bacteroides fragilis, E. coli, K. pneumoniae, Enterobacter spp, *Citrobacter* spp, *Proteus mirabilis, Serratia marsescens, A. baumanii, Pseudomonas aeruginosa*, and *Stenotrophomonas maltophilia*. Additionally, Jiménez-Rojas et al. studied Extended-Spectrum Beta-Lactamase (ESBL)-*E. coli* and ESBL-*K. pneumoniae* colonization in a Mexican neonatal intensive care unit, revealing a high prevalence (87%) and a relationship with healthcare-associated infections (22%). Variable resistance to cephalosporins, susceptibility to carbapenems, and genetic clonality underline the importance of addressing the search and study of ESBL-producing Enterobacterales in neonatal care. In this sense, another bacterium that has become one of the major causes of nosocomial infections is *A. baumannii*. Fernández-Vázquez et al. investigated the multidrug resistance profile of sequenced strains of *A. baumannii* in Mexican hospitals, identifying diverse resistance genes, including the clinically significant OXA-72 carbapenemase-encoding gene, highlighting the high adaptation of *A. baumannii* to new and variable niches. This study emphasized the role of antimicrobial resistance plasmids in disseminating resistance genes, which is crucial for effective control strategies. In the community setting, *Salmonella* is a concerning bacterium linked to outbreaks. Ma et al. analyzed 19 non-typhoidal *Salmonella* isolates, which were subjected to serovar identification, antimicrobial susceptibility testing, and biofilm formation evaluation. WGS revealed genetic relatedness, especially among *Salmonella* serovar Mbandaka isolates, suggesting the existence of a persistent source in China for more than 5 years, mediated by resistance mechanisms such as plasmids harboring $bla_{\text{CTX-M-15}}$ and virulent *mrkABCDF* operons. On the other hand, Balbuena-Alonso et al. evidenced new routes of pathogenic and multidrug-resistant bacteria transmission through food products, highlighting the role of agricultural products as reservoirs for resistance and virulence genes. This group characterized the A23EC *E. coli* strain from spinach, which belongs to the C2b sublineage of ST131, harboring three pathogenicity islands, a chromosomally integrated transposon (TnMB1860) associated with six resistance genes, and a conjugative IncF plasmid carrying a tetracycline resistance gene. Even when vaccines are available to protect against bacterial infections, AMR is a concerning issue. In a systematic review conducted by Sandoval et al., AMR in *S. pneumoniae* from invasive disease in Latin America and the Caribbean was assessed. Of 8,600 records, 103 studies were included, covering 49,660 positive samples. Penicillin resistance was observed in 21.7% of the isolates, with higher rates in children aged 0 to 5 years. Ongoing surveillance is crucial for monitoring evolving serotypes and AMR patterns, especially after the introduction of conjugated pneumococcal vaccine.

The role of emergent bacteria causing uncommon and hard-to-diagnose infections contributes to the limitation of effective treatment options. The case report by Shao et al. informs the diagnosis and treatment of *P. micra* (a Gram-positive anaerobic bacterium that exhibits colonization tendencies on oral mucosal and skin surfaces) in a 53-year-old male with recurrent hemoptysis. *P. micra* was identified using metagenomic next-generation sequencing, reflecting the importance of incorporating last-generation technologies as diagnostic tools. This infection was treated successfully with a combined beta-lactam and fluoroquinolone therapy, evidencing the importance of efficient treatment alternatives even for atypical infections.

Identifying genes associated with AMR in emerging pathogens remains a major issue. Alam et al. reported the isolation and genomic characterization of a highly MDR strain of *M. fortuitum* from a pulmonary infection harboring several genetic determinants of resistance, including acquired ones and associated mutations; interestingly, the strain investigated identified virulence genes also found in *M. tuberculosis* and *Mycobacterium abscessus*.

MGEs also harbor virulence genes that might have health implications for the host, contributing to biological variability but also representing a therapeutic challenge due to the emergence of pathogenic multidrug-resistant strains. Amer et al. investigated coagulase-negative staphylococci (CoNS) in acne lesions in Egypt, identifying *S. epidermidis* as the predominant species. Isolates from severe acne cases exhibited high antibiotic resistance and strong biofilm formation. WGS revealed multidrug resistance and virulence genes, highlighting the potential pathogenicity of CoNS in acne infections, especially the emergence of *S. warneri*, a previously reported uncommon pathogen.

In conclusion, this Research Topic contributes valuable information about the spread of AMR in emergent and re-emergent pathogenic bacteria, which is accelerated by the horizontal transfer of MGEs, reducing the efficiency of antibiotics used to control infections in humans and animals in clinical and environmental settings. Genomic-based screening strategies and new-generation technologies are prominent tools for gaining insight into the proper treatment, prevention, and control of hospital- and community-acquired diseases caused by multidrug-resistant bacteria.

Author contributions

GC-C: Investigation, Writing – original draft, Writing – review & editing. MMPA-H: Investigation, Writing – original draft, Writing – review & editing. MGB-M: Investigation, Writing – original draft, Writing – review & editing. RCR-G: Investigation, Writing – original draft, Writing – review & editing. EB-V: Investigation, Writing – original draft, Writing – review & editing.

Acknowledgments

The editor thanks the Frontiers administration team for their wonderful support with the Research Topic and the numerous peer reviewers.

Conflict of interest

The authors declare that the research was conducted in the absence of any commercial or financial relationships that could be construed as a potential conflict of interest.

Publisher's note

References

Antimicrobial Resistance Collaborators (2022). Global burden of bacterial antimicrobial resistance in 2019: a systematic analysis. *Lancet (London England)* 399, 629–655. doi: 10.1016/S0140-6736(21)02724-0

Sultan, I., Rahman, S., Jan, A. T., Siddiqui, M. T., Mondal, A. H., and Haq, Q. M. R. (2018). Antibiotics, resistome and resistance mechanisms: A bacterial perspective. *Front. Microbiol.* 9. doi: 10.3389/fmicb.2018.02066

frontiers | Frontiers in Cellular and Infection Microbiology

TYPE Original Research
PUBLISHED 04 January 2023
DOI 10.3389/fcimb.2022.1056007

OPEN ACCESS

EDITED BY
Xinmiao Jia,
Peking Union Medical College Hospital (CAMS), China

REVIEWED BY
Roberto Zenteno-Cuevas,
Universidad Veracruzana, Mexico
Cuidan Li,
Beijing Institute of Genomics (CAS), China

*CORRESPONDENCE
H. M. Adnan Hameed
adnan@gibh.ac.cn
Jianxiong Liu
ljxer64@qq.com
Tianyu Zhang
zhang_tianyu@gibh.ac.cn

SPECIALTY SECTION
This article was submitted to Molecular Bacterial Pathogenesis, a section of the journal Frontiers in Cellular and Infection Microbiology

RECEIVED 28 September 2022
ACCEPTED 05 December 2022
PUBLISHED 04 January 2023

CITATION
Alam MS, Guan P, Zhu Y, Zeng S, Fang X, Wang S, Yusuf B, Zhang J, Tian X, Fang C, Gao Y, Khatun MS, Liu Z, Hameed HMA, Tan Y, Hu J, Liu J and Zhang T (2023) Comparative genome analysis reveals high-level drug resistance markers in a clinical isolate of *Mycobacterium fortuitum* subsp. *fortuitum* MF GZ001. *Front. Cell. Infect. Microbiol.* 12:1056007.
doi: 10.3389/fcimb.2022.1056007

Comparative genome analysis reveals high-level drug resistance markers in a clinical isolate of *Mycobacterium fortuitum* subsp. *fortuitum* MF GZ001

Md Shah Alam[1,2,3,4], Ping Guan[5], Yuting Zhu[1,6], Sanshan Zeng[1,2,3,4], Xiange Fang[1,2,3,4], Shuai Wang[1,7], Buhari Yusuf[1,2,3,4], Jingran Zhang[1,2,3,4], Xirong Tian[1,2,3,4], Cuiting Fang[1,2,3,4], Yamin Gao[1,2,3,4], Mst Sumaia Khatun[1,2,3,4], Zhiyong Liu[1,2,3,4], H. M. Adnan Hameed[1,2,3,4]*, Yaoju Tan[5], Jinxing Hu[5], Jianxiong Liu[5]* and Tianyu Zhang[1,2,3,4]*

[1]State Key Laboratory of Respiratory Disease, Guangzhou Institutes of Biomedicine and Health, Chinese Academy of Sciences, Guangzhou, China, [2]Guangdong-Hong Kong-Macao Joint Laboratory of Respiratory Infectious Diseases, Guangzhou, China, [3]University of Chinese Academy of Sciences, Beijing, China, [4]China-New Zealand Joint Laboratory on Biomedicine and Health, Guangzhou, China, [5]State Key Laboratory of Respiratory Disease, Guangzhou Chest Hospital, Guangzhou, China, [6]School of Life Sciences, University of Science and Technology of China, Hefei, Anhui, China, [7]National Clinical Research Center for Infectious Diseases, Guangdong Provincial Clinical Research Center for Tuberculosis, Shenzhen Third People's Hospital, Shenzhen, China

Introduction: Infections caused by non-tuberculosis mycobacteria are significantly worsening across the globe. M. fortuitum complex is a rapidly growing pathogenic species that is of clinical relevance to both humans and animals. This pathogen has the potential to create adverse effects on human healthcare.

Methods: The MF GZ001 clinical strain was collected from the sputum of a 45-year-old male patient with a pulmonary infection. The morphological studies, comparative genomic analysis, and drug resistance profiles along with variants detection were performed in this study. In addition, comparative analysis of virulence genes led us to understand the pathogenicity of this organism.

Results: Bacterial growth kinetics and morphology confirmed that MF GZ001 is a rapidly growing species with a rough morphotype. The MF GZ001 contains 6413573 bp genome size with 66.18 % high G+C content. MF GZ001 possesses a larger genome than other related mycobacteria and included 6156 protein-coding genes. Molecular phylogenetic tree, collinearity, and comparative genomic analysis suggested that MF GZ001 is a novel member of the M. fortuitum complex. We carried out the drug resistance profile analysis and found single nucleotide polymorphism (SNP) mutations in key drug resistance genes such as rpoB, katG, AAC(2')-Ib, gyrA, gyrB, embB, pncA, blaF, thyA, embC, embR, and iniA. In addition, the MF GZ001strain contains mutations in iniA, iniC,

pncA, and ribD which conferred resistance to isoniazid, ethambutol, pyrazinamide, and para-aminosalicylic acid respectively, which are not frequently observed in rapidly growing mycobacteria. A wide variety of predicted putative potential virulence genes were found in MF GZ001, most of which are shared with well-recognized mycobacterial species with high pathogenic profiles such as M. tuberculosis and M. abscessus.

Discussion: Our identified novel features of a pathogenic member of the M. fortuitum complex will provide the foundation for further investigation of mycobacterial pathogenicity and effective treatment.

KEYWORDS

***Mycobacterium fortuitum*, morphology, comparative genomic analysis, drug resistance, pathogenesis**

Introduction

Non-tuberculosis mycobacteria (NTM) are ubiquitous, free-living, environmental saprophytic organisms that can cause human infections, including respiratory and skin diseases in both immunocompetent and immunocompromised individuals (Chan and Iseman, 2013; Maya et al., 2022). The prevalence of NTM infections has risen over the years around the world (Reves and Schluger, 2014). The yearly incidence of lung infections caused by NTM has increased from 3.13 to 4.73 per 100000 people, whereas the prevalence of NTM rose dramatically from 4.24% in 2014 to 12.68% in 2021, indicating a significant increase in the NTM outbreak in China. (Winthrop et al., 2020; Jia et al., 2021; Sun et al., 2022). The majority of NTM are rapidly growing species that have been associated with serious infectious diseases (De Groote and Huitt, 2006). Importantly, previous investigations reported that *M. abscessus* could be transmitted from person to person, and its prevalence has been widely observed in hospitals (Aitken et al., 2012; Bryant et al., 2013). The fast-growing mycobacteria comprise some clinically relevant species which include *M. fortuitum*, *M. abscessus*, *M. smegmatis*, and *M. chelonae* (De Groote and Huitt, 2006). *M. fortuitum* is frequently isolated from both respiratory and non-respiratory specimens (Park et al., 2008; Bryant et al., 2013).

M. fortuitum complex comprises opportunistic pathogens usually found in water, soil, and dust that are of clinical relevance to both humans and animals (Pavlik et al., 2021). The *M. fortuitum* complex includes *M. fortuitum*, *M. peregrinum*, *M. mageritense, M. porcinum*, *M. septicum*, *M. conceptionense*, *M. boenickei*, *M. houstonense*, *M. brisbanense*, *M. farcinogenes, M. senegalense*, and *M. setense* (Johansen and kremer, 2020; Brown-Elliott and Philley, 2017; Brown-Elliott and Wallace, 2002). *M. fortuitum* is a rapidly growing human-pathogenic species that cause pulmonary, eye, post-surgical, and catheter as well as skin and soft tissue infections (Koh et al., 2006; Brown-Elliott et al., 2012; Diaz et al., 2019; Erber et al., 2020). *M. fortuitum* in respiratory samples has been categorized based on colony morphologies, growth characteristics, and *in vitro* resistance to anti-mycobacterials (Daley and Griffith, 2002).

Whole-genome sequencing (WGS) technologies are the new strategies for understanding the molecular basis of drug resistance, metabolism, and evolution of pathogens. The conventional methodologies may have several drawbacks, particularly discordance between phenotypic and genotypic susceptibility testing outcomes. Illumina HiSeq sequencing can provide a variety of sequencing data for differentiating the distinct variable gene expressions between various samples. The sequencing data can also help in the assembly of *de novo* organism genomes (Austin et al., 2017). Highly accurate base-by-base sequencing is provided by this technique with almost no errors and up to 750 GB of data can be produced per sequencing run (Teng et al., 2017). Despite these advantages, Illumina sequencing's low-quality transcripts and short reads can significantly reduce the scope of analyses of transcriptional variations and accurate annotation (Hert et al., 2008). However, WGS employs a short-read sequencing platform that allows for the identification of additional resistance-associated mutations. For instance, due to the repetitive structure and high GC content of the mycobacterial genome, amplification bias occurs frequently during library preparation, resulting in fragmented genome assembly and other genetic variations such as INDEL and copy number variations (Treangen and Salzberg, 2011; Leung et al., 2017).

The recently developed PacBio RS II with single-molecule real-time (SMRT) sequencing methods overcome the drawbacks of conventional methods. PacBio RS II offers long-read or whole transcriptomes (Eid et al., 2009) which enable the large-scale long-read transcript collection with complete coding sequences and the characterization of the various gene families. Moreover, SMRT has enabled *de novo* assembly of the mycobacterial genome much easier (Roberts et al., 2013). SMRT sequencing can easily span highly repetitive DNA sequences due to its average read length of 10–20 kbp (Qi

et al., 2013; Zhu et al., 2016; Ferrarini et al., 2013). Additionally, it can reduce the number of gaps in the final assembled mycobacterial genome. Isolation of new rapidly growing mycobacteria (RGM) species and comprehensive analysis of the WGS of several mycobacterial isolates seem to be important for such kind of research.

In this study, we sequenced *M. fortuitum* subsp. *fortuitum* (designated as MF GZ001) isolated from a patient with pulmonary infection. This was deduced from conserved sequences of *16S rRNA hsp65*, and *rpoB* genes. We performed comparative studies with RGM and slow-growing mycobacteria (SGM) to understand the genomics, phylogeny, pathogenicity of this mycobacterial species, and the evolution of drug resistance. This investigation provides a genome-based description, which is ensuring that it's related to the *M. fortuitum* complex and displayed novel features of a potential pathogenic species.

Materials and methods

Strains collection and growth conditions

The MF GZ001 clinical strain was collected from the sputum of a 45-year-old male patient with a pulmonary infection. The patient with the symptoms of non-paroxysmal irritant cough with yellow and white sputum, chest pain, shortness of breath, headache, and low fever was admitted to the Guangzhou Chest Hospital, Guangzhou, China. The isolate was grown on Middlebrook 7H11 agar (Becton, Dickinson, and Company) supplemented with 0.2% glycerol (Shanghai Macklin Biochemical, Shanghai, China) and 10% oleic acid-albumin-dextrose-catalase (OADC) and in Middlebrook 7H9 (Difco, Becton, Dickinson and Company, New Jersey, USA) broth medium supplemented with 10% OADC, (Difco) and 0.05% Tween-80 (Amresco, USA).

Growth kinetics and morphology detection

To determine the bacterial growth curves, three mycobacterial strains MF GZ001, *M. abscessus* GZ002 (Guo et al., 2016; Chhotaray et al., 2020), and *M. smegmatis* C^2 155 were collected from Guangzhou Chest Hospital and performed phenotypic characterization. Firstly, the bacterial strains were grown in Middlebrooks 7H9 broth medium to log phase. Then the strains were diluted up to OD_{600} 0.01 in each 100 mL flask of every strain and placed in a shaking incubator for 72 hrs at 200 rmp to determine the bacterial growth curve. The bacterial growth rates were measured by detecting OD_{600} readings of bacterial strains every 6 hrs intervals using a spectrophotometer. The bacterial growth curve analysis was performed by GraphPad Prism version (8.0.2).

For the colony morphology study, the mycobacterial strains were cultured in Middlebrook 7H9 broth medium up to OD_{600} 1. Then all bacterial strains were equalized by dilution at 10^{-5} and cultured for 7 days at 37 °C. Bacterial colony images were captured after 7 days of incubation and visualized by microscope (OLYMPUS TH4-200) to determine the size and surface structure of the colony respectively.

Drug susceptibility testing (DST)

DST was performed by using broth micro-dilution methods according to the European Committee on Antimicrobial Susceptibility Testing (EUCAST) guidelines (Krishnan et al., 2009; Schon et al., 2020). The strains were grown in Middlebrook 7H9 broth medium (Difco, Becton, Dickinson and Company, New Jersey, USA) supplemented with 10% OADC, (Difco), 0.2% glycerol and 0.05% Tween-80 (Amresco, USA) for initial culture. Later, Middlebrook 7H9 (final pH 6.6 ± 0.2) broth medium supplemented with 10% OADC, 0.2% glycerol without Tween-80 was used in the preparation of inocula for DST. Based on EUCAST guidelines the inocula were fixed up to OD_{600} 0.6 with a final concentration of 1×10^5 to 5×10^5 CFU/mL. Cells in 96 well plates were incubated at 37°C. Several anti-microbials including rifabutin, imipenem, rifampicin (RIF), vancomycin, streptomycin, amikacin, clarithromycin, ethambutol, isoniazid, sulfamethoxazole, linezolid, and clofazimine were used to perform DST (Table S11). The MIC was defined based on the EUCAST formula as the lowest concentration of drugs that inhibited visible mycobacterial growth in wells.

Library construction and WGS

MF GZ001 strain was cultured in 7H9 broth and extracted the genomic DNA (gDNA) by using MAagNA Pure LC DNA Isolation Kit III. The gDNA was fragmented and collected for the preparation of SMRTbell DNA template libraries. Briefly, the DNA fragments were end-repaired and the barcode overhang adapter-ligated by removing the single-strand overhangs. The library was quantified using a Qubit (version 3.0) Fluorometer (Invitrogen, Carlsbad, CA), and checked the library size using an Agilent 2100 Bioanalyzer System. Subsequent steps were followed as per the manufacturer's instructions to prepare the SMRTbell library. The constructed library was sequenced using the Sequel II sequencing platform and PacBio reads were assembled using HGAP4 (version 4.0)/Falcon of WGS-Assembler (Version 8.2) (Myers et al., 2000; McCarthy, 2010). The genome sequence was re-corrected with Pilon software using previous Illumina data or Quiver using Pacbio reads to resolve the errors that were found during SMRT sequencing. The paired-end library was constructed by using the Illumina HiSeq instrument (Illumina, San Diego, CA, USA). The library construction protocol and bioinformatics analysis are broadly

illustrated in the supplementary material (Supplementary material 1). The preliminary Illumina raw data reads were trimmed at the percentage of bases with a Phred value greater than 20 or 30 (less than 0.1%/1% probability of error).

The unnecessary bases and reads of Pass Filter data were removed to get clean data using Cutadapt (version1.9.1) and the Burrows-Wheeler Alignment tool (BWA) (version 0.7.12) (Li and Durbin, 2009) was used to align the clean data generated from MF GZ001 to *M. fortuitum* CT6 reference complete genome sequence (NZ_CP011269.1) (Costa et al., 2015). All statistical analyses of raw data which were obtained from Illumina and SMRT sequencing are attached in the supplementary materials ((Tables S1–S6). The Prodigal (version 3.0.2, prokaryote) (Delcher et al., 2007) and Augustus (version 3.3, eukaryotes) (Stanke et al., 2006) both gene-finding software were used for predicting the coding genes. Non-coding RNA (ncRNA) includes rRNA, tRNA, snRNA, snoRNA and microRNA. Among the ncRNA, tRNAs and rRNA were detected by using tRNAscan-SE (version 1.3.1) (Lowe and Eddy, 1997), and Barrnap (version 0.9) respectively in the genome assembly. Additionally mapping Rfam (version 12.2) (Nawrocki et al., 2015) method was used to predict other ncRNAs. The coding genes were annotated with National Center for Biotechnology Information (NCBI) NR database by Diamond blastp. Functional categories in the genome were assigned to the Gene Ontology (GO) by using InterProScan software (Harris et al., 2004), to the Clusters of Orthologous Groups of proteins (COGs/KOG) (Tatusov et al., 2003; Han et al., 2018) database using rpstblastn software, and to the Kyoto Encyclopedia of Genes and Genomes (KEGG) (Kanehisa and Goto, 2000) pathway database by performing the KEGG database (http://www.genome.jp/kegg/) with Blastn software. Carbohydrate-Active Enzyme (CAZy) annotation was displayed using Diamond blastp (Luo et al., 2022). The Pfam was annotated for a large collection of protein families using the Pfam database (http://pfam.xfam.org/) (Punta et al., 2012), and Swiss_Prot was annotated by applying the Swiss_Prot database (https://www.ebi.ac.uk/uniprot) (Magrane, 2011). The Circos (version 0.69) software was used to display the circular plot and to describe the common feature of the genome.

Construction of phylogenetic trees

The evolutionary trees were constructed to represent the proximity of the relatedness between referred genome MF GZ001 and other 30 mycobacterial species. Single and combined gene-based (*16S rRNA*, *hsp65*, and *hsp65-rpoB*) three phylogenetic trees were constructed using FastTree and Mafft software (Price et al., 2010; Katoh and Standley, 2013; Robbertse et al., 2017). To generate the phylogenetic trees, the gene sequences were aligned with the reference sequences using Mafft software (version 7.310) (Katoh and Standley, 2013), and then evolutionary trees were constructed by using FastTree (Version 2.1.10.Dbl) (Price et al., 2010), which predicts nucleotide evolution using the Jukes-Cantor model and infers phylogenetic trees *via* approximately maximum-likelihood methods. Moreover, a comparison of the genetic relatedness between prokaryotic organisms is performed using average nucleotide identity (ANI) analysis. The online ANI tool was used to calculate the ANI value of the MF GZ001 genome as well as of its closely related species (https://www.ezbiocloud.net/tools/ani) (Yoon et al., 2017).

Comparative genomic analysis

SNP/INDEL detection and annotation

SNP/INDEL was performed based on the result of MUMmer alignment between assembled genome sequence of MF GZ001 and the reference genomic sequences of *M. fortuitum* CT6 (NZ_CP011269.1), *M. abscessus* GZ002 (NZ_CP034181.1) (Chhotaray et al., 2020), *M. smegmatis* C^2 155 (NZ_CP054795.1), and *M. tuberculosis* H37Rv (NC_000962.3). Annovar software (Yang and Wang, 2015; Wang, 2020) was used to understand the annotation of mutation sites, the construction of the SNP/indel distribution map, and the detection of amino acid change caused by mutations.

Collinearity analysis

The study of multiple genome alignments in the context of identified genome MF GZ001 and reference genome *M. fortuitum* strain CT6 (CP011269.1), *M. abscessus* GZ002 (NZ_CP034181.1), *M. smegmatis* C^2 155 (NZ_CP054795.1), and *M. tuberculosis* H37Rv (NC_000962.3) collinearity relationship was constructed using MAUVE software version 2.4.0 (Huang et al., 2022). For the collinearity analysis, all reference genomes were downloaded from the NCBI database.

Core and pan genes analysis

M. fortuitum complex strains, including MF GZ001, other SGM, and its closely related strains for example *M. fortuitum* CT6 (CP011269.1), *M. brisbanense* UM_WWY (NZ_BCSX00000000.1), *M. septicum* DSM44393 (NZ_CP070349.1), *M. alvei* CIP103464 (NZ_AP022565.1) and *M. mageritense* (NZ_AP022567.1) were conducted to identify the core, strain-specific genes, clusters, and uncharacterized genes by ORTHOMCL (version 1.4). Using ORTHOMCL, the annotated protein sequences from the assemblies MF GZ001, SGM, and RGM were grouped into orthologous families. The ortholog clustering output of the OrthoMCL analysis was converted into an ortholog matrix and visualized as a Venn diagram (Wang et al., 2017).

Drug-resistant genes and virulence factors distribution, prediction, and analysis

Drug-resistant gene prediction and distribution were done using the comprehensive antibiotic resistance database (CARD) (Alcock et al., 2020). The CARD is a rigorously curated collection of characterized, peer-reviewed resistance determinants and associated antibiotics, organized by the antibiotic resistance ontology (ARO) and AMR gene detection models. *M. fortuitum* CT6 (CP011269.1) strain genome sequence of drug-resistant associated genes was obtained from the NCBI database which was used as a reference sequence. A BLAST search was done against the newly identified *M. fortuitum* complex member MF GZ001 strain using these genes as the query. To find virulence genes and virulence factors related genes, the protein sequences predicted by RAST were BLAST searched against the comprehensive online resource virulence factors database (VFDB) (Yang et al., 2007). We selected the genes that were orthologous to virulence genes with at least 60% identity and 60% sequence coverage in query and subject using our own Perl scripts. For the comparative study of virulence genes, the reference sequences were compared with *M. fortuitum* complex strains and 21 other mycobacterial species by using the same approaches to indicate the alterations in species-specific genes.

Prophage and CRISPR predictions

For the prediction of prophage, the annotated sequence of the MF GZ001 genome was checked using PhiSpy software (version 4.1.16) (Akhter et al., 2012). Additionally, clustered regularly interspaced short palindromic repeats (CRISPRs) were detected in the genome by using MinCED (from the CRISPR recognition tool) (Bland et al., 2007; Grissa et al., 2007).

Data availability

The MF GZ001 genome sequence data were deposited in the NCBI database under accession number CP107719. Raw data of WGS were deposited in the NCBI Sequence Read Archive (SRA) under the accession SRR22164027. All bacterial strains and analyses are illustrated in this manuscript and its Supplementary materials.

Results

Growth kinetics and morphology study

To compare the growth kinetics of MF GZ001 and other NTM, growth curves were plotted for MF GZ001, *M. abscessus* GZ002, and *M. smegmatis* C^2 155. After culturing in Middlebrook 7H9, OD_{600} was determined at 6 hrs intervals to detect bacterial growth rates. Both MF GZ001 and *M. smegmatis* C^2 155 strains have shown faster growth than *M. abscessus* GZ002 strain in terms of their OD_{600} at various time intervals and same growth conditions (Figure 1A), though the differences were not statistically significant ($P > 0.05$). To better understand mycobacterial morphology, the MF GZ001 and *M. abscessus* GZ002 strains were grown on 7H11 Middlebrook agar plates and incubated for 7 days at 37°C. We have noticed a colony shape of MF GZ001 slightly larger than the *M. abscessus* GZ002 strain by measuring the diameter of a single colony (Figure 1B). OLYMPUS TH4-200 microscopic visualization of colony structure revealed that MF GZ001 has a wrinkled colony surface and rough morphotype, whereas *M. abscessus* GZ002 colonies are non-wrinkled and exist in a smooth morphotype (Figure 1C).

DST

We determined the *in vitro* susceptibility of MF GZ001 to several drugs using the broth micro-dilution method. The MF GZ001 strain showed high resistance to sulfamethoxazole (> 128 μg/mL), clofazimine (> 128 μg/mL), levofloxacin (> 16 μg/mL), carbapenem (> 128 μg/mL), RIF (64 μg/mL), imipenem (64 μg/mL), and streptomycin (64 μg/mL). The susceptibility of MF GZ001 to other therapeutic agents was also determined (Table S11).

General overview of MF GZ001 genome

MF GZ001 genome was sequenced using SMRT sequencing technology and Illumina HiSeq sequencing platform at high sequencing depth. The mapping ratio of the genome was 98.79% which covered 100% reads of the genome (Table S6, Figure S1). For the paired-end data of sequencing, the total number of reads and bases counts were 19187140 and 2878071000 respectively. After trimming, the average length of sequence reads was 149.50 bp. The quality evaluation of Pacbio raw reads of sequences and bases obtained from MF GZ001 were 1368432 and 4062640505, respectively. The size of the MF GZ001 genome is 6413573 bp. The final assembly of the genome was circularized with a high G +C content of 66.18% (Figure 2, Table 1). It contained 6156 protein-coding genes, whereas protein-coding genes with enzymes were 1450. In addition, a total of 98 ncRNAs, 6 rRNAs, 55 tRNAs, and 37 other ncRNAs were identified (Table 1). Moreover, a prophage with approximate size of 39521 bp (Table S7) and three repeat numbers of clustered regularly interspaced palindromic repeats (CRISPR) were predicted in the genome (Table S8).

10.3389/fcimb.2022.1056007

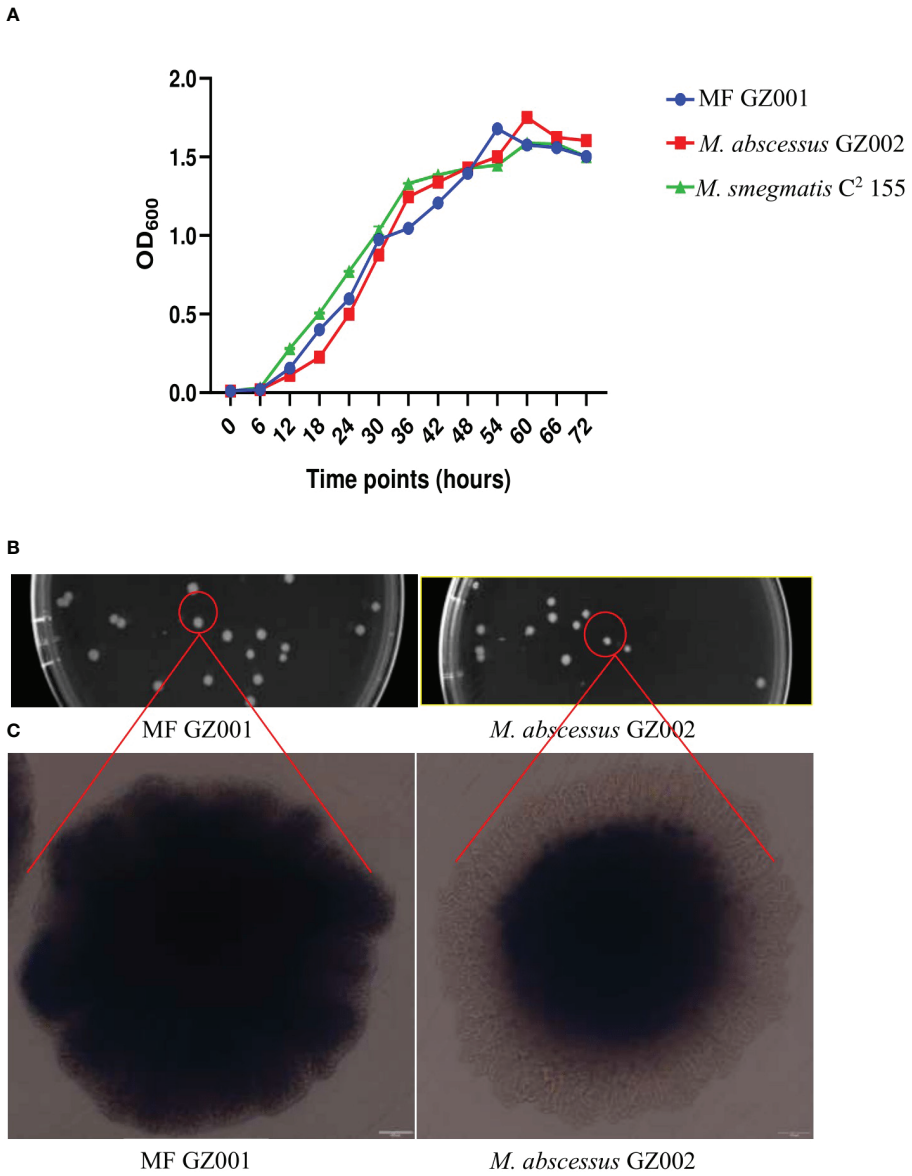

FIGURE 1
Growth kinetics and colony surface architecture of Mycobacterium species. **(A)** Growth kinetics detection of MF GZ001, *M. abscessus* GZ002, and *M. smegmatis* C^2 155. **(B)** Colony size and morphology determination. MF GZ001 and *M. abscessus* GZ002 were grown in Middlebrook 7H11 agar media supplemented with Tween 80 at 37°C. **(C)** Individual colony surface architecture was measured by OLYMPUS TH4-200.

Phylogenetic construction analysis

The phylogenetic taxonomic position of *M. fortuitum* MF GZ001 within the mycobacterium genus was constructed based on FastTree and Mafft's alignment of the target sequence of 33 mycobacterial species. Initially, the phylogenetic tree was constructed based on the worldwide known bacterial identification marker genes *16S rRNA* and *hsp65*. The *16S rRNA*-based phylogenetic tree indicated that MF GZ001 was the closest sub-species to *M. fortuitum* (Figure S8A). Among several mycobacterium species, the other closest members were *M. phocaicum, M. mucogenicum, M. septicum, and M. bacteremicum*, which belongs to *M. fortuitum* complex. In addition, *hsp65*-based phylogenetic analysis showed that MF GZ001 is closely related to *M. fortuitum* W4 (Figure S8B), which suggests that MF GZ001 is a member of the *M. fortuitum* complex. Later on, we reconstructed a phylogenetic tree based on multiple gene approaches (*16S rRNA*, *hsp65*, *rpoB*) to further

10.3389/fcimb.2022.1056007

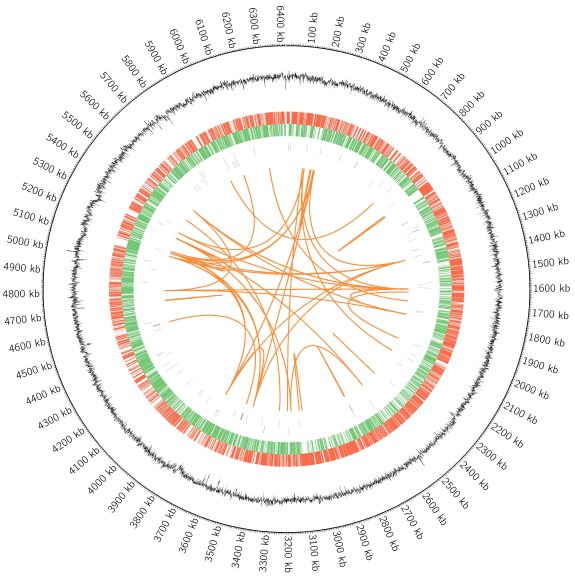

FIGURE 2
Circular representation of MF GZ001 genome displayed with Circos (version 0.69). The circular plot has seven levels. From outside to inside, the first is the information of genome position, the second is GC content information, the third is positive strand genes (marked in red color), the fourth is negative strand genes (marked in green color), the fifth is positive strand ncRNA data (marked in blue color), the sixth is negative strand ncRNA data (marked in purple color) and the seventh shows long repeats (>100 bp).

confirm the placement of MF GZ001. The multiple gene-based reconstructed phylogenetic results were most related to *M. fortuitum* CT6 (Figure S8C) and distantly related to SGM. Finally, we subjected MF GZ001 to ANI analysis using the whole genome sequences to clarify the inconsistency from the single gene-based phylogenetic predictions. The ANI values between MF GZ001 and *M. fortuitum* CT6, *M. alvei* CIP103464, *M. septicum* DSM44393, and *M. mageritense* JR2009 strains were 98.77%, 86.26%, 86.53%, and 80.38% respectively. This study revealed that the MF GZ001 strain shares the most genetic relatedness with *M. fortuitum* CT6.

Functional annotation study

The functional pathways of annotated genes were interpreted using protein-coding genes of the MF GZ001 strain in the KEGG database. A total of 2411 genes were annotated to six-factor types and 40 KEGG functional pathways along with 558 for amino acid metabolism (Figure S2; File.Xls.S1). In addition, there were 23 genes which are possibly related to different pathways in cancer, for instance central carbon metabolism in cancer, proteoglycans in cancer,

TABLE 1 General overview of MF GZ001 genome.

Features	Value	% of total
Size (bp)	6413573	100.00
G+C content (bp)	4244546	66.18
Coding region (bp)	5966586	93.03
Total genes	6254	100.00
Protein-coding genes	6156	98.43
Protein coding genes with enzymes	1450	23.19
RNA genes	98	1.57
Total number of ncRNAs	98	N/A
Number of rRNAs	6	N/A
Number of tRNAs	55	N/A
Number of other ncRNAs	37	N/A
Genes assigned to COGs	4315	69.00
COG clusters	1613	37.38
Genes with signal peptides	495	7.91
Genes with transmembrane helices	1428	22.8
N/A, Not Applicable.		

K005215 prostate cancer, and K05219 bladder cancer. These genes are not only related to cancer-associated pathways but also other pathways like lipid metabolism, pyridine metabolism, and drug metabolism. Moreover, 1 aquaporin z, 113 uncharacterized proteins, drug resistance genes, and human infectious diseases-related genes (File.Xls.S1). COG functional annotation of the MF GZ001 genome was studied by the COG database. A total of 4315 common COGs have been found in the MF GZ001 genome. For the MF GZ001 strain, the genes were functionally categorized into 21 different groups (Figure S3; File.Xl.S2). The general and unknown functions of functionally annotated MF GZ001 genome sequence have been predicted by R and S categories respectively. Notably, there were 361 genes found as unknown function categories and no homologs were identified in the COG database. The majority of the remaining functional annotation categories were represented by "transcription (K category; 530), lipid transport and metabolism (I category; 486), secondary metabolites biosynthesis, transport, and catabolism (Q category; 434), energy production and conversion (C category; 385), amino acid transport and metabolism (E; category; 383) (File.Xl.S2). In addition, the non-redundant homologous species distribution map was created for comprehensive information using the NCBI database. Among different mycobacterial species, the highest (64.83%) similarity was found with *M. fortuitum* (Figure S4, File Xl.S3). However, other analyses based on blast to GO, CAZy, Pfam, and Swiss_Prot database gene annotation result statistics table have been shown in supplementary materials (Figures S5, S6, Table S9, File. Xl.S4, S5).

Comparative genomic analysis

To investigate the genomic evolution of MF GZ001 strain, based on phylogenetic construction analysis and ANI analysis results, we compared the MF GZ001 strain with the more closely related species *M. fortuitum* CT6 as well as other RGM and SGM mycobacterium species. The evolutionary results emphasized that the MF GZ001 strain has a close relationship with *M. fortuitum* subsp. *fortuitum*. The reannotation results revealed that MF GZ001 strain genome size (6413573 bp) and CDS sequences were higher than *M. fortuitum* CT6 (6254616 bp) (Table 2). Interestingly, the MF GZ001 has the highest number of conserved unknown functional genes (1157) compared to *M. fortuitum* CT6, *M. abscessus* GZ002, *M. smegmatis* $C^2$155, and *M. tuberculosis* H37Rv (Table 2). Additionally, the MF GZ001 genome contains more unique genes (333) than the reference genome *M. fortuitum* CT6 (264) and has more gene density (base pairs per gene) compared to other mycobacterial genomes (Table 2). Moreover, the analysis endorsed that the MF GZ001 strain is substantially diversified compared to the *M. fortuitum* CT6 strain.

The advantage of high accuracy in obtaining *de novo* sequencing is to identify both major and minor variations in the genome that can reveal the origin of strains or have effects on the gene function. For instance, we have detected 74168 single-nucleotide variations (SNVs) and 2001 INDEL mutations in the MF GZ001 strains compared to the reference genome (File.Xl.S6). The sequencing data produced 50914 synonymous, 17563 non-synonymous SNVs, and 2001 INDEL mutation (Table 3). Interestingly, there were 174 intergenic mutations belonging to the two genes (*1_3425*, *1_3426*), and also obtained stop loss (33) and stop gain (110) variants in the MF GZ001 strain (File.Xl.S6 and Table 3). To know the divergence of other mycobacterium species, we investigated the SNVs data of MF GZ001 not only comparing it with closely related species but also with distantly related species. Additionally, the highest number of SNVs was obtained from MF GZ001 compared to *M. smegmatis* C^2 155. Specific positions of SNVs/INDEL in genes and mapping distribution of SNVs have been illustrated in Supplementary materials (File.Xl.S6 and Figure S7).

To study the genome modification, the collinearity analysis of the MF GZ001 strain compared to the *M. fortuitum* CT6, *M. abscessus* GZ002, *M. smegmatis* C^2 155, and *M. tuberculosis* H37Rv was performed. The collinearity outcomes predicted from the MF GZ001 genome sequence was more aligned with the *M. fortuitum* CT6 strain, exhibiting no significant genomic modifications (Figure 3). The highest matching collinearity results are consistent with our previous analysis. Using the blast core ratio algorithm, we have investigated the MF GZ001, *M. alvei* CIP103464, *M. fortuitum* CT6, *M. brisbanense* UM_WWY, *M. septicum* DSM44393, and *M. mageritense* JR2009 genome to determine the account number of core gene clusters, pan-gene clusters, specific gene clusters, unique, and other gene clusters. There were 11503 pan-gene clusters with 38843 genes, 3480 core gene clusters (21621 genes), and 4098 specific gene clusters (4359 genes) (Figure 4A). The comparative analysis of the pan-genome of the *M. fortuitum* complex detected lower and nearly similar unique gene clusters

TABLE 2 Chromosomal features of MF GZ001 compared to other RGM and SGM.

Features	MF GZ001	*M. fortuitum* CT6	*M. abscessus* GZ002	*M. smegmatis* C^2 155	*M. tuberculosis* H37Rv
Chromosome size (base pairs)	6413573	6254616	6993871	5067231	4411532
G+C (%)	66.18	66.22	64.13	67.39	65.61
Gene density (base pairs per gene)	1044.88	1039.11	1062.62	1033.41	1001.4
Average CDS length	969.23	969.78	949.29	973.43	1013.39
Protein-coding sequences (CDS)	6156	5892	4927	6531	3906
Conserved with assigned function	4999	4944	4126	5818	2851
Conserved with unknown function	1157	948	801	713	1055
Unique	333	264	1303	1820	1025
Pseudogenes	0	96	32	124	0
rRNA	6	6	3	9	3
tRNA	55	52	47	47	45

10.3389/fcimb.2022.1056007

TABLE 3 Single-nucleotide variations (SNVs) identified in MF GZ001 strain compared with the reference strains.

Identified strain	Reference strains	Synonymous	Non-synonymous	INDEL	Stop loss	stop gain
MF GZ001	*M. fortuitum* CT6	50914	17563	2001	33	110
	M. abscessus GZ002	25843	12261	1469	11	151
	M. smegmatis C^2 155	190593	83927	10764	203	875
	M. tuberculosis H37Rv	33109	15673	1887	16	181

of MF GZ001 (265) with *M. fortuitum* CT6 (197) than other *M. fortuitum* complex members (Figure 4A). This hypothesis revealed that MF GZ001 species had a significant amount of genomic variation, which was to be noted in the pan-open genome's structure and close to the *M. fortuitum* complex. Moreover, the genome sequence of MF GZ001 was compared with *M. fortuitum* CT6, *M. abscessus* GZ002, *M. smegmatis* C^2 155, and *M. tuberculosis* H37Rv to estimate the number of gene clusters that are shared between each strain. Ven diagram study predicted that the core and specific gene clusters were 2073 and 4041, respectively (Figure 4B). MF GZ001 shared the highest number of gene clusters (2352) with *M. fortuitum* CT6 than other closely related species *M. abscessus* GZ002 (1138), *M. smegmatis* C^2 155 (2126), and distantly related *M. tuberculosis* H37Rv (526) species. The reference strain *M. forturuim* CT6 obtained 260 unique gene clusters, whereas the MF GZ001 strain obtained 319 unique gene clusters which are related to the metabolic, molecular, and protein regulatory function of bacteria (Figure 4B).

Drug resistance profile and variants found in the MF GZ001 strain

From a comprehensive drug resistance analysis, the MF GZ001 strain encodes multiple drug-resistant related genes against important drugs, including RIF, macrolides, fluoroquinolones, tetracyclines, triclosan, penem, peptide antibiotics, and cephamycin. The analysis reveals that the highest (18.59%) drug-resistant related genes were associated with triclosan (71), 15.71% macrolides (60), 12.3% fluoroquinolones (47), tetracyclines (45), 5.5% RIF (21) and

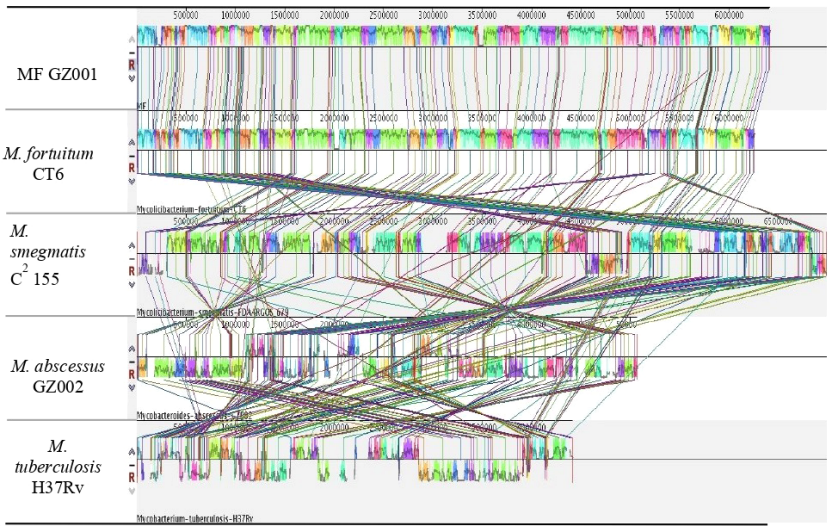

FIGURE 3
Diagram depicting genomic comparisons obtained using Mauve software. The alignment display is organized into one horizontal "panel" per input genome sequence. Each genome's panel contains the name of the genome sequence, a scale showing the sequence coordinates for that genome, and a single black horizontal center line. Colored block outlines appear above and possibly below the center line. Each of these block outlines surrounds a region of the genome sequence that is aligned to part of another genome and is presumably homologous and internally free from genomic rearrangement. Regions outside blocks lack detectable homology among the input genomes. Inside each block, Mauve draws a similar profile of the genome sequence. The height of the similarity profile corresponds to the average level of conservation in that region of the genome sequence. Areas that are completely white were not aligned and probably contain sequence elements specific to a particular genome. The height of the similarity profile is calculated to be inversely proportional to the average alignment column entropy over a region of the alignment.

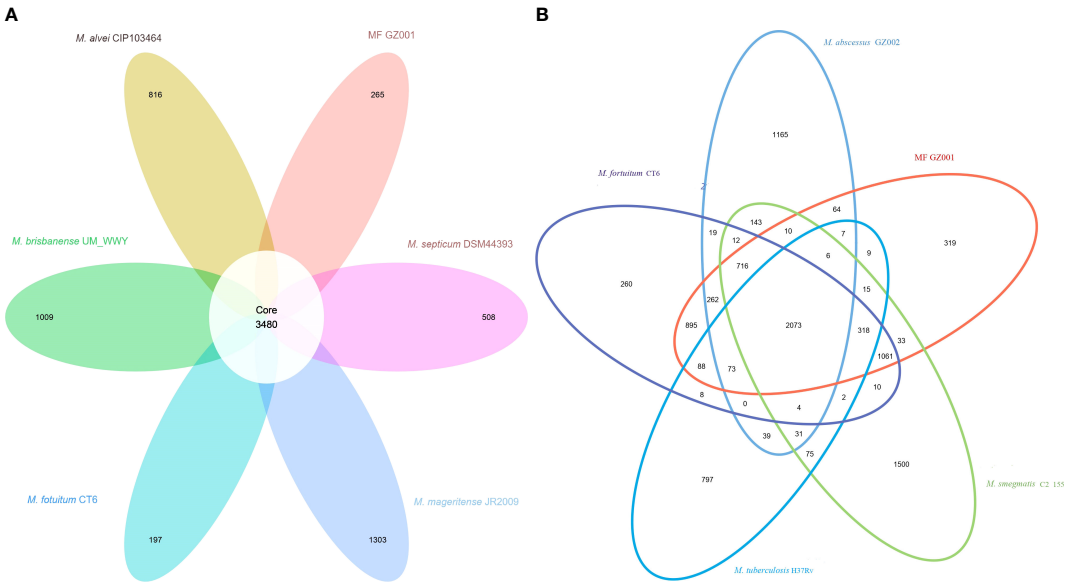

FIGURE 4
Comparative genomes representation. **(A)** Pan-genome of *M. fortuitum* complex. The white circle in the middle of the flower displayed core gene clusters, and the petals represent the unique number of clusters of each Mycobacterium species. **(B)** MF GZ001 and other mycobacterial strains genome-based Venn diagrams. The circles of different colors in the Venn diagram represent different species, and the numbers in the figure represent the numbers of gene families unique or common to each strain. In the petal diagram, each petal represents a specie. The numbers on the petals represent the number of gene families unique to the species, and the white circle in the middle represents the number of gene families shared by all strains.

7.33% cephalosporin (28) (Figure 5; Table S10). Moreover, the prevalence of the underlying SNP mutations was found in the most comprehensive drug resistance-related genes, for example, *rpoB, katG, AAC(2')-Ib, gyrA, gyrB, embB, pncA, blaF, thyA, embC, embR* and *iniA*. The most prevalent and more than 60% identity resistance-related genes have been shown in supplementary materials (Table S13). The SNP investigations showed some mutations that are not commonly observed in RGM species. For instance, the mutations in *iniA, iniC, pncA*, and *ribD* are conferred resistance to isoniazid, ethambutol, pyrazinamide, and para-aminosalicylic acid in *M. tuberculosis* (Table S13). Additionally, we have detected a mutation in the *AAC (2')-Ib* gene that causes streptomycin resistance and is more frequent in the *M. fortuitum* complex.

Comparative study of virulence genes

The virulence genes analysis reveals that the MF GZ001 genome included 167 putative virulence genes that are shared by other SGM and RGM pathogenic mycobacterium species (File.Xl.S8). We have studied the predicted virulence gene clusters across the MF GZ001 and 21 other mycobacterial strains (Table S14) based on the existence and non-existence of specific genes which indicated the relationship status between MF GZ001 and *M. fortuitum* complex. The identified 167 putative virulence genes in the mycobacterium species are responsible for inducing nitrate reductase activity, mycobacterial cell envelope, inhibition of apoptosis, lipid and protein metabolism, gene regulation, and resistance of anti-mycobacterial agents. For example, the MF GZ001 genome contains *nark2* non-redundant virulence genes which encode the nitrite transporter proteins related to exhorting nitrate reductase activity in response to reducing oxygen level by regulating its transcriptional regulation level whereas *narH*, *narG*, and *narI* (Table S14) genes encoded the proteins responsible for nitrate respiration in the absence of oxygen in the *M. tuberculosis* and *M. fortuitum* complex (Weber et al., 2000; Giffin et al., 2012). The nitrate reductase virulence factor lack in other mycobacterial species like *M. abscessus*, *M. leprae, M. marinum*, and *M. ulcerans*. Importantly, we also reported the virulence genes in MF GZ001 for instance *fbpA*, *fbpB*, *fbpC*, *hbhA*, and *mce*, encoded proteins belonging to antigen 85 complex locus (File.Xl.S8) essential for the synthesis of the bacterial cell wall (Armitige et al., 2000). These genes encoded proteins function is mycolyltransferase activity, which is essential for the development of the cell wall and the survival of mycobacteria (Mandato and Chai, 2018). We have identified five sigma factors (transcription initiation factors) that are linked to virulence in *M. tuberculosis* H37Rv (*SigAP/rpoV*, *sigE*, *sigF*, *sigH* and *sigL*), as well as the mammalian cell entry *mce* operons

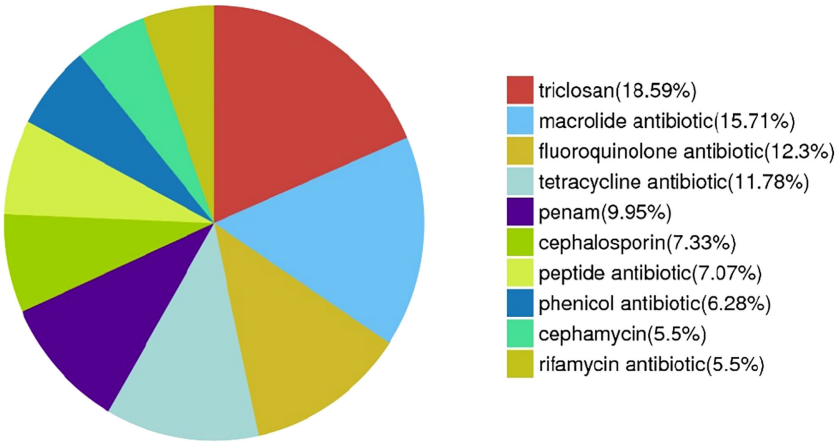

FIGURE 5
Drug resistance-related genes distribution in MF GZ001 strain.

(Table S14) that are extensively distributed across mycobacteria (Arruda et al., 1993; Wee et al., 2016). The *mce* operon has been demonstrated to be crucial for mycobacterial invasion and persistence in host macrophages and non-phagocytic mammalian cells, with *mce4* being associated with cholesterol catabolism (Zhang and Xie, 2011; Griffin et al., 2011). The MF GZ001 genome has seven operons *mce1*, *mce3*, *mce4*, *mce5*, *mce6*, *mce7*, and *mce8*, and the absence of *mce2* and *mce9* operons. MF GZ001 contained *mce1* operon homolog to *M. tuberculosis* but has not been detected in most therapeutic-resistant pathogen *M. abscessus*.

The Type VII secretion machinery is essential for mycobacterial pathophysiology and virulence (Groschel et al., 2016). Mycobacterium species include ESX 1 to 5 virulence factors and ESX-2 and ESX-5 factors are noticed in SGM. The ESX-5 is only present in SGM that could appear differentiated between RGM and SGM mycobacteria (Beckham et al., 2017). MF GZ001 genome contained ESX-1 (*espR, mycP1, eccD1, espI, esxA, eccA1, eccB1, eccCa1, eccCb1, PPE68, esxB*) virulence factor, without *espJ*, and *espK* genes that are related to SGM (File.Xl.S8). This result is consistent with *M. fortuitum*. The ESX-1 virulence factor is considered a significant virulence determinant (Madacki et al., 2021) that is associated with the inhibition of T-cell responses, inducing the differentiation of macrophages into foam cells (MacGurn and Cox, 2007; Samten et al., 2009) as well as aids in the escape of mycobacteria from phagosomes by ESAT-6 mediated perforation of vacuolar membrane (Smith et al., 2008). Moreover, we have reported that ESX-3 included *esxG, esxH, espG3, eccD3, mycP3, eccE3, eccA3, eccB3*, and *eccC3* virulence-related genes in the MF GZ001 genome. The ESX-3 factor is present in all mycobacteria and specifically essential for *in vitro* growth in *M. tuberculosis* (Sassetti et al., 2003). The ESX-3 factor is involved in iron homeostasis and uptake through the mycobactin pathway (Newton-Foot et al., 2016).

We found novel putative virulence genes homologs to *Rv1837c*, *groEL2*, *Rv0926c*, and *Rv0204c* associated with malate synthesis, dendritic cell responses, uncharacterized hypothetical protein, and transmembrane-related protein respectively that may only present in MF GZ001 strain and *M. tuberculosis* H37Rv (File.Xl.S8). Additionally, we have also identified unknown function virulence factors in the MF GZ001 strain which are related to RGM and SGM.

Furthermore, the MF GZ001 strain includes genes homologs to *katG*, *sodA*, and *sodC* that encode enzymes such as catalase-peroxidase and superoxide dismutase A which are responsible for oxidative stress tolerance (Forrellad et al., 2013). These genes may be essential for preventing the oxidative burst that occurs during macrophage survival. We have identified *nuoG* which is considered a key virulence gene of *M. tuberculosis* that encodes NADH dehydrogenase type I complex protein in the mycobacterial membrane. Similarly, some other important virulence genes are also identified for instance *secA2*, and *ptpA* (Cossu et al., 2012). These genes have been implicated as an antiapoptotic factor for macrophages (Velmurugan et al., 2007). Consequently, these genes enable the mycobacteria to avoid the host cells' built-in mechanism for cell death.

Discussion

Immunocompromised patients are particularly vulnerable to NTM infections, and the incidence of NTM infections has significantly increased globally in recent decades (Dohal et al., 2021). In this investigation, we have provided the whole genome sequencing and comparative genome analysis of a clinical strain of

NTM species, MF GZ001. In bacterial growth kinetic analysis, there was no statistically significant growth difference compared with other RGM, indicating that MF GZ001 is an RGM NTM species. The MF GZ001 has a wrinkled colony surface and rough morphotype which are consistent with a previous study (Gharbi et al., 2021). The rough morphotype *M. fortuitum* and *M. abscessus* comparatively possess more pathogenic potential (Brambilla et al., 2016; Gharbi et al., 2021). Recently, Dedrick et al., predicted the prophage length from 39.1 kb bp to 80.7 kb in clinical isolates, with an average size of ~55.3 kbp (Dedrick et al., 2021), which was closely related to prophage (39.521 kb) from our clinical strain MF GZ001 and distantly related to prophage (<11.0 kb) from *M. smegmatis* (Jordan et al., 2014; Sewell, 2017). The average prophage size indicates that the *M. fortuitum* MF GZ001 pathogenic profile may be the same as *M. abscessus*. Additionally, the DST revealed MF GZ001 strain was highly resistant to most of the therapeutic agents which also indicates that MF GZ001 strain is more virulent. Based on a single marker gene and multiple gene approaches, the phylogenetic study and ANI revealed that MF GZ001 is closely related to the *M. fortuitum* CT6. The functional reannotation analysis revealed the new mycobacterium species MF GZ001 (6254616 bp) genome size is larger than that of *M. fortuitum* CT6 (6254616 bp). Interestingly, MF GZ001 contains the highest number of conserved unknown functional genes compared to *M. fortuitum* complex members, and other RGM and SGM mycobacterium species. Moreover, MF GZ001 included more unique genes (333) than the reference genome *M. fortuitum* CT6 (264). The larger genome size of MF GZ001 may reveal the diverse genomic structure of *M. fortuitum* complex. This diverse structure was observed may be due to horizontal gene transfer, CRISPR elements, and the prophage found in this species which may have an important impact on the fitness and pathogenicity of their bacterial hosts (Cote et al., 2022). According to previous studies of prophage in NTM clinical strains, prophage was found more likely in RGM than SGM (Dedrick et al., 2021; Senhaji-Kacha et al., 2021). The clinical NTM prophages may have more abundant virulence genes than the prophages from the environmental mycobacteria (Glickman et al., 2020). Based on an overview of the MF GZ001 genome, the prophage analysis predicted that it contains a (39.521 kb) prophage region. The prophage sequence is flanked by 13 bp phage attachment sites, *attL*, and *attR* (Table S7). Though it has been studied that clinical NTM exhibits various levels of virulence, but it is not thoroughly verified yet that whether the prophage elements containing virulence genes have any impact on treatment outcomes (Gonzalez-Perez et al., 2013). The existence of virulence genes does not imply that they are being actively expressed, and the presence of a prophage in a genome does not prove that the virus is excisable or functional (Glickman et al., 2020). According to the literature contradictory review, it would be beneficial to conduct further research to characterize the prophage of the *M. fortuitum* complex. Mycobacterium species can also transfer DNA intrinsically and incorporate DNA from foreign sources between species (Rabello et al., 2012; Wee et al., 2016). In addition to comparative analysis based on genomes such as higher level of colinearity, a Venn diagram, and a pan-genome study showed a close relationship between MF GZ001 and *M. fortuitum* CT6. Although the genome variation was also observed, more characteristics were shared with *M. fortuitum* complex members than other mycobacterium species. This investigation uncovered a close link between MF GZ001 and *M. fortuitum* complex which provides insight into the deep evolution of pathogenesis in RGM species.

To our knowledge, this is the first report of SNV/INDEL mutation based on *de novo* sequencing methods in *M. fortuitum* complex members. In this report, we have detected SNV/INDEL mutations compared to the reference strains and other mycobacterium species. We have identified 74168 SNVs and 2001 INDEL mutations in the MF GZ001 strains compared to the reference genome. Moreover, we have identified stop loss (33) and stop gain (110) variants in the MF GZ001 strain. Most putative resistance mutations were observed in nonessential areas where hundreds of loss-of-function mutations might cause resistance (Miotto et al., 2017). Several variants conferred in a loss of function due to INDEL or stop codons (Richard et al., 2019). Importantly, we have found 174 intragenic mutations in two genes (*1_3425, 1_3426*) that are of unknown function. This study further emphasizes investigating the role of genes and the therapeutic resistance mechanisms in the RGM *M. fortuitum* complex.

Furthermore, the MF GZ001 drug resistance profile was studied *via in vitro* DST and prediction of drug resistance genes and variants with *in silico* analysis. *M. fortuitum* infected cases resistant to clarithromycin and fluoroquinolones have also been reported previously (Kurokawa et al., 2020). *In vitro* testing of MF GZ001 showed high resistance to macrolides, clofazimine, sulfamethoxazole, levofloxacin, streptomycin, and RIF. No frequent studies have been conducted to investigate the *M. fortuitum* complex. In this first report, drug resistance gene prediction through *in silico* approaches showed 18.59% genes associated with resistance to triclosan, 15.71% to macrolides, and 12.3% to fluoroquinolones. We have found SNPs in drug resistance-related genes such as *rpoB, arr, AAC(2')-Ib, katG, gyrA, gyrB, embB, blaF, thyA, embC* and *embR* that are previously reported in *M. fortuitum* and other mycobacterium species (Nash et al., 2005; Ramon-Garcia et al., 2006). For instance, among them recently reported, the ribosylation ADP-ribosyltransferase *arr* gene in *M. fortuitum* 7G was linked to the high level of RIF resistance which is consistent with our findings (Morgado et al., 2022a). A mutation in the *rpoB* gene's particular region known as the rifampin-resistance-determining region (RRDR) leads to the emergence of RIF resistance in NTM and *M. tuberculosis* (Saxena et al., 2021). Additionally, by expressing the *arr* gene, *M. abscessus* and *M. smegmatis* intrinsically reduced the function of RIF (Brown-Elliott et al., 2012). The *erm* gene may responsible for the intrinsic resistance to macrolides in *M. fortuitum* strains. Erm

is a member of a large family of proteins that are encoded by a variety of alleles, some of which (*erm*37-41) are specifically linked to Mycobacteriaceae species (Nash et al., 2005). Furthermore, similar to our study the mutations in *gyrA* have also been reported to be responsible for quinolone resistance in *M. fortuitum* (Kamada et al., 2021).

Importantly, the SNPs found in genes of MF GZ001, for example, *iniA, iniC, pncA*, and *ribD* conferring resistance to isoniazid, ethambutol, pyrazinamide, para-aminosalicylic acid, and isoniazid resistance respectively, are not commonly observed in RGM. We have reported a mutation in a distinctive gene *aph (3")-Ic* that is related to streptomycin resistance which is consistent with other studies (Morgado et al., 2022a). The *aph (3")-Ic* distinctive gene was first reported in environmental *M. fortuitum* and later in clinical isolates as well (Ramon-Garcia et al., 2006; Morgado et al., 2022b). We anticipate that further investigation of the novel SNPs in *iniA, iniC, ribD, pncA*, and *aph (3")-Ic* detected in this study are necessary to explore their role in the development of resistance. Particularly, these well-known drug-resistant genes are found in the MF GZ001 strain, which will be useful for further study on strain identification and characterizations enriching the genetic data sources for pathogenic diseases.

The genome of MF GZ001 comprises a variety of putative virulence genes that may have enhanced its ability for intracellular replication and persistence. *M. fortuitum* exhibits robust pathogenicity linked to various virulence genes, for instance, *mce*, *nar*, sigma, and antigen 85 complex clusters. These genes could encode potential virulence factors associated with mycobacterial cell envelope, inhibition of apoptosis, lipid and protein metabolism, gene regulation as well as nitrate reductase activity. The *mce* operons distributed across mycobacterium species are responsible for mycobacterial invasion and persistence in host macrophages and non-phagocytic mammalian cells, with *mce4* being associated with cholesterol catabolism (Zhang and Xie, 2011). *M. fortuitum* contains the *nuoG* gene, which encodes NADH dehydrogenase type I complex protein in the mycobacterial membrane which is considered as an emergent virulence factor in *M. tuberculosis* (Velmurugan et al., 2007; Cossu et al., 2012). MF GZ001 genome contains an important *trpD* gene which is also confirmed by the previous study. Among RGM, a gene copy of *trpD* was only detected in *M. abscessus* and *M. fortuitum* complex members (Gharbi et al., 2021). It encodes an anthranilate phosphoribosyltransferase associated with tryptophan biosynthesis which has contributed a significant role during infection of patients for SGM (Zhang et al., 2013). Particularly, the MF GZ001 genome has *katG*, *sodA* gene for oxidative stress resistance which may be crucial for preventing the oxidative burst that occurs during macrophage survival. These genes have been shown by Wee et al., in *M. brisbanense* which is a member of the *M. fortuitum* complex (Wee et al., 2016). Furthermore, in recent years it has been identified that the genes responsible for the biosynthesis of the many unique lipids are found in the mycobacterial cell wall. For instance, MF GZ001 contains the acyl-coenzyme A (CoA) synthase gene (*fadD28*) which is associated with the esterification of the acid to phthiocerol to produce dimycocerosyl phthiocerol which is involved in virulence (Fitzmaurice and Kolattukudy, 1997; Sirakova et al., 2002; Brodin et al., 2010).

Furthermore, we reported novel putative virulence genes that are homologous to *Rv1837c, groEL2, Rv0926c*, and *Rv0204c*, and are related to malate synthesis, dendritic cell responses, an unidentified hypothetical protein, and a transmembrane-related protein, respectively. These genes may only be found in the MF GZ001 strain and *M. tuberculosis* H37Rv. Recently, Luo et al., reported that the secretion proteins locus ESX-1, ESX-3, and ESX-5 are crucial for virulence in *M. tuberculosis* (Luo et al., 2022) and were found in the MF GZ001 strain which is consistent with the previous report (Gharbi et al., 2021; Morgado et al., 2022b). Therefore, the MF GZ001 genome sequence will provide insights into *M. fortuitum* complex potential pathogenesis. The existence of the potential virulence determinants still requires experimental evidence to detect whether the MF GZ001 strain is associated with crucial human diseases or not.

In summary, we have sequenced and analyzed the genome of the MF GZ001 strain that might be a new member of the *M. fortuitum* complex. Our comparative analysis indicated that it is a new member of the *M. fortuitum* complex and a human-pathogenic species. The findings of this study will establish a foundation for further investigations of the pathogenic mechanism of *M. fortuitum* as well as its diagnosis and treatment, especially in southern China.

Data availability statement

The original datasets generated in the study are publicly available. The MFGZ001 WGS and SRA data were deposited in the NCBI database under accession numbers CP107719 and SRR22164027.

Author contributions

All authors contributed to the article and approved the submitted version.

Funding

This work was supported by the National Key R&D Program of China (2021YFA1300904) and the Chinese Academy of Sciences (154144KYSB20190005, YJKYYQ20210026), and partially supported by the National Natural Science Foundation of China (NSFC 81973372, 21920102003), by

China-New Zealand Joint Laboratory on Biomedicine and Health, and President's International Fellowship Initiative-CAS (to H.M. Adnan Hameed), and State Key Laboratory of Respiratory Disease (SKLRD-Z-202301, SKLRD-OP-202324). We are grateful to The Alliance of International Science Organizations (ANSO) Scholarship for Young Talents PhD Fellowship Program 2022-2025 (To Md Shah Alam). The funders had no role in the study design, data collection, analysis, decision to publish, or preparation of the manuscript.

Conflict of interest

The authors declare that the research was carried out in the absence of any financial or economic relationships that could be construed as a potential conflict of interest.

Publisher's note

Supplementary material

The Supplementary Material for this article can be found online at: https://www.frontiersin.org/articles/10.3389/fcimb.2022.1056007/full#supplementary-material

References

Aitken, M. L., Limaye, A., Pottinger, P., Whimbey, E., Goss, C. H., Tonelli, M. R., et al. (2012). Respiratory outbreak of *Mycobacterium abscessus* subspecies *massiliense* in a lung transplant and cystic fibrosis center. *Am. J. Respir. Crit. Care Med.* 185 (2), 231–232. doi: 10.1164/ajrccm.185.2.231

Akhter, S., Aziz, R. K., and Edwards, R. A. (2012). PhiSpy: a novel algorithm for finding prophages in bacterial genomes that combines similarity-and composition-based strategies. *Nucleic Acids Res.* 40 (16), e126–e126. doi: 10.1093/nar/gks406

Alcock, B. P., Raphenya, A. R., Lau, T. T., Tsang, K. K., Bouchard, M., Edalatmand, A., et al. (2020). CARD 2020: antibiotic resistome surveillance with the comprehensive antibiotic resistance database. *Nucleic Acids Res.* 48 (D1), D517–D525. doi: 10.1093/nar/gkz935

Armitige, L. Y., Jagannath, C., Wanger, A. R., and Norris, S. J. (2000). Disruption of the genes encoding antigen 85A and antigen 85B of *Mycobacterium tuberculosis* H37Rv: effect on growth in culture and in macrophages. *Infect. Immun.* 68 (2), 767–778. doi: 10.1128/IAI.68.2.767-778.2000

Arruda, S., Bomfim, G., Knights, R., Huima-Byron, T., and Riley, L. W. (1993). Cloning of an *M. tuberculosis* DNA fragment associated with entry and survival inside cells. *Science* 261 (5127), 1454–1457. doi: 10.1126/science.8367727

Austin, C. M., Tan, M. H., Harrisson, K. A., Lee, Y. P., Croft, L. J., Sunnucks, P., et al. (2017). *De novo* genome assembly and annotation of australia's largest freshwater fish, the Murray cod (*Maccullochella peelii*), from illumina and nanopore sequencing read. *GigaScience* 6 (8), gix063. doi: 10.1093/gigascience/gix063

Beckham, K. S., Ciccarelli, L., Bunduc, C. M., Mertens, H. D., Ummels, R., Lugmayr, W., et al. (2017). Structure of the mycobacterial ESX-5 type VII secretion system membrane complex by single-particle analysis. *Nat. Microbiol.* 2 (6), 1–7. doi: 10.1038/nmicrobiol.2017.47

Bland, C., Ramsey, T. L., Sabree, F., Lowe, M., Brown, K., Kyrpides, N. C., et al. (2007). CRISPR recognition tool (CRT): a tool for automatic detection of clustered regularly interspaced palindromic repeats. *BMC Bioinf.* 8 (1), 1–8. doi: 10.1186/1471-2105-8-209

Brambilla, C., Llorens-Fons, M., Julian, E., Noguera-Ortega, E., Tomas-Martinez, C., Perez-Trujillo, M., et al. (2016). Mycobacteria clumping increase their capacity to damage macrophages. *Front. Microbiol.* 7. doi: 10.3389/fmicb.2016.01562

Brodin, P., Poquet, Y., Levillain, F., Peguillet, I., Larrouy-Maumus, G., Gilleron, M., et al. (2010). High content phenotypic cell-based visual screen identifies *Mycobacterium tuberculosis* acyltrehalose-containing glycolipids involved in phagosome remodeling. *PLos Pathog.* 6 (9), e1001100. doi: 10.1371/journal.ppat

Brown-Elliott, B. A., Mann, L. B., Hail, D., Whitney, C., and Wallace, J. R.J. (2012). Antimicrobial susceptibility of nontuberculous mycobacteria from eye infections. *Cornea* 31 (8), 900–906. doi: 10.1097/ICO.0b013e31823f8bb9

Brown-Elliott, B. A., and Philley, J. V. (2017). Rapidly growing mycobacteria. *Microbiol. Spectr.* 5 (1), 703–723. doi: 10.1128/microbiolspec.TNMI7-0027-2016

Brown-Elliott, B. A., and Wallace, J. R.J. (2002). Clinical and taxonomic status of pathogenic nonpigmented or late-pigmenting rapidly growing mycobacteria. *Clinc. Microbiol. Rev.* 15 (4), 716–746. doi: 10.1128/CMR.15.4.716-746.2002

Bryant, J. M., Grogono, D. M., Greaves, D., Foweraker, J., Roddick, I., Inns, T., et al. (2013). Whole-genome sequencing to identify transmission of *Mycobacterium abscessus* between patients with cystic fibrosis: a retrospective cohort study. *Lancet.* 381 (9877), 1551–1560. doi: 10.1016/S0140-6736(13)60632-7

Chan, E. D., and Iseman, M. D. (2013). Underlying host risk factors for nontuberculous mycobacterial lung disease. *Semin. Respir. Crit. Care Med.* 34 (01), 110–123. doi: 10.1055/s-0033-1333573

Chhotaray, C., Wang, S., Tan, Y., Ali, A., Shehroz, M., Zhang, T., et al. (2020). Comparative analysis of whole-genome and methylome profiles of a smooth and a rough *Mycobacterium abscessus* clinical strain. *G3 (Bethesda)* 10 (1), 13–22. doi: 10.1534/g3.119.400737

Cossu, A., Sechi, L. A., Zanetti, S., and Rosu, V. (2012). Gene expression profiling of *Mycobacterium avium* subsp. *paratuberculosis* in simulated multi-stress conditions and within THP-1 cells reveals a new kind of interactive intramacrophage behaviour. *BMC Microbiol.* 12 (1), 1–17. doi: 10.1186/1471-2180-12-87

Costa, K. C., Bergkessel, M., Saunders, S., Korlach, J., and Newman, D. K. (2015). Enzymatic degradation of phenazines can generate energy and protect sensitive organisms from toxicity. *mBio.* 6 (6), e01520–e01515. doi: 10.1128/mBio.01520-15

Cote, J., Welch, C., Kimble, M., Archambault, D., Ross, J. C., Molloy, S. D., et al. (2022). Characterization of the cluster MabR prophages of *Mycobacterium abscessus* and. *Mycobacterium chelonae. G3 (Bethesda)* 12 (9), jkac188. doi: 10.1093/g3journal/jkac188

Daley, C. L., and Griffith, D. E. (2002). Pulmonary disease caused by rapidly growing mycobacteria. *Clin. Chest. Med.* 23 (3), 623–632. doi: 10.1016/s0272-5231(02)00021-7

Dedrick, R. M., Aull, H. G., Jacobs-Sera, D., Garlena, R. A., Russell, D. A., Hatfull, G. F., et al. (2021). The prophage and plasmid mobilome as a likely driver of *Mycobacterium abscessus* diversity. *mBio.* 12 (2), e03441–e03420. doi: 10.1128/mBio.03441-20

De Groote, M. A., and Huitt, G. (2006). Infections due to rapidly growing mycobacteria. *Clinc. Infect. Dis.* 42 (12), 1756–1763. doi: 10.1086/504381

Delcher, A. L., Bratke, K. A., Powers, E. C., and Salzberg, S. L. (2007). Identifying bacterial genes and endosymbiont DNA with glimmer. *Bioinformatics* 23 (6), 673–679. doi: 10.1093/bioinformatics/btm009

Diaz, M. A. A., Huff, T. N., and Libertin, C. R. (2019). Nontuberculous mycobacterial infections of the lower extremities: A 15-year experience. *J. Clin. Tuberc. Other Mycobact. Dis.* 15, 100091. doi: 10.1016/j.jctube.2019.100091

Dohal, M., Porvaznik, I., Solovic, I., and Mokry, J. (2021). Whole genome sequencing in the management of non-tuberculous mycobacterial infections. *Microorganisms* 9 (11), 2237. doi: 10.3390/microorganisms9112237

Eid, J., Fehr, A., Gray, J., Luong, K., Lyle, J., Bettman, B., et al. (2009). Real-time DNA sequencing from single polymerase molecules. *Science* 323 (5910), 133–138. doi: 10.1126/science.1162986

Erber, J., Weidlich, S., Tschaikowsky, T., Rothe, K., Schmid, R. M., Spinner, C. D., et al. (2020). Successful bedaquiline-containing antimycobacterial treatment in post-traumatic skin and soft-tissue infection by *Mycobacterium fortuitum* complex: a case report. *BMC Infect. Dis.* 20 (1), 1–7. doi: 10.1186/s12879-020-05075-7

Ferrarini, M., Moretto, M., Ward, J. A., Surbanovski, N., Stevanovic, V., Sargent, D. J., et al. (2013). Anevaluation of the PacBioRS platform for sequencing and denovoassembly of achloroplast genome. *BMC Genomics* 14 (1), 1–12. doi: 10.1186/1471-2164-14-670

Fitzmaurice, A. M., and Kolattukudy, P. E. (1997). Open reading frame 3, which is adjacent to the mycocerosic acid synthase gene, is expressed as an acyl coenzyme a synthase in *Mycobacterium bovis* BCG. *J. @ Bact* 179 (8), 2608–2615. doi: 10.1128/jb.179.8.2608-2615.1997

Forrellad, M. A., Klepp, L. I., Gioffre, A., Sabio y Garcia, J., Morbidoni, H. R., Bigi, F., et al. (2013). Virulence factors of the *Mycobacterium tuberculosis* complex. *Virulence* 4 (1), 3–66. doi: 10.4161/viru.22329

Gharbi, R., Khanna, V., Frigui, W., Mhenni, B., Brosch, R., and Mardassi, H. (2021). Phenotypic and genomic hallmarks of a novel, potentially pathogenic rapidly growing mycobacterium species related to the *Mycobacterium fortuitum* complex. *Sci. Rep.* 11 (1), 1–12. doi: 10.1038/s41598-021-91737-8

Giffin, M. M., Raab, R. W., Morganstern, M., and Sohaskey, C. D. (2012). Mutational analysis of the respiratory nitrate transporter NarK2 of *Mycobacterium tuberculosis*. *PLos One.* 7 (9), e45459. doi: 10.1371/journal.pone.0045459

Glickman, C., Kammlade, S. M., Hasan, N. A., Epperson, L. E., Davidson, R. M., and Strong, M. (2020). Characterization of integrated prophages within diverse species of clinical nontuberculous mycobacteria. *Viro. J.* 17(1), 1–13. doi: 10.1186/s12985-020-01394-y

Gonzalez-Perez, M., Marino-Ramirez, L., Parra-Lopez, C. A., Murcia, M. I., Marquina, B., Hernandez-Pando, R., et al. (2013). Virulence and immune response induced by *Mycobacterium avium* complex strains in a model of progressive pulmonary tuberculosis and subcutaneous infection in BALB/c mice. *Infect. Immun.* 81 (11), 4001–4012. doi: 10.1128/IAI.00150-13

Griffin, J. E., Gawronski, J. D., DeJesus, M. A., Ioerger, T. R., Akerley, B. J., and Sassetti, C.M. (2011). High-resolution phenotypic profiling defines genes essential for mycobacterial growth and cholesterol catabolism. *PLos Pathog.* 7 (9), e1002251. doi: 10.1371/journal.ppat.1002251

Grissa, I., Vergnaud, G., and Pourcel, C. (2007). CRISPRFinder: a web tool to identify clustered regularly interspaced short palindromic repeats. *Nucleic Acids Res.* 35 (suppl_2), W52–W57. doi: 10.1093/nar/gkm360

Groschel, M. I., Sayes, F., Simeone, R., Majlessi, L., and Brosch, R. (2016). ESX secretion systems: mycobacterial evolution to counter host immunity. *Nat. Rev. Microbiol.* 14 (11), 677–691. doi: 10.1038/nrmicro.2016.131

Guo, J., Wang, C., Han, Y., Liu, Z., Wu, T., Zhang, T., et al. (2016). Identification of lysine acetylation in *Mycobacterium abscessus* using LC–MS/MS after immunoprecipitation. *J. Proteome Res.* 15 (8), 2567–2578. doi: 10.1021/acs.jproteome.6b00116

Han, R., Xie, D., Tong, X., Zhang, W., Liu, G., Yu, N., et al. (2018). Transcriptomic landscape of *Dendrobium huoshanense* and its genes related to polysaccharide biosynthesis. *AGRIS* 87 (1), 3574. doi: 10.5586/asbp.3574

Harris, M. A., Clark, J., Ireland, A., Lomax, J., Ashburner, M., Hill.,, et al. (2004). The gene ontology (GO) database and informatics resource. *Nucleic Acids Res.* 32 (Database issue), D258–D261. doi: 10.1093/nar/gkh036

Hert, D. G., Fredlake, C. P., and Barron, A. E. (2008). Advantages and limitations of next-generation sequencing technologies: a comparison of electrophoresis and non-electrophoresis methods. *Electrophoresis* 29 (23), 4618–4626. doi: 10.1002/elps.200800456

Huang, Z., Yu, K., Xiao, Y., Wang, Y., Xiao, D., and Wang, D. (2022). Comparative genomic analysis reveals potential pathogenicity and slow-growth characteristics of genus *Brevundimonas* and description of *Brevundimonas pishanensis* sp. nov. *Microbiol. Spect.* 10 (2), e02468–e02421. doi: 10.1128/spectrum.02468-21

Jia, X., Yang, L., Li, C., Xu, Y., Yang, Q., and Chen, F. (2021). Combining comparative genomic analysis with machine learning reveals some promising diagnostic markers to identify five common pathogenic non-tuberculous mycobacteria. *Microb. Biotechnol.* 14 (4), 1539–1549. doi: 10.1111/1751-7915.13815

Johansen, M. D., and Kremer, L. (2020). CFTR depletion confers hypersusceptibility to *Mycobacterium fortuitum* in a zebrafish model. *Front. Cell Infect. Microbiol.* 10. doi: 10.3389/fcimb.2020.00357

Jordan, T. C., Burnett, S. H., Carson, S., Caruso, S. M., Clase, K., Hatfull, G. F., et al. (2014). A broadly implementable research course in phage discovery and genomics for first-year undergraduate students. *mBio.* 5 (1), e01051–e01013. doi: 10.1128/mBio.01051-13

Kamada, K., Yoshida, A., Iguchi, S., Arai, Y., Uzawa, Y., Kikuchi, K., et al. (2021). Nationwide surveillance of antimicrobial susceptibility of 509 rapidly growing mycobacteria strains isolated from clinical specimens in Japan. *Sci. Rep.* 11 (1), 1–10. doi: 10.1038/s41598-021-91757-4

Kanehisa, M., and Goto, S. (2000). KEGG: kyoto encyclopedia of genes and genomes. *Nucleic Acids Res.* 28 (1), 27–30. doi: 10.1093/nar/28.1.27

Katoh, K., and Standley, D. M. (2013). MAFFT multiple sequence alignment software version 7: improvements in performance and usability. *Mol. Biol. Evol.* 30 (4), 772–780. doi: 10.1093/molbev/mst010

Koh, W. J., Kwon, O. J., Jeon, K., Kim, T. S., Lee, K. S., Bai, G. H., et al. (2006). Clinical significance of nontuberculous mycobacteria isolated from respiratory specimens in Korea. *Chest* 129 (2), 341–348. doi: 10.1378/chest.129.2.341

Krishnan, M. Y., Manning, E. J., and Collins, M. T. (2009). Comparison of three methods for susceptibility testing of *Mycobacterium avium subsp. paratuberculosis* to 11 antimicrobial drugs. *J. Antimicrob. Chemother.* 64 (2), 310–316. doi: 10.1093/jac/dkp184

Kurokawa, K., Harada, N., Sasano, H., Takagi, H., Takei, S., Takahashi, K., et al. (2020). Pulmonary infection due to fluoroquinolone-resistant *Mycolicibacterium fortuitum*: a case report. *BMC Infect. Dis.* 20 (1), 1–6. doi: 10.1186/s12879-020-05596-1

Leung, K. S. S., Siu, G. K. H., Tam, K. K. G., To, S. W. C., Rajwani, R., Yam, W. C., et al. (2017). Comparative genomic analysis of two clonally related multidrug resistant *mycobacterium tuberculosis* by single molecule real-time sequencing. *Front. Cell. Infect. Microbiol.* 7. doi: 10.3389/fcimb.2017.00478

Li, H., and Durbin, R. (2009). Fast and accurate short read alignment with burrows–wheeler transform. *Bioinformatics* 25 (14), 1754–1760. doi: 10.1093/bioinformatics/btp324

Lowe, T. M., and Eddy, S. R. (1997). tRNAscan-SE: a program for improved detection of transfer RNA genes in genomic sequence. *Nucleic Acids Res.* 25 (5), 955–964. doi: 10.1093/nar/25.5.955

Luo, Z., Hao, S., Bai, X., Zhang, Z., Ma, Y., Zhang, D., et al. (2022). Identification and genomic analysis of *Mycobacterium ulcerans* ecovar liflandii from the farmed Chinese tongue sole, *Cynoglossus semilaevis* gunther. *Aquaculture* 548, 737614. doi: 10.1016/j.aquaculture.2021.737614

MacGurn, J. A., and Cox, J. S. (2007). A genetic screen for *Mycobacterium tuberculosis* mutants defective for phagosome maturation arrest identifies components of the ESX-1 secretion system. *Infect. Immun.* 75 (6), 2668–2678. doi: 10.1128/IAI.01872-06

Madacki, J., Orgeur, M., Mas Fiol, G., Frigui, W., Ma, L., and Brosch, R. (2021). ESX-1-independent horizontal gene transfer by *Mycobacterium tuberculosis* complex strains. *mBio.* 12 (3), e00965–e00921. doi: 10.1128/mBio.00965-21

Magrane, M. (2011). UniProt knowledgebase: a hub of integrated protein data. *Database (Oxford)* 2011, bar009. doi: 10.1093/database/bar009

Mandato, A., and Chai, Y. C. (2018). Regulation of antigen 85C activity by reversible s-glutathionylation. *IUBMB Life.* 70 (11), 1111–1114. doi: 10.1002/iub.1923

Maya, T. G., Komba, E. V., Mensah, G. I., Mbelele, P. M., Mpagama, S. G., Kazwala, R. R., et al. (2022). Drug susceptibility profiles and factors associated with non-tuberculous mycobacteria species circulating among patients diagnosed with pulmonary tuberculosis in Tanzania. *PLos One* 17 (3), e0265358. doi: 10.1371/journal.pone.0265358

McCarthy, A. (2010). Third generation DNA sequencing: pacific biosciences' single molecule real time technology. *Chem. Bio.* 17 (7), 675–676. doi: 10.1016/j.chembiol.2010.07.004

Miotto, P., Tessema, B., Tagliani, E., Chindelevitch, L., Starks, A. M., Rodwell, T. C., et al. (2017). A standardised method for interpreting the association between mutations and phenotypic drug resistance in *Mycobacterium tuberculosis*. *Eur. Respir. J.* 50 (6), 1701354. doi: 10.1183/13993003.01354-2017

Morgado, S., de Veiga Ramos, N., do Nascimento Pereira, B. B., Freitas, F., da Fonseca, E. L., and Vicente, A. C. (2022a). Multidrug-resistant *Mycolicibacterium fortuitum* infection in a companion cat (*Felis silvestris catus*) in Brazil. *Access Microbiol.* 4 (2), 317. doi: 10.1099/acmi.0.000317

Morgado, S., Ramos, N. D. V., Freitas, F., da Fonseca, E. L., and Vicente, A. C. (2022b). *Mycolicibacterium fortuitum* genomic epidemiology, resistome and virulome. *Mem. Inst. Oswaldo. Cruz.* 116, e210247. doi: 10.1590/0074-02760210247

Myers, E. W., Sutton, G. G., Delcher, A. L., Dew, I. M., Fasulo, D. P., Venter, J. C., et al. (2000). A whole-genome assembly of *Drosophila*. *Science* 287 (5461), 2196–2204. doi: 10.1126/science.287.5461.2196

Nash, K. A., Zhang, Y., Brown-Elliott, B. A., and Wallace, J. R.J. (2005). Molecular basis of intrinsic macrolide resistance in clinical isolates of *Mycobacterium fortuitum*. *J. Anti Chem.* 55 (2), 170–177. doi: 10.1093/jac/dkh523

Nawrocki, E. P., Burge, S. W., Bateman, A., Daub, J., Eberhardt, R. Y., Finn, R. D., et al. (2015). Rfam 12.0: updates to the RNA families database. *Nucleic Acids Res.* 43 (D1), D130–D137. doi: 10.1093/nar/gku1063

Newton-Foot, M., Warren, R. M., Sampson, S. L., Van Helden, P. D., and Gey van Pittius, N. C. (2016). The plasmid-mediated evolution of the mycobacterial ESX (Type VII) secretion systems. *BMC Evo. Bio.* 16 (1), 1–12. doi: 10.1186/s12862-016-0631-2

Park, S., Suh, G. Y., Chung, M. P., Kim, H., Kwon, O. J., Koh, W. J., et al. (2008). Clinical significance of *Mycobacterium fortuitum* isolated from respiratory specimens. *Respt. Med.* 102 (3), 437–442. doi: 10.1016/j.rmed.2007.10.005

Pavlik, I., Ulmann, V., and Weston, R. T. (2021). Clinical relevance and environmental prevalence of *Mycobacterium fortuitum* group members. comment on mugetti et al. gene sequencing and phylogenetic analysis: powerful tools for an improved diagnosis of fish mycobacteriosis caused by mycobacterium fortuitum group members. microorganisms 2021, 9, 797. *Microorganisms* 9 (11), 2345. doi: 10.3390/microorganisms9112345

Price, M. N., Dehal, P. S., and Arkin, A. P. (2010). FastTree 2–approximately maximum-likelihood trees for large alignments. *PLos One* 5 (3), e9490. doi: 10.1371/journal.pone.0009490

Punta, M., Coggill, P. C., Eberhardt, R. Y., Mistry, J., Tate, J., Finn, R. D., et al. (2012). The pfam protein families database. *Nucleic Acids Res.* 40 (D1), D290–D301. doi: 10.1093/nar/gkr1065

Qi, J., Zheng, N., Zhang, B., Sun, P., Hu, S., Li, X., et al. (2013). Mining genes involved in the stratification of Paris polyphylla seeds using high-throughput embryo transcriptome sequencing. *BMC Genomics* 14 (1), 1–14. doi: 10.1186/1471-2164-14-358

Rabello, M. C. D. S., Matsumoto, C. K., de Almeida, L. G. P., Menendez, M. C., de Oliveira, R. S., Leao, S. C., et al. (2012). First description of natural and experimental conjugation between mycobacteria mediated by a linear plasmid. *PLos One* 7 (1), e29884. doi: 10.1371/journal.pone

Ramon-Garcia, S., Otal, I., Martin, C., Gomez-Lus, R., and Ainsa, J. A. (2006). Novel streptomycin resistance gene from *Mycobacterium fortuitum*. *Antimicrob. Agents Chemother.* 50 (11), 3920–3922. doi: 10.1128/AAC.00223-06

Reves, R., and Schluger, N. W. (2014). Update in tuberculosis and nontuberculous mycobacterial infections 2013. *Am. J. Respir. Crit. Care Med.* 189 (8), 894–898. doi: 10.1164/rccm.201402-0210UP

Richard, M., Gutierrez, A. V., Viljoen, A., Rodriguez-Rincon, D., Roquet-Baneres, F., Kremer, L., et al. (2019). Mutations in the *MAB_2299c* TetR regulator confer cross-resistance to clofazimine and bedaquiline in *Mycobacterium abscessus*. *Antimicrobial Agents chemother.* 63 (1), e01316–e01318. doi: 10.1128/AAC.01316-18

Robbertse, B., Strope, P. K., Chaverri, P., Gazis, R., Ciufo, S., Schoch, C. L., et al. (2017). Improving taxonomic accuracy for fungi in public sequence databases: applying 'one name one species' in well-defined genera with trichoderma/hypocrea as a test case. *Database (Oxford)* 2017, bax072. doi: 10.1093/database/bax072

Roberts, R. J., Carneiro, M. O., and Schatz, M. C. (2013). The advantages of SMRT sequencing. *Gen. Biol.* 14 (6), 1–4. doi: 10.1186/gb-2013-14-6-405

Samten, B., Wang, X., and Barnes, P. F. (2009). *Mycobacterium tuberculosis* ESX-1 system-secreted protein ESAT-6 but not CFP10 inhibits human T-cell immune responses. *Tuberculosis* 89 (Suppl 1), S74–S76. doi: 10.1016/S1472-9792(09)70017-4

Sassetti, C. M., Boyd, D. H., and Rubin, E. J. (2003). Genes required for mycobacterial growth defined by high density mutagenesis. *Mol. Microbiol.* 48 (1), 77–84. doi: 10.1046/j.1365-2958.2003.03425.x

Saxena, S., Spaink, H. P., and Forn-Cuni, G. (2021). Drug resistance in nontuberculous mycobacteria: mechanisms and models. *Biology* 10 (2), 96. doi: 10.3390/biology10020096

Schon, T., Werngren, J., Machado, D., Borroni, E., Wijkander, M., Cambau, E., et al. (2020). Antimicrobial susceptibility testing of *Mycobacterium tuberculosis* complex isolates–the EUCAST broth microdilution reference method for MIC determination. *Clinc. Microbiol. Infect.* 26 (11), 1488–1492. doi: 10.1016/j.cmi.2020.07.036

Senhaji-Kacha, A., Esteban, J., and Garcia-Quintanilla, M. (2021). Considerations for phage therapy against *Mycobacterium abscessus*. *Front. Microbiol.* 11. doi: 10.3389/fmicb.2020.609017

Sewell, E. (2017). Characterizing the intact prophage of *Mycobacterium chelonae bergey*. *Honors College* 265. Available at: https://digitalcommons.library.umaine.edu/honors/265

Sirakova, T. D., Fitzmaurice, A. M., and Kolattukudy, P. (2002). Regulation of expression of mas and *fadD28*, two genes involved in production of dimycocerosyl phthiocerol, a virulence factor of *Mycobacterium tuberculosis*. *J. Bacteriol.* 184 (24), 6796–6802. doi: 10.1128/JB.184.24.6796-6802.2002

Smith, J., Manoranjan, J., Pan, M., Bohsali, A., Xu, J., Gao, L. Y., et al. (2008). Evidence for pore formation in host cell membranes by ESX-1-secreted ESAT-6 and its role in *Mycobacterium marinum* escape from the vacuole. *Infect. Immun.* 76 (12), 5478–5487. doi: 10.1128/IAI.00614-08

Stanke, M., Schoffmann, O., Morgenstern, B., and Waack, S. (2006). Gene prediction in eukaryotes with a generalized hidden Markov model that uses hints from external sources. *BMC Bioinf.* 7 (1), 1–11. doi: 10.1186/1471-2105-7-62

Sun, Q., Yan, J., Liao, X., Wang, C., Wang, C., Pan, J., et al. (2022). Trends and species diversity of nontuberculous mycobacteria isolation from respiratory samples in northern china 2014–2021. *Front. Public Health* 10. doi: 10.3389/fpubh.2022.923968

Tatusov, R. L., Fedorova, N. D., Jackson, J. D., Jacobs, A. R., Kiryutin, B., Natale, D. A., et al. (2003). The COG database: an updated version includes eukaryotes. *BMC Bioinf.* 4, 41. doi: 10.1186/1471-2105-4-41

Teng, J. L., Yeung, M. L., Chan, E., Jia, L., Lin, C. H., Woo, P. C., et al. (2017). PacBio but not illumina technology can achieve fast, accurate and complete closure of the high GC, complex *Burkholderia pseudomallei* two-chromosome genome. *Front. Microbiol.* 8. doi: 10.3389/fmicb.2017.01448

Treangen, T. J., and Salzberg, S. L. (2011). Repetitive DNA and next-generation sequencing: computational challenges and solutions. *Nat. Rev. Genet.* 13 (1), 36–46. doi: 10.1038/nrg3117

Velmurugan, K., Chen, B., Miller, J. L., Azogue, S., Gurses, S., Briken, V., et al. (2007). *Mycobacterium tuberculosis nuoG* is a virulence gene that inhibits apoptosis of infected host cells. *PLos Pathog.* 3 (7), e110. doi: 10.1371/journal.ppat.0030110

Wang, K. (2020). *ANNOVAR documentation*. Available at: https://annovar.openbioinformatics.org/en/latest/

Wang, J., Haapalainen, M., Schott, T., Thompson, S. M., Smith, G. R., Pirhonen, M., et al. (2017). Genomic sequence *of 'Candidatus liberibacter* solanacearum haplotype c and its comparison with haplotype a and b genomes. *PLos One* 12 (2), e0171531. doi: 10.1371/journal.pone.0171531

Weber, I., Fritz, C., Ruttkowski, S., Kreft, A., and Bange, F. C. (2000). Anaerobic nitrate reductase (narGHJI) activity of *Mycobacterium bovis* BCG *in vitro* and its contribution to virulence in immunodeficient mice. *Mol. Microbiol.* 35 (5), 1017–1025. doi: 10.1046/j.1365-2958.2000.01794.x

Wee, W. Y., Tan, T. K., Jakubovics, N. S., and Choo, S. W. (2016). Whole-genome sequencing and comparative analysis of *Mycobacterium brisbanense* reveals a possible soil origin and capability in fertiliser synthesis. *PLos One* 11 (3), e0152682. doi: 10.1371/journal.pone.0152682

Winthrop, K. L., Marras, T. K., Adjemian, J., Zhang, H., Wang, P., and Zhang, Q. (2020). Incidence and prevalence of nontuberculous mycobacterial lung disease in the large US managed care health plan 2008–2015. *Ann. Am. Thorac. Soc* 17 (2), 178–185. doi: 10.1513/AnnalsATS.201804-236OC

Yang, J., Chen, L., Sun, L., Yu, J., and Jin, Q. (2007). VFDB 2008 release: an enhanced web-based resource for comparative pathogenomics. *Nucleic Acids Res.* 36 (suppl_1), D539–D542. doi: 10.1093/nar/gkm951

Yang, H., and Wang, K. (2015). Genomic variant annotation and prioritization with ANNOVAR and ANNOVAR. *Nat. Protoc.* 10 (10), 1556–1566. doi: 10.1038/nprot.2015.105

Yoon, S. H., Ha, S. M., Lim, J., Kwon, S., and Chun, J. (2017). A large-scale evaluation of algorithms to calculate average nucleotide identity. *Antonie Van Leeuwenhoek* 110 (10), 1281–1286. doi: 10.1007/s10482-017-0844-4

Zhang, Y. J., Reddy, M. C., Ioerger, T. R., Rothchild, A. C., Dartois, V., Rubin, E. J., et al. (2013). Tryptophan biosynthesis protects mycobacteria from CD4 T-cell-mediated killing. *Cell* 155 (6), 1296–1308. doi: 10.1016/j.cell.2013.10.045

Zhang, F., and Xie, J. P. (2011). Mammalian cell entry gene family of *Mycobacterium tuberculosis*. *Mol. Cell Biochem.* 352 (1), 1–10. doi: 10.1007/s11010-011-0733-5

Zhu, L., Zhong, J., Jia, X., Liu, G., Kang, Y., Chen, F., et al. (2016). Precision methylome characterization of *Mycobacterium tuberculosis* complex (MTBC) using PacBio single-molecule real-time (SMRT) technology. *Nucleic Acids Res.* 44 (2), 730–743. doi: 10.1093/nar/gkv1498

frontiers | Frontiers in Cellular and Infection Microbiology

TYPE Original Research
PUBLISHED 09 October 2023
DOI 10.3389/fcimb.2023.1237725

OPEN ACCESS

EDITED BY
F-X Campbell-Valois,
University of Ottawa, Canada

REVIEWED BY
David W. Ussery,
University of Arkansas for Medical Sciences, United States
Frederic Auvray,
Ecole Nationale Vétérinaire de Toulouse (ENVT), France

*CORRESPONDENCE
Rosa del Carmen Rocha-Gracia
rochagra@yahoo.com;
rosa.rocha@correo.buap.mx

RECEIVED 09 June 2023
ACCEPTED 15 September 2023
PUBLISHED 09 October 2023

CITATION
Balbuena-Alonso MG, Camps M, Cortés-Cortés G, Carreón-León EA, Lozano-Zarain P and Rocha-Gracia RdC (2023) Strain belonging to an emerging, virulent sublineage of ST131 *Escherichia coli* isolated in fresh spinach, suggesting that ST131 may be transmissible through agricultural products.
Front. Cell. Infect. Microbiol. 13:1237725.
doi: 10.3389/fcimb.2023.1237725

Strain belonging to an emerging, virulent sublineage of ST131 *Escherichia coli* isolated in fresh spinach, suggesting that ST131 may be transmissible through agricultural products

Maria G. Balbuena-Alonso[1], Manel Camps[2], Gerardo Cortés-Cortés[1,2], Eder A. Carreón-León[3], Patricia Lozano-Zarain[1] and Rosa del Carmen Rocha-Gracia[1]*

[1]Posgrado en Microbiología, Centro de Investigaciones Microbiológicas, Instituto de Ciencias, Benemérita Universidad Autónoma de Puebla, Puebla, Mexico, [2]Departament of Microbiology and Environmental Toxicology, University of California at Santa Cruz, Santa Cruz, CA, United States, [3]Facultad de Ciencias Químicas, Universidad Autónoma de Chihuahua, Chihuahua, Mexico

Food contamination with pathogenic *Escherichia coli* can cause severe disease. Here, we report the isolation of a multidrug resistant strain (A23EC) from fresh spinach. A23EC belongs to subclade C2 of ST131, a virulent clone of Extraintestinal Pathogenic *E. coli* (ExPEC). Most A23EC virulence factors are concentrated in three pathogenicity islands. These include PapGII, a fimbrial tip adhesin linked to increased virulence, and *CsgA* and *CsgB*, two adhesins known to facilitate spinach leaf colonization. A23EC also bears Tn*MB1860*, a chromosomally-integrated transposon with the demonstrated potential to facilitate the evolution of carbapenem resistance among non-carbapenemase-producing enterobacterales. This transposon consists of two IS*26*-bound modular translocatable units (TUs). The first TU carries *aac(6')-Ib-cr*, bla_{OXA-1}, *ΔcatB3*, *aac(3)-IIe*, and *tmrB*, and the second one harbors $bla_{CXT-M-15}$. A23EC also bears a self-transmissible plasmid that can mediate conjugation at 20°C and that has a mosaic IncF [F(31,36):A(4,20):B1] and Col156 origin of replication. Comparing A23EC to 86 additional complete ST131 sequences, A23EC forms a monophyletic cluster with 17 other strains that share the following four genomic traits: (1) virotype E (*papGII*+); (2) presence of a PAI II_{536}-like pathogenicity island with an additional *cnf1* gene; (3) presence of chromosomal Tn*MB1860*; and (4) frequent presence of an F(31,36):A(4,20):B1 plasmid. Sequences belonging to this cluster (which we named "C2b sublineage") are highly enriched in septicemia samples and their associated genetic markers align with recent reports of an emerging, virulent sublineage of the C2 subclade, suggesting significant pathogenic potential. This is the first report of a ST131 strain belonging to subclade C2 contaminating green leafy vegetables. The detection of this

uropathogenic clone in fresh food is alarming. This work suggests that ST131 continues to evolve, gaining selective advantages and new routes of transmission. This highlights the pressing need for rigorous epidemiological surveillance of ExPEC in vegetables with One Health perspective.

KEYWORDS

ExPEC, ST131, food safety, virulence, mobile genetic elements, conjugative transfer

1 Introduction

Food products are a key source for transmission of pathogenic bacteria, such *as Salmonella* and *Escherichia coli*. (Gizaw, 2019) *E. coli* colonizes the human gastrointestinal tract as a commensal but some pathotypes of *E. coli* can cause serious disease (Denamur et al., 2021). Pathogenic strains of *E. coli* can be grouped into intestinal (InPEC) and extraintestinal (ExPEC) pathotypes depending on whether they cause primarily gastrointestinal symptoms or whether they affect other organs, including urinary tract, bloodstream, wounds, kidney, brain, and other internal organs (Sora et al., 2021). ExPEC strains are responsible for a large fraction of urinary tract and bloodstream infections in humans (Sarowska et al., 2019) and can be classified into 4 pathotypes: uropathogenic *E. coli* (UPEC, primarily associated with urinary tract infections-UTIs), avian pathogenic *E. coli* (APEC, which causes colibacillosis in poultry but that can also infect humans), septicemia-associated *E. coli* (SEPEC) and neonatal meningitis-causing *E. coli* (NMEC) (Meena et al., 2023).

Community and hospital ExPEC infections are generally treated with 2nd and 3rd generation cephalosporins, fluoroquinolones, or with trimethoprim-sulfamethoxazole (Pitout, 2012). Resistance to cephalosporins can generally be attributed to the acquisition of genes with extended-spectrum β-lactamase (ESBL) activity; in ExPEC, the most frequent ones are $bla_{\text{CTX-M}}$ variants. Resistance to fluoroquinolones is largely due to mutations that reduce the affinity of these drugs for their targets (gyrase -*gyrAB*- and topoisomerase IV -*parCE*-), although resistance can also be provided or enhanced by a fluoroquinolone-degrading enzyme (*aac(6')-lb-cr*), by DNA-protecting enzymes (*qnr* genes), or by efflux regulation mutations (*marR*, *acrR* and *soxR*) (Huseby et al., 2017; Poirel et al., 2018). Resistance to dihydrofolate metabolism inhibitors is generally provided by dihydrofolate synthetase genes that are insensitive to sulfonamides (*sul*) or by dihydrofolate reductase mutants (*dfr*) that are insensitive to trimethoprim (Van Duijkeren et al., 2000). Topoisomerase genes represent core functions and are most frequently found in the chromosome. The other resistance genes are accessory and tend to be found in plasmids, which in turn facilitate their spread, mostly by conjugation. Over time, plasmid-borne genes tend to get incorporated into chromosomes with the assistance of mobile genetic elements (MGEs) such as insertion sequences and transposons (Wang Y. et al., 2022).

Sequence type 131 (ST131) is a globally-dominant multidrug resistance (MDR) clone and a major driver of the current ExPEC pandemic. Compared to other globally dispersed clones, ST131 stands out for its highly dynamic accessory genome (Decano et al., 2021). Like most UPEC strains, ST131 resides in the human gut as a commensal but can cause mild to severe infections of urinary tract and asymptomatic urinary bacteriuria (Biggel et al., 2020; Tchesnokova et al., 2020). The ST131's genome exhibits a broad range of known or suspected virulence factors that likely contributed to its dominance in the clinic. These include siderophores, adhesins, toxins, protectins and other elements contributing to the successful establishment and persistence of an infection. Some of these factors are specific to ST131 sublineages, notably *hly* (hemolysin), *iro* (siderophore), AAF (aggregative adherence fimbriae), and *papGII* (P fimbrial tip adhesin variant).

The complex population structure of ST131 has been elucidated (Price et al., 2013; Petty et al., 2014). Two ancestral clades have been identified, namely clade A (which carries the *fimH41* allele) and clade B (which carries the *fimH22* and *fimH35* allelic variants). Strains belonging to these two clades, which are now infrequent, are generally sensitive to fluoroquinolones and rarely carry ESBL plasmids, although they occasionally have $bla_{\text{CTX-M}}$ genes integrated in the chromosome. Clade C is an emerging epidemic lineage characterized by multidrug resistance and higher virulence (Denamur et al., 2021). This clade appears to have evolved from clade B by the acquisition of the *fimH30* allele and of several prophages and it expresses serotype O25b:H4. Within clade C, three subclades can be distinguished by divergent antimicrobial resistance profiles: C0, which is sensitive to fluoroquinolones, and C1 and C2, which have acquired fluoroquinolone resistance mutations in *gyrA* and *parC*. C1 and C2 in turn, differ in the $bla_{\text{CTX-M}}$ gene associated with them: subset C1 (with *fimH30*R1), is typically associated with $bla_{\text{CTX-M-14}}$ or with $bla_{\text{CTX-M-27}}$, whereas

Abbreviations: MDR, multidrug resistance; ExPEC, Extraintestinal pathogenic *E. coli*; PTU, Plasmid Taxonomic Unit; MLST, Multilocus Sequence Typing; STs, Sequence Types; TA, Toxin-Antitoxin systems; MGEs, Mobile Genetic Elements; ESBL, Extended-Spectrum B-lactamases; CRE, Carbapenem-resistant Enterobacteriales; ARG, Antibiotic Resistance Gene; TU, Translocatable Unit; MDR, MultiDrug Resistance; RDR, Resistance Determining Region; UPEC, UroPathogenic *Escherichia coli*; APEC, Avian Pathogenic *Escherichia coli;* PAI, Pathogenicity Island; UTI, Urinary Tract Infection; CAT, Chloramphenicol Acetyl Transferase; IS, Insertion Sequence; PFGE, Pulsed-Field Gel Electrophoresis.

subset C2 (with *fimH30*RX), is generally associated with $bla_{CTX\text{-}M\text{-}15}$. The $bla_{CTX\text{-}M\text{-}15}$ gene was initially carried by IncF plasmids but more recently the mobilization of this gene to the chromosome has been reported through transposition events frequently involving insertion sequences belonging to the IS*26* family (Dhanji et al., 2011; Stoesser et al., 2016). The C2 subclade has been found to be enriched in highly virulent and multidrug resistance isolates, with the virulence associated with the presence of the gene *papGII* (Pajand et al., 2021; Biggel et al., 2022).

ST131's main reservoir is thought to be the human intestine and the usual route of transmission to be person-to-person contact (Lopez et al., 2014; Pitout and Finn, 2020); however, an increasing (although still small) number of studies are reporting its isolation from non-human sources, such as food, food animals, pets, and environmental sources, suggesting that these may represent vectors for the transmission of this strain (Meena et al., 2023). ST131 strains recovered from food have been associated primarily with meat products, particularly pork and chicken (Meena et al., 2021); because of ST131's ability for long-time residence in the gastrointestinal tract, animal carcasses contaminated with intestinal content are considered the likely source in meat products. It also needs to be noted that, in addition to contaminating food, *E. coli* food strains can also function as reservoirs of virulence and antibiotic resistance genes, which can be frequently exchanged with clinical strains *via* horizontal gene transfer (HGT) (Balbuena-Alonso et al., 2022).

Here we report the isolation, phenotypic characterization, and genomic sequence of an *E. coli* isolate from a spinach sample that we named A23EC. We describe the presence of a large number of virulence factors, mainly located in three pathogenicity islands, that suggest a uropathogenic pathotype. Also, we show that this strain presents a multidrug resistance profile that is consistent with its antibiotic resistance gene (ARG) content, and we describe a conjugative plasmid that is capable of self-transmission even at room temperature. Finally, we compare A23EC's genomic sequence with that of other fully-assembled ST131 genomes in *GenBank* and find that A23EC belongs to a virulent, emerging sublineage of the ST131 subclade C2. We identify genetic markers unique to this sublineage and report on their alignment with earlier studies of virulent sublineages of the C2 subclade that were based on partially assembled sequences. These results highlight the pressing need for rigorous epidemiological surveillance of ExPEC in vegetables with a One Health perspective.

2 Materials and methods

2.1 Produce fresh sampling and bacterial isolation

During the period from April 2017 to November 2018, ready-to-eat raw vegetables were collected from fixed and mobile food service establishments, in Puebla, Mexico (19.03 N, -98.20 W). A total of 183 samples were obtained from 82 establishments with lettuce (21%), tomato (17%), onion with coriander (13%), cucumber (12%), onion (9%), carrot (6%), radish (6%), coriander (5%), brussels sprouts (3%), red onion (3%), celery (1%), spinach (1%), a mix of tomato, onion and coriander (1%), squash (1%), and green bell pepper (1%). All samples were stored at 4°C and processed within 24 h. For bacterial isolation, 10g of food were inoculated in 20 mL of sodium lauryl sulfate broth (BD Bioxon ®) and incubated at 37°C with shaking at 30 rpm for 24 h. Subsequently, the cultures were streaked onto MacConkey agar plates (BD Bioxon) supplemented with cefotaxime (CTX) (2ug/ml). Colonies were picked from the selective plates, subcultured and streaked to obtain pure cultures. Putative strains were identified according to biochemical tests with Vitek system (bioMérieux, France) following the schemes in MacFaddin's Manual of Biochemical Tests for the Identification of Clinically Important Bacteria (MacFaddin, 2003). Also, *E. coli*-specific *ybbW* and *uidA* genes were used to confirm their identity by PCR (Silkie et al., 2008; Walker et al., 2017).

2.2 Antimicrobial susceptibility testing and detection of resistance genes

The antibiotic susceptibility profile was obtained by agar dilution methods using criteria from Clinical and Laboratory Standards Institute (CLSI) guidelines as a reference (CLSI, 2022); as a control, the strain *E. coli* ATCC 25922 was used. Twenty-one antimicrobial agents belonging to 12 antibiotic classes were tested: amikacin (30 ug), gentamicin (10 ug), streptomycin (10 ug), tobramycin (10 ug), ampicillin (10 ug), amoxicillin/clavulanic acid (20/10 ug), cefuroxime (30 ug), cefotaxime (30 ug), ceftazidime (30 ug), cefepime (30 ug), cefoxitin (30 ug), aztreonam (30 ug), trimethoprim (5 ug), trimethoprim/sulfamethoxazole (1.25/23.75 ug), nalidixic acid (30 ug), ciprofloxacin (5 ug), chloramphenicol (30 ug), tetracycline (30 ug), meropenem (10 ug), imipenem (10 ug) and fosfomycin/G6P (200/50 ug) (BBLTM Sensi-DiscTM; Becton Dickinson and Co). Cefotaxime resistant (CTX-resistant) *E. coli* isolates were screened for ESBL production by the double-disk synergy test using disks containing cefotaxime, ceftazidime, aztreonam and cefepime, with a centrally positioned disk of amoxicillin/clavulanic acid (20/10 ug).

2.3 DNA isolation and whole-genome sequencing analysis

The ESBL-producing *E. coli* strain isolated from spinach was selected for whole-genome sequencing (WGS). This strain (A23EC) was cultured overnight at 37°C in brain heart infusion broth; total DNA extraction was performed using the Wizard® genomic DNA purification kit (Promega, United States) according to the manufacturer's instruction. Sequencing was perform using two platforms: shorts reads were generated on the Illumina Nextseq 500 plataform using 75-bp paired-end (Ilumina, United States) and long reads were generated on the Nanopore Minion plataform depth 80x (Nanopore, United, States). Quality check of the raw sequencing data was performed using Quast v0.11.5 (https://www.bioinformatics.babraham.ac.uk/projects/fastqc/) (Wingett

and Andrews, 2018). In the next step, hybrid genome assembly was generated with SPAdes v3.9.0 and Unicycler v0.5.0 assemblers (Bankevich et al., 2012; Wick et al., 2017). Finally, annotation was performed by the Rapid Annotations using Subsystems Technology (RAST) server (https://rast.nmpdr.org/rast.cgi (accessed on June 17, 2022) (Aziz et al., 2008) and using PROKKA v1.2 (Seemann, 2014). Sequence type was characterized using MLST v2.0 (https://pubmlst.org/organisms/escherichia-spp (accessed on June 25, 2022), and pMLST (http://pubmlst.org/plasmid/) (Villa et al., 2010); the serotypes (O:H) were predict with SerotypeFinder v2.0 (Joensen et al., 2015) whereas phylogroup was determined using the ClermonTyping 1.4 (Clermont et al., 2013) (http://clermontyping.iame-research.center), and finally the variant of the *fimH* gene was determined using FimTyper v1.0 (https://cge.cbs.dtu.dk/services/FimTyper) (Roer et al., 2017).

2.4 Plasmid analysis

PFGE with S1 nuclease (S1 Nuclease Thermo Scientific) digestion of whole genomic DNA was used for determinate the number and size of plasmids of strain A23EC (Ben Sallem et al., 2014). PlasmidFinder 2.1 (Carattoli et al., 2014) (https://cge.cbs.dtu.dk/services/PlasmidFinder/) (85% identity and 70% minimum length) was used to identify the replicon present for each plasmid and the replicase type. The presence of conjugation elements in plasmids was performed by using the tool OriTfinder 1.1 (Li et al., 2018) (https://bioinfo-mml.sjtu.edu.cn/oriTfinder/) with modificated parameters (Blast E-value 0.00001) and the identity of relaxase was confirmed with MOBScan (Garcillán-Barcia et al., 2020) (https://castillo.dicom.unican.es/mobscan). Also, Plasmid Taxonomic Units (PTU) were identified by COPLA (a taxonomic classifier of plasmids) using the recommended parameters (Redondo-Salvo et al., 2020) (https://castillo.dicom.unican.es/copla/). The search for type I (*pndAD, srnBC* and *hok-sok*) and type II (*ccdAB, relEB, parDE, pemKI* and *vagCD*) addiction systems was performed by BLASTn alignment with the parameters 90% coverage, 80% identity and E-value ≤ 0.000001; the system was considered to be present if the Antitoxin-Toxin (AT) sequences were adjacent. Finally, Blast Ring Image Generator (BRIG) v0.95 was used with default settings to compare our plasmid sequences to publicly available sequence (Alikhan et al., 2011) and visualized using Proksee.ca 1.0 (Stothard et al., 2018).

2.5 Detection of virulence and resistance genes

Antimicrobial resistance genes were detected using ResFinder v4.1 (https://cge.cbs.dtu.dk/services/ResFinder/)(Bortolaia et al., 2020) (with parameters 80% of coverage and 90% of identity) and the Comprehensive Antibiotic Resistance Database (CARD) v3.2.5 (https://card.mcmaster.ca/analyze) (McArthur et al., 2013) by the Resistance Gene Identifier (RGI) with the "strict" algorithm. The virulence gene profile of the isolate was established based on the detection of these genes in VirulenceFinder v2.0 (the cut-off values for genes identity was 90% and alignment coverage was 70%) (https://cge.cbs.dtu.dk/services/VirulenceFinder/) (Tetzschner et al., 2020), Virulence Factor database (VFDB) and VFanalyzer with default parameters (http://www.mgc.ac.cn/cgi-bin/VFs/v5/main.cgi, accessed on October 20, 2022) (Liu et al., 2019). The virotype was assigned according to the presence of virulence genes following the scheme described by Nicholas-Chanoine et al, and the additional ones suggested by Barrios-Villa et al. (Nicolas-Chanoine et al., 2014; Barrios-Villa et al., 2018). The Pathogenicity Islands were predicted using IslandViewer 4, which uses three independent methods for island prediction: IslandPick, IslandPath-DIMOB and SIGI-HMM (https://www.pathogenomics.sfu.ca/islandviewer) (Bertelli et al., 2017), sequence comparison of each island was performed using Blastn v2.13.and Easyfig v2.2.5 (Sullivan et al., 2011) using the sequences of the prototype strains reported by Desvaux et al., 2020. Finally, PHASTER web server was used to predict prophage regions in the genome of A23EC strain (https://phaster.ca/) (Arndt et al., 2016). Insertion sequences and transposons were identified with Mobile Element Finder v1.0.3 (https://cge.food.dtu.dk/services/MobileElementFinder/) (Johansson et al., 2021) and the identity of the insertion sequences was confirmed using ISfinder (Siguier et al., 2006); while VRprofile2 (https://tool2-mml.sjtu.edu.cn/VRprofile/) (Wang M. et al., 2022) was used to identify the genetic environment of the resistance genes. CD-HIT-EST (Li and Godzik, 2006) was used to cluster similar structures with more than 99% coverage and similarity, and a multiple genetic structural comparison was represented using Easyfig v2.2.5 (Sullivan et al., 2011).

2.6 Phylogenetic analysis

We compared the *E. coli* strain A23EC with other 86 fully assembled *E. coli* ST131 genomes deposited in *GenBank*, belonging to clades A, B and C. The metadata collected was the source of isolation, year of sampling, and country of origin (Table S1). All the *E. coli* genomes referred to as "Clinical" (66 strains) were associated with human infections recovered from urine, blood, sputum, and feces. The category "Animal" (4 strains) represented samples of dog, cat, and pig. The category "Environmental" (3 strains) includes strains isolated from wastewater bodies. Thirteen strains were not classified according to their sample type, and they were marked as "No data available". The unweighted Pair-Group Method using Arithmetic averages (UPGMA) was performed based on SNPs, using the newick graph obtained with CSI Phylogeny (https://cge.cbs.dtu.dk/services/CSIPhylogeny-1.2/, accessed on June 27, 2022) (Kaas et al., 2014) with EC598 as reference genome (accession number NZ_HG941718.1) (Forde et al., 2014). The SNP tree was visualized using iTOL software (https://itol.embl.de) (Letunic and Bork, 2021).

2.7 Conjugation assays

The two strains : donor ($A23EC^{Tet+}$) and recipient ($C600^{Rif+}$): donor ($A23EC^{Tet+}$) and recipient ($C600^{Rif+}$) were cultured

separately in 5mL Luria Bertani broth (LB) and incubated at 37°C overnight. Subsequently, 1000 µL of the recipient and 250 µL of the donor were mixed and inoculated into 20 mL of LB, incubated for 24 hours at 37°C and 20°C with shaking at 130 rpm. Finally, serial dilutions from 100 to 10-6 or 1,000,000 were performed and plated for selection of transconjugants (Cortés-Cortés et al., 2016). Transconjugants were selected using MacConkey agar (BD Bioxon) supplemented with rifampicin (100µg/mL) and tetracycline (10µg/mL). To confirm the identity of the transconjugants, PCR amplifications of the *tetA* (plasmid location) and $bla_{\text{CTX-M-15}}$ (chromosomal location) genes were performed. Only *tetA* was expected to be amplified in the transconjugants. Each experiment was performed in triplicate. The plasmid transference under the two temperatures was compared by *t-student* in Rstudio statistical software 1.4.1103. The frequency of conjugation (Fc) is described in this study as the ratio of the number of transconjugants divided by the number of recipients (Huisman et al., 2022; Mota-Bravo et al., 2023), expressed by the following equation:

$$FC = \frac{Transconjugants/(\frac{CFU}{mL})}{Recipient/(\frac{CFU}{mL})}$$

2.8 Accession numbers

GenBank accession numbers of the strain A23EC genome sequenced for this study are Chromosome CP118558.1 and plasmid pA23EC CP118559.1 Bioproject: PRJNA936840. BioSample: SAMN33377322.

3 Results

3.1 Isolation of an ExPEC strain from spinach

As part of a study involving 183 vegetable samples, in 2017-2018 we isolated a CTX-resistant strain from a spinach sample obtained in a supermarket in the city of Puebla, Mexico. The spinach sample came from a bulk-salad section that was not contained in sealed packaging. The sample was collected into an individual sterile bag, stored at 4°C and transported immediately to the laboratory for processing. Biochemical tests identified the isolate as being *E. coli* and this identity was confirmed using conventional PCR amplification of two diagnostic markers for *E. coli* (*ybbW* and *uidA*, not shown).

Next, we obtained the complete genomic sequence of this strain, which we named A23EC, using the Illumina Nextseq 500 and Nanopore Minion platforms, generating a hybrid assembly using short and long sequences, respectively. According to its sequence, A23EC belongs to phylogroup B2, sequence type ST131 and serotype O25:H4. The presence of allelic variant *fimH30Rx* identifies this strain as belonging to clade C, subclade C2, a lineage that includes highly virulent clones (Stoesser et al., 2016; Pajand et al., 2021; Biggel et al., 2022). The closest relative to A23EC in *GenBank* is the p4A strain (CP049085.2), isolated from a patient suffering from bacteremia in the United States in 2015 (Table S2) and reported in Shropshire et al., 2021. The genome features, virulome and resistome of *E. coli* A23EC strain are summarized in Table 1.

To see how A23EC relates to other ST131 strains, we performed a phylogenetic analysis of A23EC along with all other complete ST131 genomes of *E. coli* deposited in *GenBank* until June 2022. The results, shown in the form of a cladogram are presented in Figure 1. The 86 ST131 genomes included in this analysis group into the three known ST131 clades, namely A, B, and C. Within the C clade, they group into two main subclades (C1 and C2). Within the C2 subclade, we see two distinct monophyletic clusters (sublineages), that we named C2a (13 strains) and C2b (18 strains). A23EC belongs to sublineage C2b. Figure 1 also lists the source of the samples (when known). Genomes corresponding to sublineage C2b largely correspond to human clinical strains, with three environmental strains isolated from wastewater. The geographic origin of sublineage C2b samples is listed in Table S1, and includes samples from Europe, Asia, Australia and North and South America.

3.2 Pathogenicity molecular profile

Using IslandViewer 4, we identified three pathogenicity islands, mapped to the chromosome in Figure 2. The first one was PAI I A23EC (this PAI is similar to PAI II_{536}), which contained the genes *hlyABCD* (hemolysin encoding cluster), *fimC (*chaperone-like periplasmic protein*)* and *papABCDEHKX* and *papGII* (P-fimbrial tip adhesin). Unlike PAI II_{536}, PAI I_{A23EC} also carries *cnf1* (cytotoxic necrotizing factor). The second pathogenicity island is PAI II A23EC (which is similar to PAI I_{CFT073}), which harbored the *iucABCD* genes, members of a family of non-ribosomal peptide synthetase-independent siderophore (NIS), *sat* (secreted autotransporter toxin), *kpsMII-K5* (capsular protein variant K5), *iha* (iron-regulated gene homologue adhesin), and *iutA* (ferric aerobactin receptor). Finally, the third pathogenicity island is PAI III A23EC. This PAI is similar to PAI II_{CFT073} corresponding to high pathogenicity island (HPI) (Schubert et al., 2004; Llyod et al., 2009) including the siderophore yersiniabactin biosynthesis and uptake genes *irp1, irp2, fyuA* and *ybtAEPQSTX* (Perry et al., 1999).

Virulencefinder identified twenty-four additional virulence genes in the genome of A23EC. These genes can be grouped into the following five functional categories: 1) bacterial adhesion (*csgAB, yfcV* and operon *fimABCDFGHI*); 2) iron acquisition (*sitA, chuA, iucD and iutA*); 3) serum resistance (*iss*, and *traT*); 4) colonization and invasion (*ompT, yehABCD* and *malX*); and 5) toxin genes (*usp* and *senB*) (Figures 2, S1).

3.3 Phenotypic and genotypic antibiotic resistance profile

A23EC's antibiotic resistance profile and ESBL status was determined using the Kirby-Bauer method. Phenotypically,

TABLE 1 Genome features, virulome and resistome of *E. coli* A23EC strain.

Feature	Chromosome	Plasmid pA23EC
Size (bp)	5,239,797	157,470
GC (%)	50.6	50.3
No. of genes	5253	217
Inc group (pMLST)	NA	FII : FIA:FIB : Col156
Virulome		
Virulence genes	*csgAB, iss, sitA, malX, yehABCD, yfcV, chuA, fimABCDFGH, usp, ompT*	*senB, iutA, traT, iucD*
Pathogenicity island (PAI)	CFT073 (I, II), 536 (II)	
Resistome		
Aminoglycosides	*aac(3)-IIe, aac(6')-lb-cr*	
Betalactams	$bla_{\text{CTX-M-15}}$, $bla_{\text{OXA-1}}$	
Quinolones	*aac(6')-lb-cr*	
QRDR quinolones	*gyrA* (S83L, D87N), *parC* (S80I)	
Macrolides	*mdfA*	
Phenicols	Δ*catB3*	
Tetracyclines		*tetAR*
Metals	*baeRS, cpxA, pmrF*	
Biocides	*acrABDFS, evgAS, mdtBCEFGHMNOP, sitA, marA, emrABEKRY, tolC, gadWX*	
Heat stress tolerance	*KpnEF*	

NA, not applicable; QRDR, quinolone resistance-determining region.

A23EC is a MDR strain (Magiorakos et al., 2012), exhibiting resistance to at least one member of six different antibiotic families: aminoglycosides, penicillin, cephalosporins, tetracyclines, quinolones and monobactams. In addition, our A23EC strain showed a positive ESBL phenotype and intermediate resistance profile for amikacin and amoxicillin with clavulanic acid. The only antibiotics tested that this strain remained susceptible to were carbapenems, fosfomycin, chloramphenicol and trimethoprim with sulfamethoxazole (Table S3).

Using Resfinder and RGI CARD, we found the following ARGs (Table 1): two genes encoding β-lactamase ($bla_{\text{CTX-M-15}}$ and $bla_{\text{OXA-1}}$), one aminoglycoside resistance gene (*aac(3)-IIe*) and an aminoglycoside and quinolone resistance gene (*aac(6')-lb-cr*), an efflux pump (*mdfA*), a truncated chloramphenicol resistance gene (Δ*catB3*), a tunicamycin resistance determinant (*tmrB*) (Noda et al., 1992), and the gene *tetA* associated with resistance to tetracycline (alongside *tetR*, transcriptional repressor). The truncated Δ*catB3* gene harbors two in-frame deletions involving a total of 28 amino-acids (see nucleotide alignment in Figure S3). These two deletions reduce the size of this 210 amino-acid protein to 182 amino acids, and result in a loss of homology with respect to the WT beginning at amino acid position 147 (see amino acid alignment in Figure S3B), thus deleting the entire C-terminal α-helical domain.

The *gyrA* subunit of gyrase and the *parC* subunit of topoisomerase IV had three point mutations conferring fluoroquinolone resistance: S83I, D87N in gyrase and S80L in topoisomerase IV. The presence of $bla_{\text{CTX-M-15}}$ and of fluoroquinolone resistance mutations in *gyrA* and *parC* are consistent with the placement of this strain in subclade C2 of ST131.

3.4 Genomic structure of chromosomal ARGs

Looking at the distribution of ARG genes in the chromosome, we found Tn*MB1860*, a 12,837 bp- *IS26*-bounded transposon structure integrated in the chromosome, previously described by Shropshire et al, 2021. Tn*MB1860* is made up of two discrete, modular translocatable units (TUs): MB1860TU_A and MB1860TU_B (Figure 3A). MB1860TU_A carries the *aac(6')-lb-cr*, $bla_{\text{OXA-1}}$ and truncated Δ*catB3* genes flanked by two IS*26* elements in opposite orientations, followed by two additional antibiotic resistance genes (*aac(3)-lle* and *tmrB*) and is bordered on the 3' end by a ΔIS*3*, IS*Kpn11*, IS*26* and ΔTn*2* cluster. MB1860TU_B is bounded by two IS*26* elements in the sense orientation and it has a partial IS*Ecp* sequence, a $bla_{\text{CXT-M-15}}$ gene and the *wbuC* gene (also known as *orf477*) in the opposite orientation; its genetic organization is common for $bla_{\text{CTX-M-15}}$ (Dhanji et al., 2011; Ludden et al., 2020).

Chromosomal TnMB1860 was previously reported in two non-carbapenemase producing septicemia isolates by Shropshire et al., 2021 (Shropshire et al., 2021), that (like A23EC) belonged to subclade C2 of ST131. To establish the distribution of Tn*MB1860* (flanked by IS*26*) more widely, we looked for the presence of the

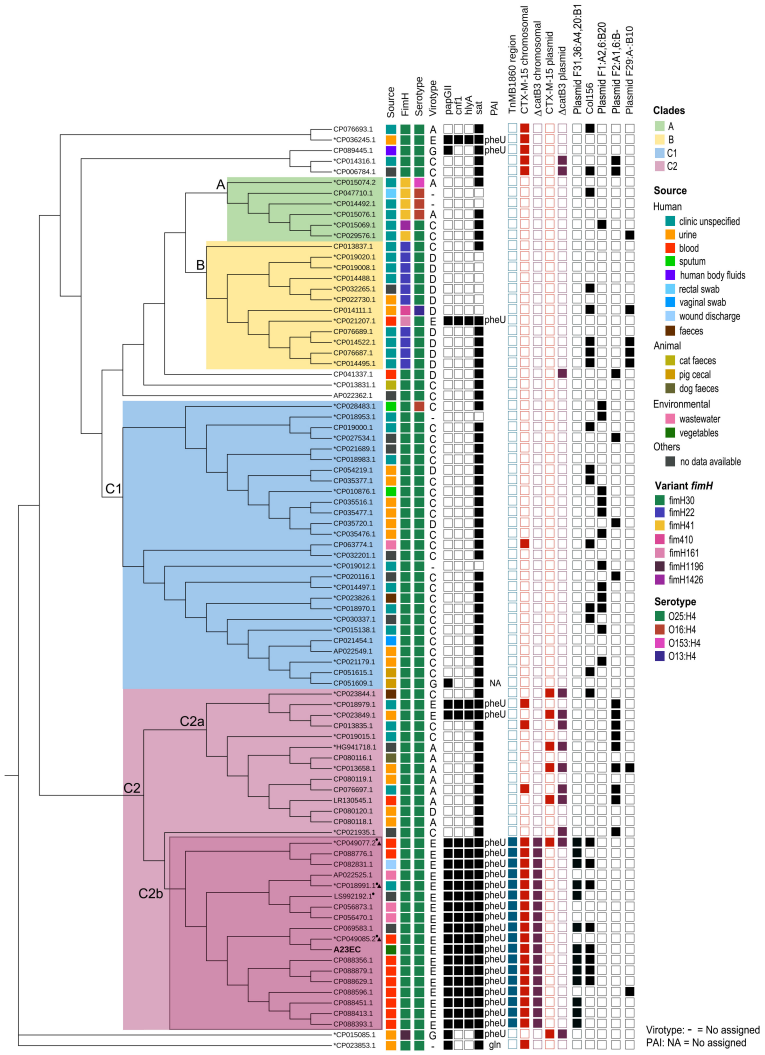

FIGURE 1
Distribution of selected genetic elements across ST131 sublineages. Cladogram showing the phylogenetic relationships between the 87 genomes included in this study. The first column indicates the source of isolation. The second column indicates the allelic variant of FimH identified. The third column indicates the serotype. The fourth column shows lists the virotype assigned. The 5th to 8th columns indicate the virulence genes that define virotype E. The 9th column indicates the tRNA insertion site of the pathogenicity island harbouring *cnf1, papGII* and *hly* genes. The 10th shows the presence of the compound transposon Tn*MB1860*. Columns 11-14 show the presence of Δ*catB3* and CTX-M-15 and whether they are found in a plasmid or in the chromosome). The 15th column indicates the presence of plasmid (F31,36:A4,20:B1). Next column shows presence of the Col156 replicon. The last three columns indicate the presence the other frequent F plasmid replicons (those with a frequency of occurrence > 5 plasmids) listed according to their pMLST classification. The asterisk next to the *GenBank* accession number indicates strains contained in the study of Biggel et al., 2022 and those with a small triangle belong to the L1 sublineage. The circle indicates strains included in the study of Shropshire et al., 2021. This graphical representation was generated using the CSI Phylogeny platform with EC598 (NZ_HG941718.1) as the reference genome.

complete sequence in 2,387complete genomes of *E. coli*. As a threshold, we selected 98% sequence identity with a coverage >70%, then further confirmed that it was a similar arrangement by detecting the presence of the six relevant resistance genes within a 20,000 bp window. Based on these criteria, we found 18 highly significant hits, all of them chromosomal except for one (Table S2). Remarkably, all the 17 chromosomal sequences belong to the C2b sublineage of subclade C2 identified by our phylogenetic analysis shown in Figure 1. This observation suggests that Tn*MB1860* was captured during the evolution of the C2 subclade C2b and passed down vertically, making it a good identifier for sublineage C2b (Figure 1). In sixteen of these sequences (including that of strain A23EC) the insertion site of Tn*MB1860* is found ~4,400 bp away from the gene encoding methionyl-tRNA synthetase, *metG*, in a molybdopterin cofactor biosynthesis operon. In only one strain (p4A; sequence CP049085.1) Tn*MB186* was located adjacent to the gene encoding colicin I receptor, disrupting it (Δ*cirA*) (Figure 3C). The consistency between insertion sites and the observed clustering of this transposon's representation in the cladogram (which points to vertical transmission) suggests that this is likely the result of a single capture event. The one exception in strain p4A presumably appears to be the result of an additional IS*26*-mediated intramolecular transposition event so it is still consistent with the hypothesis of a single capture event (Shropshire et al., 2021).

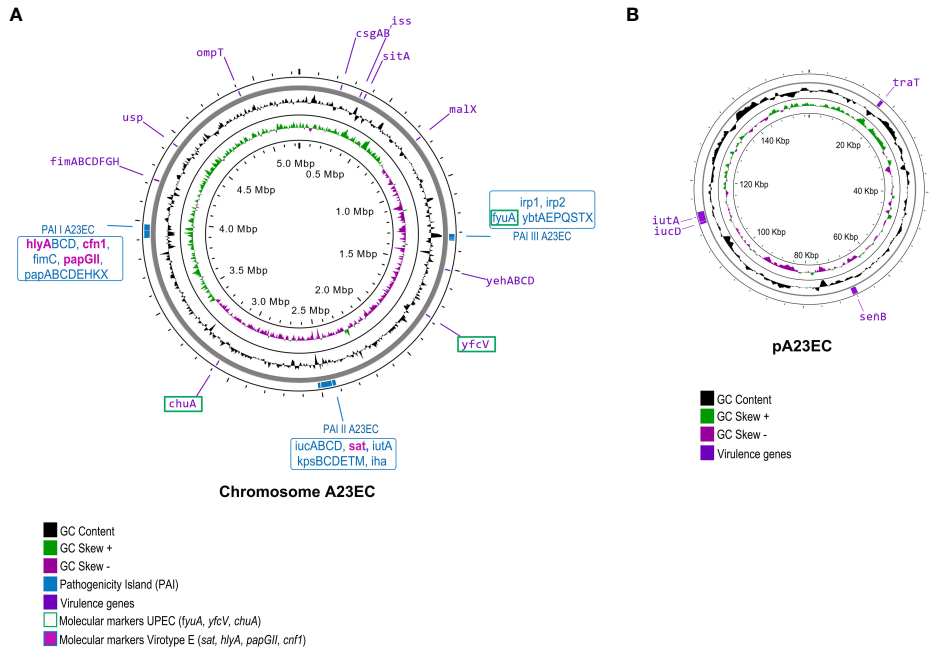

FIGURE 2
Virulome of *E. coli* A23EC. The genome is shown, with GC content, + and – skew in the inner circles. The outer circle indicates the location of individual virulence genes, labelled in their genomic positions. The labels corresponding to virulence factors serving as molecular markers of uropathogenic strains are boxed in green. **(A)** Chromosomal virulome. The three PAI I pathogenicity islands identified in A23EC are shown. PAI I A23EC (similar to PAI-II-536-pheU [PAI II_{536}]), PAI II A23EC (similar to PAI-CFT073-pheV [PAI I_{CFT073}]), and PAI III A23EC (similar to PAI-CFT073-asnT [PAI II_{CFT073}] and corresponding to pathogenicity island [HPI]) (Llyod et al., 2009). The virulence genes harbored in each PAIs are listed in blue boxes. Virotype E-defining genes, all found within these PAIs, are highlighted in bold and pink. **(B)** Plasmid (pA23EC) virulome. Genes encoding virulence factors are labeled and their position is shown in purple boxes.

We also found a single Tn*MB1860* sequence located in a plasmid. This plasmid was p11A_p2, a 180,962 bp plasmid described by Shropshire et al, 2021. Plasmid p11A_p2 includes the MB1860TU_A and MB1860TU_B TUs located downstream of the class I integron carrying *dfrA17*, *aadA5*, *qacE*Δ1 and *sul1*. The two Tn*MB1860* TUs are not contiguous, though, but separated by a large insertion sequence (18,314 bp in length) containing 9 ORFs that include several virulence factors (Figure 3B). Plasmid p11A_p2 was found in strain 11A (CP049077.2), which also contained Tn*MB1860* integrated in the chromosome (Shropshire et al., 2021).

A comparative analysis of the structure of the Tn*MB1860* region in the sequences included in the C2b sublineage resulted in five distinct clusters (clusters #1 to 5). The canonical gene arrangements for each cluster are shown in Figures 3B, C and S4. The majority of genomic sequences (n=12) belong to cluster 3; all strains in this cluster show an identical structural profile of Tn*MB1860* (delimited by IS*26*); as mentioned above, strain p4A (CP049085.2) differs from the remaining eleven, including strain A23EC, in its insertion site (Δ*cirA*), but it shows an otherwise identical structure (Figure 3C). Cluster 1 contains the single plasmid Tn*MB1860* sequence (described above). Cluster 2, with two sequences, has MB1860TU_B translocated just upstream of MB1860TU_A in an inverted orientation, as well as an inversion of the IS*26* elements flanking the composite transposon (Figure 3B). Cluster 4, with two sequences, exhibits a loss of Tn*2* (Figure 3C). Finally, cluster 5, also with two sequences, exhibits a loss of IS*26* flanking the 5' end of the MB1860TU_A region, as well as a Tn*2* element (Figure 3B).

3.5 Identification and characterization of plasmid content

Whole genome sequencing identified a single plasmid in the A23EC genome, which we named pA23EC. The presence of this plasmid was confirmed using the S1-PFGE technique (Cortés-Cortés et al., 2016). This plasmid is 157,470 bp in size, has a GC content of 50.3% and contains 172 putative coding regions (CDS) according to Prokka and RAST. Of these, only two CDSs (*tetA* and *tetR*) corresponded to ARGs, both part of a tetracycline resistance operon. These two genes were located contiguously and flanked by Tn*As1*. VirulenceFinder and VFanalyzer identified four virulence genes in pA23EC, namely *iutA, iucD* (related to iron uptake), *traT* (associated with serum resistance) and *senB* (encoding enterotoxin) (Figure 2).

In terms of plasmid regulatory elements, PlasmidFinder identified four replicons, namely Col156, IncFII, IncFIA, and IncFIB. The three IncF replicons are widely separated from each other in the plasmid sequence and their alleles correspond to the F (31,36):A(4,20):B1 subclassification proposed by Villa et al. (Villa et al., 2010). The Col156 replicon is separated from the closest IncF replicon by 30,748 bp. COPLA, which is the most accurate method available for plasmid classification according to phylogenetic relatedness (Redondo-Salvo et al., 2021), ascribed pA23EC to the FE plasmid taxonomic unit (PTU-FE). We also found an abundance of plasmid maintenance systems, these including three type II toxin-antitoxin systems (*ccdAB, vapBC* and *pemKI*) and the

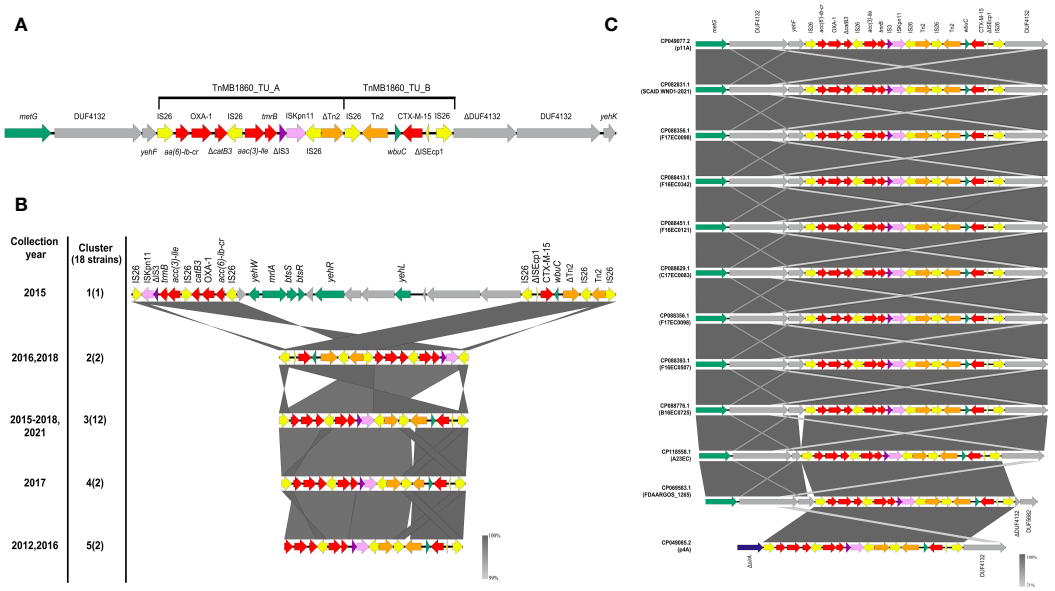

FIGURE 3
Genomic structure and genetic context of the Tn*MB1860* sequence in the C2b sublineage of the C2 subclade of ST131 genomes included in our study. The different genetic elements are shown as arrows. Resistance genes are shown in red; IS26 insertion sequences in yellow, ΔIS3 in purple, IS*Kpn11* in lilac, transposons in orange, *metG* in green, Δ*cirA* in blue and genes encoding hypothetical proteins in gray. Genes within and in the vicinity of Tn*MB1860* are labelled. **(A)** Structure of Tn*MB1860*. The genetic structure of Tn*MB1860* with its two transposable units and a total of six ARGs, as described in Shropshire et al, 2021 (Shropshire et al., 2021) **(B)** Comparative genetic arrangement of Tn*MB1860* in genomes belonging to sublineage C2b. The five clusters reflect distinct genetic distribution profiles of Tn*MB1860*. The *GenBank* accession numbers for the genomic sequences included in each group are shown in Table S2. The numbers on the left indicate the cluster corresponding to the set of sequences shown on the right, with number of sequences in each cluster shown in parentheses. All sequences were chromosomal, except for the single sequence in Cluster 1. The comparison was performed with Easyfig and the BLASTn algorithm. The percent sequence identity is shown in the form of a heatmap ranging between 99 and 100%, as shown in the legend. **(C)** Comparative genetic arrangement of the sequences in cluster 3. In eleven of the sequences, including strain A23EC, the insertion site of Tn*MB1860* was close to the gene encoding methionyl-tRNA synthetase, *metG*. A single sequence (CP049085.1) was instead inserted in the gene encoding for the truncated colicin I receptor (*cirA*), as previously described by Shropshire et al., 2021 (Shropshire et al., 2021).

parAB genes coding for a partitioning system that ensures accurate plasmid segregation (Figure 4, outer circle).

We looked for the presence of additional F(31,36):A(4,20):B1 plasmids in the 86 genomes shown in Figure 1 and found eleven other examples, all within the C2 subclade C2b sublineage that includes strain A23EC. These plasmids showed a 99% percentage of identity to pA23EC, although the coverage (*i.e.* the degree of overlap) varied between 76% and 99%. A comparison of the 12 pA23EC-like plasmids identified is shown in Figure 4. The % coverage and elements that are absent in other plasmids relative to pA23EC are shown in Table 2. We see that two areas tend to get lost as the % overlap decreases. The first area is located between 50 kb and 80 kb and includes the genes *nemR, nemA* (involved in protection against oxidative stress) (Gray et al., 2013), the virulence gene *senB* and the Col156 replicase *repA*. The second area that is prone to deletion is located between positions 110 and 120 kb and includes the iron acquisition genes *iucD, iutA*, the partitioning system *parAB* and *vapBC*, and the addiction systems *ccdAB*. Tetracycline resistance is only lost in one of the plasmids (pTO217_2).

3.6 Mobilization properties

In terms of propagation, the plasmid pA23EC was classified as self-transmissible (conjugative) based on the presence of a complete set of mobilization genes, which includes an *oriT* sequence, the type F relaxase protein (MOBF) and the type IV secretion system (TSS4) (Smillie et al., 2010). The type IV coupling protein (T4CP) showed intact domains (Garcillán-Barcia et al., 2020). We tested the conjugation ability of pA23EC at two temperatures, 20°C (the approximate temperature in the field) and 37°C (body temperature). As a recipient, we used a standard recipient strain $C600^{Rif+}$. We did detect a low frequency of conjugation and this frequency did not differ significantly depending on the temperature, with a frequency of 2.65×10^{-5} at 37°C and a frequency of 2.82×10^{-5} at 20°C (*t-student*, p>0.05).

4 Discussion

Here we describe the isolation of a strain (A23EC) from a spinach sample at point-of-sale in Mexico and present a detailed genomic characterization of this isolate. Based on its sequence, this strain belongs to the C2 subclade of ST131, which is recognized as a pandemic clone that is highly virulent, multidrug resistant, and widely distributed around the world (Petty et al., 2014).

A phylogenetic analysis of all complete genomes corresponding to ST131 *E. coli* deposited in the *Genbank* database as of June 2022, places A23EC in a monophyletic sublineage of subclade C2, which we named C2b, clustered with seventeen other strains. These 18

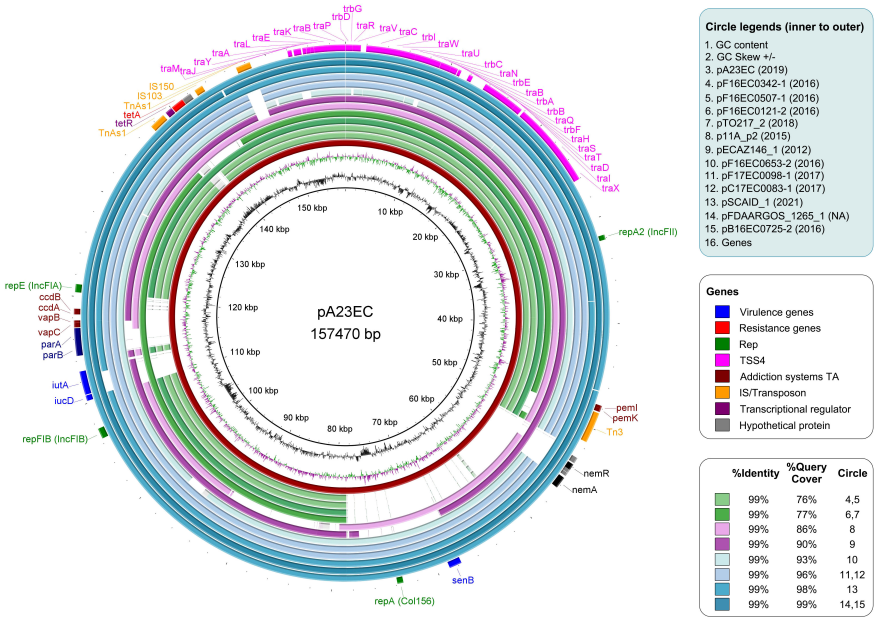

FIGURE 4
Comparative analysis of plasmid pA23EC with the other 11 F subtype FII_31/36:FIA_4/20:B1 plasmids identified within the sublineage C2b of subclade C2. From inner to outer relative to the distance map, the circles represent the following: Circle 1-2: GC content and GC Skew. Circle 3: plasmid pA23EC (highlighted in red). Circles 4-15: other plasmids belonging to subtype FII(31/36):FIA (4/20):B1 carried by the C2b sublineage of the C2 subclade of *E. coli* ST131; the names of the plasmids are listed in the legend, with their year of isolation in parenthesis. The % identity and % coverage are color-coded as indicated in the legend and shown in increasing coverage order. Circle 16: pA23EC gene content annotated with Prokka, with virulence, resistance, replication, conjugation, addiction systems, insertion sequences/transposons, transcription factors and hypothetical proteins in different colors, as indicated in the legend.

genomes showed four unique commonalities, illustrated in Figure 1: 1) They carry a Tn*MB1860* transposon structure flanked by IS*26* elements. This transposon is chromosomally integrated in all cases and its chromosomal integration site in these genomes is consistent with a single capture event. 2) They carry a PAI II536-like pathogenicity island with an additional *cnf1* gene. 3) They consistently belong to virotype E. 4) Thirteen of the eighteen isolates (including A23EC) also carry a F(31,36):A(4,20):B1 plasmid. We did not detect this pMLST type in any other ST131 sample included in our analysis, suggesting that it is specific for sublineage C2b samples.

By contrast, strains belonging to the C2a sublineage included in the analysis lack the Tn*MB1860* transposon and frequently carry $bla_{\text{CTX-M-15}}$ in plasmids, belong mostly to virotypes A or C (only two out of thirteen belong to virotype E); and consistently have F2:A-:B- plasmids when plasmids are present.

Note that all strains belonging to sublineage C2a were collected before 2014 (mean isolation date, 2009), whereas 16 of the 18 strains belonging to sublineage C2b were collected after 2014 (mean collection date, 2017), suggesting that C2b represents an emerging sublineage of the C2 subclade; this could be confirmed by further analysis with a larger number of strains.

Recent studies of ST131 clade C clinical strain collections already point to the emergence of new lineages of subclade C2 exhibiting higher virulence and antibiotic resistance. These virulent lineages are consistent with C2b, although in these studies, the identification of genomic markers was less comprehensive because most of the sequences were not completely assembled. Specifically, one study looked into the association of the gene *papGII* with the expansion of ST131 (Biggel et al., 2022). This report noted a large expansion of *papGII*+ isolates within the C2 subclade and distinguished three *papGII*+ sublineages: L1, L2 and L3. We noticed that the three fully sequenced strains from that study correspond to sublineage C2b in our analysis (marked with a triangle next to the accession number in Figure 1) and carry all the genetic markers that we defined as diagnostic for C2b. In that study, these strains were ascribed to L1 sublineage of *papGII*+ C2 strains (along with 233 additional samples). The L1 sublineage was defined by the dominant presence of F(31,36):A(4,20):B1 alleles in IncF plasmids, and by the dominant presence of $bla_{\text{CTX-M-15}}$ as ESBL-encoding gene; further, the sub-branch they were ascribed to, L1a, consisting of 184 sequences is (like C2b) characterized by the insertion of Tn*MB1860* in the vicinity of the *metG* gene and by the presence of the two virulence genes *hly*/*cnf1* in the *papGII*+ PAI. Thus, our proposed C2b sublineage appears to align perfectly with the L1a sub-branch of the Biggle et al., 2022 study (Biggel et al., 2022). They found two additional distinct *papGII*+ sublineages within the C2 subclade. Given that these additional sublineages (L2 and L3) were less frequent and more geographically restricted (Ludden et al., 2020; Biggel et al., 2022), their absence in our study can likely be attributable to our much smaller sample size.

A second study identified a monophyletic cluster of 22 C2 strains enriched for virulence and for ARG markers that was named by the authors “C2 subset” (Pajand et al., 2021). Similar to our proposed C2b sublineage, this C2 subset was characterized by the presence of *hlyABCD* virulence genes found in a PAI II_{536}-like

TABLE 2 Genetic elements that are absent relative to pA23EC; pA23EC-related plasmids are listed in decreasing order of overlap.

Plasmid	% query cover	*RepA*	*tetAR*	*nemR*	*nemA*	*senB*	*iucD*	*iutA*	*parAB*	*vapBC*	*pemIK*	*ccdAB*	Tn3	IS150
pA23EC	100	+	+	+	+	+	+	+	+	+	+	+	+	+
pB16EC0725-2	99	+	+	+	+	+	+	+	+	+	+	+	+	+
pFDAARGOS_1265_1	99	+	+	+	+	+	+	+	+	+	+	+	+	+
pSCAID_1	98	+	+	+	+	+	+	+	+	+	+	+	+	+
pF17EC0083-1	96	+	+	-	-	+	+	+	+	+	+	+	+	-
pF17EC0098-1	96	+	+	-	-	+	+	+	+	+	+	+	+	-
pF16EC0653-2	93	+	+	-	-	+	+	+	+	+	+	+	+	-
pECAZ146	90	-	+	+	+	-	+	+	-	-	+	+	+	-
p11A_p2	86	+	+	-	+	+	-	-	-	+	+	+	+	+
pTO217_2	77	-	-	-	-	-	+	+	+	+	-	+	-	+
pF16EC0121-2	77	-	+	-	-	-	-	-	-	-	+	-	+	+
pF16EC0507-1	76	-	+	-	-	-	-	-	-	-	+	-	+	+
pF16EC0342-1	76	-	+	-	-	-	-	-	-	-	+	-	+	+

genomic island containing *cnf1*, by largely belonging to virotype E (therefore being *papGII*+), and by frequently carrying plasmids with F31 or F36:A4:B1 replicons. This study also describes the presence of *aac(3)-IIa* and of a IS*15DIV*-bounded transposon with *aac(6')-lb-cr*, bla_{OXA-1}, Δ*catB3*, although they report the frequent presence of *aac(3)-IId* instead of that of *aac(3)-IIe* (an arrangement similar to that of MB1860TU_A, given that IS*15DIV* is very closely related to IS*26*), and $bla_{CTX-M-15}$ with an IS*Ecp1* upstream of and in the same orientation as $bla_{CTX-M-15}$, the reversed *wbuC* and a Tn*2* transposon (possibly MB1860TU_B). The concordance between the markers associated with this "C2 subset" and our proposed C2b sublineage, is striking.

We noted the presence of a plasmid in strain A23EC. This plasmid (named pA23EC) was classified as PTU-FE by COPLA and has four replicons, three of which belong to incompatibility group F: F(31,36):A(4,20):B1, which can be annotated as F-:A-:B1. As it happens, PTU-FE F-:A-:B1 is one of four PTU-replicon combinations previously proposed to mediate most of the flow of resistance and virulence genes between food and clinical strains, so the present work supports the idea that the plasmid flow between food and clinical strains is preferentially mediated by a specific subset of plasmids (Balbuena-Alonso et al., 2022), although the presence of A23EC in food may be incidental in this case. The fourth replicon belongs to the Col156 type, which has been previously described in isolates of the C1 subclade, carrying CTX-M-14 or -27 (Kondratyeva et al., 2020) (seen also in Figure 1). The presence of Col156 replicons, which are infrequent, in separate subclades of ST131 raises the possibility of plasmid exchanges across ST131 subclades.

Plasmid pA23EC had a complete set of mobilization genes, suggesting that this plasmid is capable of conjugation. Indeed, we detected conjugation at both 20 and 37°C. Conjugation frequencies were similar at both temperatures, which is surprising, as lower temperature slows growth down; however, it appears that the frequency of conjugation of A23EC to the $C600^{Rif+}$ recipient strain is not influenced by incubation temperature. Thus, our report is the first to show efficient conjugation for a subclade C2 strain of ST131 at a temperature under 37°C. These observations suggest that pA23EC has the potential to spread *via* conjugation, not only in human hosts but also in environmental reservoirs. Also note that pA23EC is classified as PTU-FE, which exhibits a host range of III on a six-grade scale, with a level of promiscuity to the level of family, and therefore has the potential to contribute to genetic exchange across multiple species in the Enterobacteriaceae.

A23EC is a multidrug-resistant strain, with resistance to aminoglycosides, penicillin, cephalosporins, tetracyclines, quinolones and monobactam. The prevalence of strains that are resistant to all first-line drugs is rising at an alarming rate (Manges, 2016), and multidrug-resistant ExPEC has been categorized by the WHO as a high-risk pathogen of critical priority (Tacconelli et al., 2018). Genotypically, we found nine ARGs in A23EC. Six of these mapped to Tn*MB1860* in the chromosome, in two separate TUs. The first TU (MB1860TU_A) carried *aac(6')-lb-cr*, bla_{OXA-1}, Δ*catB3*, *aac(3)-IIe* and *tmrB*, whereas the second TU (MB1860TU_B) carried $bla_{CTX-M-15}$. Two additional ARGs were found elsewhere in the chromosome >1 Mb away from TnMB1860, namely *aac(3)-IIa* and *mdfA*; *tetA/tetR* were the only ARGs found in the pA23EC plasmid.

The ARGs that we identified are likely responsible for the observed resistance to penicillins and first-generation cephalosporins (bla_{OXA-1} and $bla_{CTX-M-15}$), to synthetic cephalosporins ($bla_{CTX-M-15}$), monobactams ($bla_{CTX-M-15}$), (Zhu et al., 2022), fluoroquinolones (*aac(6')-lb-cr*, and mutations at position S83L, D87N of gyrase and position S80L of ParC (Redgrave et al., 2014; Huseby et al., 2017), to gentamicin (*aac(3)-IIe*), to tobramycin (*aac(6')-lb-cr* and *aac(3)-IIe*), to amikacin (*aac(6')-lb-cr*, intermediate resistance) (Ojdana et al., 2018; Stogios et al., 2022) and to tetracycline (*tetA*/*tetR*) (Møller et al., 2016).

The genes *mdfA* and *tmrB* could enhance resistance to a variety of drugs rather than being primarily responsible for resistance to a specific drug. *MdfA* (also known as *cmlA* or *cmr*) is a proton-dependent pump with a very wide range of substrates that include chloramphenicol, erythromycin, roxithromycin and certain aminoglycosides and fluoroquinolones (Edgar and Bibi, 1997). TmrB is an ATP-binding membrane protein that protects against tunicamycin exposure, binding tunicamycin and functioning either as an efflux pump or as a permeability barrier for this drug (Noda et al., 1992; Noda et al., 1995). Given that tunicamycin is an experimental drug not used as an antibiotic in the clinic or as growth promoter for animals, the frequent presence of the *tmrB* gene in resistance-determining regions (Grevskott et al., 2020; Pungpian et al., 2022) is intriguing and points to a possible role as modulator of resistance to other antibiotics.

Chloramphenicol acetyl transferases acetylate the antibiotic chloramphenicol at the 30-hydroxyl position using acetyl coenzyme as an acetyl donor (White et al., 1999). CatB3 is a B-type acetyltransferase, which tends to have low activity against chloramphenicol, and forms homotrimers. Trimer formation requires the C-terminal α-helical domain and is important for catalysis because the acetyl acceptor site of each protein is located in a pocket formed between monomers of the trimer. Therefore, the loss of the C-terminal α-helical domain in A23EC's Δ*catB3* is expected to destabilize the trimer (Alcala et al., 2020). Belonging to a CAT family with low activity against chloramphenicol to begin with and having a truncation that likely suppresses its catalytic activity could explain the sensitivity of A23EC to chloramphenicol despite carrying Δ*catB3*. Indeed, in a previous report, a strain with this exact truncation was reported as sensitive to chloramphenicol (Hubbard et al., 2020). However, the fact that the two deletions observed in Δ*catB3* of A23EC are in-frame, and that this allele is fully conserved in our proposed C2b sublineage and even in other STs (strain CP048934.1 is classified as ST315) suggests that *ΔcatB3* might retain some residual function that is being maintained through selection.

One of the C2b genomes (strain 11A CP049077.2) carries the Tn*MB1860* transposon integrated in the chromosome and also in plasmid p11A_2. This results in a gene dosage duplication for all the genes encoded in Tn*MB1860* that likely makes this transposon structure and all the ARGs that it contains redundant in strain 11A. The concurrent presence of a given ARG in a chromosome and in a plasmid within the same isolate is not uncommon and is interpreted as an intermediate stage in the incorporation of genetic content from a plasmid into the chromosome (Wang et al., 2022). This interpretation is also consistent with the incomplete penetrance of the F(31,36):A(4,20):B1 plasmid in sublineage C2b, which appears to have been lost independently four times (Figure 1).

The A23EC strain bears the seven virulence markers that are characteristic of ExPEC, as expected for ST131 (Figure S1) (Johnson et al., 2003; van Hoek et al., 2016); the presence of *chuA*, *fyuA*, and *yfcV* identifies A23EC as a potentially UPEC strain and its *papGII+* status suggests it may be particularly virulent. Indeed, the PapGII fimbrial tip adhesin was shown to promote inflammation in renal tissue through transcriptional reprogramming of kidney cells (Biggel et al., 2020), and *papGII+* strains have been reported to be enriched in blood isolates relative to urine/UTI infections (Ambite et al., 2019). Other virulence genes in A23EC including P fimbriae, hemolysins, siderophores, toxins and capsular synthesis, all located within PAIs, have previously been linked to the development of invasive infections (Sabaté et al., 2006; Tsoumtsa Meda et al., 2022). Outside PAIs, we identified *fimH*, which is associated with adherence on biotic and abiotic surfaces (Cookson et al., 2002), and *iss, sitA* and *ompT*, which are genes associated with serum resistance and favoring colonization and invasion mainly described in APEC strains (Olsen et al., 2012), as well as the presence of toxin gene *usp* associated with strains causing pyelonephritis, prostatitis and bacteremia (Nipič et al., 2013).

A high virulence of the C2b sublineage of the C2 subclade is also supported by the sources of isolation of C2b samples. Out of eighteen samples, ten were isolated from patients suffering from septicemia (58.8%) and none from urine. For comparison, out of thirteen C2a samples, five were isolated from urine (38.5%) and only one was isolated from the bloodstream (7.7%). Consistent with these observations, Pajand et al., 2021 report that the "C2 subset" (which as explained above aligns with our proposed C2b sublineage) accounted for the excess resistance and virulence of subclade C2 relative to C1 subclade strains (Pajand et al., 2021). However, the observed difference in sample origin between the C2a and C2b sublineages of the C2 subclade could also be attributed to unknown variables affecting the sampling and is based in both cases on a small number of samples.

Based on epidemiological surveillance studies that have been carried out in different parts of the world in the "One Health" context, non-animal agricultural products have been proposed to be important vectors for the circulation of multidrug-resistant ExPEC strains between humans, animals and the environments (Meena et al., 2023). Our report of an isolate belonging to the C2 subclade of ST131 contaminating green leafy vegetables adds support to this hypothesis. We searched for additional relevant reports in the literature. Table S4 lists examples of *E. coli* strains isolated from vegetables, along with their phylotypes (when known) and their corresponding reference. A few sequence types stand out, namely ST10, ST38, ST23, ST69 and ST155, which to our knowledge have been independently reported 8, 4, 3, 3, and 3 times, respectively out of a total of 36 annotated examples. Note that while most of the isolates reported likely represent commensals (based on their phylotype), about ⅓ of them (including ST69) belong to likely ExPEC phylotypes (B2, and D), supporting the idea that agricultural products can indeed serve as vectors for the transmission of ExPEC strains.

Humans represent the main reservoirs of *E. coli* ST131 by colonizing the intestine (Morales Barroso et al., 2018; Sarkar et al., 2018; Johnson et al., 2022). When isolated in foods, the source of ST131 *E. coli* are typically animal products such as meat and dairy products (Platell et al., 2011; Liu et al., 2018) and the C2 (O25:H4/H30) subclade of *E. coli* is much less frequent in foods other ST131 lineages such as H22 (Manges, 2016; Massella et al., 2020). The isolation of a $bla_{CXT\text{-}M\text{-}15}$-bearing ST131 strain from an agricultural product has only been previously reported once, from a

bitter cucumber imported from the Dominican Republic (Müller et al., 2016), and we ignore further details about its molecular classification. Thus, to our knowledge, this is the first report of an ST131 clone belonging to the C2 subclade (O25:H4/H30) contaminating green leafy vegetable. The isolation of an emerging, potentially uropathogenic strain of ST131 from spinach is relevant to public health because the consumption of fresh produce has increased as a result of a healthier lifestyle (Castro-Rosas et al., 2012).

Three other strains of the C2b sublineage described here were isolated from wastewater (Figure 1). Further, ST131 clade C strains have been observed to survive wastewater treatment and release to surface water (Tausova et al., 2012; Zurfluh et al., 2013; Müller et al., 2016). Thus, A23EC could have reached spinach *via* contaminated water. Admittedly, the present study cannot determine the point at which A23EC contaminated the spinach, and it is therefore possible that contamination happened after the spinach was harvested (during processing, transport or at the supermarket itself) but we can say that this strain is able to persist in spinach long enough for transmission. Whether the ability of A23EC and possibly other C2b strains to persist in fresh vegetables represents a new adaptation or it was simply previously missed is unclear. The presence of virulence factors facilitating adherence to human and animal cells (*papABCD*, *papGII*, *iha*, *yfcV*, *kpsm-TII-k5*, *fimABCDEFGHI* and *csgABCDEFG*) (Sarowska et al., 2019) may be relevant. This is particularly true of adhesins CsgA and CsgB, which have been described to be significantly involved in adhesion and colonization in spinach leaves (Saldaña et al., 2011; MacArisin et al., 2012), and allow their proliferation on the food surface through the formation of biofilms (Zhao et al., 2022). In addition, previous studies have demonstrated the ability of *E. coli* strains to reside within the internal cavity of stomata and internal tissues; this internalization protects the bacteria from disinfecting and bactericidal products, thereby increasing their survival. Internalization also contributes to inefficient washing and sanitizing treatments in vegetables (Gullian-Klanian and Sánchez-Solis, 2018; Querido et al., 2020). However, these previous studies have focused on STEC and EHEC strains and may have missed the presence of ExPEC in these foods.

Some reports interpret the occurrence of ST131 strain in different hosts such as companion and food animals or in different environmental niches such as sewage and other aquatic environments as overflow from its main niche (Melo et al., 2019; Finn et al., 2020); in contrast, other studies report specialization in ST131 strains depending on their origin, suggesting that they are adapting to different niches. This raises complex questions about the role of reservoirs in ST131 evolution and spread (Bonnet et al., 2021; Denamur et al., 2021). The isolation of ST131 strains in foods such as A23EC paves the ground for understanding the epidemiology and evolutionary dynamics of ST131 through rigorous and systematic monitoring using selected molecular markers.

In conclusion, our results add to previous knowledge about the global dissemination of ST131 by confirming the emergence of a distinct sublineage of subclade C2 (C2b), that has the potential to be highly pathogenic and that bears a transposon structure that has the potential to facilitate the evolution of carbapenem resistance among non-carbapenemase-producing enterobacterales (Shropshire et al., 2021). The genetic content of virulence and resistance genes and associated mobilization elements described here for the A23EC strain, together with the plasticity of *E. coli* ST131 genome, suggests that this ExPEC strain has the potential to evolve persistence in new environments and to infect humans and/or animals through new routes of transmission. These observations call for a more comprehensive surveillance and monitoring system for ExPEC strains in non-clinical settings.

Data availability statement

The datasets presented in this study can be found in online repositories. The names of the repository/repositories and accession number(s) can be found in the article/Supplementary material.

Author contributions

MB-A organized the database and performed the formal analysis. MB-A, GC-C, EC-L, and MC participated in the research. MC, PL-Z, and RR-G supervised the experimental and bioinformatics analysis. MC performed extensive review of the original draft. RR-G performed resources and project administration and funding acquisition. All authors contributed to the article and approved the submitted version.

Funding

This work was supported by the Consejo Nacional de Ciencia y Tecnología (CONACyT) [CB-2017-2018/A1-S-22136]. The CONACyT also provided a fellowship [589143 to MB-A]. We are also grateful for the UC MEXUS-CONACYT Postdoctoral Fellowship 2017-2019 and the CONACYT National Postdoctoral Fellowship across "Convocatoria de Estancias Posdoctorales por México 2020" during the development of the research to GC-C [335026].

Acknowledgments

The authors thank Margarita Maria de la Paz Hernández Arenas, Candelerario Vázquez Cruz and Miguel Castañeda Lucio from "Centro de Investigaciones en Ciencias Microbiológicas, Instituto de Ciencias" of Benemérita Universidad Autónoma de Puebla, for their invaluable contribution, guidance and support to the development of this work.

Conflict of interest

The authors declare that the research was conducted in the absence of any commercial or financial relationships that could be construed as a potential conflict of interest.

Publisher's note

All claims expressed in this article are solely those of the authors and do not necessarily represent those of their affiliated organizations, or those of the publisher, the editors and the reviewers. Any product that may be evaluated in this article, or claim that may be made by its manufacturer, is not guaranteed or endorsed by the publisher.

Supplementary material

The Supplementary Material for this article can be found online at: https://www.frontiersin.org/articles/10.3389/fcimb.2023.1237725/full#supplementary-material

References

Alcala, A., Ramirez, G., Luna, O., Nguyen, K., Vazquez, D., Tan, K., et al. (2020). Structural and functional characterization of three Type B and C chloramphenicol acetyltransferases from Vibrio species. *Protein Sci.* 29 (3), 695–710. doi: 10.1002/pro.3793

Alikhan, N. F., Petty, N. K., Ben Zakour, N. L., and Beatson, S. A. (2011). BLAST Ring Image Generator (BRIG): Simple prokaryote genome comparisons. *BMC Genomics* 12 (1), 402. doi: 10.1186/1471-2164-12-402

Ambite, I., Butler, D. S. C., Stork, C., Grönberg-Hernández, J., Köves, B., Zdziarski, J., et al. (2019). Fimbriae reprogram host gene expression – Divergent effects of P and type 1 fimbriae. *PloS Pathog.* 15 (6), 1–30. doi: 10.1371/journal.ppat.1007671

Arndt, D., Grant, J. R., Marcu, A., Sajed, T., Pon, A., Liang, Y., et al. (2016). PHASTER: a better, faster version of the PHAST phage search tool. *Nucleic Acids Res.* 44 (W1), W16–W21. doi: 10.1093/nar/gkw387

Aziz, R. K., Bartels, D., Best, A., DeJongh, M., Disz, T., Edwards, R. A., et al. (2008). The RAST Server: Rapid annotations using subsystems technology. *BMC Genomics* 9, 1–15. doi: 10.1186/1471-2164-9-75

Balbuena-Alonso, M. G., Cortés-Cortés, G., Kim, J. W., Lozano-Zarain, P., Camps, M., and del Carmen Rocha-Gracia, R. (2022). Genomic analysis of plasmid content in food isolates of E. coli strongly supports its role as a reservoir for the horizontal transfer of virulence and antibiotic resistance genes. *Plasmid* 123–124. doi: 10.1016/j.plasmid.2022.102650

Bankevich, A., Nurk, S., Antipov, D., Gurevich, A. A., Dvorkin, M., Kulikov, A. S., et al. (2012). SPAdes: A new genome assembly algorithm and its applications to single-cell sequencing. *J. Comput. Biol.* 19 (5), 455–477. doi: 10.1089/cmb.2012.0021

Barrios-Villa, E., Cortés-Cortés, G., Lozano-Zaraín, P., Arenas-Hernández, M. M. D. L. P., Martínez de la Peña, C. F., Martínez-Laguna, Y., et al. (2018). Adherent/invasive Escherichia coli (AIEC) isolates from asymptomatic people: New E. coli ST131 O25: H4/H30-Rx virotypes. *Ann. Clin. Microbiol. Antimicrobials* 17 (1), 1–11. doi: 10.1186/s12941-018-0295-4

Ben Sallem, R., Ben Slama, K., Rojo-Bezares, B., Porres-Osante, N., Jouini, A., Klibi, N., et al. (2014). IncI1 plasmids carrying blaCTX-M-1or blaCMY-2genes in Escherichia coli from healthy humans and animals in Tunisia. *Microbial Drug Resist* 20 (5), 495–500. doi: 10.1089/mdr.2013.0224

Bertelli, C., Laird, M. R., Williams, K. P., Lau, B. Y., Hoad, G., Winsor, G. L., et al. (2017). IslandViewer 4: Expanded prediction of genomic islands for larger-scale datasets. *Nucleic Acids Res.* 45 (W1), W30–W35. doi: 10.1093/nar/gkx343

Biggel, M., Moons, P., Nguyen, M. N., Goossens, H., and Van Puyvelde, S. (2022). Convergence of virulence and antimicrobial resistance in increasingly prevalent Escherichia coli ST131 papGII+ sublineages. *Commun. Biol.* 5 (1), 1–10. doi: 10.1038/s42003-022-03660-x

Biggel, M., Xavier, B. B., Johnson, J. R., Nielsen, K. L., Frimodt-Møller, N., Matheeussen, V., et al. (2020). Horizontally acquired papGII-containing pathogenicity islands underlie the emergence of invasive uropathogenic Escherichia coli lineages. *Nat. Commun.* 11 (1), 1–15. doi: 10.1038/s41467-020-19714-9

Bonnet, R., Beyrouthy, R., Haenni, M., Nicolas-Chanoine, M. H., Dalmasso, G., and Madec, J. Y. (2021). Host colonization as a major evolutionary force favoring the diversity and the emergence of the worldwide multidrug-resistant escherichia coli st131. *MBio* 12 (4), 1–12. doi: 10.1128/mBio.01451-21

Bortolaia, V., Kaas, R. S., Ruppe, E., Roberts, M. C., Schwarz, S., Cattoir, V., et al. (2020). ResFinder 4.0 for predictions of phenotypes from genotypes. *J. Antimicrobial. Chemother* 75 (12), 3491–3500. doi: 10.1093/jac/dkaa345

Carattoli, A., Zankari, E., Garciá-Fernández, A., Larsen, M. V., Lund, O., Villa, L., et al. (2014). In Silico detection and typing of plasmids using plasmidfinder and plasmid multilocus sequence typing. *Antimicrobial. Agents Chemother* 58 (7), 3895–3903. doi: 10.1128/AAC.02412-14

Castro-Rosas, J., Cerna-Cortés, J. F., Méndez-Reyes, E., Lopez-Hernandez, D., Gómez-Aldapa, C. A., and Estrada-Garcia, T. (2012). Presence of faecal coliforms, Escherichia coli and diarrheagenic E. coli pathotypes in ready-to-eat salads, from an area where crops are irrigated with untreated sewage water. *Int. J. Food Microbiol.* 156 (2), 176–180. doi: 10.1016/j.ijfoodmicro.2012.03.025

Clermont, O., Christenson, J. K., Denamur, E., and Gordon, D. M. (2013). The Clermont Escherichia coli phylo-typing method revisited: Improvement of specificity and detection of new phylo-groups. *Environ. Microbiol. Rep.* 5 (1), 58–65. doi: 10.1111/1758-2229.12019

CLSI (2022). *Performance standards for antimicrobial susceptibility testing 32nd edition: M100s.* (Pennaylvania, USA)

Cookson, A. L., Cooley, W. A., and Woodward, M. J. (2002). The role of type 1 and curli fimbriae of Shiga toxin-producing Escherichia coli in adherence to abiotic surfaces. *Int. J. Med. Microbiol.* 292 (3–4), 195–205. doi: 10.1078/1438-4221-00203

Cortés-Cortés, G., Lozano-Zarain, P., Torres, C., Castañeda, M., Sánchez, G. M., Alonso, C. A., et al. (2016). Detection and molecular characterization of escherichia coli strains producers of extended-spectrum and CMY-2 type beta-lactamases, isolated from turtles in Mexico. *Vector-Borne. Zoonot. Dis.* 16 (9), 595–603. doi: 10.1089/vbz.2014.1725

Decano, A. G., Tran, N., Foori, H.–., Awadi, B.–., Campbell, L., Ellison, K., et al. (2021). Plasmids shape the diverse accessory resistomes of Escherichia coli ST131. *Access Microbiology* 3 (1), acmi000179. doi: 10.1099/acmi.0.000179

Denamur, E., Clermont, O., Bonacorsi, S., and Gordon, D. (2021). The population genetics of pathogenic Escherichia coli. *Nat. Rev. Microbiol.* 19 (1), 37–54. doi: 10.1038/s41579-020-0416-x

Desvaux, M., Dalmasso, G., Beyrouthy, R., Barnich, N., Delmas, J., and Bonnet, R. (2020). Pathogenicity factors of genomic islands in intestinal and extraintestinal Escherichia coli. *Front. Microbiol.* 11. doi: 10.3389/fmicb.2020.02065

Dhanji, H., Patel, R., Wall, R., Doumith, M., Patel, B., Hope, R., et al. (2011). Variation in the genetic environments of bla CTX-M-15 in Escherichia coli from the faeces of travellers returning to the United Kingdom. *The Journal of Antimicrobial Chemotherapy* 66(5), 1005–1012. doi: 10.1093/jac/dkr041

Edgar, R., and Bibi, E. (1997). MdfA, an escherichia coli multidrug resistance protein with an extraordinarily broad spectrum of drug recognition. *J Bacteriol* 179 (7), 2274–2280. doi: 10.1128/jb.179.7.2274-2280.1997

Finn, T. J., Scriver, L., Lam, L., Duong, M., Peirano, G., Lynch, T., et al. (2020). A comprehensive account of escherichia coli sequence type 131 in wastewater reveals an abundance of fluoroquinolone-resistant clade a strains. *Appl. Environ. Microbiol.* 86 (4), 1–11. doi: 10.1128/AEM.01913-19

Forde, B. M., Ben Zakour, N. L., Stanton-Cook, M., Phan, M. D., Totsika, M., Peters, K. M., et al. (2014). The complete genome sequence of escherichia coli EC958: A high quality reference sequence for the globally disseminated multidrug resistant E. coli O25b:H4-ST131 clone. *PloS One* 9 (8), 1–13. doi: 10.1371/journal.pone.0104400

Garcillán-Barcia, M. P., Redondo-Salvo, S., Vielva, L., and de la Cruz, F. (2020). MOBscan: Automated Annotation of MOB Relaxases. *Methods in molecular biology* (Clifton, N. J.), 295–308. doi: 10.1007/978-1-4939-9877-7_21

Gizaw, Z. (2019). Public health risks related to food safety issues in the food market: A systematic literature review. *Environ. Health Prev. Med.* 24 (1), 1–21. doi: 10.1186/s12199-019-0825-5

Gray, M. J., Wholey, W. Y., Parker, B. W., Kim, M., and Jakob, U. (2013). NemR is a bleach-sensing transcription factor. *J. Biol. Chem.* 288 (19), 13789–13798. doi: 10.1074/jbc.M113.454421

Grevskott, D. H., Salvà-serra, F., Moore, E. R. B., and Marathe, N. P. (2020). Nanopore sequencing reveals genomic map of CTX-M-type extended-spectrum β -lactamases carried by Escherichia coli strains isolated from blue mussels (Mytilus edulis) in Norway. *BMC Microbiology* 20(1), 134. doi: 10.1186/s12866-020-01821-8

Gullian-Klanian, M., and Sánchez-Solis, M. J. (2018). Growth kinetics of Escherichia coli O157:H7 on the epicarp of fresh vegetables and fruits. *Braz. J. Microbiol.* 49 (1), 104–111. doi: 10.1016/j.bjm.2017.08.001

Hubbard, A. T. M., Mason, J., Roberts, P., Parry, C. M., Corless, C., Aartsen, J., et al. (2020). Piperacillin/tazobactam resistance in a clinical isolate of Escherichia coli due to IS 26 -mediated ampli fi cation of bla. *Nat. Commun.* 11 (1), 1–9. doi: 10.1038/s41467-020-18668-2

Huisman, J. S., Benz, F., Duxbury, S. J. N., de Visser, J. A. G. M., Hall, A. R., Fischer, E. A. J., et al. (2022). Estimating plasmid conjugation rates: A new computational tool and a critical comparison of methods. *Plasmid* 121, 102627. doi: 10.1016/j.plasmid.2022.102627

Huseby, D. L., Pietsch, F., Brandis, G., and Tegehall, A. (2017). Mutation supply and relative fitness shape the genotypes of ciprofloxacin-resistant escherichia coli. *Mol Biol Evol* 34 (5), 1029–1039. doi: 10.1093/molbev/msx052

Joensen, K. G., Tetzschner, A. M. M., Iguchi, A., Aarestrup, F. M., and Scheutz, F. (2015). Rapid and easy in silico serotyping of Escherichia coli isolates by use of whole-genome sequencing data. *J. Clin. Microbiol.* 53 (8), 2410–2426. doi: 10.1128/JCM.00008-15

Johansson, M. H. K., Bortolaia, V., Tansirichaiya, S., Aarestrup, F. M., Roberts, A. P., and Petersen, T. N. (2021). Detection of mobile genetic elements associated with antibiotic resistance in Salmonella enterica using a newly developed web tool: MobileElementFinder. *J. Antimicrobial. Chemother* 76, 101–109. doi: 10.1093/jac/dkaa390

Johnson, J. R., Clabots, C., Porter, S. B., Bender, T., Johnston, B. D., and Thuras, P. (2022). Intestinal persistence of colonizing escherichia coli strains, especially ST131-H30, in relation to bacterial and host factors. *J. Infect. Dis.* 225 (12), 2197–2207. doi: 10.1093/infdis/jiab638

Johnson, J. R., Murray, A. C., Gajewski, A., Sullivan, M., Snippes, P., Kuskowski, M. A., et al. (2003). Isolation and molecular characterization of nalidixic acid-resistant extraintestinal pathogenic Escherichia coli from retail chicken products. *Antimicrobial. Agents Chemother* 47 (7), 2161–2168. doi: 10.1128/AAC.47.7.2161-2168.2003

Kaas, R. S., Leekitcharoenphon, P., Aarestrup, F. M., and Lund, O. (2014). Solving the problem of comparing whole bacterial genomes across different sequencing platforms. *PloS One* 9 (8), 1–8. doi: 10.1371/journal.pone.0104984

Kondratyeva, K., Salmon-Divon, M., and Navon-Venezia, S. (2020). Meta-analysis of pandemic escherichia coli ST131 plasmidome proves restricted plasmid-clade associations. *Sci. Rep.* 10 (1), 1–11. doi: 10.1038/s41598-019-56763-7

Letunic, I., and Bork, P. (2021). Interactive tree of life (iTOL) v5: An online tool for phylogenetic tree display and annotation. *Nucleic Acids Res.* 49 (W1), W293–W296. doi: 10.1093/nar/gkab301

Li, W., and Godzik, A. (2006). Cd-hit: A fast program for clustering and comparing large sets of protein or nucleotide sequences. *Bioinformatics* 22 (13), 1658–1659. doi: 10.1093/bioinformatics/btl158

Li, X., Xie, Y., Liu, M., Tai, C., Sun, J., Deng, Z., et al. (2018). OriTfinder: A web-based tool for the identification of origin of transfers in DNA sequences of bacterial mobile genetic elements. *Nucleic Acids Res.* 46 (W1), W229–W234. doi: 10.1093/nar/gky352

Liu, C. M., Stegger, M., Aziz, M., Johnson, T. J., Waits, K., Nordstrom, L., et al. (2018). Escherichia coli ST131-H22 as a foodborne uropathogen. *MBio* 9 (4), 1–11. doi: 10.1128/MBIO.00470-18

Liu, B., Zheng, D., Jin, Q., Chen, L., and Yang, J. (2019). VFDB 2019: A comparative pathogenomic platform with an interactive web interface. *Nucleic Acids Res.* 47 (D1), D687–D692. doi: 10.1093/nar/gky1080

Lloyd, A. L., Henderson, T. A., Vigil, P. D., and Mobley, H. L. (2009). Genomic islands of uropathogenic Escherichia coli contribute to virulence. *Journal of Bacteriology* 191 (11), 3469–3481. doi: 10.1128/JB.01717-08

Lopez, L., Vin, L., Cisneros, M., Go, S. L., Sa, H., and Morales, I. (2014). Escherichia coli belonging to the worldwide emerging epidemic clonal group O25b/ST131 : risk factors and clinical implications. *The Journal of Antimicrobial Chemotherapy* 69(3), 809–814. doi: 10.1093/jac/dkt405

Ludden, C., Decano, A. G., Jamrozy, D., Pickard, D., Morris, D., Parkhill, J., et al. (2020). Genomic surveillance of Escherichia coli ST131 identifies local expansion and serial replacement of subclones. *Microbial Genomics* 6(4), e000352. doi: 10.1099/mgen.0.000352

MacArisin, D., Patel, J., Bauchan, G., Giron, J. A., and Sharma, V. K. (2012). Role of curli and cellulose expression in adherence of escherichia coli O157:H7 to spinach leaves. *Foodborne Pathog. Dis.* 9 (2), 160–167. doi: 10.1089/fpd.2011.1020

MacFaddin, J. F. (2003). *MacFaddin's manual of biochemical tests for the identification of clinically important bacteria* (Buenos Aires, Argentina: Williams and Wilkins Co).

Magiorakos, A. P., Srinivasan, A., Carey, R. B., Carmeli, Y., Falagas, M. E., Giske, C. G., et al. (2012). Multidrug-resistant, extensively drug-resistant and pandrug-resistant bacteria: An international expert proposal for interim standard definitions for acquired resistance. *Clin. Microbiol. Infection* 18 (3), 268–281. doi: 10.1111/j.1469-0691.2011.03570.x

Manges, A. R. (2016). Escherichia coli and urinary tract infections: The role of poultry-meat. *Clin. Microbiol. Infection* 22 (2), 122–129. doi: 10.1016/j.cmi.2015.11.010

Massella, E., Reid, C. J., Cummins, M. L., Anantanawat, K., Zingali, T., Serraino, A., et al. (2020). Snapshot study of whole genome sequences of *Escherichia coli* from healthy companion animals, livestock, wildlife, humans and food in Italy. *Antibiotics* 9 (11), 1–22. doi: 10.3390/antibiotics9110782

McArthur, A. G., Waglechner, N., Nizam, F., Yan, A., Azad, M. A., Baylay, A. J., et al. (2013). The comprehensive antibiotic resistance database. *Antimicrobial. Agents Chemother* 57 (7), 3348–3357. doi: 10.1128/AAC.00419-13

Meena, P. R., Priyanka, P., and Singh, A. P. (2023). Extraintestinal pathogenic Escherichia coli (ExPEC) reservoirs, and antibiotics resistance trends: a one-health surveillance for risk analysis from "farm-to-fork" *Lett. Appl. Microbiol.* 76 (1), 1–12. doi: 10.1093/lambio/ovac016

Meena, P. R., Yadav, P., Hemlata, H., Tejavath, K. K., and Singh, A. P. (2021). Poultry-origin extraintestinal Escherichia coli strains carrying the traits associated with urinary tract infection, sepsis, meningitis and avian colibacillosis in India. *J. Appl. Microbiol.* 130 (6), 2087–2101. doi: 10.1111/JAM.14905

Melo, L. C., Haenni, M., Saras, E., Duprilot, M., Nicolas-Chanoine, M. H., and Madec, J. Y. (2019). Emergence of the C1-M27 cluster in ST131 Escherichia coli from companion animals in France. *J. Antimicrobial. Chemother* 74 (10), 3111–3113. doi: 10.1093/jac/dkz304

Møller, T. S. B., Overgaard, M., Nielsen, S. S., Bortolaia, V., Sommer, M. O. A., Guardabassi, L., et al. (2016). Relation between tetR and tetA expression in tetracycline resistant Escherichia coli. *BMC Microbiol.*, 1–8. doi: 10.1186/s12866-016-0649-z

Morales Barroso, I., López-Cerero, L., Navarro, M. D., Gutiérrez-Gutiérrez, B., Pascual, A., and Rodríguez-Baño, J. (2018). Intestinal colonization due to Escherichia coli ST131: Risk factors and prevalence. *Antimicrobial. Resist Infection Control* 7 (1), 1–6. doi: 10.1186/s13756-018-0427-9

Mota-Bravo, L., Camps, M., Muñoz-Gutiérrez, I., Tatarenkov, A., Warner, C., Suarez, I., et al. (2023). Detection of horizontal gene transfer mediated by natural conjugative plasmids in E. coli. *J. Visual. Exp.* 193, 1–23. doi: 10.3791/64523

Müller, A., Stephan, R., and Nüesch-Inderbinen, M. (2016). Distribution of virulence factors in ESBL-producing Escherichia coli isolated from the environment, livestock, food and humans. *Sci. Tot. Environ.* 541, 667–672. doi: 10.1016/j.scitotenv.2015.09.135

Nicolas-Chanoine, M.-H., Bertrand, X., and Madec, J.-Y. (2014). Escherichia coli ST131, an intriguing clonal group. *Clin. Microbiol. Rev.* 27 (3), 543. doi: 10.1128/CMR.00125-13

Nipič, D., Podlesek, Z., Budič, M., Črnigoj, M., and Žgur-Bertok, D. (2013). Escherichia coli uropathogenic-specific protein, USP, is a bacteriocin-like genotoxin. *J. Infect. Dis.* 208 (10), 1545–1552. doi: 10.1093/infdis/jit480

Noda, Y., Takatsuki, A., Yoda, K., and Yamasaki, M. (1995). TmrB protein, which confers resistance to tunicamycin on bacillus subtilis, binds tunicamycin. *Biosci. Biotechnol. Biochem.* 8451 (59(2), 321–322. doi: 10.1271/bbb.59.321

Noda, Y., Yoda, K., and Yamasaki, M. (1992). TmrB protein, responsible for tunicamycin resistance of Bacillus subtilis, is a novel ATP-binding membrane protein. *J Bacteriol* 174 (13), 4302–4307. doi: 10.1128/jb.174.13.4302-4307.1992

Ojdana, D., Sienko, A., Sacha, P., Majewski, P., Wieczrek, P., Wieczorek, A., et al. (2018). Genetic basis of enzymatic resistance of E. coli to aminoglycosides. *Adv Med Sci* 63 (1), 9–13. doi: 10.1016/j.advms.2017.05.004

Olsen, R. H., Christensen, H., and Bisgaard, M. (2012). Comparative genomics of multiple plasmids from APEC associated with clonal outbreaks demonstrates major similarities and identifies several potential vaccine-targets. *Veterinary Microbiol.* 158 (3–4), 384–393. doi: 10.1016/j.vetmic.2012.03.008

Pajand, O., Rahimi, H., Darabi, N., Roudi, S., Ghassemi, K., Aarestrup, F. M., et al. (2021). Arrangements of Mobile Genetic Elements among Virotype E Subpopulation of Escherichia coli Sequence Type 131 Strains with High Antimicrobial Resistance and Virulence Gene Content. *mSphere* 6 (4), e0055021. doi: 10.1128/mSphere.00550-21

Perry, R. D., Balbo, P. B., Jones, H. A., Fetherston, J. D., and Demoll, E. (1999). Yersiniabactin from Yersinia pestis: Biochemical characterization of the siderophore and its role in iron transport and regulation. *Microbiology* 145 (5), 1181–1190. doi: 10.1099/13500872-145-5-1181

Petty, N. K., Zakour, N. L. B., Stanton-Cook, M., Skippington, E., Totsika, M., Forde, B. M., et al. (2014). Global dissemination of a multidrug resistant Escherichia coli clone. *Proc. Natl. Acad. Sci. United States America* 111 (15), 5694–5699. doi: 10.1073/pnas.1322678111

Pitout, J. D. D. (2012). Extraintestinal pathogenic Escherichia coli: A combination of virulence with antibiotic resistance. *Front. Microbiol.* 3 (JAN). doi: 10.3389/fmicb.2012.00009

Pitout, J. D. D., and Finn, T. J. (2020). The evolutionary puzzle of Escherichia coli ST131. *Infection Genet. Evol.* 81 (February), 104265. doi: 10.1016/j.meegid.2020.104265

Platell, J. L., Johnson, J. R., Cobbold, R. N., and Trott, D. J. (2011). Multidrug-resistant extraintestinal pathogenic Escherichia coli of sequence type ST131 in animals and foods. *Veterinary Microbiol.* 153 (1–2), 99–108. doi: 10.1016/j.vetmic.2011.05.007

Poirel, L., Madec, J.-Y., Lupo, A., Schink, A.-K., Kieffer, N., Nordmann, P., et al. (2018). Antimicrobial resistance in Escherichia coli. *Microbiol. Spectr.* 6 (4), 1–27. doi: 10.1128/MICROBIOLSPEC.ARBA-0026-2017

Price, L. B., Johnson, J. R., Aziz, M., Clabots, C., Johnston, B., Tchesnokova, V., et al. (2013). The epidemic of extended-spectrum-β-lactamase-producing Escherichia coli ST131 is driven by a single highly pathogenic subclone, H30-Rx. *MBio* 4 (6), 1–10. doi: 10.1128/mBio.00377-13

Pungpian, C., Angkititrakul, S., and Chuanchuen, R. (2022). Genomic characterization of antimicrobial resistance in mcr carrying ESBL producing

Escherichia coli from pigs and humans. *Microbiology (Reading, England)* 168 (6), 1–13. doi: 10.1099/mic.0.001204

Querido, M. M., Paulo, J., Aguiar, L., Neves, P., and Pereira, C. C. (2020). Self-disinfecting surface and infection control. *Colloids Surface B: Biointerfaces* 178 (January), 8–21. doi: 10.1016/j.colsurfb.2019.02.009

Redgrave, L. S., Sutton, S. B., Webber, M. A., and Piddock, L. J. V. (2014). Fluoroquinolone resistance : mechanisms, impact on bacteria, and role in evolutionary success. *Trends Microbiol.* 22 (8), 438–445. doi: 10.1016/j.tim.2014.04.007

Redondo-Salvo, S., Bartomeus-Peñalver, R., Vielva, L., Tagg, K. A., Webb, H. E., Fernández-López, R., et al. (2021). COPLA, a taxonomic classifier of plasmids. *BMC Bioinf.* 22 (1), 1–9. doi: 10.1186/s12859-021-04299-x

Redondo-Salvo, S., Fernández-López, R., Ruiz, R., Vielva, L., de Toro, M., Rocha, E. P. C., et al. (2020). Pathways for horizontal gene transfer in bacteria revealed by a global map of their plasmids. *Nat. Commun.* 11 (1), 1–13. doi: 10.1038/s41467-020-17278-2

Roer, L., Tchesnokova, V., Allesøe, R., Muradova, M., Chattopadhyay, S., Ahrenfeldt, J., et al. (2017). Development of a Web Tool for Escherichia coli Subtyping Based on fimH Alleles. *J. Clin. Microbiol.* 55 (8), 2538–2543. doi: 10.1128/JCM.00737-17

Sabaté, M., Moreno, E., Pérez, T., Andreu, A., and Prats, G. (2006). Pathogenicity island markers in commensal and uropathogenic Escherichia coli isolates. *Clin. Microbiol. Infection* 12 (9), 880–886. doi: 10.1111/j.1469-0691.2006.01461.x

Saldaña, Z., Sánchez, E., Xicohtencatl-Cortes, J., Puente, J. L., and Girón, J. A. (2011). Surface structures involved in plant stomata and leaf colonization by Shiga-toxigenic Escherichia coli O157: H7. *Front. Microbiol.* 2 (MAY). doi: 10.3389/fmicb.2011.00119

Sarkar, S., Hutton, M. L., Vagenas, D., Ruter, R., Schüller, S., Lyras, D., et al. (2018). Intestinal colonization traits of pandemic multidrug-resistant Escherichia coli ST131. *J. Infect. Dis.* 218 (6), 979–990. doi: 10.1093/infdis/jiy031

Sarowska, J., Futoma-Koloch, B., Jama-Kmiecik, A., Frej-Madrzak, M., Ksiazczyk, M., Bugla-Ploskonska, G., et al. (2019). Virulence factors, prevalence and potential transmission of extraintestinal pathogenic Escherichia coli isolated from different sources: recent reports. *Gut Pathog.* 11 (1), 1–16. doi: 10.1186/S13099-019-0290-0

Schubert, S., Rakin, A., and Heesemann, J. (2004). The Yersinia high-pathogenicity island (HPI): evolutionary and functional aspects. *Int. J. Med. Microbiol.* 294 (2-3), 83–94. doi: 10.1016/j.ijmm.2004.06.026

Seemann, T. (2014). Prokka: Rapid prokaryotic genome annotation. *Bioinformatics* 30 (14), 2068–2069. doi: 10.1093/bioinformatics/btu153

Shropshire, W. C., Aitken, S. L., Pifer, R., Kim, J., Bhatti, M. M., Li, X., et al. (2021). IS26-mediated amplification of blaOXA-1and blaCTX-M-15with concurrent outer membrane porin disruption associated with *de novo* carbapenem resistance in a recurrent bacteraemia cohort. *J. Antimicrobial. Chemother* 76 (2), 385–395. doi: 10.1093/jac/dkaa447

Siguier, P., Perochon, J., Lestrade, L., Mahillon, J., and Chandler, M. (2006). ISfinder : the reference centre for bacterial insertion sequences. *Nucleic Acids Res* 34, 32–36. doi: 10.1093/nar/gkj014

Silkie, S. S., Tolcher, M. P., and Nelson, K. L. (2008). Reagent decontamination to eliminate false-positives in Escherichia coli qPCR. *J. Microbiol. Methods* 72 (3), 275–282. doi: 10.1016/j.mimet.2007.12.011

Smillie, C., Garcillán-Barcia, M. P., Francia, M. V., Rocha, E. P., and de la Cruz, F. (2010). Mobility of plasmids. *Microbiol. Mol. Biol. Rev.* 74 (3), 434–452. doi: 10.1128/MMBR.00020-10

Sora, V. M., Meroni, G., Martino, P. A., Soggiu, A., Bonizzi, L., and Zecconi, A. (2021). Extraintestinal pathogenic escherichia coli: Virulence factors and antibiotic resistance. *Pathogens* 10 (11), 1–25. doi: 10.3390/pathogens10111355

Stoesser, N., Sheppard, A. E., Pankhurst, L., de Maio, N., Moore, C. E., Sebra, R., et al. (2016). Evolutionary history of the global emergence of the Escherichia coli epidemic clone ST131. *MBio* 7 (2), 1–15. doi: 10.1128/mBio.02162-15

Stogios, P. J., Bordeleau, E., Xu, Z., Skarina, T., Evdokimova, E., Chou, S., et al. (2022). Structural and molecular rationale for the diversification of resistance mediated by the Antibiotic_NAT family. *Communications Biology* 5(1), 263. doi: 10.1038/s42003-022-03219-w

Stothard, P., Grant, J. R., and Van Domselaar, G. (2018). Visualizing and comparing circular genomes using the CGView family of tools. *Briefings Bioinf.* 20 (4), 1576–1582. doi: 10.1093/bib/bbx081

Sullivan, M. J., Petty, N. K., and Beatson, S. A. (2011). Easyfig: A genome comparison visualizer. *Bioinformatics* 27 (7), 1009–1010. doi: 10.1093/bioinformatics/btr039

Tacconelli, E., Carrara, E., Savoldi, A., Harbarth, S., Mendelson, M., Monnet, D. L., et al. (2018). Discovery, research, and development of new antibiotics: the WHO priority list of antibiotic-resistant bacteria and tuberculosis. *Lancet Infect. Dis.* 18 (3), 318–327. doi: 10.1016/S1473-3099(17)30753-3

Tausova, D., Dolejska, M., Cizek, A., Hanusova, L., Hrusakova, J., Svoboda, O., et al. (2012). Escherichia coli with extended-spectrum β-lactamase and plasmid-mediated quinolone resistance genes in great cormorants and mallards in central europe. *J. Antimicrobial. Chemother* 67 (5), 1103–1107. doi: 10.1093/jac/dks017

Tchesnokova, V. L., Rechkina, E., Chan, D., Haile, H. G., Larson, L., Ferrier, K., et al. (2020). Pandemic uropathogenic fluoroquinolone-resistant escherichia coli have enhanced ability to persist in the gut and cause bacteriuria in healthy women. *Clin Infect Dis* 70, 937–939. doi: 10.1093/cid/ciz547

Tetzschner, A. M. M., Johnson, J. R., Johnston, B. D., Lund, O., and Scheutz, F. (2020). In Silico genotyping of Escherichia coli isolates for extraintestinal virulence genes by use of whole-genome sequencing data. *J. Clin. Microbiol.* 58 (10), 1–13. doi: 10.1128/JCM.01269-20

Tsoumtsa Meda, L. L., Landraud, L., Petracchini, S., Descorps-Declere, S., Perthame, E., Nahori, M. A., et al. (2022). The cnf1 gene is associated with an expanding Escherichia coli ST131 H30Rx/C2 subclade and confers a competitive advantage for gut colonization. *Gut Microbes* 14 (1), 1–20. doi: 10.1080/19490976.2022.2121577

Van Duijkeren, E., Schink, A.-K., Roberts, M. C., Wang, Y., and Schwarz, S. (2000). Mechanisms of bacterial resistance to antimicrobial agents. *J. Med. Libanais* 48 (4), 186–198. doi: 10.1128/microbiolspec.arba-0019-2017

van Hoek, A. H. A. M., Stalenhoef, J. E., van Duijkeren, E., and Franz, E. (2016). Comparative virulotyping of extended-spectrum cephalosporin-resistant E. coli isolated from broilers, humans on broiler farms and in the general population and UTI patients. *Veterinary Microbiol.* 194 (2015), 55–61. doi: 10.1016/j.vetmic.2016.04.008

Villa, L., García-Fernández, A., Fortini, D., and Carattoli, A. (2010). Replicon sequence typing of IncF plasmids carrying virulence and resistance determinants. *J. Antimicrobial. Chemother* 65 (12), 2518–2529. doi: 10.1093/jac/dkq347

Walker, D. I., McQuillan, J., Taiwo, M., Parks, R., Stenton, C. A., Morgan, H., et al. (2017). A highly specific Escherichia coli qPCR and its comparison with existing methods for environmental waters. *Water Res.* 126, 101–110. doi: 10.1016/j.watres.2017.08.032

Wang, Y., Batra, A., Schulenburg, H., and Dagan, T. (2022). Gene sharing among plasmids and chromosomes reveals barriers for antibiotic resistance gene transfer. *Philos. Trans. R. Soc. B: Biol. Sci.* 377 (1842), 1–11. doi: 10.1098/rstb.2020.0467

Wang, M., Goh, Y. X., Tai, C., Wang, H., Deng, Z., and Ou, H. Y. (2022). VRprofile2: Detection of antibiotic resistance-associated mobilome in bacterial pathogens. *Nucleic Acids Res.* 50 (W1), 768–773. doi: 10.1093/nar/gkac321

White, P. A., Stokes, H. W., Bunny, K. L., and Hall, R. M. (1999). Characterization of a chloramphenicol acetyltransferase determinant found in the chromosome of Pseudomonas aeruginosa. *FEMS microbiology Letters* 175 (1), 27–35. doi: 10.1111/j.1574-6968. 1999.tb 13598.x

Wick, R. R., Judd, L. M., Gorrie, C. L., and Holt, K. E. (2017). Unicycler: Resolving bacterial genome assemblies from short and long sequencing reads. *PloS Comput. Biol.* 13 (6), 1–22. doi: 10.1371/journal.pcbi.1005595

Wingett, S. W., and Andrews, S. (2018). Fastq screen: A tool for multi-genome mapping and quality control. *F1000Research* 7 (0), 1–13. doi: 10.12688/f1000research.15931.1

Zhao, X., Sun, Y., Ma, Y., Xu, Y., Guan, H., and Wang, D. (2022). Research advances on the contamination of vegetables by Enterohemorrhagic Escherichia coli: pathways, processes and interaction. *Crit. Rev. Food Sci. Nutr.* 15, 1–15. doi: 10.1080/10408398.2022.2146045

Zhu, Y., Huang, W. E., and Yang, Q. (2022). Clinical perspective of antimicrobial resistance in bacteria. *Infection and Drug Resistance* 15, 735–746. doi: 10.2147/IDR.S345574

Zurfluh, K., Hächler, H., Nüesch-Inderbinen, M., and Stephan, R. (2013). Characteristics of extended-spectrum β-lactamase- and carbapenemase-producing Enterobacteriaceae isolates from rivers and lakes in Switzerland. *Appl. Environ. Microbiol.* 79 (9), 3021–3026. doi: 10.1128/AEM.00054-13

frontiers | Frontiers in Cellular and Infection Microbiology

TYPE Original Research
PUBLISHED 14 November 2023
DOI 10.3389/fcimb.2023.1274573

OPEN ACCESS

EDITED BY
Manuel Gerardo Ballesteros Monrreal,
University of Sonora, Mexico

REVIEWED BY
Edwin Barrios-Villa,
Universidad de Sonora, Mexico
Mark T. Anderson,
University of Michigan, United States

*CORRESPONDENCE
Claudio Neidhöfer
claudio.neidhoefer@ukbonn.de

†These authors have contributed equally to this work

RECEIVED 08 August 2023
ACCEPTED 18 September 2023
PUBLISHED 14 November 2023

CITATION
Neidhöfer C, Neuenhoff M, Jozič R, Atangcho B, Unsleber S, Neder U, Grumaz S and Parčina M (2023) Exploring clonality and virulence gene associations in bloodstream infections using whole-genome sequencing and clinical data. *Front. Cell. Infect. Microbiol.* 13:1274573. doi: 10.3389/fcimb.2023.1274573

Exploring clonality and virulence gene associations in bloodstream infections using whole-genome sequencing and clinical data

Claudio Neidhöfer[1,2*†], Marcel Neuenhoff[3†], Robert Jozič[1], Brenda Atangcho[1,4], Sandra Unsleber[5], Ulrike Neder[5], Silke Grumaz[5] and Marijo Parčina[1]

[1]Institute of Medical Microbiology, Immunology and Parasitology. University Hospital Bonn, Bonn, Germany, [2]Institute of Experimental Haematology and Transfusion Medicine, University of Bonn, Bonn, Germany, [3]Bioinformatics and Systems Biology, Justus Liebig University Giessen, Giessen, Germany, [4]Institute for Functional Gene Analytics, Bonn-Rhein-Sieg University of Applied Sciences, Sankt Augustin, Germany, [5]Noscendo GmbH, Duisburg, Germany

Background: Bloodstream infections (BSIs) remain a significant cause of mortality worldwide. Causative pathogens are routinely identified and susceptibility tested but only very rarely investigated for their resistance genes, virulence factors, and clonality. Our aim was to gain insight into the clonality patterns of different species causing BSI and the clinical relevance of distinct virulence genes.

Methods: For this study, we whole-genome-sequenced over 400 randomly selected important pathogens isolated from blood cultures in our diagnostic department between 2016 and 2021. Genomic data on virulence factors, resistance genes, and clonality were cross-linked with *in-vitro* data and demographic and clinical information.

Results: The investigation yielded extensive and informative data on the distribution of genes implicated in BSI as well as on the clonality of isolates across various species.

Conclusion: Associations between survival outcomes and the presence of specific genes must be interpreted with caution, and conducting replication studies with larger sample sizes for each species appears mandatory. Likewise, a deeper knowledge of virulence and host factors will aid in the interpretation of results and might lead to more targeted therapeutic and preventive measures. Monitoring transmission dynamics more efficiently holds promise to serve as a valuable tool in preventing in particular BSI caused by nosocomial pathogens.

KEYWORDS

bloodstream infections, whole-genome sequencing, clonality patterns, virulence factors, resistance genes, genotype-phenotype correlation, genomic characterization of BSI, molecular epidemiology of BSI

Introduction

Bloodstream infections (BSIs) pose a substantial global health threat, leading to increased morbidity and mortality rates (McNamara et al., 2018). While identifying the causative pathogen and its antibiotic susceptibility remains a clinical priority, exploring additional factors such as genetic relatedness, virulence genes, and antibiotic resistance genes can significantly enhance patient outcomes and alleviate the overall burden (Wren, 2000; Leavis et al., 2006; Wyres et al., 2020; Allen et al., 2021). Whole-genome sequencing (WGS) studies have revolutionized our understanding of pathogen identification, antibiotic resistance, and epidemiology (Wren, 2000). Insights into clonality patterns can guide interventions to curtail the dissemination of specific strains and inform targeted prevention strategies (Wren, 2000; Leavis et al., 2006; Wyres et al., 2020). Furthermore, studying pathogen clonality provides valuable insights into the evolutionary dynamics of BSI pathogens, facilitating the prediction of future trends in antibiotic resistance and virulence (Wren, 2000; Allen et al., 2021).

Virulence factors play a crucial role in the colonization, invasion, and evasion of the host immune system by pathogens. Understanding the specific virulence factors associated with BSI-causing bacteria provides insights into disease mechanisms, severity, and potential therapeutic targets (Wren, 2000; L Thomas and Lee, 2012; Wyres et al., 2020). In-depth investigations of bacterial virulence factors associated with BSI have yielded significant findings concerning pathogenesis and host–pathogen interactions (Wren, 2000; Leavis et al., 2006; L Thomas and Lee, 2012; Wyres et al., 2020). Studying resistance genes and correlating them with phenotypical susceptibility are of paramount importance for addressing key research questions in the field of antimicrobial resistance leading to a comprehensive understanding of the interplay between genotype and phenotype (Wren, 2000; L Thomas and Lee, 2012; Mahfouz et al., 2020; Allen et al., 2021). It enables the validation and verification of resistance mechanisms and provides a more accurate assessment of the clinical implications of specific genetic variants.

In this study, we conducted a comprehensive whole-genome sequencing of over 400 randomly selected common BSI-causing pathogens to elucidate clonality patterns and assess the clinical significance of virulence and resistance genes, including their association with mortality. Our study findings advance the understanding of BSI pathogenesis and hold implications for more targeted therapeutic interventions.

Methods

Study design and data collection

For this study, over 400 bacterial isolates of common pathogens detected in blood cultures between January 2019 and December 2021 in our microbiological diagnostic unit, which services a tertiary referral and maximum care hospital and other hospitals in the area, were randomly selected for the genera *Acinetobacter*, *Bacteroides*, *Citrobacter*, *Enterobacter*, and *Serratia* and the species *Enterococcus faecalis*, *Enterococcus faecium*, *Escherichia coli*, *Klebsiella pneumonia*, *Proteus mirabilis*, *Pseudomonas aeruginosa*, *Staphylococcus aureus*, *Stenotrophomonas maltophilia*, *Streptococcus pneumoniae*, and *Streptococcus pyogenes* from cryo-storage. These were thawed, subcultured twice on Columbia 5% sheep blood agar (Becton Dickinson, Heidelberg, Germany), and inspected by two experienced operators prior to sequencing. Isolate information was complemented by accessible laboratory information on phenotypical susceptibility, growth of additional bacteria in the same blood culture, and routine diagnostic resistance gene detection, as well as accessible patient information on age, sex, hospitalization, 30-day mortality, and outcome. We constructed a database that was password-protected and accessible by only three operators who ensured that all patient data were fully de-identified prior to analysis. Unless specifically mentioned or reported, the minimum inhibitory concentrations (MICs) were determined by the VITEK 2 system (bioMérieux, Marcy-l'Etoile, France). Isolate susceptibility was inferred based on EUCAST Cl. Br. Tables v. 13.0.

DNA preparation and sequencing

DNA isolation, library preparation, sequencing, and sequence assembly were carried out by Noscendo GmbH, Germany. Genomic DNA was prepared from pellets obtained from 5 ml of culture in a brain heart infusion (BHI) medium (Becton Dickinson, Heidelberg, Germany). Cell pellets were prepared, shipped on dry ice, and stored at −80°C until further processing. DNA was isolated with the ZymoBIOMICS DNA Miniprep Kit (Zymo Research, Irvine, CA, USA) according to the manufacturer's instructions with a Vortex Genie 2 device equipped with an SI-H524 horizontal tube holder (Scientific Industries, Bohemia, NY, USA) to perform mechanical cell disruption for 10 min. DNA concentration was measured with the Qubit 1X dsDNA Assay-Kit on a Qubit 2.0 instrument (Thermo Fisher Scientific, Waltham, MA, USA), and size distribution was checked with the Agilent Genomic DNA 50 kb Kit on a 5200 Fragment Analyzer System (Agilent Technologies, Santa Clara, CA, USA). The libraries were prepared using the Ligation Sequencing Kit SQK-LSK109 with Native Barcoding Expansion 1–12 (PCR-free) EXP-NBD104 and Native Barcoding Expansion 13–24 (PCR-free) EXP-NBD114 according to the manufacturer's instructions (Oxford Nanopore Technologies, Oxford, UK) together with NEB Blunt/TA Ligase Master Mix and NEBNext Companion Module for Oxford Nanopore Technologies Ligation Sequencing (New England Biolabs, MA, USA). Then, the libraries were prepared, pooled in equimolar ratio, quality checked, loaded on a MinION Flow Cell (R9.4.1), and finally sequenced on a MinION benchtop sequencer (Mk1B). For each batch preparation, a pellet of a 1.5-ml overnight culture (BHI medium) of DSM 1576–*Escherichia coli* was used as an internal quality control during the whole process, starting with DNA isolation.

Bioinformatics analysis

After sequencing, fast5 data were basecalled using the Oxford Nanopore Technologies neural-network-based basecalling software Guppy (version 5.0.7) applying a high accuracy mode (config dna_r9.4.1_450bps_hac.cfg). Fastq statistics on read length distributions, expected coverages, and N50 values were calculated. Following closely the manual of the tool Trycycler (Wick et al., 2021) (https://github.com/rrwick/Trycycler, version 0.4.2), long-read consensus assemblies were produced from multiple input assemblies of the same input data set by using the following assemblers: Flye (https://github.com/fenderglass/Flye, version 2.8.3), Miniasm and Minipolish (https://github.com/rrwick/Minipolish, version 0.1.3), and Raven (https://github.com/lbcb-sci/raven, version 1.4.0). Before assembly, reads below a length of 1,000 bp were removed using the tool Filtlong (https://github.com/rrwick/Filtlong, version 0.2.0), at most removing 5% of the original data set. Nine subsamples were created, providing a minimum read depth of 100×. In cases in which average coverages were below 100×, the minimum read depth after subsampling was lowered to 50×. Subsampled data sets were then forwarded to the assemblers, producing nine assemblies in total, three of every assembler. The Trycycler then clustered similar contigs to detect spurious, incomplete, or misassembled contigs. After manual inspection, the conspicuous clusters were removed. The remaining clusters were further processed to result in circular chromosomes and plasmids. Consensus sequences were polished using Medaka (https://github.com/nanoporetech/medaka, version 1.4.3) to increase base accuracy and minimize assembly and sequencing errors.

Assembly quality was finally evaluated by Busco (https://busco.ezlab.org/, https://gitlab.com/ezlab/busco/-/releases/5.2.1, version 5.2.1). Furthermore, reads were mapped to the consensus sequence by using Minimap2 (https://github.com/lh3/minimap2, version 2.18) and Flye-samtools to get coverage values of every consensus base. Assemblies having a Busco completeness value above 95% and every consensus base covered with at least 5× coverage were regarded as high quality. All isolates with valid results and sufficient coverage were included in the analysis.

Detection of antimicrobial resistance (AMR) genes, stress response genes, and virulence factors was detected with AMRFinderPlus (3.11.4) "–plus" option/NCBI reference gene database (2023-02-23.1) (Feldgarden et al., 2021; Feldgarden et al., 2022). If species were present in the list of curated organisms, the "–organism" option was used to ignore universal species mutations and resistance genes and to screen for known point mutations. Only results with identity and coverage >90% were included. For further analysis, assemblies were imported into bactopia (Shen, ; Ewels et al., 2020; Petit and Read, 2020). FastANI (v1.33) was used to calculate the average nucleotide identity within species (Jain et al., 2018). MLST types were determined with the PubMLST database using MLST (2.23.0, https://github.com/tseemann/mlst) (Jolley et al., 2018). For *Enterobacterales*, plasmids were detected using plasmidFinder (2.1.6) (Camacho et al., 2009; Carattoli et al., 2014).

Strain-specific tools were used to obtain more in-depth information: *E. coli*—ECTyper (1.0.0) (Iguchi et al., 2015), *K. pneumoniae*—Kleborate (2.3.2) (Lam et al., 2021), *P. aeruginosa*—pasty (1.0.2, https://github.com/rpetit3/pasty) (Camacho et al., 2009; Thrane et al., 2016), and *S. pneumoniae*—Seroba (1.0.2) (Epping et al., 2018).

Phylogenetic trees and ANI values in supplementary data were created with Anvi'o v7.1 (Eren et al., 2021) using "anvi'o pangenomics workflow" (Edgar, 2004; Hyatt et al., 2010; Buchfink et al., 2015; Pritchard et al., 2016; Chan and Lowe, 2019). All detected resistance genes, stress response genes, and virulence factors for each species can be found in the Supplementary Material. (Sequence names are mentioned yellow for findings with shared gene symbol but multiple possible alleles. These were merged for our purposes if the genes belong to the same subclass.)

All data relevant to the study are included in the article or uploaded as supplementary information. Due to collaboration agreements, genomes have not been uploaded to any publicly accessible platform but can be shared upon reasonable request.

The Ethics Committee of the University Hospital Bonn confirmed that no ethics approval was required for this study.

Results

Isolate and patient information

The 364 isolates for which genomes were available with satisfactory coverage and quality belonged to 364 different patients of which the majority were men (60.16%). Detailed information on patients and isolates is listed in Table 1. In 55 cases (15.11%), the pathogen under study was not the only one isolated from the respective blood culture. In 7, there were 2 additional pathogens, and in another three, 3. Fourteen isolates were methicillin-resistant *S. aureus* (MRSA), 10 were vancomycin-resistant *enterococci* (VRE), and 26 were gram-negative rods falling into the German guideline classification of multidrug-resistant gram-negative rods on the basis of resistance against three (3MRGN) or four (4MRGN) of the following antibiotic groups: acylureidopenicillins, third- and fourth-generation cephalosporins, carbapenems, and fluoroquinolones.

Species characteristics

The most frequently detected AMR genes were *fosA* (107), *oqxA* (73), and *emrD* (70). These were, however, only detected in *Enterobacterales* and *P. aeruginosa* that made up a large part of all isolates. An overview of detected virulence, stress response, and AMR genes can be found in the Supplementary Material. Figure 1 displays to what degree the average nucleotide identity could vary across different pathogens and the number of virulence genes, AMR genes, stress response genes, and plasmids that different pathogens carried. The 30-day and 90-day mortality did not correlate with the number of resistance, AMR, or stress response genes but with

10.3389/fcimb.2023.1274573

TABLE 1 Patient and isolate information.

Age (years) Mean (min, max)	62.15 (0, 95)	
Sex		
Female	145	39.84%
Male	219	60.16%
Ward type		
Emergency center	92	25.28%
ICU	112	30.77%
Non-ICU ward	154	42.31%
Outpatient clinics	6	1.65%
Clinic		
Anesthesiology	20	5.49%
Emergency departments	89	24.45%
General surgery	19	5.22%
Rehabilitation	49	13.46%
Gynecology	8	2.2%
Heart surgery	10	2.75%
Internal medicine	77	21.15%
Neonatology	6	1.65%
Neurosurgery	8	2.2%
Neurology	17	4.67%
Oncology	40	10.99%
Orthopedics	5	1.37%
Pediatrics	10	2.75%
Urology	4	1.1%
Others	2	0.55%
Year		
2016	77	21.15%
2017	71	19.51%
2018	83	22.80%
2019	62	17.03%
2020	61	16.76%
2021	10	2.75%
Isolates		
***Acinetobacter* spp.**	12	3.3%
***Bacteroides* spp.**	4	1.1%
***Citrobacter* spp.**	15	4.12%
***Enterobacter* spp.**	45	12.36%
Enterococcus faecalis	19	5.22%
Enterococcus faecium	19	5.22%
Escherichia coli	40	10.99%
Klebsiella pneumoniae	40	10.99%
Proteus mirabilis	20	5.5%
Pseudomonas aeruginosa	38	10.44%
***Serratia* spp.**	27	7.42%
Staphylococcus aureus	48	13.19%
Stenotrophomonas maltophilia	5	1.37%
Streptococcus pneumoniae	13	3.57%
Streptococcus pyogenes	18	4.95%

patient age (rpb = 0.22, n = 248, p = 0.001 and rpb = 0.25, n = 201, p = <0.001, respectively).

Enterococcus faecalis

The majority of the isolates originated from patients in intensive care units (ICUs) with eight cases, followed by the emergency center (EC) with four cases. None of the isolates were identified as VRE either phenotypically or genotypically. There were 11 unique multilocus sequence typing (MLST) types represented once and four types represented twice. The isolates showed an average nucleotide identity of 98.78% to each other, ranging from 98.40% to 98.97%. Notably, patients infected with *E. faecalis* isolates encoding *dfrF*, *gyrA_S83I*, and *parC_S80I* exhibited significantly lower 30-day (all p = 0.015) and 90-day survival rates (all p = 0.047), although the assumptions for the χ^2 test were not met due to low cell frequencies. Out of all the isolates, only two showed higher MICs for trimethoprim/sulfamethoxazole than the threshold of ≤10, and both of these isolates tested positive for the *dfrG* gene.

Enterococcus faecium

Out of the *E. faecium* isolates, 10 were classified as VRE, but their presence was not associated with a lower 30-day or 90-day survival rate. Among these isolates, the MLST types of seven could not be determined, while six belonged to ST117 and three to ST80. Five ST117 isolates and two ST80 isolates were identified as VRE. No significant differences were observed in the 30-day and 90-day survival rates based on the presence or absence of specific genes. However, a positive correlation was found between survival and younger age (rpb = 0.71, p = 0.001). The isolates displayed an average nucleotide identity of 98.84% to each other, with a range of 94.29% to 99.27%.

Staphylococcus aureus

Fourteen isolates were MRSA, of which all were *mecA*-positive. Two isolates were resistant to tetracycline, while *tet(k)* was only encoded by one of them and by one phenotypically susceptible isolate; *tet(38)* was encoded by both resistant ones but also by all but one of those susceptible. Out of four that were resistant to rifampicin, only one was found to have genes conferring resistance to it (*rboB_H481Y*, *rboB_L466S*, and *rpoB_S486L*). Resistance to levofloxacin well matched the presence of resistance genes *gyrA_S84L*, *parC_E84G*, *parC_E84K*, *parC_S80F*, and/or *parE_P585S*. While all isolates were susceptible to linezolid, in nine, *23S_C2220T* was found. Out of 23 resistant to erythromycin, 11 encoded *erm(A)*, 4 *erm(C)*, 2 *erm(T)*, and another 2 *msr(A)* and *mph(C)*; in 4, no macrolide resistance genes were detected. For 40 isolates, information on the 30-day survival could be retrieved, as well as for 37 on 90-day survival and 30-day and 90-day outcomes. The only significant difference that was found was that of a lower 30-day survival in patients with *S. aureus* isolates that encoded *splE* (p = 0.045; Cramér's V 0.32) but without meeting χ^2 test assumptions due to low cell frequencies and without significant Fisher exact test (p = 0.072). Isolates had an average nucleotide identity to each other of 98.36, ranging from 97.73 to 98.75 (see also Figure A1 in the Supplementary Material). The two most represented MLST types were 225 (10) and 22 (9).

Streptococcus pneumoniae

In 11 out of 13 cases in which *S. pneumoniae* grew, blood cultures were collected in the EC. The available data were insufficient to perform statistical analyses pertaining to hypotheses involving 30-day and 90-day outcomes and survival rates. Only three isolates had MICs to penicillin sufficiently high to be considered susceptible only at increased dosage (I). Of these, two

10.3389/fcimb.2023.1274573

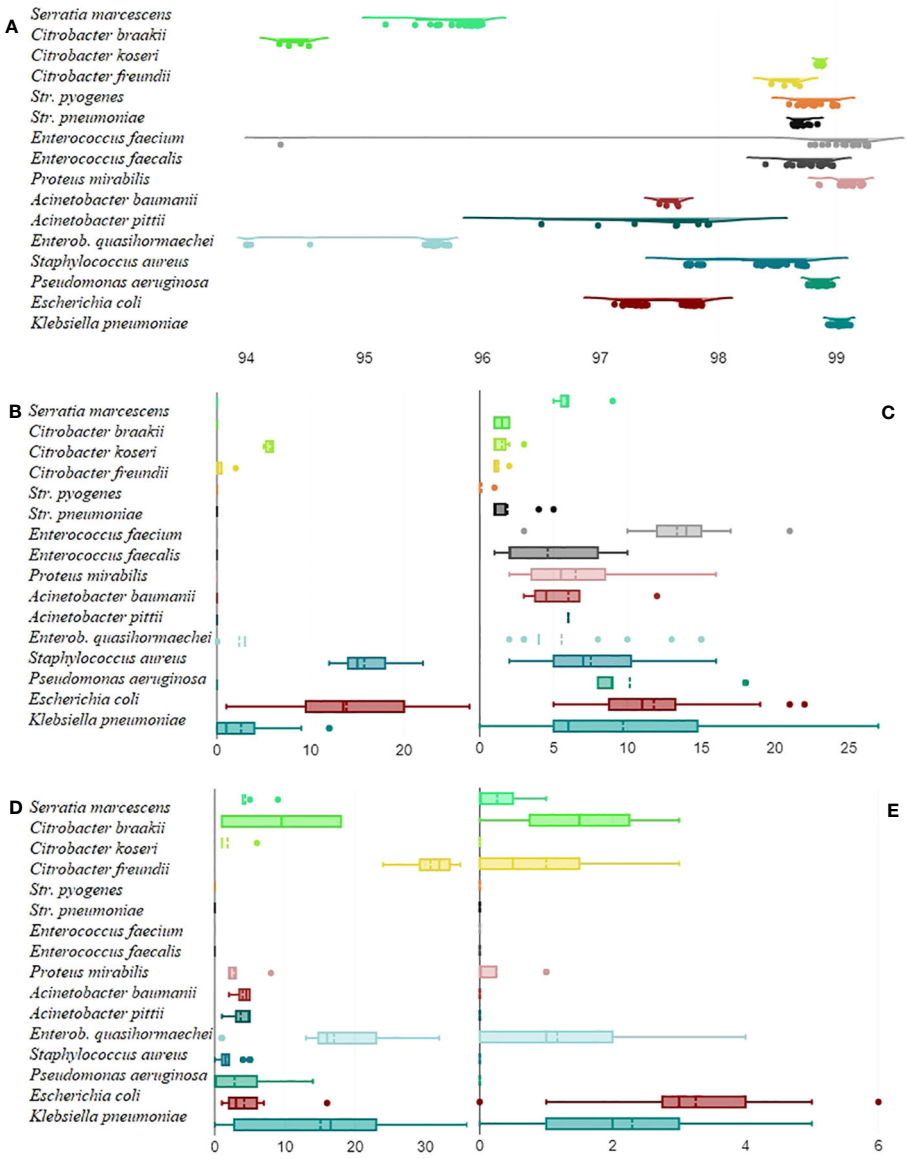

FIGURE 1
Mean average nucleotide identity by pathogen. For each isolate, the average nucleotide identity it had to all the other isolates within the same group in percent (*x*-axis) was calculated and displayed as a raincloud plot **(A)**. Boxplots on the number (*x*-axis) of virulence genes **(B)**, AMR genes **(C)**, stress response genes **(D)**, and plasmids **(E)** that pathogens carried.

encoded *pbp1a* and *pbp2b*. Two out of three isolates resistant to erythromycin encoded *erm(B)*. Three out of four isolates resistant to tetracycline encoded *tet(M)*. Isolates had an average nucleotide identity to each other of 98.71, ranging from 98.63 to 98.84. Isolates belonged to 10 different serotypes, the most frequent being 8, with 16F and 17F having two isolates each, and these isolates had 13 different MLST types.

Streptococcus pyogenes

In 12 out of 18 cases in which *S. pyogenes* grew, blood cultures were collected in the EC. Here, too, the available data were insufficient to perform statistical analyses pertaining to hypotheses involving 30-day and 90-day outcomes and survival rates. Both isolates resistant to tetracycline carried *tet(M)*. Isolates had an average nucleotide identity to each other of 98.82, ranging from 98.60 to 99.01. The two most represented MLST types were ST28 (5) and ST39 (4).

Bacteroides fragilis

The four *B. fragilis* isolates had an average nucleotide identity of 98.97 to each other that ranged from 98.91 to 99.03. One MLST type could not be determined, while the remaining were ST40, ST67, and ST129. The only isolate resistant to clindamycin was also the only one to encode *mef(A)*, as well as the only isolate to have an increased MIC to meropenem was the only one to encode *cfxA*.

Escherichia coli

The mean nucleotide identity of *E. coli* isolates ranged from 96.74 to 98.42 (see also Figure A2 in the Supplementary Material) with an average of 97.63, with MLST type ST69 being the most frequent (6). Four isolates belonged to ST12, ST73, and ST131 each, and two isolates to ST88 and ST95 each. Two isolates could not be assigned and the remaining isolates all belonged to different MLST types. The most represented O-antigen types were O4, O6, and O25, with four isolates each, and the most represented H-antigen type was H4 (9). The majority of isolates carried one or more plasmids with the most frequent being *IncFIB(APec01918)* (32), *Col156* (17), *IncFII* (14), and *IncFIA* (13). The significant differences found were only that of a lower 30-day and 90-day survival in patients with isolates encoding *IncFII(pSE11)* and *p0111* ($p = 0.001$, Cramér's $V = 0.69$) but without χ^2 test assumptions being met due to low cell frequencies.

Klebsiella pneumoniae

For three *K. pneumoniae* isolates, the MLST type could not be determined, and another three belonged to ST147. Six MLST types were represented twice (ST14, ST15, ST20, ST78, ST661, and ST3328), and another 22 just once. With Kleborate, the missing MLSTs were identified as ST307, ST223-1LV, and ST1013-1LV. Isolates had an average nucleotide identity of 99.03 to each other, ranging from 98.93 to 99.12 (see also Figure A3 in the Supplementary Material), and carried an average of 2.4 plasmids, ranging from two isolates carrying none to three carrying five. The number of encoded stress tolerance, AMR, and virulence genes varied from none to 36, from none to 27, and from none to 12, respectively, with only one isolate encoding neither of each. significant differences found were that of a lower 30-day and 90-day survival in patients with isolates encoding *iucA*, *iucB*, and *iucC* ($p = 0.039$, Cramér's $V = 0.35$) and *iroB* and *iroN* ($p = 0.039$, Cramér's $V = 0.35$), but all violating χ^2 test assumptions due to low cell frequencies, and for *aac(3)-IId*, *aph(3')-VI*, *gyrA_D87G*, and *phoQ_R16C* ($p = 0.046$, Cramér's $V = 0.34$) and *blaSHV*, *dfrA1*, *iucC*, and *ompK36_D135DGD* ($p = 0.039$, Cramér's $V = 0.35$), additionally without significant Fisher exact test. The four isolates encoding *blaOXA-48* and the three isolates encoding *blaNDM-1* were all correctly identified as such in routine diagnostics.

Enterobacter spp.

The sequenced *Enterobacter* isolates were all reported in routine diagnostics as *Enterobacter cloacae* complex isolates, but WGS revealed these to be *E. quasihormaechei* (31), *E. quasiroggenkampii* (4), *E. sichuanensis* (3), *E. cloacae* (2), *E. chengduensis* (2), and *E. wuhouensis* (1). Isolates either encoded no virulence genes or three (*iroB*, *iroC*, *iroN*), with all isolates encoding three being *E. quasihormaechei* isolates. The number of carried AMR and stress response genes varied significantly among the isolates, ranging from 1 to 15 for AMR genes and 1 to 35 for stress response genes. Isolates encoded between none and four plasmids, the most frequent being *IncFII(pECLA)* (12), *IncFIB (pECLA)* (10), and *Col440I* (8). The one *blaVIM-1*-positive isolate was phenotypically susceptible to imipenem and meropenem and was, hence, not investigated for carrying carbapenemases in routine diagnostics. MLST type could not be determined in 11 cases; in seven, ST50 was identified, and in three, ST118 was identified. Other MLST types were only represented once or twice. No significant differences were found regarding the 30-day and 90-day survival and the presence or absence of investigated genes.

Citrobacter spp.

Four *Citrobacter* isolates were *C. freundii*, another four were *C. braakii*, and seven were *C. koseri*. The average nucleotide identity of *C. koseri* (98.88) and *C. freundii* (98.59) isolates was higher than that of *C. braakii* (94.41) isolates, despite *C. freundii* isolates belonging to four different MLST types. Among all eight *C. freundii* and *C. braakii* isolates, there was only one isolate carrying virulence genes (*ybtP* and *ybtQ*), whereas all *C. koseri* isolates encoded the same virulence factors (*iucA*, *iucB*, *iucC*, *ybtP*, and *ybtQ*) with the exception of *senB*, which was only encoded by four. Isolates encoded between one and three AMR genes. The most significant variation was observed in the number of stress response genes encoded by the isolates. Two *C. braakii* isolates and six *C. koseri* isolates only encoded a single stress response gene, which was *fief*, while the remaining *C. koseri* isolates encoded six, the remaining *C. braakii* isolates encoded 17, and *C. freundii* isolates encoded between 24 and 35. Isolates carried from none to four plasmids with not a single plasmid carried by more than one isolate. The only two *Citrobacter* isolates encoding *qnrB38* were the only ones to have MICs to moxifloxacin above the lowest measurable level.

Proteus mirabilis

Proteus mirabilis isolates had an average nucleotide identity of 99.12 to each other, ranging from 98.83 to 99.25. The significant differences found were that of a lower 30-day survival when isolates encoded *aph(3')-la* ($p = 0.028$; Cramér's V 0.63); however, χ^2 test assumptions were violated due to low cell frequencies and the Fisher exact test was not significant ($p = 0.091$). All isolates carrying *blaTEM-1* were resistant to ampicillin and all but one isolate to ampicillin/sulbactam. All isolates resistant to trimethoprim/sulfamethoxazole carried *dfrA1* and in addition either *sul1* or *sul2*. Four isolates carried an *IncQ1* plasmid.

Serratia marcescens

More than half of the isolates were isolated from patients in the ICU, but isolates only had an average nucleotide identity to each other of 95.79, ranging from 95.18 to 96.00 (see also Figure A4 in the Supplementary Material). No significant differences were found in the 30-day and 90-day survival linked to the presence or absence of certain genes, age, or ward type. Four isolates carried a *pSM22* plasmid and another three isolates either *Col440I*, *IncX5*, or *IncX6*. The *IncX5* carrying isolate carried a *blaVIM-1* alongside it that was neither specifically investigated nor detected in routine diagnostics. That isolate was resistant to piperacillin–tazobactam, tested cephalosporins, and imipenem but had a MIC to meropenem of 0.19 as determined by the gradient strip test (Liofilchem, Roseto degli

Abruzzi, Italy). It was also the only one to be *sul1*-positive although it was just as susceptible to trimethoprim/sulfamethoxazole as all the other isolates. Isolates carried four or five out of 10 stress response genes and either five or six out of 13 AMR genes. The most frequent AMR genes were *ssmE*, *smdB*, *smdA*, *sdeY*, *sdeA* (27 each), *smfY*, *sdeB* (26 each), *aac(6′)* (25), *blaSRT* (22), and *tet(41)* (21).

Acinetobacter baumannii complex

Among the isolates of the *A. baumannii* complex, four were *A. baumannii* isolates and eight were *A. pittii*. Among the *A. baumannii* isolates, the MLST types represented were ST1, ST40, and ST213, with one isolate unassigned and with an average nucleotide identity to each other ranging from 97.54 to 97.69 and from 96.52 to 98.03 among the *A. pittii* isolates. No virulence genes were identified; however, between one and five stress tolerance genes were identified in all isolates and either five or six AMR genes in *A. pittii* and between 3 and 12 in *A. baumannii*. In both species, the most frequently encoded stress tolerance genes were *nreB* (12), *clpK* (6), *yfdX2* (5), *trxLHR* (5), and *hdeD-GI* (5), while the most frequent AMR genes were *amvA* (12) and *ant(3″)-IIa* (10). The available data were insufficient to perform statistical analyses pertaining to hypotheses involving 30-day and 90-day outcomes and survival rates.

Pseudomonas aeruginosa

The average nucleotide identity of *P. aeruginosa* isolates was 98.85 and ranged from 98.66 to 98.94. For 11 isolates, no MLST type could be determined, while three belonged to ST234, ST253, and ST823 each, two to ST308, ST316, and ST446 each, and all the remaining isolates to different MLST types. Isolates belonged mainly to serogroups O11 (13), O6 (9), O1 (5), and O10 (4). No virulence genes were detected, and stress response genes were only detected in less than half of the isolates in which they ranged from 2 to 14 in number. The most frequently encoded were *merE* (14), *merT* (12), *merR* (12), *merP* (12), *merD* (11), and *merA* (11). No isolate had fewer than 8 AMR genes with some carrying up to 18. By far, the most frequent were *mexE* (38), *mexA* (38), *fosA* (38), *aph(3′)-llb* (38), *mexX* (37), *catB7* (37), and *crpP* (29). Thirty-five isolates carried *blaOXA* genes and four *blaVIM* (three *blaVIM-2* and one *blaVIM-11*). Five isolates were classified as 4MRGN and three as 3MRGN. One *blaVIM-2* encoding isolate did not previously classify as 4MRGN as it had below-resistant MICs to piperacillin–tazobactam and cefepime and the *blaVIM-2* gene was neither investigated nor detected in routine diagnostics. It was resistant to imipenem, meropenem, ciprofloxacin, and ceftazidime. No significant differences were found in the 30-day and 90-day survival linked to the presence or absence of certain genes. Isolates exhibited a distinct clustering pattern, roughly partitioning into three distinct branches. Notably, one of these branches encompassed all but one isolate from patients with negative 30-day survival (see Figure A5 in the Supplementary Material) ($p = 0.038$).

Stenotrophomonas maltophilia

Stenotrophomonas maltophilia isolates only had an average nucleotide identity of 93.15 to each other, ranging from 92.09 to 94.17. One MLST type could not be determined, while all remaining were of different ones: ST4, ST23, ST224, and ST233. Only one did not have any stress response genes, the others had from three to nine, and all isolates carried either seven or eight antimicrobial resistance genes. Those shared among all isolates were *aph(6)*, *emrA*, *emrB*, *emrC*, and *smeF*.

Discussion

The present study aimed to conduct a comprehensive analysis of blood culture isolates' genomes, with a retrospective correlation between the detected virulence genes, resistance genes, and stress tolerance genes with the phenotypical susceptibilities and patient outcomes. The findings of this investigation yielded extensive and informative data on the distribution of genes implicated in bloodstream infections across various species. However, the interpretation of these results necessitates careful consideration due to several noteworthy factors. The intriguing observed associations between survival outcomes and the presence of specific resistance genes warrant caution, particularly given the limited knowledge regarding many of the identified virulence factors. The χ^2 test assumptions were persistently violated due to the relatively small sample sizes in the groups of patients with negative 30-day and 90-day survival available for each species, making it imperative to validate and strengthen these associations by replicating the study with larger sample sizes for different species. One key consideration is the possibility that host factors may play a more significant role than pathogen factors in determining the outcomes of bloodstream infections and the inherent difficulty in fully accounting for such factors in studies of this nature (Hekker et al., 2000; Casadevall and Pirofski, 2001; Tseng et al., 2002; Beck et al., 2004; Tseng et al., 2005; Newman et al., 2017).

For example, research on *splE* in *S. aureus* still aims to uncover its precise functions and mechanisms. It seems that *splE* plays a significant role in *S. aureus* pathogenesis by promoting immune evasion through the degradation of immune components and facilitating tissue invasion by breaking down extracellular matrix proteins (Stach et al., 2018). Confirming its role in survival would further emphasize the importance of understanding *splE* for developing effective strategies against staphylococcal infections. The *IncFII(pSE11)* and *p0111* plasmids that were linked to lower survival in *E. coli* are known for disseminating AMR genes (Tasleem Jan and Tiwari, 2017; Wang et al., 2022), and their likely correlation with factors such as prolonged hospitalizations cannot be excluded to confound results, emphasizing that interpretation of the results warrants considered caution. The lower survival in *aph(3′)-la* encoding *P. mirabilis* isolate is probably the most questionable finding, because aside from resistance to aminoglycosides, it is not reported to contribute to virulence (Shaw et al., 1993), and aminoglycosides are infrequently used in our setting.

The study highlights important differences in genetic variation across different species and might be representative to some degree for these pathogens involved in BSI, while it is certainly important to exercise caution in generalizing these findings or applying them to other settings. The identity and coverage values for *E. faecium* ST117 and *E. coli* ST131 were both 100% for their exact alleles. Notably, ECO 131 has been highlighted in several studies as a rapidly expanding multidrug-resistant pathogen with high receptivity and the potential to

develop resistance to last-resort antibiotics such as carbapenems and colistin (Pitout and Finn, 2020; Li et al., 2021; Taati Moghadam et al., 2021; Brumwell et al., 2023). Serotypes H4 and O25 were found to match all isolates in our investigation, consistent with previous studies (Brumwell et al., 2023), but none of the isolates exhibited the antimicrobial MDR profile of 3MRGN or 4MRGN. *Enterococcus faecium* ST117 was previously identified as a rising factor in vancomycin-resistant enterococci (VRE) (Weber et al., 2020), and five out of six isolates in our study were found to carry *vanB* genes. A comparison with this recent comprehensive study involving 120 isolates revealed that all the genes mentioned in the study (*msrC*, *efmA*, *erm(B)*, *dfrG*, *aac(6')-Ii*, *gyrA*, *parC*, and *pbp5*) matched those present in our isolates, except for *efmA*, which was absent in the NCBI database used. The notable clustering of ST50 *E. quasihormaechei* isolates calls for focused investigations, given the escalating local and global issue of sewage-related clonal colonization in hospital sanitary facilities (Babouee Flury et al., 2016; Kehl et al., 2022; Stokes et al., 2022). Similarly, the recurring identification of ST147 *K. pneumoniae* and ST235 and ST823 *P. aeruginosa* isolates, even in wards geographically distant from those assumed to have a contamination source in our setting (Kehl et al., 2022; Neidhöfer et al., 2023a), urges us to implement transmission dynamics monitoring networks (Bohl et al., 2022; Ko et al., 2022; Neidhöfer et al., 2023b).

Conclusion

Conducting replication studies with larger sample sizes for each species is imperative to cautiously interpret associations between survival outcomes and the presence of specific genes, emphasizing the need for further research in this area. A deeper understanding of virulence and host factors will not only aid in the interpretation of results but also pave the way for the development of more targeted therapeutic and preventive measures, thus enhancing patient outcomes. In addition, implementing more efficient transmission dynamics monitoring holds significant promise as a valuable tool in preventing bloodstream infections caused by certain pathogens, highlighting the importance of establishing robust surveillance systems.

Data availability statement

All data and original contributions presented in the study are included in the article/Supplementary Material, except for genomes that cannot be readily made available because of binding collaboration agreements. These can, however, be made available upon request directed to the corresponding author.

Ethics statement

The studies involving humans were approved by the Ethics Committee of the University Hospital Bonn. The studies were conducted in accordance with the local legislation and institutional requirements. Written informed consent for participation was not required from the participants or the participants' legal guardians/next of kin in accordance with the national legislation and institutional requirements.

Author contributions

CN: Conceptualization, Data curation, Formal Analysis, Investigation, Methodology, Project administration, Supervision, Visualization, Writing – original draft, Writing – review & editing. MN: Formal Analysis, Investigation, Methodology, Software, Visualization, Writing – original draft, Writing – review & editing, Conceptualization, Data curation. RJ: Data curation, Formal Analysis, Methodology, Project administration, Writing – review & editing. BA: Data curation, Writing – review & editing. SU: Data curation, Methodology, Software, Writing – original draft, Writing – review & editing. UN: Data curation, Methodology, Software, Writing – original draft, Writing – review & editing. SG: Data curation, Methodology, Software, Writing – original draft, Writing – review & editing. MP: Conceptualization, Funding acquisition, Project administration, Resources, Supervision, Writing – review & editing.

Funding

The authors declare that no financial support was received for the research, authorship, and/or publication of this article.

Conflict of interest

SG is coinventor of one pending international patent on diagnostic algorithms and chief scientific officer and cofounder of Noscendo GmbH in Duisburg, Germany. SU and UN are employed by Noscendo GmbH.

The remaining authors declare that the research was conducted in the absence of any commercial or financial relationships that could be construed as a potential conflict of interest.

Publisher's note

Supplementary material

The Supplementary Material for this article can be found online at: https://www.frontiersin.org/articles/10.3389/fcimb.2023.1274573/full#supplementary-material

References

Allen, J. P., Snitkin, E., Pincus, N. B., and Hauser, A. R. (2021). Forest and trees: exploring bacterial virulence with genome-wide association studies and machine learning. *Trends Microbiol.* 29 (7), 621–633. doi: 10.1016/j.tim.2020.12.002

Babouee Flury, B., Ellington, M. J., Hopkins, K. L., Turton, J. F., Doumith, M., Loy, R., et al. (2016). Association of novel nonsynonymous single nucleotide polymorphisms in ampD with cephalosporin resistance and phylogenetic variations in ampC, ampR, ompF, and ompC in Enterobacter cloacae isolates that are highly resistant to carbapenems. *Antimicrobial Agents chemotherapy* 60 (4), 2383–2390. doi: 10.1128/AAC.02835-15

Beck, M. A., Handy, J., and Levander, O. A. (2004). Host nutritional status: the neglected virulence factor. *Trends Microbiol.* 12 (9), 417–423. doi: 10.1016/j.tim.2004.07.007

Bohl, J. A., Lay, S., Chea, S., Ahyong, V., Parker, D. M., Gallagher, S., et al. (2022). Discovering disease-causing pathogens in resource-scarce Southeast Asia using a global metagenomic pathogen monitoring system. *Proc. Natl. Acad. Sci.* 119, 11, e2115285119. doi: 10.1073/pnas.2115285119

Brumwell, A., Sutton, G., Lantos, P. M., Hoffman, K., Ruffin, F., Brinkac, L., et al. (2023). Escherichia coli ST131 associated with increased mortality in bloodstream infections from urinary tract source. *J. Clin. Microbiol.*, e00199–e00123. doi: 10.1128/jcm.00199-23

Buchfink, B., Xie, C., and Huson, D. (2015). Fast and sensitive protein alignment using DIAMOND. *Nat. Methods* 12 (1), 59–60. doi: 10.1038/nmeth.3176

Camacho, C., Coulouris, G., Avagyan, V., Ma, N., Papadopoulos, J., Bealer, K., et al. (2009). BLAST+: architecture and applications. *BMC Bioinf.* 10, 421. doi: 10.1186/1471-2105-10-421

Carattoli, A., Zankari, E., García-Fernández, A., Voldby Larsen, M., Lund, O., Villa, L., et al. (2014). In silico detection and typing of plasmids using PlasmidFinder and plasmid multilocus sequence typing. *Antimicrob. Agents Chemother.* 58 (7), 3895–3903. doi: 10.1128/aac.02412-14

Casadevall, A., and Pirofski, L.-a. (2001). Host-pathogen interactions: the attributes of virulence. *J. Infect. Dis.* 184 (3), 337–344. doi: 10.1086/322044

Chan, P. P., and Lowe, T. M. (2019). tRNAscan-SE: searching for tRNA genes in genomic sequences. *Methods Mol. Biol.* 1962, 1–14. doi: 10.1007/978-1-4939-9173-0_1

Edgar, R. C. (2004). MUSCLE: multiple sequence alignment with high accuracy and high throughput. *Nucleic Acids Res.* 32 (5), 1792–1797. doi: 10.1093/nar/gkh340

Epping, L., van Tonder, A. J., Gladstone, R. A.The Global Pneumococcal Sequencing Consortium, , Bentley, S. D., Page, A. J., et al. (2018). SeroBA: rapid high- throughput serotyping of Streptococcus pneumoniae from whole genome sequence data. *Microbial Genomics* 4 (7):e000186. doi: 10.1099/mgen.0.000186

Eren, A. M., Kiefl, E., Shaiber, A., Veseli, I., Miller, S. E., Schechter, M. S., et al. (2021). Community-led, integrated, reproducible multi-omics with anvi'o. *Nat. Microbiol.* 6 (1), 3–6. doi: 10.1038/s41564-020-00834-3

Ewels, P., Peltzer, A., Fillinger, S., Patel, H., Alneberg, J., Wilm, A., et al. (2020). Nahnsen S The nf-core framework for community-curated bioinformatics pipelines. *Nat. Biotechnol.* 38 (3), 276–278. doi: 10.1038/s41587-020-0439-x

Feldgarden, M., Brover, V., Fedorov, B., Haft, D. H., Prasad, A. B., and Klimke, W. (2022). Curation of the AMRFinderPlus databases: applications, functionality and impact. *Microb. Genom.* 8 (6), mgen000832. doi: 10.1099/mgen.0.000832

Feldgarden, M., Brover, V., Gonzalez-Escalona, N., Frye, J. G., Haendiges, J., Haft, D. H., et al. (2021). AMRFinderPlus and the reference gene catalog facilitate examination of the genomic links among antimicrobial resistance, stress response, and virulence. *Sci. Rep.* 11 (1), 12728. doi: 10.1038/s41598-021-91456-0

Hekker, T. A., Groeneveld, A. B., Simoons-Smit, A. M., de Man, P., Connell, H., and MacLaren, D. M. (2000). Role of bacterial virulence factors and host factors in the outcome of Escherichia coli bacteraemia. *Eur. J. Clin. Microbiol. Infect. Dis.* 19, 312–316. doi: 10.1007/s100960050483

Hyatt, D., Chen, G. L., Locascio, P. F., Land, M. L., Larimer, F. W., and Hauser, L. J. (2010). Prodigal: prokaryotic gene recognition and translation initiation site identification. *BMC Bioinf.* 11, 119. doi: 10.1186/1471-2105-11-119

Iguchi, A., Iyoda, S., Kikuchi, T., Ogura, Y., Katsura, K., Ohnishi, M., et al. (2015). A complete view of the genetic diversity of the Escherichia coli O-antigen biosynthesis gene cluster. *DNA Res.* 22 (1), 101–107. doi: 10.1093/dnares/dsu043

Jain, C., Rodriguez-R, L. M., Phillippy, A. M., Konstantinidis, K. T., and Aluru, S. (2018). Aluru S High throughput ANI analysis of 90K prokaryotic genomes reveals clear species boundaries. *Nat. Commun.* 9 (1), 5114. doi: 10.1038/s41467-018-07641-9

Jolley, K. A., Bray, J. E., and Maiden, M. C. J. (2018). Open-access bacterial population genomics: BIGSdb software, the PubMLST.org website and their applications. *Wellcome Open Res.* 3, 124. doi: 10.12688/wellcomeopenres.14826.1

Kehl, K., Schallenberg, A., Szekat, C., Albert, C., Sib, E., Exner, M., et al. (2022). Dissemination of carbapenem resistant bacteria from hospital wastewater into the environment. *Sci. Total Environ.* 806, 151339. doi: 10.1016/j.scitotenv.2021.151339

Ko, K. K. K., Chng, K. R., and Nagarajan, N. (2022). Metagenomics-enabled microbial surveillance. *Nat. Microbiol.* 7 (4), 486–496. doi: 10.1038/s41564-022-01089-w

Lam, M. M. C., Wick, R. R., Watts, S. C., Cerdeira, L. T., Wyres, K. L., and Holt, K. E. (2021). A genomic surveillance framework and genotyping tool for Klebsiella pneumoniae and its related species complex. *Nat. Commun.* 12, 4188. doi: 10.1038/s41467-021-24448-325

Leavis, H. L., Bonten, M. J. M., and Willems, R. J. L. (2006). Identification of high-risk enterococcal clonal complexes: global dispersion and antibiotic resistance. *Curr. Opin. Microbiol.* 9 (5), 454–460. doi: 10.1016/j.mib.2006.07.001

Li, D., Wyrsch, E. R., Elankumaran, P., Dolejska, M., Marenda, M. S., Browning, G. F., et al. (2021). Genomic comparisons of Escherichia coli ST131 from Australia. *Microbial Genomics* 7 (12), 000721. doi: 10.1099/mgen.0.000721

Thomas, C. L., and Lee, S. W. (2012). Knowing is half the battle: Targeting virulence factors of group A streptococcus for vaccine and therapeutics. *Curr. Drug Targets* 13 (3), 308–322. doi: 10.2174/138945012799424679

Mahfouz, N., Ferreira, I., Beisken, S., von Haeseler, A., and Posch, A. E. (2020). Large-scale assessment of antimicrobial resistance marker databases for genetic phenotype prediction: a systematic review. *J. Antimicrobial Chemotherapy* 75 (11), 3099–3108. doi: 10.1093/jac/dkaa257

McNamara, J. F., Righi, E., Wright, H., Hartel, G. F., Harris, P. N. A., and Paterson, D. L. (2018). Long-term morbidity and mortality following bloodstream infection: a systematic literature review. *J. Infection* 77 (1), 1–8. doi: 10.1016/j.jinf.2018.03.005

Neidhöfer, C., Sib, E., Neuenhoff, M., Schwengers, O., Dummin, T., Buechler, C., et al. (2023a). Hospital sanitary facilities on wards with high antibiotic exposure play an important role in maintaining a reservoir of resistant pathogens, even over many years. *Antimicrobial Resistance Infection Control* 12 (1), 1–17. doi: 10.1186/s13756-023-01236-w

Neidhöfer, C., Sib, E., Benhsain, A. H., Mutschnik-Raab, C., Schwabe, A., Wollkopf, A., et al. (2023b). Examining different analysis protocols targeting hospital sanitary facility microbiomes. *Microorganisms* 11 (1), 185. doi: 10.3390/microorganisms11010185

Newman, J. W., Floyd, R. V., and Fothergill, J. L. (2017). The contribution of Pseudomonas aeruginosa virulence factors and host factors in the establishment of urinary tract infections. *FEMS Microbiol. Lett.* 364 (15). doi: 10.1093/femsle/fnx124

Petit, R. A. III, and Read, T. D. (2020). Bactopia: a flexible pipeline for complete analysis of bacterial genomes. *mSystems.* 5 (4), e00190–20. doi: 10.1128/mSystems.00190-2024

Pitout, J. D. D., and Finn, T. J. (2020). The evolutionary puzzle of Escherichia coli ST131. *Infection Genet. Evol.* 81, 104265. doi: 10.1016/j.meegid.2020.104265

Pritchard, L., Glover, R. H., Humphris, S., Elphinstone, J. G., and Toth, I. K. (2016). Genomics and taxonomy in diagnostics for food security: soft-rotting enterobacterial plant pathogens. *Anal. Methods* 8, 12–24. doi: 10.1039/C5AY02550H

Shaw, K. J., Rather, P. N., Hare, R. S., and Miller, G. H. (1993). Molecular genetics of aminoglycoside resistance genes and familial relationships of the aminoglycoside-modifying enzymes. *Microbiological Rev.* 57 (1), 138–163. doi: 10.1128/mr.57.1.138-163.1993

Shen, W. (2021). Csvtk–A Cross-Platform. *Efficient and Practical CSV/TSV Toolkit in Golang.*

Stach, N., Kalinska, M., Zdzalik, M., Kitel, R., Karim, A., Serwin, K., et al. (2018). Unique substrate specificity of SplE serine protease from Staphylococcus aureus. *Structure* 26 (4), 572–579. doi: 10.1016/j.str.2018.02.008

Stokes, W., Peirano, G., Matsumara, Y., Nobrega, D., and Pitout, J. D. D. (2022). Population-based surveillance of Enterobacter cloacae complex causing blood stream infections in a centralized Canadian region. *Eur. J. Clin. Microbiol. Infect. Dis.* 41, 119–125. doi: 10.1007/s10096-021-04309-z

Taati Moghadam, M., Mirzaei, M., Fazel Tehrani Moghaddam, M., Babakhani, S., Yeganeh, O., Asgharzadeh, S., et al. (2021). The challenge of global emergence of novel colistin-resistant Escherichia coli ST131. *Microbial Drug resistance* 27 (11), 1513–1524. doi: 10.1089/mdr.2020.0505

Hemlata, J. A. T., and Tiwari, A. (2017). The ever changing face of antibiotic resistance: Prevailing problems and preventive measures. *Curr. Drug Metab.* 18 (1), 69–77. doi: 10.2174/1389200217666161014163324

Thrane, S. W., Taylor, V. L., Lund, O., Lam, J. S., and Jelsbak, L. (2016). Application of whole- genome sequencing data for O-specific antigen analysis and in silico serotyping of pseudomonas aeruginosa isolates. *J. Clin. Microbiol.* 54 (7), 1782–1788. doi: 10.1128/JCM.00349-16

Tseng, C.-C., Wu, J. J., Liu, H. L., Sung, J. M., and Huang, J. J. (2002). Roles of host and bacterial virulence factors in the development of upper urinary tract infection caused by Escherichia coli. *Am. J. Kidney Dis.* 39 (4), 744–752. doi: 10.1053/ajkd.2002.32992

Tseng, C.-C., Wu, J. J., Wang, M. C., Hor, L. I., Ko, Y. H., and Huang, J. J. (2005). Host and bacterial virulence factors predisposing to emphysematous pyelonephritis. *Am. J. Kidney Dis.* 46 (3), 432–439. doi: 10.1053/j.ajkd.2005.05.019

Wang, M., Jiang, L., Wei, J., Zhu, H., Zhang, J., Liu, Z., et al. (2022). Similarities of P1-like phage plasmids and their role in the dissemination of bla CTX-M-55. *Microbiol. Spectr.* 10 (5), e01410-22. doi: 10.1128/spectrum.01410-22

Weber, A., Maechler, F., Schwab, F., Gastmeier, P., and Kola, A. (2020). Increase of vancomycin-resistant Enterococcus faecium strain type ST117 CT71 at Charité - Universitätsmedizin Berlin, 2008 to 2018. *Antimicrob. Resist. Infect. Control* 9 (1), 109. doi: 10.1186/s13756-020-00754-1

Wick, R. R., Judd, L. M., Cerdeira, L. T., Hawkey, J., Méric, G., Vezina, B., et al. (2021). Trycycler: consensus long-read assemblies for bacterial genomes. *Genome Biol.* 22, 266. doi: 10.1186/s13059-021-02483-z

Wren, B. W. (2000). Microbial genome analysis: insights into virulence, host adaptation and evolution. *Nat. Rev. Genet.* 1 (1), 30–39. doi: 10.1038/35049551

Wyres, K. L., Lam, M. M. C., and Holt, K. E. (2020). Population genomics of Klebsiella pneumoniae. *Nat. Rev. Microbiol.* 18 (6), 344–359. doi: 10.1038/s41579-019-0315-1

frontiers | Frontiers in Cellular and Infection Microbiology

TYPE Original Research
PUBLISHED 18 December 2023
DOI 10.3389/fcimb.2023.1278819

OPEN ACCESS

EDITED BY
Margarita María de la paz Arenas-Hernandez,
Benemérita Universidad Autónoma de Puebla, Mexico

REVIEWED BY
Paul G Higgins,
University of Cologne, Germany
German Matias Traglia,
Universidad de La Republica, Salto, Uruguay, Uruguay
Andres Felipe Opazo-Capurro,
University of Concepcion, Chile

*CORRESPONDENCE
María Dolores Alcántar-Curiel
alcantar@unam.mx

RECEIVED 16 August 2023
ACCEPTED 01 December 2023
PUBLISHED 18 December 2023

CITATION
Fernández-Vázquez JL, Hernández-González IL, Castillo-Ramírez S, Jarillo-Quijada MD, Gayosso-Vázquez C, Mateo-Estrada VE, Morfín-Otero R, Rodríguez-Noriega E, Santos-Preciado JI and Alcántar-Curiel MD (2023) Pandrug-resistant *Acinetobacter baumannii* from different clones and regions in Mexico have a similar plasmid carrying the bla_{OXA-72} gene. *Front. Cell. Infect. Microbiol.* 13:1278819. doi: 10.3389/fcimb.2023.1278819

Pandrug-resistant *Acinetobacter baumannii* from different clones and regions in Mexico have a similar plasmid carrying the bla_{OXA-72} gene

José Luis Fernández-Vázquez[1], Ismael Luis Hernández-González[2], Santiago Castillo-Ramírez[2], Ma Dolores Jarillo-Quijada[1], Catalina Gayosso-Vázquez[1], Valeria Eréndira Mateo-Estrada[2], Rayo Morfín-Otero[3], Eduardo Rodríguez-Noriega[3], José Ignacio Santos-Preciado[1] and María Dolores Alcántar-Curiel[1]*

[1]Laboratorio de Infectología, Microbiología e Inmunología Clínica, Unidad de Investigación en Medicina Experimental, Facultad de Medicina, Universidad Nacional Autónoma de México, Ciudad de México, Mexico, [2]Programa de Genómica Evolutiva, Centro de Ciencias Genómicas, Universidad Nacional Autónoma de México, Cuernavaca, Mexico, [3]Hospital Civil de Guadalajara "Fray Antonio Alcalde" e Instituto de Patología Infecciosa y Experimental, Centro Universitario de Ciencias de la Salud, Universidad de Guadalajara, Guadalajara, Mexico

Background: Multidrug-resistant *Acinetobacter baumannii* is a common hospital-acquired pathogen. The increase in antibiotic resistance is commonly due to the acquisition of mobile genetic elements carrying antibiotic resistance genes. To comprehend this, we analyzed the resistome and virulome of Mexican *A. baumannii* multidrug-resistant isolates.

Methods: Six clinical strains of *A. baumannii* from three Mexican hospitals were sequenced using the Illumina platform, the genomes were assembled with SPAdes and annotated with Prokka. Plasmid SPAdes and MobRecon were used to identify the potential plasmid sequences. Sequence Type (ST) assignation under the MLST Oxford scheme was performed using the PubMLST database. Homologous gene search for known virulent factors was performed using the virulence factor database VFDB and an *in silico* prediction of the resistome was conducted via the ResFinder databases.

Results: The six strains studied belong to different STs and clonal complexes (CC): two strains were ST208 and one was ST369; these two STs belong to the same lineage CC92, which is part of the international clone (IC) 2. Another two strains were ST758 and one was ST1054, both STs belonging to the same lineage CC636, which is within IC5. The resistome analysis of the six strains identified between 7 to 14 antibiotic resistance genes to different families of drugs, including beta-lactams, aminoglycosides, fluoroquinolones and carbapenems. We detected between 1 to 4 plasmids per strain with sizes from 1,800 bp to 111,044 bp. Two strains from hospitals in Mexico City and

Guadalajara had a plasmid each of 10,012 bp pAba78r and pAba79f, respectively, which contained the bla_{OXA-72} gene. The structure of this plasmid showed the same 13 genes in both strains, but 4 of them were inverted in one of the strains. Finally, the six strains contain 49 identical virulence genes related to immune response evasion, quorum-sensing, and secretion systems, among others.

Conclusion: Resistance to carbapenems due to pAba78r and pAba79f plasmids in Aba pandrug-resistant strains from different geographic areas of Mexico and different clones was detected. Our results provide further evidence that plasmids are highly relevant for the horizontal transfer of antibiotic resistance genes between different clones of *A. baumannii*.

KEYWORDS

***Acinetobacter baumannii*, pandrug-resistant, bla_{OXA-72} gene, plasmid, Mexico**

Introduction

Acinetobacter baumannii is a Gram-negative, non-spore-forming, strictly aerobic, non-flagellated exhibiting twitching motility catalase positive, oxidase negative bacterium (Wilharm et al., 2013). It is an opportunistic pathogen that can colonize the skin and cause various healthcare-associated infections (HAIs); predominantly pneumonia and catheter-associated bacteremia but can also cause soft tissue and urinary tract infections (Wong et al., 2017). Infections caused by *A. baumannii* commonly occur in immunocompromised patients with a high incidence in hospital settings. These infections contribute to attributable mortality rates that range from 5% in general hospital wards to as high as 54% in ICUs (Shahryari et al., 2021).

Due to its intrinsic resistance to numerous antimicrobial agents and its ability to efficiently acquire various resistance mechanisms, *A. baumannii* isolates are frequently multi-drug-resistant (MDR) or extensively drug-resistant (XDR). In this regard, carbapenem-resistant *A. baumannii* (CRAB) has been recognized as a critical priority pathogen in the World Health Organization´s priority list of antibiotic-resistant bacteria (Kabic et al., 2023). This species belongs to the so-called "ESKAPE group", which also includes *Enterococcus faecium*, *Staphylococcus aureus*, *Klebsiella pneumoniae*, *Pseudomonas aeruginosa*, and *Enterobacter* species (Karlowsky et al., 2017). These bacteria not only cause the majority of HAIs but also represent different paradigms of pathogenicity, transmission, and antimicrobial resistance, posing a serious threat to hospitals (Jie et al., 2021).

One significant mechanism of carbapenem resistance involves the hydrolysis of carbapenems by carbapenemase enzymes, which are predominantly encoded on plasmids and, in some cases, on the chromosome, such as oxacillinases. The enzymes carbapenemases exhibited a high degree of transmissibility (Nordmann and Poirel, 2013; Nordmann and Poirel, 2019; Graña-Miraglia et al., 2020). Among carbapenem-resistant *A. baumannii* strains from Latin American countries, the most widely disseminated carbapenemases belong to the class D enzymes (Rodríguez et al., 2018), which include OXA-23, OXA-58, OXA-72, OXA-143 and OXA-253; however, NDM-1, VIM-1, IMP-1, and IMP-10 have also been detected (Nordmann and Poirel, 2019).

Several studies have demonstrated that *A. baumannii* has a natural ability to incorporate exogenous DNA through horizontal gene transfer (HGT), including antibiotic resistance determinants (Traglia et al., 2014). The frequent identification of foreign DNA in its genome explains the genomic plasticity of this pathogen (Lee et al., 2017); HGT is the main mechanism for acquiring new traits, such as antimicrobial resistance genes, allowing the survival of bacterial species with high genetic plasticity (Partridge et al., 2018). Currently, there is a particular interest in studying plasmids carrying genes encoding OXA-type beta-lactamases, which are the primary mechanism of carbapenem resistance in *A. baumannii* (Salgado-Camargo et al., 2020).

Whole-genome sequencing techniques, combined with bioinformatic tools, have been of great help not only to identify the entire gene background that a strain possesses but also to determine different replicons and the genes encoded within them (Graña-Miraglia et al., 2020). Here, we sequenced six Mexican strains of *A. baumannii* sampled from three hospitals to obtain information about the resistome, virulome, and structural dynamics of antimicrobial resistance plasmids.

Materials and methods

Study design, settings, and isolates

We selected six *A. baumannii* strains isolated from patients with healthcare-associated infections (HAIs) from three tertiary referral hospitals in different geographic areas in Mexico: four strains were

collected at Hospital Regional General Ignacio Zaragoza (HRGIZ), Instituto de Seguridad y Servicios Sociales de los Trabajadores del Estado (ISSSTE) in Mexico City, Mexico; one strain at Pediatric ward of the Hospital General de México Eduardo Liceaga (HGM-P) in Mexico City, Mexico and one strain at Hospital Civil de Guadalajara, Fray Antonio Alcalde (HCG) in Guadalajara Jalisco, Mexico (Alcántar-Curiel et al., 2019b). Strains were grown in LB medium overnight at 37°C and stored in glycerol 20% at -80°C until analysis.

Antimicrobial susceptibility testing

Antimicrobial susceptibility testing was done by the automated VITEK®-2 System. Microdilution broth method was used to determinate MICs of colistin according to Clinical and Laboratory Standards Institute guidelines (CLSI) (Lewis and Pharm, 2023) using *Escherichia coli* ATCC 25922 as quality control strain. We employed the antimicrobial categories as proposed by Magiorakos including the multidrug-resistant (MDR), extensively drug-resistant (XDR), and pandrug-resistant (PDR) phenotypes (Magiorakos et al., 2012).

Pulsed-field gel electrophoresis

Genotyping of *A. baumannii* strains was determined by Pulsed-Field Gel Electrophoresis (PFGE) as described previously (Naas et al., 2005; Alcántar-Curiel et al., 2014). Briefly, genomic DNA from all strains was digested with ApaI (New England Biolabs, Beverly, MA) embedded in 1% agarose plugs and then subjected to PFGE with a Gene Path system (BioRad) and using lambda ladder PFGE marker (New Englands Biolabs, Beverly) as molecular marker. The PFGE patterns were analyzed using the GelJ Software (Heras et al., 2015), and individual pulse type (PT) were defined according to the interpretative criteria proposed by Tenover (Tenover et al., 1995). The similarity between profiles was calculated using the Dice coefficient (Dice, 1945), every strain with a correlation greater than 85% was considered as member of the same PT.

Plasmids characterization

Plasmids content in *A. baumannii* isolates was detected using a gentle lysis procedure for both chromosomal and plasmid DNA, followed by separation through electrophoresis using the Eckhardt technique (Eckhardt, 1978; Alcántar-Curiel et al., 2019a). As a source for the high molecular weight DNA bacterial artificial chromosomes (BAC) of 67, 86, 101, 122, 145, and 195 Kb were used (González et al., 2006). 1Kb Plus DNA Ladder (ThermoFisher Scientific) was used as low molecular weight markers.

Whole-genome sequence analysis

Total DNA from an isolated colony was extracted using the QIAamp® DNA Mini Kit (Qiagen, Hilden, Germany) according to the manufacturer's instructions. DNA quality and quantity were evaluated by agarose gel electrophoresis. The genome sequencing of the isolates was carried out at of Instituto Nacional de Medicina Genómica (https://www.inmegen.gob.mx/) in Mexico City, Mexico. Samples were sequenced on the Illumina MiSeq platform at 2 x 250 base pair-end read (Mateo-Estrada et al., 2021). Data were assembled using SPAdes 3.13.1 (Bankevich et al., 2012), and genome annotation was performed using Prokka v.1.14.6 (Seemann, 2014). The Multi Locus Sequence Typing (MLST) was performed according to Oxford MLST scheme, as previously described by Bartual et al. (2005) and Pasteur MLST scheme, as previously described by Diancourt et al. (2010). The ST was designated according to the allelic profiles in the PubMLST database (http://pubmlst.org/abaumannii/). Based on the eBURST and neighbour-joining diagram approach generated by the Phyloviz 2.0 program, MLST clonal complexes (CC) and evolutionary relationships between *A. baumannii* strains were defined (Toledano-Tableros et al., 2021). Antibiotic resistance genes (ARGs) were identified using ResFinder 4.1 (Bortolaia et al., 2020). Virulence-associated genes were identified using the virulence factor database VFDB 2.0 (Darmancier et al., 2022). The mobile genetic elements were characterized using plasmidSPAdes v3.11.1 (Antipov et al., 2016) y MOB-suite v3.0.3 (Robertson and Nash, 2018; Robertson et al., 2020).

Data access

The whole genome sequences have been deposited at GenBank under the accession numbers JAUPJZ000000000, JAUPJY000000000, JAUPJX000000000, JAUPJW000000000, JAUPJV000000000, JAUPJU000000000 (BioProject PRJNA997334). The accession number of the plasmids is OR436916, OR436917, OR436918, OR436919, OR436920, OR436921, OR436922, OR436923.

Results

Clinical data and antibiotic susceptibility pattern

The six *A. baumannii* strains investigated in this study were obtained from clinical samples. The strains Aba/76 and Aba/78 were isolated from cerebrospinal fluid, while Aba/75, Aba/77, Aba/79, and Aba/80 were derived from blood samples. Aba/76, Aba/77, and Aba/78 were isolated from patients who were admitted to the Intensive Care Unit, Aba/75 from a patient in the Internal Medicine department, Aba/79 from a Cardiology patient, and Aba/80 from a Pediatrics patient. Regarding comorbidities, Aba/79 and Aba/80 were isolated from patients with catheter-associated bacteremia, Aba/75 from a patient with septic shock, Aba/76 from a patient with an aneurysm, Aba/77 from a patient who had suffered traumatic brain injury, and Aba/79 from a patient with a pituitary microadenoma. Strains Aba/75, Aba/78 and Aba/79 exhibited a PDR profile demonstrating resistance to aminoglycosides, second- and third-generation cephalosporins, fluoroquinolones,

10.3389/fcimb.2023.1278819

tetracyclines, carbapenems and colistin. The remaining three strains Aba/76, Aba/77 and Aba80 displayed an XDR profile, with one of them showcasing resistance to colistin (Table 1).

The isolates belong to IC2 and IC5

The isolates were genotyped using PFGE. Among the four strains obtained from ISSSTE, Aba/75 and Aba/76 exhibited macrorestriction patterns with over 85% similarity, both assigned to PT1. We further evaluated the genomic similarity between Aba/75 and Aba/76 using CJ Bioscience's online Average Nucleotide Identity (ANI) calculator, which revealed a remarkable 99.97% identity in their genomic sequences. Strain Aba/77 was categorized as PT2, while strain Aba/78 was assigned to PT3. Notably, Aba/78 was associated with a nosocomial outbreak. Strain Aba/79 from HCG was designated as PT4, and the strain from HGM, Aba/80, was classified as PT5 (Figure 1).

Pasteur MLST analysis identified that isolates Aba/75, Aba/76, and Aba/78 belonged to ST2, whereas isolates Aba/77, Aba/79, and Aba/80 belonged to ST156. Using the Oxford MLST data, we ascertained that Aba/75 and Aba/76 PT1 strains belonged to ST208, which is part of CC92 within IC2. The strain Aba/77 PT2 and Aba/79 PT4 belonged to ST758, CC636, a member of IC5. The strain Aba/78 PT3 belonged to ST369, CC92, a member of IC2, and strain Aba/80 PT5, belonged to ST1054, CC636, a member of IC5 (Table 2). Interestingly, three strains belonged to CC92, a member of IC2, and the other three strains belonged to CC636, a member of IC5 (Table 2; Figure 2).

Resistome and virulome of *A. baumannii* strains

Molecular analysis identified the highest number of ARGs in strain Aba/78 with 14 genes. The strains of the same PT1 Aba/75 and Aba/76 harboured the same number of the ARGs, with 10 genes. Strains Aba/77 and Aba/79 (both ST758) harboured 8 and 7 genes respectively, while strain Aba/80 harboured 8 genes (Table 2). The identified ARGs mainly belonged to the families of macrolides, fluoroquinolones, and aminoglycosides. Additionally, genes for resistance to carbapenems (last-line drugs against *A. baumannii*) were identified in all strains.

Analysis of the virulome of six strains revealed the presence of 49 similar genes in all clinical isolates. These genes are involved in adherence, biofilm formation, enzymes, immune evasion, iron uptake, regulation, serum resistance, and stress adaptation (Supplementary Table 1). These findings underscore the pathogenic potential exhibited by the majority of strains within the *A. baumannii* complex.

Plasmids identification, genome rearrangements, and carriage of ARGs

Experimental assays showed that strain Aba/79 had the highest number of replicons, with four plasmids of sizes 14,000 bp, 6,500

TABLE 1 Antimicrobial susceptibility profiles of six isolates of *A. baumannii* from Mexican hospitals.

No. Isolate-Hospital	Categories[a] antimicrobial resistance	MIC µg/mL[b]							
		Amikacin	Gentamicin	Cefotaxime	Cefepime	Levofloxacin	Tetracycline	Imipenem	Meropenem	Colistin
Aba/75-HRGIZ	PDR	>128 (R)	>128 (R)	>128 (R)	64 (R)	32 (R)	>128 (R)	8 (R)	8 (R)	16 (R)
Aba/76-HRGIZ	XDR	>128 (R)	>128 (R)	>128 (R)	32 (R)	8 (R)	>128 (R)	4 (I)	8 (R)	1 (S)
Aba/77-HRGIZ/	XDR	32 (I)	2 (S)	>128 (R)	>128 (R)	16 (R)	16 (R)	64 (R)	16 (R)	32 (R)
Aba/78-HRGIZ	PDR	>128 (R)	>128 (R)	>128 (R)	>128 (R)	16 (R)	>128 (R)	128 (R)	>128 (R)	32 (R)
Aba/79-HCG	PDR	32 (I)	32 (R)	>128 (R)	32 (R)	16 (R)	32 (R)	64 (R)	128 (R)	32 (R)
Aba/80-HGM-P	XDR	>128 (R)	>128 (R)	>128 (R)	128 (R)	32 (R)	>128 (R)	>128 (R)	128 (R)	2 (S)

[a]Multidrug resistance criterion proposed by Magiorakos et al., 2012; MDR, multidrug-resistant; XDR, extensively drug-resistant; PDR, pandrug-resistant.
[b]MIC, Minimum Inhibitory Concentration; I, intermediate susceptibility; R, resistant; S, susceptible; HRGIZ, Hospital Regional General Ignacio Zaragoza, Instituto de Seguridad y Servicios Sociales de los Trabajadores del Estado, Mexico City; HGM-P, Pediatric ward of the Hospital General de México Eduardo Liceaga, Mexico City; HCG, Hospital Civil de Guadalajara, Fray Antonio Alcalde, Guadalajara, Jalisco.

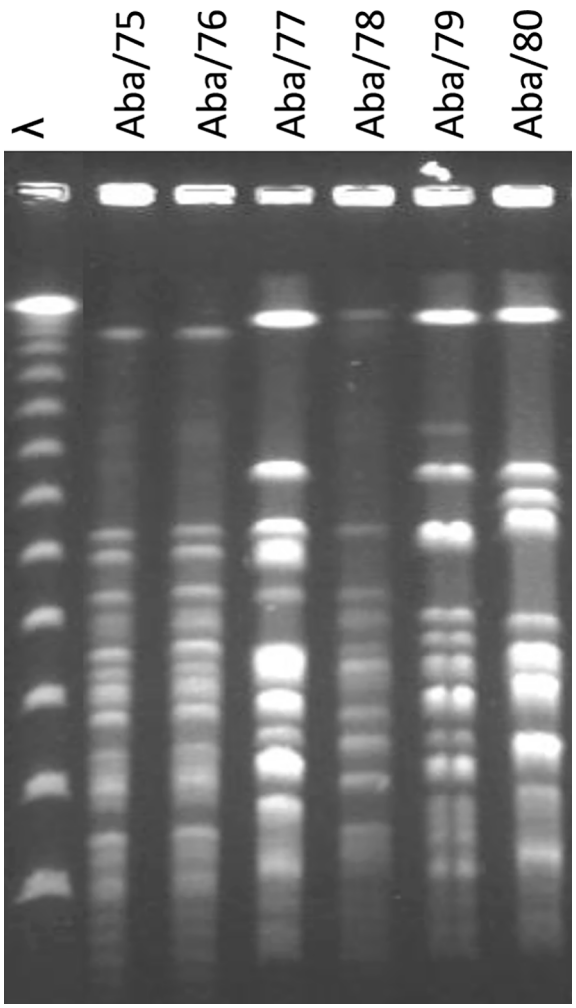

FIGURE 1
Electrophoretic PFGE pattern of *A. baumannii* strains. λ: Molecular marker.

bp, 3,200 bp and 1,800 bp. Strain Aba/77 harbour two plasmids with sizes of 14,000 bp and 3,200 bp. Strain Aba/80 harboured three plasmids with sizes of 14,000 bp, 3,200 bp and 2,100 bp. Finally strains Aba/75, Aba/76 and Aba/78 do not harbor plasmids (Table 3; Figure 3). Based on *in silico* analysis and genome assemblies, four plasmids of sizes 16,610 bp, 10,012 bp, 5,358 bp, and 2,803 bp were identified in the Aba/79 strain. In the Aba/77 strain, two plasmids of sizes 15,362 bp and 5,358 bp were identified, while in the Aba/80 strain, two plasmids of sizes 15,365 bp and 5,358 bp were identified. Additionally, a plasmid of 111,044 bp was detected in the Aba/75 and Aba/76 strains and a plasmid of 10,012 bp in Aba/78 strain (Table 3). However, as previously indicated, no plasmids were identified in these three strains through experimental assays.

Using ResFinder, the ARGs carried in each replicon were identified. In the case of strain Aba/79, which had four replicons, only the 10,012 bp plasmid harbored the bla_{OXA-72} gene, conferring carbapenem resistance, we named this plasmid pAba79f. The plasmid of the same size 10,012 bp in strain Aba/78 also contained the bla_{OXA-72} gene (ID GenBank: AY739646), which we named pAba78r. The nucleotide sequence alignment of these two plasmids of the same size that contained the bla_{OXA-72} gene showed a 73% close relationship. In these two plasmids, we identified an IS701 sequence located 433 base pairs upstream of the bla_{OXA-72} gene. It was found that the plasmids in strains Aba/75, Aba/76 and Aba/80 did not contain any ARGs.

The analysis of the sequences of both plasmids pAba79f and pAba78r strains using BLASTN (https://blast.ncbi.nlm.nih.gov/Blast.cgi) showed that these plasmids have matched with the circular plasmid pAba10042a of 10,062 bp from *A. baumannii* strain 10042 (ID Gen Bank: NZ_CP023027.1). The analysis of the genome information revealed that both plasmids had 13 coding sequences (CDS) (Figure 4A). Among these, six encode hypothetical proteins, one encodes an IS701 transposase, one encodes the carbapenemase bla_{OXA-72}, one encodes a plasmid mobilization protein MobA/MobB, one encodes a replication inhibitor protein RepM, one encodes a Mer regulatory protein, one encodes a DNA-binding protein Arc, and one encodes a MarR transcriptional regulator.

Although the plasmids pAba79f and pAba78r have the same size and the same number of CDS, their structures are different. A region of 4 CDS which includes a hypothetical protein, MobA, RepM and Mer, is inverted between the two plasmids (Figure 4A). The nucleotide sequence of the pAba10042a plasmid obtained from Gen Bank exhibits the same genetic organization as the pAba79f plasmid from Aba/79 strain (Figure 4A).

To delve deeper into the dynamics and persistence of plasmids, resistance gene transfer and genetic rearrangements, we selected the genome sequences of five *A baumannii* strains belonging to ST369 (53, 58, 64, 70, 73), from Mateo 2021 et al. and three strains belonging to ST758 (43, 63, 69) sharing the same ST as strains Aba/78 y Aba/79, respectively. Plasmid analysis was conducted in these strains, revealing that strain 73 possesses the pAba10042a plasmid of 10,062 bp, while strain 58 has a plasmid with the same size but a lower number of CDS (13 and 12, respectively), which we named pAba58. Strain 70 harbours a plasmid of 5,464 bp, which we named pAba70F. However, strains 53 and 64 do not have any replicons. As for the three ST758 strains, the pAba10042a of 10,062 bp was identified in all of them. Interestingly, the search for ARGs revealed that all the 10,062 bp and 5,464 bp plasmids harbour the bla_{OXA-72} gene (Figure 4B). From the analysis of gene structure in the plasmids, we observed that, except for strains 58 and 70, which lack one or more genes, all other strains retained the same structure and orientation as the pAba10042a plasmid (Figure 4B). Finally, it is noteworthy that no virulence genes were found in the sequence of the pAba10042a plasmids in each strain.

Discussion

A. baumannii is a bacterium of significant interest and concern in the hospital environment due to its ability to cause HAIs. This pathogen has become a global public health problem due to its increasing antimicrobial resistance, which hinders its treatment and control. One of the main features of *A. baumannii* is its capacity to acquire antimicrobial resistance genes through the lateral transfer of

TABLE 2 Antibiotic resistance genes in *A. baumannii* strains.

No. strain	Aba/75	Aba/76	Aba/77	Aba/78	Aba/79	Aba/80
Pulse Type/Sequence Type/Clonal Complex/ International Clonal	PT1/ST208/ CC92/IC2	PT1/ST208/ CC92/IC2	PT2/ST758/ CC636/IC5	PT3/ST369/ CC92/IC2	PT4/ST758/ CC636/IC5	PT5/ST1054/ CC636/IC5
Total resistance genes	10 genes	10 genes	8 genes	14 genes	7 genes	8 genes
Antibiotic resistance gene	*bla*$_{ADC-25}$	*bla*$_{ADC-25}$	*bla*$_{ADC-25}$	*bla*$_{ADC-25}$	*bla*$_{ADC-25}$	*bla*$_{ADC-25}$
	bla$_{OXA-66}$	*bla*$_{OXA-66}$		*bla*$_{OXA-66}$		
			bla$_{OXA-65}$		*bla*$_{OXA-65}$	*bla*$_{OXA-65}$
			bla$_{OXA-239}$			*bla*$_{OXA-239}$
			bla$_{OXA-72}$	*bla*$_{OXA-72}$	*bla*$_{OXA-72}$	
				bla$_{TEM-1}$		
	aph(3'')-Ib	*aph(3'')-Ib*	*aph(3'')-Ib*	*aph(3'')-Ib*	*aph(3'')-Ib*	*aph(3'')-Ib*
	aph(6)-Id	*aph(6)-Id*	*aph(6)-Id*	*aph(6)-Id*	*aph(6)-Id*	*aph(6)-Id*
	aph(3')-Ia	*aph(3')-Ia*				
						aph(3')-VIa
				aac(6')-Ib-cr		
				aac(6')-Ib3		
				aadA1		
	armA	*armA*		*arma*		
			aac(6')-Ian		*aac(6')-Ian*	*aac(6')-Ian*
	mph(E)	*mph(E)*				
	msr(E)	*msr(E)*				
	sul2	*sul2*	*sul2*		*sul2*	*sul2*
				sul1		
				catB8		
	tet(B)	*tet(B)*		*tet(B)*		
				qacE		

bla$_{ADC-25}$, Cephalosporinase. *bla*$_{OXA-66}$ and *bla*$_{OXA-65}$, Beta-lactam resistance. *bla*$_{OXA-239}$, and *bla*$_{OXA-72}$, Carbapenem resistance. *bla*$_{TEM-1}$, Beta-lactam resistance. aph(3'')-Ib, *aph(6)-Id, aph(3')-Ia, aph(3')-vIa, aac(6')-Ib3, aadA1, armA*, and *aac(6')-Ian, aac(6')-Ib-cr*, Aminoglycoside resistance. *mph(E)*, Macrolide resistanc. *msr(E)*, Macrolide, Lincosamide and Streptogramin B resistance. *sul1* and *sul2*, Sulphonamide resistance. *catB8*, Phenicol resistance. *tet(B)*, Tetracycline resistance; *qacE*, Disinfectant resistance.

genetic material between different strains, with diverse geographical origins (Graña-Miraglia et al., 2020). In this study, conducted on *A. baumannii* PDR and *A. baumannii* XDR strains from three hospitals and two geographic areas in Mexico, the dissemination of strains with similar PFGE patterns was observed (Figure 1). For example, PT1 detected in 2 strains from ISSSTE (Aba/1 and Aba/2), corresponds to clone G previously reported by Alcántar-Curiel in 2019 at ISSSTE, México City, from where these isolates originated. It also corresponds to clone 22 previously reported by Alcántar-Curiel in 2014 strains from HCG, Guadalajara. The distance between these two hospitals is 540 Km. Therefore, we can conclude that this pulse type has been disseminated for at least five years in Mexico.

The eBURST and ST assignment analyses of the strains identified two groups. Group IC2 comprises Aba/75 and Aba/76 of ST208, and Aba/78 of ST369, all of which are members of CC92 (Figure 2). Group IC5 includes Aba/77 and Aba/79 of ST758, and Aba/80 of ST1054, all of which are members of CC636 (Figure 2). Although ST208 was identified in a strain from ISSSTE in Mexico City, it has been previously identified in San Luis Potosí, México (Tamayo-Legorreta et al., 2016), Guadalajara, Jalisco, México (Mateo-Estrada et al., 2021), and Mexico City (Alcántar-Curiel et al., 2019b; Alcántar-Curiel et al., 2023). Similarly, ST369 identified in a strain from ISSSTE in Mexico City, has been previously described in Nuevo León, Mexico (Bocanegra-Ibarias et al., 2015), Guadalajara, Jalisco, Mexico (Mateo-Estrada et al., 2021), and by our group (Alcántar-Curiel et al., 2019b; Alcántar-Curiel et al., 2023).

The IC5 strains were identified in all three hospitals included in the study. The strains Aba/77 from ISSSTE and Aba/79 from HCG belong to ST758, which has been previously described in four hospitals in Mexico City (Tamayo-Legorreta et al., 2014; Graña-Miraglia et al., 2017; Mancilla-Rojano et al., 2019) and Guadalajara, Jalisco, México (Alcántar-Curiel et al., 2019b; Mateo-Estrada et al.,

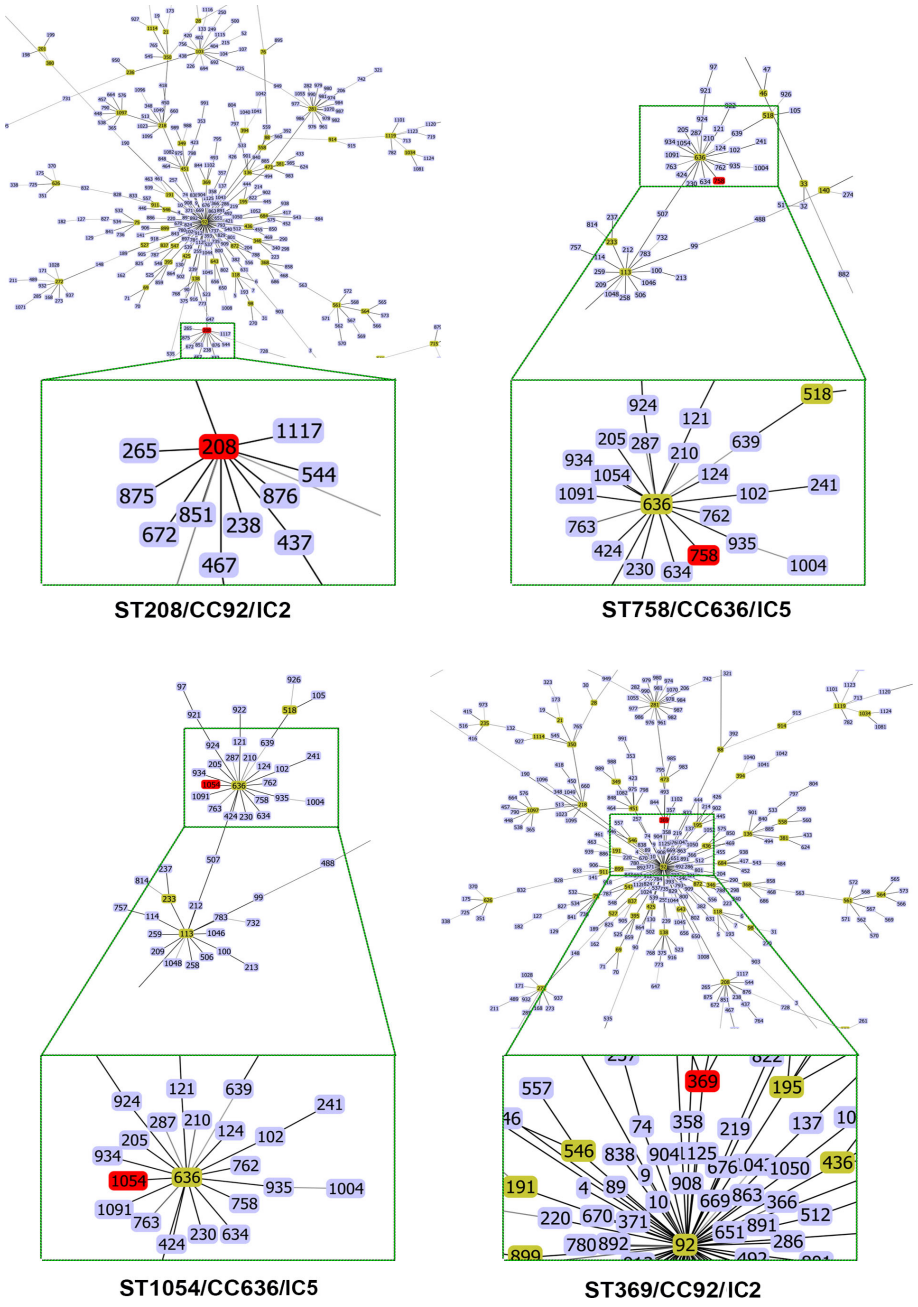

FIGURE 2
eBurst diagrams for Oxford MLST schemes of *A. baumannii* strains with clonal complexes and STs of close-up.

2021). Recently, in 2020 Graña-Miraglia described that ST758 is an endemic clade that emerged recently within IC5 and exhibits considerable variation in terms of antibiotic resistance genes in Mexican strains. According to the PubMLST database, several studies have reported isolates of this ST in Canada (Loewen et al., 2014), Mexico and Honduras (Graña-Miraglia et al., 2017; López-Leal et al., 2019), and in Colombia (Vanegas et al., 2015). Regarding the Aba/80 strain from HGM, it belongs to ST1054, which has been previously described in other hospitals in Mexico City by Alcántar-Curiel in 2019.

The geographic distribution of IC2 is worldwide, including countries in Latin America (Levy-Blitchtein et al., 2018) and the United States of America (Hujer et al., 2017), which share borders with Mexico. Although this clone has not been described as one of the most relevant in Mexico (Graña-Miraglia et al., 2017; Graña-Miraglia et al., 2020), our results highlight its importance in Mexico. As for IC5, it has mainly spread in Latin America. Studies conducted in Brazil, Argentina, Chile and Paraguay (Nodari et al., 2020) report that the main carbapenemase-producing clones belong to CC15 and CC79, corresponding to IC4 and IC5, respectively (Chagas et al., 2014). Due to its presence in North, Central, and South America, IC5 is considered a Pan-American clone, although it has been described in southeastern Europe (Graña-Miraglia et al., 2020). Our results confirm the dissemination of IC2 and IC5 strains

10.3389/fcimb.2023.1278819

TABLE 3 Plasmids identified in *A. baumannii* using Gel Eckhardt and the SPAdes Plasmid/Mobrecon programs.

Strain	Aba/75		Aba/76		Aba/77		Aba/78		Aba/79		Aba/80	
Metodology	Eckhardt	PlasmidSPAdes/MOB-suite	Eckhardt	PlasmidSPAdes/MOB-suite	Eckhardt	PlasmidSPAdes/MOB-suite	Eckhardt	PlasmidSPAdes/MOB-suite	Eckhardt	PlasmidSPAdes/MOB-suite	Eckhardt	PlasmidSPAdes/MOB-suite
Plasmids	N/D	111,044	N/D	111,044	14,000	15,362	N/D	10,012	14,000	16,610	14,000	15,365
					3,200	5,358			6,500	10,012	3,200	5,358
									3,200	5,358	2,100	
									1,800	2,803		

The size is expressed in base pairs. N/D, Not detected.

in Mexico, often exhibiting XDR and PDR (Nodari et al., 2020). Therefore, it is suggested to maintain close surveillance in the hospital environment.

A. *baumannii* strains with XDR and PDR are becoming increasingly prevalent in hospital settings. Therefore, it is becoming more crucial to identify the types of ARGs these pathogens harbor to provide targeted and effective therapies that promote patient health.

To address the increasing problem of antimicrobial resistance and safeguard the effectiveness of antimicrobials, studying the resistome is essential. Our data showed significant diversity in the number of ARGs (Table 2), highlighting that IC2 strains harbored the highest number of AGRs Aba/78 having 14, and Aba/75 and Aba/76 having 10 each. While IC5 strains contained a lower number of AGRs, Aba/77 had 8, Aba/79 had 7 and Aba/80 had 8. Hernández-González et al. (2022) conducted a genomic study of the resistome using complete genomes of *baumannii* published and reported an average of 29.38 ARGs per genome using the CARD program. This number is higher to the number of AGRs detected in the IC2 strains in this study, a clone that has a longer divergence time and is globally distributed. However, the number of AGRs is lower in the ST758 and ST1054 strains belonging to IC5. The first one has recently expanded as reported by Graña-Miraglia in 2017, while there are few reported cases of the second ST.

Another significant finding was the presence of genes encoding carbapenemases. All strains contained $bla_{\text{OXA-51-like}}$ genes, which are intrinsic resistance genes, but the allele, differed for each IC; IC2 strains harbored $bla_{\text{OXA-66}}$, while IC5 strains carried $bla_{\text{OXA-65}}$. IC5 strains Aba/77 and Aba/80 carried $bla_{\text{OXA-239}}$ in the chromosome, which belongs to the $bla_{\text{OXA-23-like}}$ family. Particularly, IC2 strain Aba/78 and IC5 strain Aba/79 shared the presence of the $bla_{\text{OXA-72}}$ gene, which belongs to the $bla_{\text{OXA-40-like}}$ family. Notably, the presence of the IS701 element 433 base pairs upstream of $bla_{\text{OXA-72}}$ strongly supports its association with the carbapenem resistance phenotype. Except for the consistent presence of the $bla_{\text{OXA-72}}$ gene in both IC groups, these findings imply a selective pattern of cephalosporinases and carbapenemase genes within the strains of IC2 and IC5. This selective trend could serve as a potential determinant in tracing their lineage. Our findings align with Ingti et al.'s study (Ingti et al., 2020), highlighting the coexistence of ADC-type and OXA genes in *A. baumannii*, collectively contributing to resistance against extended-spectrum cephalosporins and carbapenems. Nevertheless, the resistance profile of strain Aba/75 to both carbapenems, and the resistance of strain Aba/76 to meropenem in the absence of carbapenemases, suggests the potential involvement of an alternative resistance mechanism, possibly associated with efflux pump activity or the loss of porins.

The virulome of the *A. baumannii* strains was found to be highly conserved in this study. Forty-nine virulence genes were identified in all strains, and the main categories in which they were grouped included biofilm formation, lipopolysaccharide production, acinetobactin synthesis, and regulatory systems. These mechanisms coincide with those described by (Wong et al., 2017; Harding et al., 2018; Ibrahim et al., 2021), which enable the bacteria to persist in adverse environmental conditions.

The acquisition of genetic material through horizontal transfer in *A. baumannii* is a highly successful process that allows the

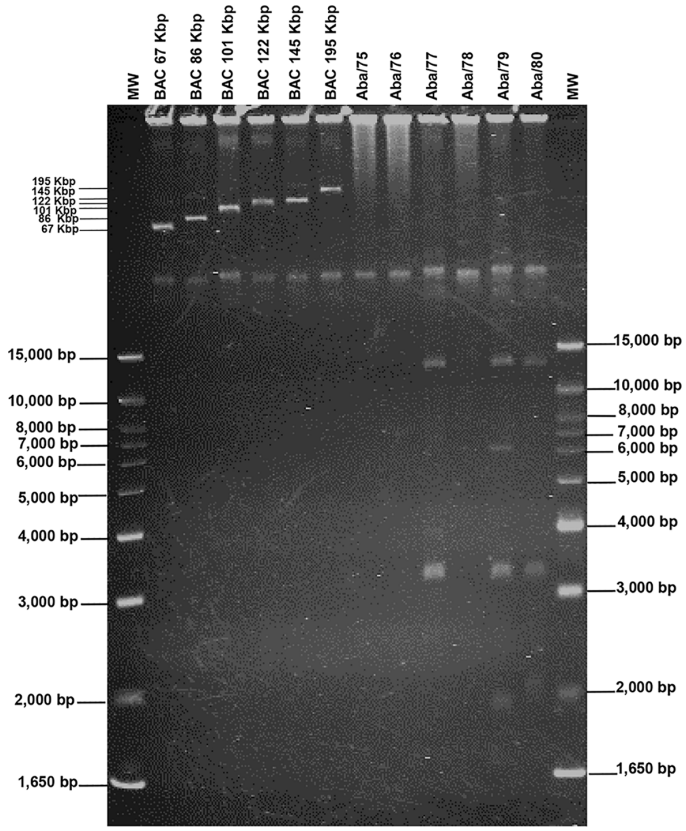

FIGURE 3
Electrophoretic pattern of plasmids in *A. baumannii* strains. BACs, Bacterial Artificial Chromosome used as reference markers for high molecular weight. MW, Molecular Weight (1KB plus DNA Ladder).

bacteria to make changes in its genome, even faster than the mutation process (Graña-Miraglia et al., 2017). The diversity in plasmid sizes found in strains of this study is consistent with the sizes described in various studies, ranging from 1.8 kb to over 100 kb, with smaller plasmids being carriers of ARGs generating the most interest (Lean and Yeo, 2017). Gel electrophoresis and *in silico* analysis showed that the number and size of small plasmids are quite similar. However, in the gel electrophoresis assay, the

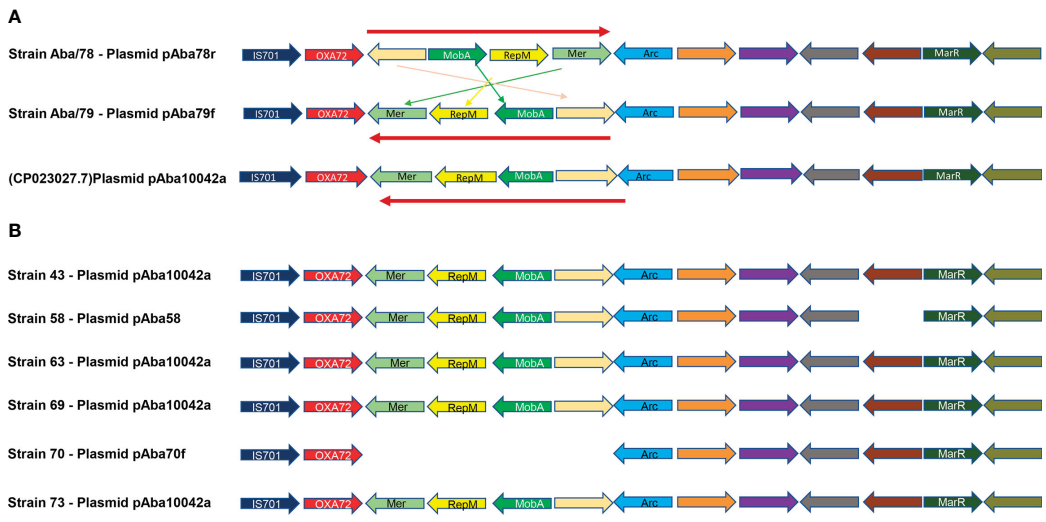

FIGURE 4
Genetic structure in *A. baumannii* plasmids. **(A)**- Genetic structure of plasmids pAba10042a (CP023027.1), pAba78r and pAba79f. **(B)**- Genetic structure of plasmids identified in *A. baumannii* strains from Mateo-Estrada et al., 2021, pAba10042a, pAba58 and pAba70f.

megaplasmids that were identified through *in silico* analysis were not visualized. The limitations of gel electrophoresis lie in the non-identification of large-sized plasmids, probably due to the low copy numbers of the replicon. On the other hand, the limitations of bioinformatic techniques include the updating of program databases, genome coverage, read depth, as well as the presence of repetitive regions that make genome assembly challenging, among others. Significantly, we managed to identify concordances between both methodologies, enabling us to gain insight into the mobile elements contain in *A. baumannii* and determine the resistance genes they harbor.

This is one the first studies where the size of plasmids was compared using both experimental and bioinformatic methodologies, which proved to be complementary. In the Eckhardt method, gel electrophoresis allows each plasmid to be obtained in its linearized form due to the denaturing properties of the system. Meanwhile, the bioinformatic power of *in silico* analysis enabled the identification of plasmids in the genome content. This approach can be of great assistance in future studies concerning plasmid dynamics.

The sequence analysis for ARGs within each of the identified replicons revealed that strains Aba/78 and Aba/79, belonging to ST369/CC92/IC2 and ST758/CC636/IC5, respectively, contained a 10,012 bp plasmid harboring the carbapenem resistance gene $bla_{\text{OXA-72}}$ in both strains. This plasmid contains 13 coding regions, including the replication and mobilization machinery, allowing it to undergo horizontal transfer to these strains (Figure 4A). Despite the significant identity in size and number of identified CDS, these plasmids were not identical to each other. In their structure, they exhibited the inversion of four of their genes involved in plasmid mobilization. The inverted locus is composed of hypothetical protein, followed by MobA, which enables plasmid mobilization, the RepM protein, which serves as an initiator of replication, and the regulatory protein Mer (Figure 4A). The sequence of these plasmids showed that the plasmid pAba79f from Aba/79 strain, ST758/CC636/IC5, exhibited 100% identity with plasmid pAba10042a (NZ_CP023027.1) of 10,062 bp (Salgado-Camargo et al., 2020).

To determine whether the genetic structure of these plasmids had been previously identified in reported strains, we selected genomes from a study conducted by Mateo-Estrada in 2021. We included five strains belonging to ST369/CC92/IC2 and three strains from ST758/CC636/IC5, corresponding to Aba/78 and Aba/79 strains respectively. In these genomes, we identified two ST369 strains with a 10,062 bp plasmid and one strain with a 5,464 bp plasmid, and both plasmids contained the $bla_{\text{OXA-72}}$ gene. As for ST758, we identified three strains carrying a 10,062 bp plasmid with the $bla_{\text{OXA-72}}$ gene. The sequence of each plasmid showed that four strains harboured the plasmid pAba10042a with identical structures. However, strain 58 had almost the same structure but lacked a hypothetical protein. The plasmid had the same size of 10,062 bp, but in the gene annotation, it only presented 12 of the 13 CDS that strain Aba/79 had. Likewise, strain 70, which carried the 5,464 bp plasmid, lacked the entire locus that was inverted in strains Aba/78 and Aba/79, although the rest of the sequence remained unchanged, including the remaining 9 CDS. This analysis revealed significant plasticity of this plasmid, as it exhibited various structural rearrangements and lengths in several strains. However, in all cases, it retained the $bla_{\text{OXA-72}}$ resistance gene, which belongs to the serine carbapenemases family $bla_{\text{OXA-24-like}}$. This gene represents one of the predominant mechanisms for carbapenem resistance in *A. baumannii* (Salgado-Camargo et al., 2020). It is noteworthy that the Aba/78 strain with the inverted locus in the resistance plasmid harboured the highest number of ARGs, totalling 14, including a cephalosporinase and two carbapenemases, and was responsible for a nosocomial outbreak. The epidemiological surveillance of this particular clone is crucial to prevent its spread; importantly, the plasmid it carries can be transferred to strains of different IC.

Our study highlighted the significant ability of *A. baumannii* to persist in the hospital environment for extended periods. Moreover, it revealed the broad range of resistance determinants that *A. baumannii* possesses and the structural versatility of certain plasmids capable of transmitting resistance genes among different clones. Epidemiological studies supported by genetic-molecular data will be increasingly necessary to comprehend the extent of genetic diversity and monitor the transmission of resistance determinants in *A. baumannii* populations.

Data availability statement

The datasets presented in this study can be found in online repositories. The names of the repository/repositories and accession number(s) can be found in the article/Supplementary Material.

Author contributions

JF-V: Conceptualization, Data curation, Formal analysis, Investigation, Methodology, Software, Writing – original draft. IH-G: Writing – review & editing, Data curation, Software, Methodology. SC-R: Formal analysis, Supervision, Writing – review & editing. MJ-Q: Writing – review & editing, Methodology, Validation. CG-V: Methodology, Formal analysis, Writing – review & editing. VM-E: Methodology, Software, Writing – review & editing. RM-O: Writing – review & editing, Data curation, Methodology. ER-N: Data curation, Methodology, Writing – review & editing. JS-P: Formal analysis, Writing – review & editing. MA-C: Formal analysis, Funding acquisition, Supervision, Writing – original draft, Writing – review & editing.

Funding

The author(s) declare financial support was received for the research, authorship, and/or publication of this article. This work was supported by Programa de Apoyo a Proyectos de Investigación e Innovación Tecnológica (UNAM-PAPIIT-DGAPA) grant number IN217721 and Consejo Nacional de Ciencia y Tecnología (CONACyT México) grant number Ciencia de Frontera 2019-171880.

Conflict of interest

The authors declare that the research was conducted in the absence of any commercial or financial relationships that could be construed as a potential conflict of interest.

Publisher's note

All claims expressed in this article are solely those of the authors and do not necessarily represent those of their affiliated organizations, or those of the publisher, the editors and the reviewers. Any product that may be evaluated in this article, or claim that may be made by its manufacturer, is not guaranteed or endorsed by the publisher.

Supplementary material

The Supplementary Material for this article can be found online at: https://www.frontiersin.org/articles/10.3389/fcimb.2023.1278819/full#supplementary-material

SUPPLEMENTARY TABLE 1
Virulence factor genes identified in *A. baumannii* strains.

References

Alcántar-Curiel, M. D., Fernández-Vázquez, J. L., Toledano-Tableros, J. E., Gayosso-Vázquez, C., Jarillo-Quijada, M. D., López-Álvarez, M. D. R., et al. (2019a). Emergence of IncFIA Plasmid-Carrying blaNDM-1 Among *Klebsiella pneumoniae* and *Enterobacter cloacae* Isolates in a Tertiary Referral Hospital in Mexico. *Microbial Drug Resistance (Larchmont N.Y.)* 25 (6), 830–838. doi: 10.1089/mdr.2018.0306

Alcántar-Curiel, M. D., García-Torres, L. F., González-Chávez, M. I., Morfín-Otero, R., Gayosso-Vázquez, C., Jarillo-Quijada, M. D., et al. (2014). Molecular mechanisms associated with nosocomial carbapenem-resistant *Acinetobacter baumannii* in Mexico. *Arch. Med. Res.* 45 (7), 553–560. doi: 10.1016/j.arcmed.2014.10.006

Alcántar-Curiel, M. D., Huerta-Cedeño, M., Jarillo-Quijada, M. D., Gayosso-Vázquez, C., Fernández-Vázquez, J. L., Hernández-Medel, M. L., et al. (2023). Gram-negative ESKAPE bacteria bloodstream infections in patients during the COVID-19 pandemic. *PeerJ* 11, e15007. doi: 10.7717/peerj.15007

Alcántar-Curiel, M. D., Rosales-Reyes, R., Jarillo-Quijada, M. D., Gayosso-Vázquez, C., Fernández-Vázquez, J. L., Toledano-Tableros, J. E., et al. (2019b). Carbapenem-resistant *Acinetobacter baumannii* in three tertiary care hospitals in Mexico: Virulence profiles, innate immune response and clonal dissemination. *Front. Microbiol.* 10. doi: 10.3389/fmicb.2019.02116

Antipov, D., Hartwick, N., Shen, M., Raiko, M., Lapidus, A., and Pevzner, P. A. (2016). plasmidSPAdes: assembling plasmids from whole genome sequencing data. *Bioinf. (Oxford England)* 32 (22), 3380–3387. doi: 10.1093/bioinformatics/btw493

Bankevich, A., Nurk, S., Antipov, D., Gurevich, A. A., Dvorkin, M., Kulikov, A. S., et al. (2012). SPAdes: a new genome assembly algorithm and its applications to single-cell sequencing. *J. Comput. Biology: A J. Comput. Mol. Cell Biol.* 19 (5), 455–477. doi: 10.1089/cmb.2012.0021

Bartual, S. G., Seifert, H., Hippler, C., Luzon, M. A. D., Wisplinghoff, H., and Rodríguez-Valera, F. (2005). Development of a multilocus sequence typing scheme for characterization of clinical isolates of *Acinetobacter baumannii*. *J. Clin. Microbiol.* 43 (9), 4382–4390. doi: 10.1128/JCM.43.9.4382-4390.2005

Bocanegra-Ibarias, P., Peña-López, C., Camacho-Ortiz, A., Llaca-Díaz, J., Silva-Sánchez, J., Barrios, H., et al. (2015). Genetic characterisation of drug resistance and clonal dynamics of *Acinetobacter baumannii* in a hospital setting in Mexico. *Int. J. Antimicrobial Agents* 45 (3), 309–313. doi: 10.1016/j.ijantimicag.2014.10.022

Bortolaia, V., Kaas, R. S., Ruppe, E., Roberts, M. C., Schwarz, S., Cattoir, V., et al. (2020). ResFinder 4.0 for predictions of phenotypes from genotypes. *J. Antimicrobial Chemotherapy* 75 (12), 3491–3500. doi: 10.1093/jac/dkaa345

Chagas, T. P. G., Carvalho, K. R., de Oliveira Santos, I. C., Carvalho-Assef, A. P. D., and Asensi, M. D. (2014). Characterization of carbapenem-resistant *Acinetobacter baumannii* in Brazil, (2008-2011): countrywide spread of OXA-23-producing clones (CC15 and CC79). *Diagn. Microbiol. Infect. Dis.* 79 (4), 468–472. doi: 10.1016/j.diagmicrobio.2014.03.006

Darmancier, H., Domingues, C. P. F., Rebelo, J. S., Amaro, A., Dionísio, F., Pothier, J., et al. (2022). Are virulence and antibiotic resistance genes linked? A comprehensive analysis of bacterial chromosomes and plasmids. *Antibiotics (Basel Switzerland)* 11 (6), 706. doi: 10.3390/antibiotics11060706

Diancourt, L., Passet, V., Nemec, A., Dijkshoorn, L., and Brisse, S. (2010). The population structure of *Acinetobacter baumannii*: expanding multiresistant clones from an ancestral susceptible genetic pool. *PloS One* 5 (4), e10034. doi: 10.1371/journal.pone.0010034

Dice, L. R. (1945). Measures of the amount of ecologic association between species. *Ecology* 26 (3), 297–302. doi: 10.2307/1932409

Eckhardt, T. (1978). A rapid method for the identification of plasmid desoxyribonucleic acid in bacteria. *Plasmid* 1 (4), 584–588. doi: 10.1016/0147-619x(78)90016-1

González, V., Santamaría, R. I., Bustos, P., Hernández-González, I., Medrano-Soto, A., Moreno-Hagelsieb, G., et al. (2006). The partitioned *Rhizobium etli* genome: genetic and metabolic redundancy in seven interacting replicons. *Proc. Natl. Acad. Sci. United States America* 103 (10), 3834–3839. doi: 10.1073/pnas.0508502103

Graña-Miraglia, L., Evans, B. A., López-Jácome, L. E., Hernández-Durán, M., Colín-Castro, C. A., Volkow-Fernández, P., et al. (2020). Origin of OXA-23 variant OXA-239 from a recently emerged lineage of *Acinetobacter baumannii* international clone V. *MSphere* 5 (1). doi: 10.1128/mSphere.00801-19

Graña-Miraglia, L., Lozano, L. F., Velázquez, C., Volkow-Fernández, P., Pérez-Oseguera, Á., Cevallos, M. A., et al. (2017). Rapid gene turnover as a significant source of genetic variation in a recently seeded population of a healthcare-associated pathogen. *Front. Microbiol.* 8. doi: 10.3389/fmicb.2017.01817

Harding, C. M., Hennon, S. W., and Feldman, M. F. (2018). Uncovering the mechanisms of *Acinetobacter baumannii* virulence. *Nat. Rev. Microbiol.* 16 (2), 91–102. doi: 10.1038/nrmicro.2017.148

Heras, J., Domínguez, C., Mata, E., Pascual, V., Lozano, C., Torres, C., et al. (2015). GelJ – a tool for analyzing DNA fingerprint gel images. *BMC Bioinf.* 16 (1). doi: 10.1186/s12859-015-0703-0

Hernández-González, I. L., Mateo-Estrada, V., and Castillo-Ramirez, S. (2022). The promiscuous and highly mobile resistome of *Acinetobacter baumannii*. *Microbial Genomics* 8 (1). doi: 10.1099/mgen.0.000762

Hujer, A. M., Higgins, P. G., Rudin, S. D., Buser, G. L., Marshall, S. H., Xanthopoulou, K., et al. (2017). Nosocomial Outbreak of Extensively Drug-Resistant *Acinetobacter baumannii* Isolates Containing bla OXA-237 Carried on a Plasmid. *Antimicrobial Agents Chemotherapy* 61 (11). doi: 10.1128/aac.00797-17

Ibrahim, S., Al-Saryi, N., Al-Kadmy, I. M. S., and Aziz, S. N. (2021). Multidrug-resistant *Acinetobacter baumannii* as an emerging concern in hospitals. *Mol. Biol. Rep.* 48 (10), 6987–6998. doi: 10.1007/s11033-021-06690-6

Ingti, B., Upadhyay, S., Hazarika, M., Khyriem, A. B., Paul, D., Bhattacharya, P., et al. (2020). Distribution of carbapenem resistant *Acinetobacter baumannii* with blaADC-30 and induction of ADC-30 in response to beta-lactam antibiotics. *Res. Microbiol.* 171 (3–4), 128–133. doi: 10.1016/j.resmic.2020.01.002

Jie, J., Chu, X., Li, D., and Luo, Z. (2021). A set of shuttle plasmids for gene expression in *Acinetobacter baumannii*. *PloS One* 16 (2), e0246918. doi: 10.1371/journal.pone.0246918

Kabic, J., Novovic, K., Kekic, D., Trudic, A., Opavski, N., Dimkic, I., et al. (2023). Comparative genomics and molecular epidemiology of colistin-resistant *Acinetobacter baumannii*. *Comput. Struct. Biotechnol. J.* 21, 574–585. doi: 10.1016/j.csbj.2022.12.045

Karlowsky, J. A., Hoban, D. J., Hackel, M. A., Lob, S. H., and Sahm, D. F. (2017). Resistance among Gram-negative ESKAPE pathogens isolated from hospitalized patients with intra-abdominal and urinary tract infections in Latin American countries: SMART 2013–2015. *Braz. J. Infect. Diseases: Off. Publ. Braz. Soc. Infect. Dis.* 21 (3), 343–348. doi: 10.1016/j.bjid.2017.03.006

Lean, S. S., and Yeo, C. C. (2017). Small, enigmatic plasmids of the nosocomial pathogen, *Acinetobacter baumannii*: Good, bad, who knows? *Front. Microbiol.* 8. doi: 10.3389/fmicb.2017.01547

Lee, C.-R., Lee, J. H., Park, M., Park, K. S., Bae, I. K., Kim, Y. B., et al. (2017). Biology of *Acinetobacter baumannii*: Pathogenesis, antibiotic resistance mechanisms, and prospective treatment options. *Front. Cell. infection Microbiol.* 7. doi: 10.3389/fcimb.2017.00055

Levy-Blitchtein, S., Roca, I., Plasencia-Rebata, S., Vicente-Taboada, W., Velásquez-Pomar, J., Muñoz, L., et al. (2018). Emergence and spread of carbapenem-resistant *Acinetobacter baumannii* international clones II and III in Lima, Peru. *Emerging Microbes Infections* 7 (1), 1–9. doi: 10.1038/s41426-018-0127-9

Lewis, J. S., and Pharm, D. (2023). *FIDSA. CLSI—M100: Performance Standards for Antimicrobial Susceptibility Testing. 33rd ed* (Berwyn, IL, USA: Clinical and Laboratory Standards Institute).

Loewen, P. C., Alsaadi, Y., Fernando, D., and Kumar, A. (2014). Genome sequence of an extremely drug-resistant clinical isolate of *Acinetobacter baumannii* strain AB030. *Genome Announcements* 2 (5). doi: 10.1128/genomeA.01035-14

López-Leal, G., Zuniga-Moya, J. C., Castro-Jaimes, S., Graña-Miraglia, L., Pérez-Oseguera, Á., Reyes-García, H. S., et al. (2019). Unexplored genetic diversity of multidrug- and extremely drug-resistant *Acinetobacter baumannii* isolates from tertiary hospitals in Honduras. *Microbial Drug Resistance (Larchmont N.Y.)* 25 (5), 690–695. doi: 10.1089/mdr.2018.0311

Magiorakos, A.-P., Srinivasan, A., Carey, R. B., Carmeli, Y., Falagas, M. E., Giske, C. G., et al. (2012). Multidrug-resistant, extensively drug-resistant and pandrug-resistant bacteria: an international expert proposal for interim standard definitions for acquired resistance. *Clin. Microbiol. Infection: Off. Publ. Eur. Soc. Clin. Microbiol. Infect. Dis.* 18 (3), 268–281. doi: 10.1111/j.1469-0691.2011.03570.x

Mancilla-Rojano, J., Castro-Jaimes, S., Ochoa, S. A., Bobadilla Del Valle, M., Luna-Pineda, V. M., Bustos, P., et al. (2019). Whole-genome sequences of five *Acinetobacter baumannii* strains from a child with leukemia M2. *Front. Microbiol.* 10. doi: 10.3389/fmicb.2019.00132

Mateo-Estrada, V., Fernández-Vázquez, J. L., Moreno-Manjón, J., Hernández-González, I. L., Rodríguez-Noriega, E., Morfín-Otero, R., et al. (2021). Accessory genomic epidemiology of cocirculating *Acinetobacter baumannii* clones. *MSystems* 6 (4), e0062621. doi: 10.1128/mSystems.00626-21

Naas, T., Levy, M., Hirschauer, C., Marchandin, H., and Nordmann, P. (2005). Outbreak of carbapenem-resistant *Acinetobacter baumannii* producing the carbapenemase OXA-23 in a tertiary care hospital of Papeete, French Polynesia. *J. Clin. Microbiol.* 43 (9), 4826–4829. doi: 10.1128/JCM.43.9.4826-4829.2005

Nodari, C. S., Cayô, R., Streling, A. P., Lei, F., Wille, J., Almeida, M. S., et al. (2020). Genomic analysis of carbapenem-resistant *Acinetobacter baumannii* isolates belonging to major endemic clones in South America. *Front. Microbiol.* 11. doi: 10.3389/fmicb.2020.584603

Nordmann, P., and Poirel, L. (2013). Strategies for identification of carbapenemase-producing *Enterobacteriaceae*. *J. Antimicrobial Chemotherapy* 68 (3), 487–489. doi: 10.1093/jac/dks426

Nordmann, P., and Poirel, L. (2019). Epidemiology and diagnostics of carbapenem resistance in gram-negative bacteria. *Clin. Infect. Diseases: Off. Publ. Infect. Dis. Soc. America* 69 (Supplement_7), S521–S528. doi: 10.1093/cid/ciz824

Partridge, S. R., Kwong, S. M., Firth, N., and Jensen, S. O. (2018). Mobile genetic elements associated with antimicrobial resistance. *Clin. Microbiol. Rev.* 31 (4). doi: 10.1128/cmr.00088-17

Robertson, J., Bessonov, K., Schonfeld, J., and Nash, J. H. E. (2020). Universal whole-sequence-based plasmid typing and its utility to prediction of host range and epidemiological surveillance. *Microbial Genomics* 6 (10). doi: 10.1099/mgen.0.000435

Robertson, J., and Nash, J. H. E. (2018). MOB-suite: software tools for clustering, reconstruction and typing of plasmids from draft assemblies. *Microbial Genomics* 4 (8). doi: 10.1099/mgen.0.000206

Rodríguez, C. H., Nastro, M., and Famiglietti, A. (2018). Carbapenemases in *Acinetobacter baumannii*. Review of their dissemination in Latin America. *Rev. Argent. Microbiologia* 50 (3), 327–333. doi: 10.1016/j.ram.2017.10.006

Salgado-Camargo, A. D., Castro-Jaimes, S., Gutierrez-Rios, R.-M., Lozano, L. F., Altamirano-Pacheco, L., Silva-Sanchez, J., et al. (2020). Structure and evolution of *Acinetobacter baumannii* plasmids. *Front. Microbiol.* 11. doi: 10.3389/fmicb.2020.01283

Seemann, T. (2014). Prokka: rapid prokaryotic genome annotation. *Bioinf. (Oxford England)* 30 (14), 2068–2069. doi: 10.1093/bioinformatics/btu153

Shahryari, S., Mohammadnejad, P., and Noghabi, K. A. (2021). Screening of anti-*Acinetobacter baumannii* phytochemicals, based on the potential inhibitory effect on OmpA and OmpW functions. *R. Soc. Open Sci.* 8 (8), 201652. doi: 10.1098/rsos.201652

Tamayo-Legorreta, E., Turrubiartes-Martínez, E., Garza-Ramos, U., Niño-Moreno, P., Barrios, H., Sánchez-Pérez, A., et al. (2016). Outbreak caused by blaOXA-72-producing *Acinetobacter baumannii* ST417 detected in clinical and environmental isolates. *Microbial Drug Resistance (Larchmont N.Y.)* 22 (2), 129–133. doi: 10.1089/mdr.2015.0157

Tamayo-Legorreta, E. M., Garza-Ramos, U., Barrios-Camacho, H., Sanchez-Perez, A., Galicia-Paredes, A., Meza-Chavez, A., et al. (2014). Identification of OXA-23 carbapenemases: novel variant OXA-239 in *Acinetobacter baumannii* ST758 clinical isolates in Mexico. *New Microbes New Infections* 2 (6), 173–174. doi: 10.1002/nmi2.60

Tenover, F. C., Arbeit, R. D., Goering, R. V., Mickelsen, P. A., Murray, B. E., Persing, D. H., et al. (1995). Interpreting chromosomal DNA restriction patterns produced by pulsed-field gel electrophoresis: criteria for bacterial strain typing. *J. Clin. Microbiol.* 33 (9), 2233–2239. doi: 10.1128/jcm.33.9.2233-2239.1995

Toledano-Tableros, J. E., Gayosso-Vázquez, C., Jarillo-Quijada, M. D., Fernández-Vázquez, J. L., Morfin-Otero, R., Rodríguez-Noriega, E., et al. (2021). Dissemination of bla NDM- 1 gene among several *Klebsiella pneumoniae* sequence types in Mexico associated with horizontal transfer mediated by IncF-like plasmids. *Front. Microbiol.* 12. doi: 10.3389/fmicb.2021.611274

Traglia, G. M., Chua, K., Centrón, D., Tolmasky, M. E., and Ramírez, M. S. (2014). Whole-genome sequence analysis of the naturally competent *Acinetobacter baumannii* clinical isolate A118. *Genome Biol. Evol.* 6 (9), 2235–2239. doi: 10.1093/gbe/evu176

Vanegas, J. M., Higuita, L. F., Vargas, C., Vargas, C., Cienfuegos, A. V., Rodríguez, E., et al. (2015). *Acinetobacter baumannii* resistente a carbapenémicos causando osteomielitis e infecciones en piel y tejidos blandos en hospitales de Medellín, Colombia. *Biomedica: Rev. del Instituto Nacional Salud* 35 (4), 522–530. doi: 10.7705/biomedica.v35i4.2572

Wilharm, G., Piesker, J., Laue, M., and Skiebe, E. (2013). DNA Uptake by the Nosocomial Pathogen *Acinetobacter baumannii* Occurs during Movement along Wet Surfaces. *J. Bacteriology* 195 (18), 4146–4153. doi: 10.1128/jb.00754-13

Wong, D., Nielsen, T. B., Bonomo, R. A., Pantapalangkoor, P., Luna, B., and Spellberg, B. (2017). Clinical and pathophysiological overview of *Acinetobacter* infections: A century of challenges. *Clin. Microbiol. Rev.* 30 (1), 409–447. doi: 10.1128/cmr.00058-16

frontiers | Frontiers in Cellular and Infection Microbiology

TYPE Original Research
PUBLISHED 09 January 2024
DOI 10.3389/fcimb.2023.1327092

OPEN ACCESS

EDITED BY
Manuel Gerardo Ballesteros Monrreal,
University of Sonora, Mexico

REVIEWED BY
María Cristina González Vázquez,
Benemérita Universidad Autónoma
de Puebla, Mexico
Asive Myataza,
National Health Laboratory Service (NHLS),
South Africa

*CORRESPONDENCE
Mingju Hao
haomingju@163.com

†These authors contribute equally to this work

RECEIVED 24 October 2023
ACCEPTED 20 December 2023
PUBLISHED 09 January 2024

CITATION
Ma W, Cui X, Dong X, Li X, Liu K, Wang Y, Shi X, Chen L and Hao M (2024) Characterization of nontyphoidal *Salmonella* strains from a tertiary hospital in China: serotype diversity, multidrug resistance, and genetic insights. *Front. Cell. Infect. Microbiol.* 13:1327092. doi: 10.3389/fcimb.2023.1327092

Characterization of nontyphoidal *Salmonella* strains from a tertiary hospital in China: serotype diversity, multidrug resistance, and genetic insights

Wanshan Ma[1†], Xiaodi Cui[2†], Xiutao Dong[1], Xinpeng Li[3], Ke Liu[1], Yujiao Wang[1], Xiaohong Shi[1], Liang Chen[4,5] and Mingju Hao[1*]

[1]Department of Clinical Laboratory Medicine, The First Affiliated Hospital of Shandong First Medical University & Shandong Provincial Qianfoshan Hospital, Shandong Medicine and Health Key Laboratory of Laboratory Medicine, Jinan, China, [2]School of Clinical Medicine, Jining Medical University, Jining, China, [3]Department of Bacterial Infectious Disease Control and Prevention, Shandong Center for Disease Control and Prevention, Jinan, China, [4]Center for Discovery and Innovation, Hackensack Meridian Health, Nutley, NJ, United States, [5]Department of Medical Sciences, Hackensack Meridian School of Medicine, Nutley, NJ, United States

Objective: Nontyphoidal *Salmonella* is a significant public health concern due to its ability to cause foodborne illnesses worldwide. This study aims to characterize the nontyphoidal *Salmonella* strains isolated from patients in China.

Methods: A total of 19 nontyphoidal *Salmonella* strains were characterized through serovar identification, antimicrobial susceptibility testing (AST), biofilm formation assessment. Genetic relatedness was determined using pulsed-field gel electrophoresis (PFGE). WGS was employed to decipher the resistance mechanism and to contextualize the *S.* serovar Mbandaka strains among previously sequenced isolates in China. The biofilm associated *mrkA* gene was examined by PCR.

Results: The predominant serovar identified was *S.* Enteritidis, followed by *S.* Mbandaka, *S.* Thompson, *S.* Livingston, *S.* Alachua, and *S.* Infantis. PFGE analysis indicated a notable genetic similarity among the *S.* Mbandaka isolates. Phylogenetic analysis suggested that these strains were likely derived from a single source that had persisted in China for over five years. One multidrug resistance (MDR) *S.* Enteritidis isolate carried a highly transferable IncB/O/K/Z plasmid with $bla_{CTX\text{-}M\text{-}15}$. One *S.* Thompson strain, harboring the *mrkABCDF* operon in an IncX1 plasmid, isolated from cutaneous lesions, demonstrated robust biofilm formation. However, no *mrkABCDF* loci were detected in other strains.

Conclusion: Our study emphasizes the importance of persisted surveillance and prompt response to *Salmonella* infections to protect public health. The dissemination of $bla_{CTX\text{-}M\text{-}15}$-harboring IncB/O/K/Z plasmid and the spread of virulent *mrkABCDF* operon among *Salmonella* in China and other global regions warrant close monitoring.

KEYWORDS

nontyphoidal *Salmonella*, antibiotic resistance, *mrkABCDF* operon, phylogenetic analysis, biofilm

Introduction

Nontyphoidal *Salmonella* (NTS) is one of the most common agents of gastrointestinal disease globally (Amuasi and May, 2019). It is estimated that NTS cause about 129.5 million cases each year, resulting in about 100,000 to 1 million deaths per year worldwide (Wen et al., 2017; Branchu et al., 2018). Salmonella infections frequently occur in humans when they consume contaminated foods, including poultry, eggs, beef, pork, milk, seafood, and fresh fish products. Additionally, direct interactions with animals can lead to the transmission of Salmonella to humans (Zhao et al., 2003). While most infections result in self-limiting gastroenteritis, individuals such as infants, the elderly or those with compromised immune systems are susceptible to life-threatening invasive infections (Marchello et al., 2022).

To date, over 2600 *Salmonella* serovars have been identified, of which only a few NTS serovars are responsible for most human infections (Akinyemi et al., 2023). *S.* Typhimurium and *S.* Enteritidis accounts for the majority of NTS infections in humans (Wang et al., 2023). Alarmingly, the emergence of multi-drug-resistant (MDR) *Salmonella* serovars, particularly against 3rd-generation cephalosporins and fluoroquinolones, is having a great impact on the efficacy of antibiotic treatment, and an increasing prevalence of MDR strains may lead to an increase in mortality rates of *Salmonella* infections (Crump et al., 2015). Of note, MDR strains can carry specific virulence factors which are more virulent than their susceptible counterparts (Gebreyes et al., 2009).

In China, surveillance data spanning from 2006 to 2019 reveals an average of 62 serovars are detected annually from human origin (Wang et al., 2023). *S.* Typhimurium and *S.* Enteritidis were the most common serovar causing human infections in China. Moreover, the proportion of antimicrobial-resistant *Salmonella* isolates occur with increasing frequency during 2006–2019, especially beta-lactam, quinolone, tetracycline, and rifampicin resistance (Wang et al., 2023). These findings highlight the need for continuous monitoring of *Salmonella* infection with particular emphasis on MDR *Salmonella* strains.

In this study, we identified and examined a total of 19 NTS isolates from patients at a tertiary hospital in eastern China in 2022. The majority of cases were reported between July and October, with the peak incidence occurring in October. Through a combination of phenotypic and molecular analyses, we aimed to gain comprehensive insights into the characteristics of these *Salmonella* strains.

Materials and methods

Bacterial isolates

During the period from March 20, 2022, to December 16, 2022, a total of 19 isolates of NTS were investigated in this study (Figure 1). All strains were the first isolates collected from each patient. Ten of the isolates were obtained from feces. Other clinical specimens included blood cultures, bronchoalveolar lavage fluid,

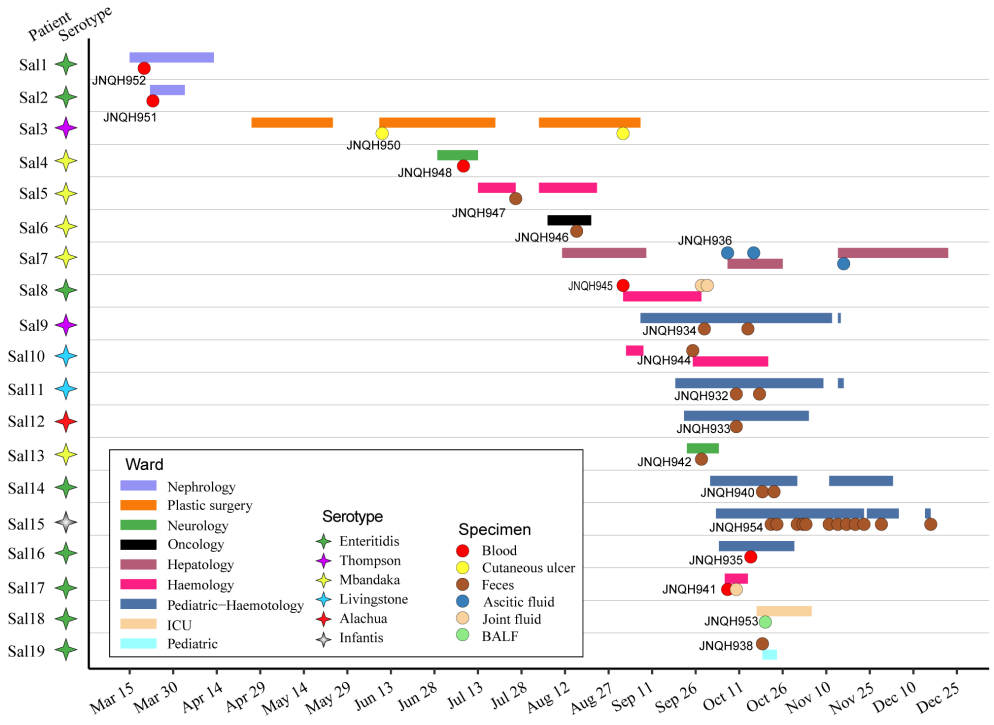

FIGURE 1
Time frame of stays in hospitalization for the 19 patients involved in NTS infection. Horizontal bars represent the duration of hospitalization for each patient, with distinct colors indicating the respective ward departments. Circles represent the time of isolation for each patient with colored circles representing the specimen source. Colored stars represent different serovars.

cutaneous ulcer, ascitic fluid, joint fluid. For routine use samples were inoculated on Blood Agar (TSA w/5% Sheep Blood) and selective SS Agar (Salmonella-Shigella agar) and were grown at 37°C overnight.

Patient information

The median age of infected patients was 35.5 years (range: 1-78 years). 17 of the patients were males. The median duration of illness was 9 days (range: 5-89 days). Predominant symptoms included diarrhea (68.4%), fever (47.4%), abdominal pain (47.4%). Lower respiratory tract infection-related symptoms and signs are prominent in a patient with lung infection (patient Sal18). All the patients were administered antimicrobial agents, with 14 (73.7%) patients showing effective outcomes. Short descriptions of the investigated isolates are presented in Table 1.

Antimicrobial susceptibility testing

AST was performed using the disk diffusion method or microdilution method as recommended by the Clinical and Laboratory Standards Institute guidelines (CLSI, 2021). Antimicrobial discs were manufactured by Oxoid in UK. The following antimicrobial agents were tested: ampicillin (AMP, disk content 10μg), ceftazidime (CAZ, 30μg), ciprofloxacin (CIP, 5μg), ceftriaxone (CRO, 30μg), trimethoprim-sulfamethoxazole (TMP-SMZ, 1.25/23.75μg), meropenem (MEM, 10μg). Levofloxacin (LEV) was tested by microdilution method. Results were interpreted using the CLSI breakpoints (CLSI M100, 2021). MDR was defined as acquired non-susceptibility to at least one agent in three or more antimicrobial categories (Magiorakos et al., 2012). Each of the antibiotics was tested with 3 duplicates. ATCC 25922 (*E. coli*) were used as quality control strains for susceptibility testing.

Salmonella serotyping

The isolated *Salmonella* were serotyped on slides by slide agglutination as described in the manufacturer's instructions (Statens Serum Institut, Copenhagen, Denmark). Briefly, the *Salmonella* strains were grown overnight on Blood Agar then colonies were transferred to the drop of antiserum. The "O" antigen type was determined based on oligosaccharides associated with lipopolysaccharide. Then the "H" antigen was determined based on flagellar proteins. The reaction was read with the naked eye by holding the slide in front of a light source against a black background. A positive reaction was seen as a visible agglutination. A negative

TABLE 1 Overall strain features collected in this study.

Patient ID	Strain	Gender	Age (Year)	Specimen type	Serovar	Ward department	Main Diagnosis
Sal1	JNQH952	Male	25	Blood	Enteritidis	nephrology	Post-renal transplantation
Sal2	JNQH951	Male	40	Blood	Enteritidis	nephrology	Systemic vasculitis
Sal3	JNQH950	Male	58	Skin secretion	Thompson	Plastic surgery	Diabetes mellitus
Sal4	JNQH948	Male	78	Blood	Mbandaka	Neurology	Encephalitis
Sal5	JNQH947	Male	67	Feces	Mbandaka	Haemology	Lymphoma
Sal6	JNQH946	Male	58	Feces	Mbandaka	Oncology	Cholangiocarcinoma
Sal7	JNQH936	Male	39	Ascites	Mbandaka	Hepatology	Acute pancreatitis
Sal8	JNQH945	Male	40	Blood/Joint fluid	Enteritidis	Haemology	Acute lymphocytic leukemia
Sal9	JNQH934	Male	1	Feces	Thompson	Pediatric-Haemotology	Acute myeloid leukemia
Sal10	JNQH944	Female	39	Feces	Livingstone	Haemology	Aplastic anemia
Sal11	JNQH932	Male	10	Feces	Livingstone	Pediatric-Haemotology	Aplastic anemia
Sal12	JNQH933	Male	12	Feces	Alachua	Pediatric-Haemotology	Aplastic anemia
Sal13	JNQH942	Male	71	Feces	Mbandaka	Neurology	Cerebral infarction
Sal14	JNQH940	Male	10	Feces	Enteritidis	Pediatric-Haemotology	Hematopoietic stem cell transplantation
Sal15	JNQH954	Female	3	Feces	Infantis	Pediatric-Haemotology	Acute lymphocytic leukemia
Sal16	JNQH935	Male	11	Blood	Enteritidis	Pediatric-Haemotology	Acute lymphocytic leukemia
Sal17	JNQH941	Male	32	Blood	Enteritidis	Haemology	Thrombocytopenia
Sal18	JNQH953	Male	65	BALF	Enteritidis	ICU	Pneumoniae
Sal19	JNQH938	Male	5	Feces	Enteritidis	Pediatric	Gastroenteritis

reaction was persistence of the homogeneous milky turbidity. The serovar was assigned according to the Kauffmann-White scheme, which is a comprehensive system employed for the discrimination of serological variations within the *Salmonella* genus.

Pulsed-field gel electrophoresis

All isolates were analyzed for genetic relatedness by PFGE. PFGE of XbaI-digested genomic DNA samples were performed with a CHEF MAPPER XA apparatus (Bio-Rad, USA), as previously described (Ma et al., 2023). In brief, genomic DNA was prepared by embedding cells in agarose plugs, followed by XbaI digestion for 2 h at 37°C. Electrophoresis conditions consisted of one phase from 2.2 to 63.8 s at a run time of 17 h. *Salmonella* serovar Branderup H9812 strain was used as the reference strain. PFGE patterns were analyzed and compared using GelJ software 2.0v (Heras et al., 2015).

Biofilm formation

The process of biofilm formation was assessed using crystal violet staining as described previously with minor modifications (Hao et al., 2021a). Briefly, overnight cultures of the bacteria were diluted 1:1,000 in LB medium. A total volume of 200 µl of the diluted culture was then transferred to each well of a microtiter plate. The plate was incubated at 37°C for 24 hours. After incubation, the wells were washed four times with distilled water to remove any planktonic (free-floating) bacteria. The remaining adherent bacteria were then stained with 125 µl of a 0.1% crystal violet dye solution. Following incubation for 10 minutes, the crystal violet solution was carefully removed, and the wells were washed six times with distilled water. After that, 150 µl of a 30% glacial acetic acid in water solution was added to each well. The plate was incubated for an additional 10 minutes at room temperature, allowing the acetic acid to dissolve the crystal violet-stained biofilms. The optical density (OD) of the solubilized biofilms was then measured at a wavelength of 590 nm using a microplate reader (Thermo Scientific). At least three replicates were performed for each sample. Statistical significance in biofilm assays was calculated using Student's t-test and any differences between strains with a P value of <0.05 were considered significant.

Whole-genome sequencing

Complete sequencing was performed on four selected strains, which included a strong biofilm-forming *S.* Thompson strain (JNQH950), *S.* Mbandaka (JNQH948), as well as two resistant *S.* Enteritidis strains (JNQH940 and JNQH952). Genomic DNA was isolated using a WizardR Genomic DNA Purification Kit as described in the manufacturer's instructions (Promega, Madison, WI, USA). The DNA samples were subject to next generation sequencing using the Illumina HiSeq (Illumina, San Diego, CA, USA) and Oxford Nanopore (MinION system). The hybrid assembly was performed by Unicycler v0·5.0 (Wick et al., 2017). The whole-genome sequences were annotated by Prokka (Seemann, 2014) automatically followed by manual curation.

Genomic analysis

In silico multi-locus sequence typing was performed using MLST 2.0 (Larsen et al., 2012). Seven housekeeping genes, including *aroC, dnaN, hemD, hisD, purE, sucA*, and *thrA*, were chosen for MLST analysis. The antibiotic resistome(s) were predicted by the Resistance Gene Identifier (RGI) (https://github.com/arpcard/rgi) to query the CARD database (https://card.mcmaster.ca) (Alcock et al., 2020). The virulence genes and plasmid replicons in the sequenced isolates were identified using VFDB (Liu et al., 2022) and PlasmidFinder 2.0 (Carattoli et al., 2014) respectively. In order to contextualize our isolates among the corresponding strains in China, genomes of *S.* Mbandaka were downloaded from EnteroBase in combination with the genomes reported in a large-scale one-health study (Wang et al., 2023). SNPs were detected using Snippy v3.2 (https://github.com/tseemann/snippy) based on recombination filtration by Gubbins v. 2.4.1 (Croucher et al., 2015) and core SNP extraction by SNP-sites v. 2.5.1 (Page et al., 2016). SNPs located in phage regions, repetitive and recombinogenic regions, were removed before phylogenetic analysis. Genomic coordinates corresponding to phage sequences and repetitive elements in the reference genome were determined using Phast (http://phaster.ca) and Mummer (Kurtz et al., 2004), respectively. All extracted SNPs in core genome regions were concatenated as pseudosequences. The approximately-maximum-likelihood phylogenetic tree was inferred from alignments of nucleotide sequences with FastTree (Price et al., 2009). The visualization and annotation of the phylogenetic tree were carried out using R ggtree package (Yu et al., 2017).

OriT Finder was used to determine the conjugation module (Li et al., 2018). ISFinder was used to identify ISs (https://isfinder.biotoul.fr/). Plasmid similarity was examined comparing against the PLSDB plasmid database (Schmartz et al., 2022). Comparison between homologous plasmids were performed using BLASTn and illustrated by Easyfig v2.2.2 (Sullivan et al., 2011). To examine the distribution and features of *mrkABCDF* operon in global plasmids, plasmid reference sequences were downloaded from NCBI (https://ftp.ncbi.nlm.nih.gov/refseq/release/plasmid) and compared using Mashtree (Katz et al., 2019). Serovars assigned from Kauffmann-White scheme were confirmed by SeqSero2 v1.1.1 (Zhang et al., 2019).

Conjugal transference of $bla_{CTX\text{-}M\text{-}15}$ harboring plasmid

In order to examine the conjugal transference of $bla_{CTX\text{-}M\text{-}15}$ harboring plasmid in JNQH940, conjugation experiments were conducted using *E. coli* J53AziR as recipients, following a previously described method (Hao et al., 2021b). Overnight

cultures of JNQH940 and *E. coli* J53AziR were mixed in a 1:1 ratio and applied separately onto 0.45-μm filter paper. The filter papers were then placed on LB agar plates and incubated overnight at 37°C. Transconjugants were selected on Mueller–Hinton agar containing sodium azide (100 mg/L) and ceftazidime (16 mg/L). The presence of transconjugants was confirmed using PCR targeting the $bla_{CTX\text{-}M\text{-}15}$ gene. Conjugation frequency was determined by dividing the number of transconjugants by the number of recipient cells.

Detection of m*rkABCDF* loci by PCR

The *mrkABCDF* virulence loci were identified via a colony Polymerase Chain Reaction (PCR) assay, wherein the target gene *mrkA* was amplified using specific primers (mrkAF: 5'-ACCAGCAAACAACAGGGCTA-3', mrkAR: 5'-TGATTTTGTTGGTCAGCGCG-3'). The occurrence of a positive outcome in this assay was determined by the generation of a DNA fragment with a length of 106 base pairs. For the purpose of assay validation, a well-characterized *K. variicola* isolate JNQH473, which had previously undergone comprehensive sequencing in our prior research (Wang et al., 2021a), was utilized as a positive control.

Nucleotide sequence accession numbers

Complete sequences of the chromosomes and plasmids of strain JNQH940, 948, 950 and 952 have been deposited in the GenBank databases under accession numbers CP136141-CP136151.

Results

Serovar identification and antimicrobial susceptibility

Six different serovars were assigned according to the Kauffmann-White scheme. *S.* Enteritidis was the most common serovar, accounting for 42.1% of the isolates, followed by *S.* Mbandaka (26.3%), Thompson (10.5%), Livingston (10.5%), Alachua (5.3%), Infantis (5.3%) (Figure 1). Antimicrobial-susceptibility testing results showed that isolates of *S.* Mbandaka, Infantis, Livingston, and Alachua exhibited susceptibility to the tested antibiotics. In contrast, JNQH934 (*S.* Thompson) and JNQH940 (*S.* Enteritidis) demonstrated significant resistance to AMP, CIP, and TMP-SMZ, displaying multidrug resistance (Table 2).

TABLE 2 Antimicrobial susceptibility testing for NTS isolates collected from this study.

No. Strains (Serovar)	Antibiotic agents						
	AMP[a]	CAZ[a]	CIP[a]	CRO[a]	LEV[b]	TMP-SMZ[a]	MEM[a]
JNQH933 (Alachua)	22	30	35	32	0.125	30	29
JNQH952 (Enteritidis)	6	22	34	32	0.06	22	30
JNQH953 (Enteritidis)	6	27	31	27	0.125	16	31
JNQH935 (Enteritidis)	6	24	38	30	1	20	31
JNQH941 (Enteritidis)	23	27	35	30	1	20	35
JNQH945 (Enteritidis)	6	25	31	30	0.25	20	35
JNQH940 (Enteritidis)	6	6	21	6	2	6	30
JNQH938 (Enteritidis)	6	25	27	30	0.25	17	32
JNQH951 (Enteritidis)	6	25	31	30	0.03	6	38
JNQH954 (Infantis)	24	29	30	29	0.125	30	32
JNQH944 (Livingstone)	19	25	36	27	0.125	26	30
JNQH932 (Livingstone)	19	27	36	29	0.125	27	31
JNQH946 (Mbandaka)	22	22	34	30	0.06	27	33
JNQH948 (Mbandaka)	23	26	38	30	0.125	24	31
JNQH936 (Mbandaka)	23	24	39	30	0.125	20	30
JNQH947 (Mbandaka)	22	25	35	30	0.125	27	30
JNQH942 (Mbandaka)	20	21	35	30	0.125	25	30
JNQH950 (Thompson)	6	28	31	34	0.125	6	36
JNQH934 (Thompson)	6	22	6	30	1	6	32

[a]Disk infusion method (mm); [b]Microdilution method (μg/ml). AMP, ampicillin; CAZ, ceftazidime; CIP, ciprofloxacin; CRO, ceftriaxone; LEV, levofloxacin; TMP-SMZ, trimethoprim-sulfamethoxazole; MEM, meropenem. All tests were performed in duplicate, and each test included three biological replicates.

Genetic relatedness of *Salmonella* isolates

PFGE analysis utilizing XbaI restriction enzyme was employed to evaluate the genetic relatedness among the isolates. The PFGE patterns of *S.* Enteritidis isolates were similar but distinguishable except JNQH941 and JNQH935. Two *S.* Thompson isolates (JNQH950, 934) had notably different PFGE patterns, indicative of genetic diversity. However, two *S.* Livingston isolates (JNQH932, 944) demonstrated similar PFGE patterns, suggesting a potential genetic relatedness between these isolates. Of note, the *S.* Mbandaka serovar isolates displayed very similar PFGE patterns, suggesting a closer genetic relationship (Figure 2). Interestingly, SNP-based phylogenetic tree uncovered a close relationship between *S.* Mbandaka JNQH948 and a strain (GCA_030099325.1) obtained from human feces in Zhejiang in 2017 (Figure 3), with only 8 SNP differences. These results highlight the occurrence of small-scale clonal spread of *S.* Mbandaka in China.

Genomic and phenotypic characterization of *Salmonella* strains

Whole-genome sequences were obtained for four strains (JNQH948, 950, 952, 940). *S.* Enteritidis strains JNQH940 and JNQH952 harbored three and two plasmids respectively. *S.* Thompson strain JNQH950 carried two plasmids whereas no plasmids were identified in *S.* Mbandaka strain JNQH948. The serovars of all isolates predicted to be consistent with *Salmonella* serotyping by slide agglutination. MLST revealed the *S.* Mbandaka isolate (JNQH948) belonged to ST413. *S.* Enteritidis (JNQH940, 952) and S. Thompson (JNQH950) were classified as ST11 and ST26 respectively. The resistance genotypes predicted by RGI revealed ampicillin resistance were mediated by $bla_{\text{TEM-1}}$. For the MDR JNQH940, resistance to quinolone (CIP) was conferred by *qnrS1*. The resistance of TMP-SMZ was associated with the presence of trimethoprim resistant *sul1/sul2* genes. JNQH940 was found to carry the $bla_{\text{CTX-M-15}}$ gene. Notably, the virulence cluster

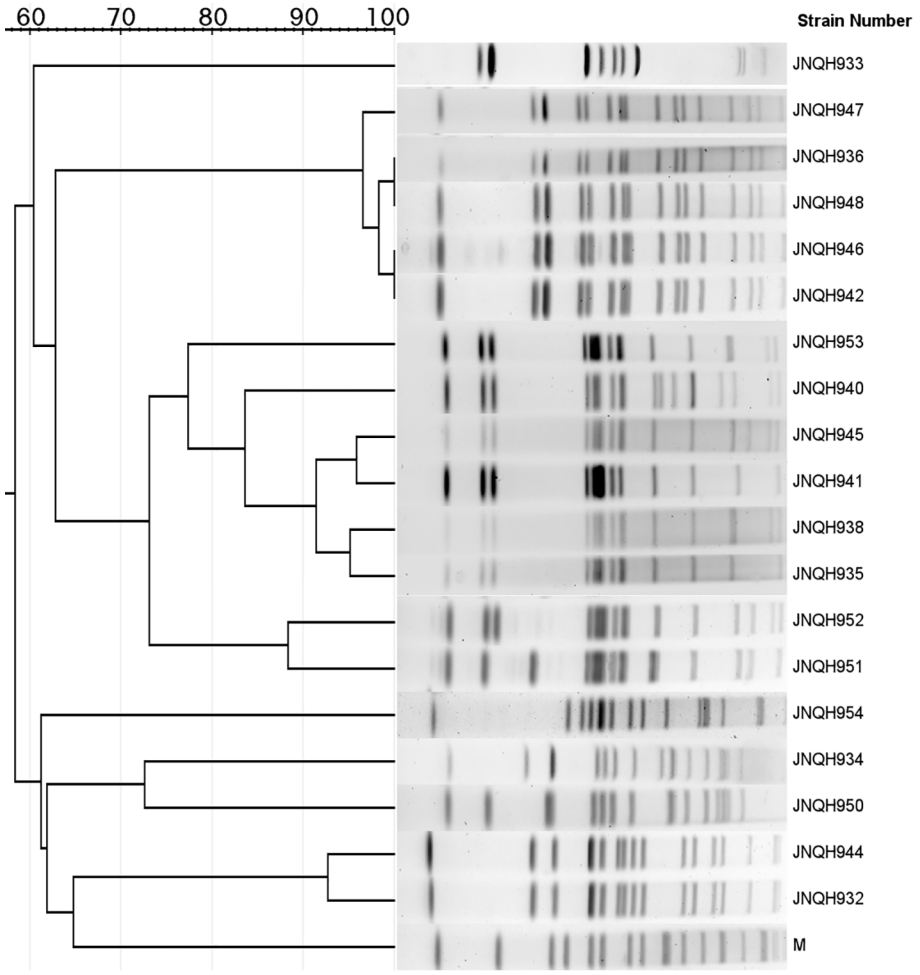

FIGURE 2
Dendrogram of the pulsed-field gel electrophoresis (PFGE) patterns of NTS isolates collected from this study. M, PFGE marker strain (*S.* Braenderup H9812).

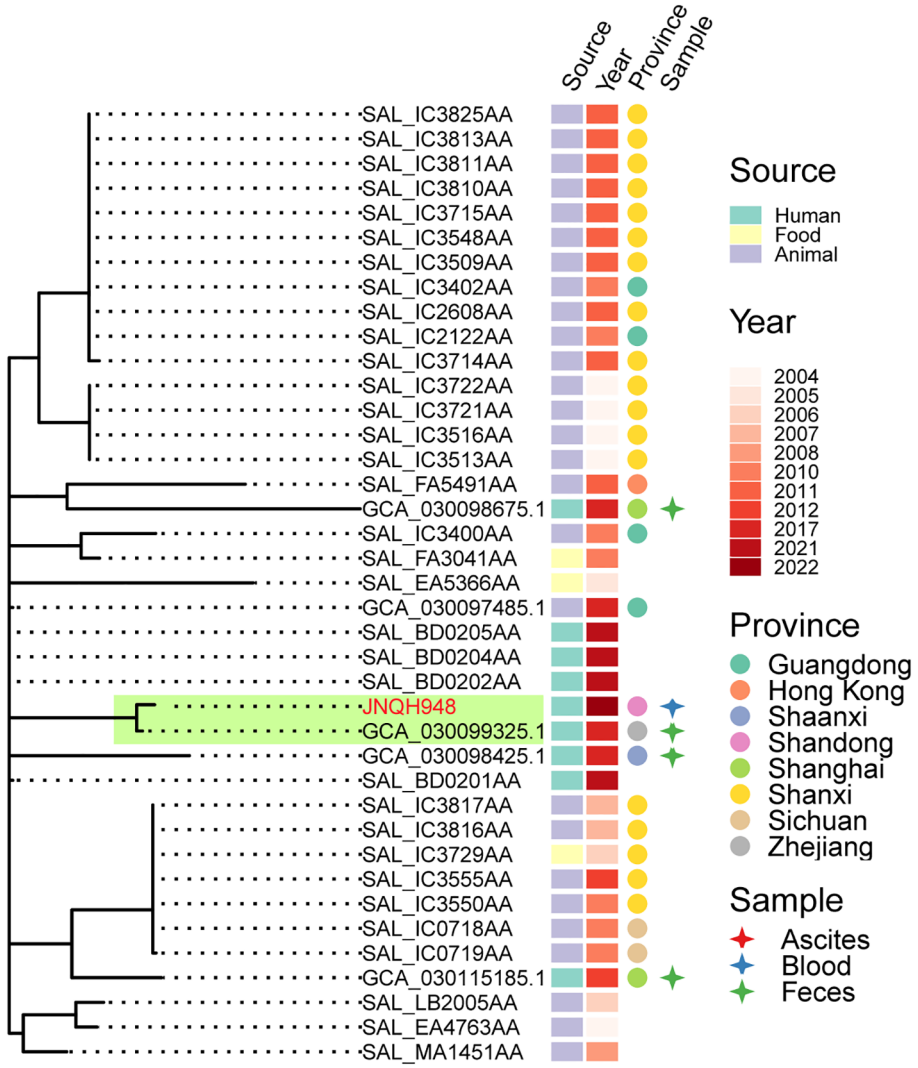

FIGURE 3
Phylogenetic relationships within *S.* Mbandaka strain JNQH948 and publicly available sequences from EnteroBase and a Chinese study. Phylogeny (left) showing the relationships. The strain source, collection year, location and specimen types were shown for each isolate. Subclade containing the JNQH948 and the closely related *S.* Mbandaka strain were indicated in light green shade.

of *mrkABCDF* was detected in *S.* Thompson strain JNQH950 but absent in other strains.

$bla_{CTX\text{-}M\text{-}15}$ was carried by a highly transferrable IncB/O/K/Z plasmid in *S.* Enteritidis strain JNQH940

The $bla_{CTX\text{-}M\text{-}15}$-harboring plasmid in strain JNQH940 was determined to be an IncB/O/K/Z plasmid type, with a length of 127,061bp base pairs. The plasmid contains genes associated with plasmid conjugation, as well as a region comprising genes to encode a type IV pilus system. The conjugation elements included the origin of transfer site (oriT), type IV coupling protein gene (T4CP), and genes encoding the relaxase and some type IV secretion components (T4SS) (Figure 4). Conjugation assays showed the IncB/O/K/Z plasmid was successfully transferred into *E. coli* J53 from JNQH940 strain. The conjugation frequency was 10^{-3} per recipient cell, which was further confirmed by PCR targeting the $bla_{CTX\text{-}M\text{-}15}$ gene and IncB/O/K/Z replicon. In addition to $bla_{CTX\text{-}M\text{-}15}$, the plasmid also harbored 9 additional antimicrobial resistance genes encoding resistance to fluroquinolone (*qnrS1*), macrolide (*mphA*, *mrx*), sulfonamide (*sul1/sul2*), antiseptics (*qacE*) and aminoglycoside [*aadA5, APH(3')-Ib, APH(6)-Id*].

JNQH950 exhibited significantly higher biofilm-forming capabilities mediated by *mrkABCDF* operon in an IncX1 plasmid

We investigated the biofilm-forming capabilities of various *Salmonella* strains. The OD_{590} for JNQH950 was determined to be 1.187, while the other strains exhibited an OD_{590} measurement below 0.29. ATCC14028, which served as a reference, was measured to be

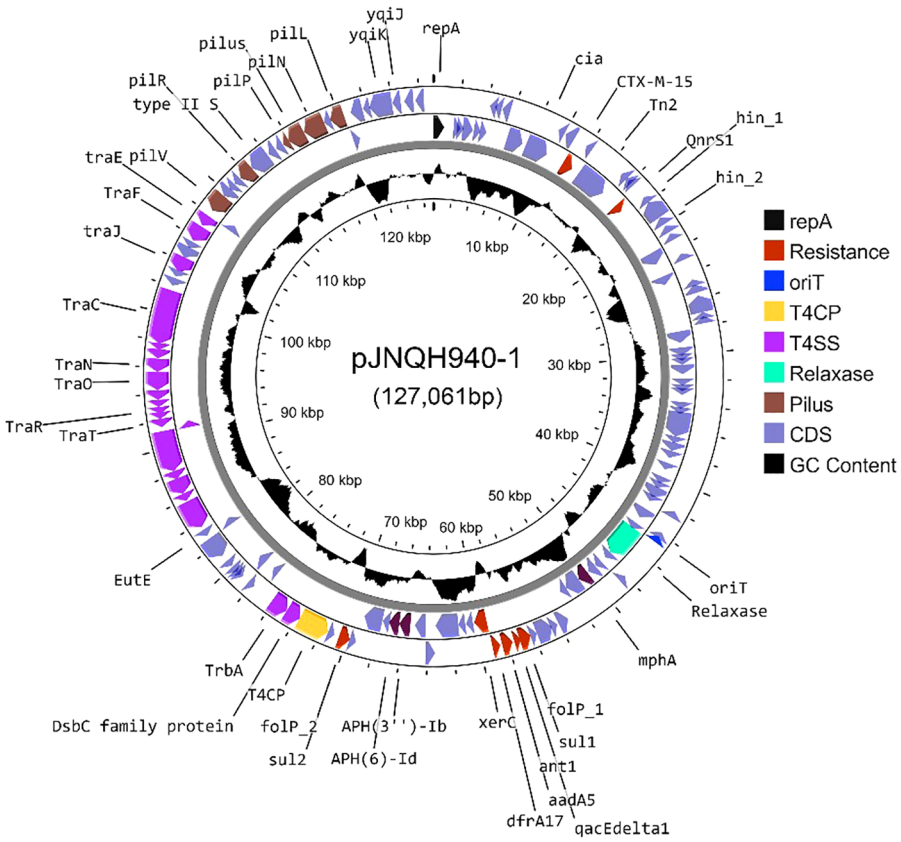

FIGURE 4
A circle map of the *bla*$_{CTX-M-15}$-bearing IncB/O/K/Z type plasmid pJNQH940-1 in strain JNQH940. Open reading frames (ORFs) of pJNQH940-1 are shown as the outermost ring, with plasmid replicons, transconjugation elements (T4CP, T4SS, oriT, relaxase), type IV pilus system and antimicrobial resistance genes highlighted.

0.284. These results underscore the unique biofilm-forming potential of JNQH950 when compared to other tested strains (Figure 5). Further WGS analysis revealed the backbone structure of *mrkABCDF* cluster harboring plasmid belonged to an IncX1 plasmid, with a length of 40,394 base pairs. The *mrkABCDF* cassettes were contained within two IS1A elements of the IS1 family, constituting a transposon of Tn6011. These *mrkABCDF* cassettes encode the main structural subunit and assembly machinery of type 3 fimbriae, which are associated with biofilm formation. In addition, the MGEs associated with plasmid replication, stability, transfer integration was predicted. BLAST query against GenBank database showed that plasmid was closely related to plasmid pCP8-3-IncX1 (NZ_CP053740.1, with 90% coverage and 99.65% identity), pOLA52 (NC_010378.1, with 95% coverage and 99.47% identity), and some others plasmids hosted by *Enterobacterales* (Figure 6).

Tracking key virulence loci encoding *mrkABCDF* operon in global plasmids revealed their prevalence in *Enterobacteriaceae*

A total of 195 plasmids harboring *mrkABCDF* operon were identified in the reference plasmids in NCBI database, most of which are carried by *Enterobacteriaceae*. *K. pneumoniae* is the dominant host strain, followed by *E. coli*, *E. hormaechei*, *K. quasipneumoniae*. These plasmids belong to several incompatibility groups, predominant by IncFIB, IncFII, IncFIA, IncX, IncR. Plasmid sequence analysis by oriTfinder revealed the presence of four crucial conjugation elements (oriT, T4SS, T4CP, relaxase gene) in 31.2% (61/195) of the plasmids. The majority of these plasmids were found in host strains isolated in the environmental sources. The top 5 countries were UK, China, USA, India and Austria. Notably, plasmids originating from homo sapiens were most commonly detected in urine samples. It is noteworthy that 60 of the analyzed plasmids coharbored antibiotic resistance genes, including 6 carbapenem resistance genes and 17 *mcr* genes. *mrkABCDF* operon harboring plasmids has been present in *E. coli* strains dating back to the 1950s. Eight plasmids comprised of a cluster which had a close relationship with our plasmids, all of which belonged to IncX1 plasmid type and were carried by *E. coli* strains (Figure 7).

Discussion

During the year 2022, our hospital diagnosed a total of 19 patients with *Salmonella* infections, as determined through

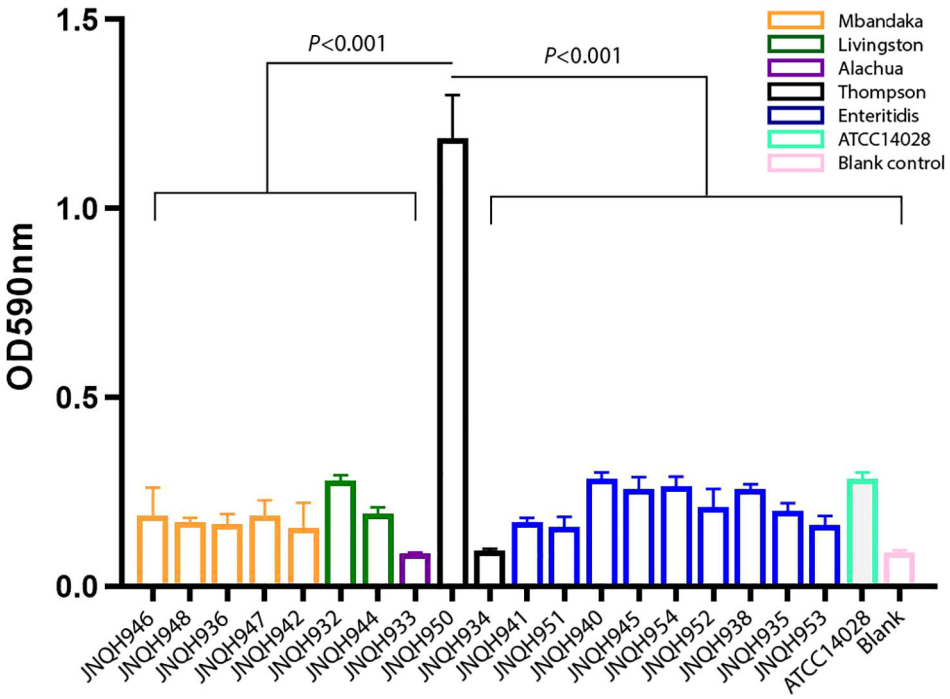

FIGURE 5
Biofilm formation of NTS strains. Data are represented as mean ± standard deviation from at least three independent experiments.

microbiologic cultures. The most commonly identified serovar was *S.* Enteritidis, closely followed by *S.* Mbandaka and some other sporadic serovars including *S.* Thompson, Livingston, Alachua and Infantis. The majority of cases were reported between the months of July and October, with the highest peak occurring in October. Genetic relatedness analysis suggested that *S.* Mbandaka isolates were part of a single clonal expansion whereas *S.* Enteritidis strains were composed of diverse clonal linages. A significant observation was that *S.* Alachua was isolated from the feces of a patient suffering from a gastro-infection, marking the first observation of this particular serovar in China.

Non-typhoidal *Salmonella* infections typically manifest as mild and self-limiting acute enterocolitis in the majority of individuals (Crump et al., 2015). Parenteral infections, resulting from the dissemination of the bacterium beyond the gastrointestinal tract, are infrequent complications of gastroenteritis (Graham et al., 2000). However, reports of nontyphoidal *Salmonella* causing intravascular, bone, and joint infections are widespread on a global scale. In Africa, NTS strains cause invasive disease with bacteraemia more often in children, with 4100 deaths per year (Crump et al., 2015; Akinyemi et al., 2023). Such invasive infections are particularly associated with various forms of immunocompromise, with individuals at the extremes of age or those

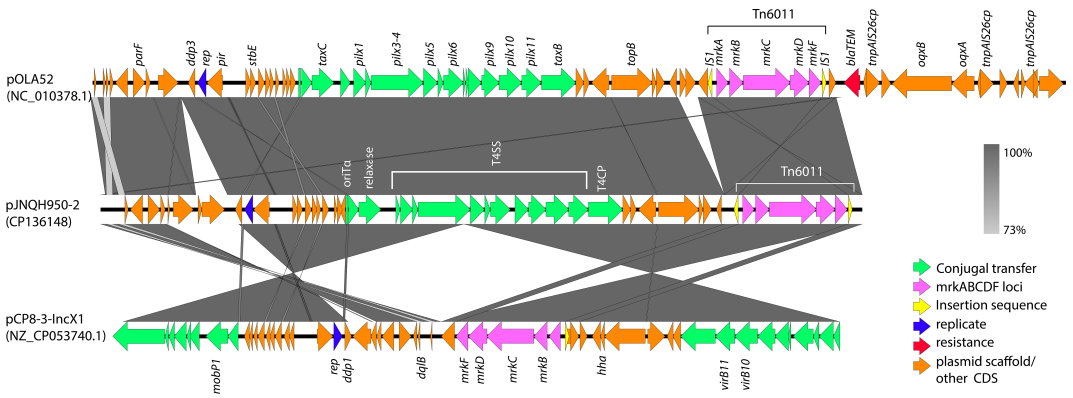

FIGURE 6
Genetic comparison of *mrkABCDF* harboring plasmid pJNQH950-2 and two closely related to plasmid pCP8-3-IncX1 (NZ_CP053740.1), pOLA52 (NC_010378.1). *mrkABCDF* transposon (Tn6011) are shown as the outermost ring. The genes are exhibited in arrows with different colors to note on their functional classes. Shades indicate shared regions of homology. The plasmid accession numbers are listed below the plasmid names.

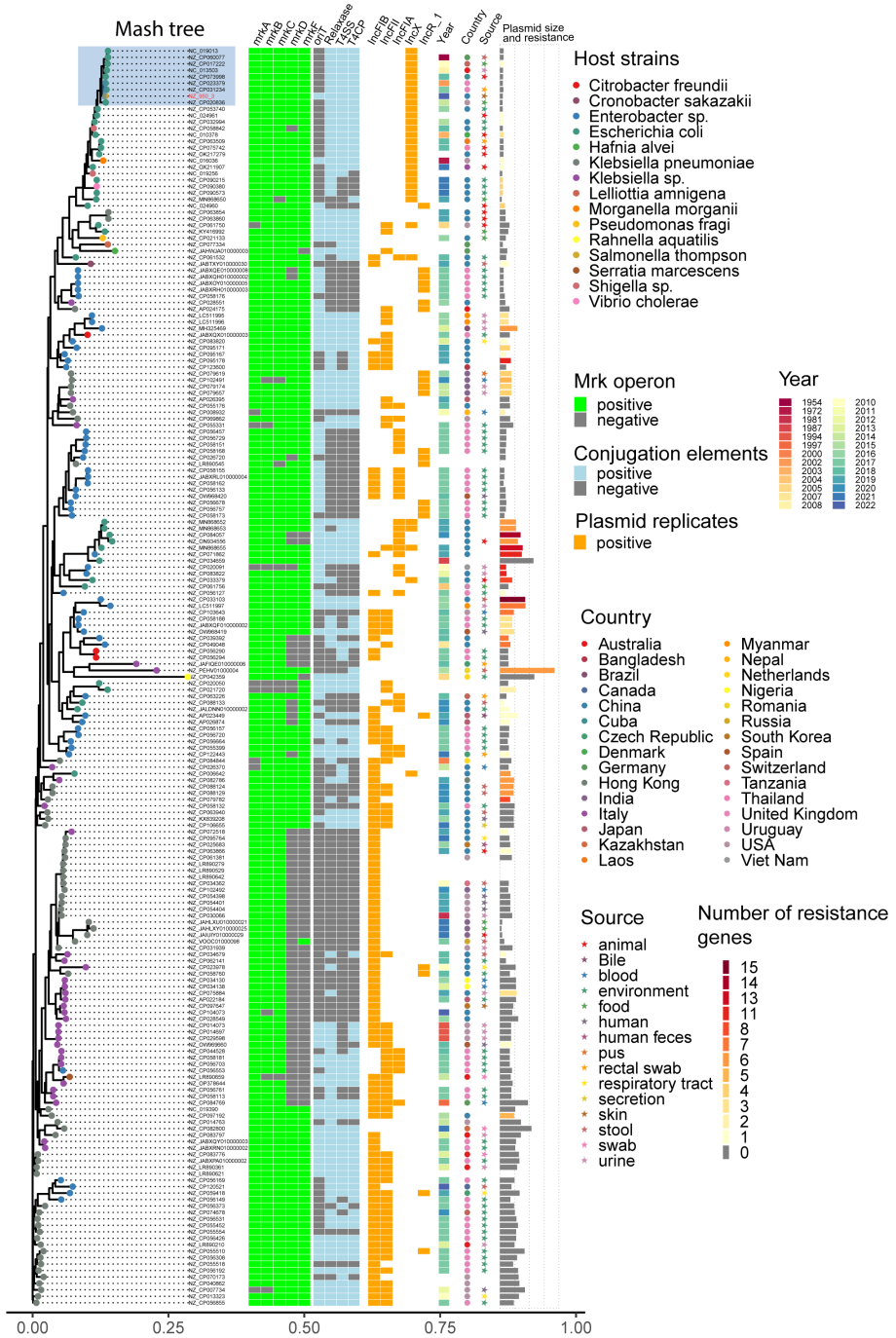

FIGURE 7
Distance tree of plasmids harboring *mrkABCDF* operon in reference NCBI database. Phylogeny (left) showing the relationships between 195 *mrkABCDF* operons harboring plasmids. The presence of *mrkABCDF* virulence loci, plasmid conjugation elements (oriT, T4SS, T4CP, relaxase), top five plasmid types, host strain properties (collection year, country, source), as well as the plasmid size and number of resistance genes were illustrated for each isolate. Grey tiles indicate gene's absence. The isolates' tip points are colored by the host species.

with compromised immune systems (Crump et al., 2011; Parry et al., 2013; Crump et al., 2015; Akinyemi et al., 2021). In our study, nine of our patients experienced extra-intestinal infections, underscoring the potential severity of the encountered *Salmonella* strains. Our cases demonstrated a heightened vulnerability to these infections, possibly due to the presence of multiple comorbidities, including acute leukemia, diabetes, autoimmune diseases, and organ transplantation. Given the impaired immunity in these patients, swift and comprehensive clinical intervention is essential. This is because *Salmonella* can penetrate the compromised intestinal barrier and disseminate to multiple organs, potentially leading to sepsis and severe complications. Therefore, proactive and diligent medical management is crucial for these individuals to minimize adverse outcomes.

Cutaneous infections caused by *Salmonella* are exceedingly rare occurrences. Only a few reports have documented cutaneous manifestations in patients with *S. enterica* infection (Marzano et al., 2003; Desikan et al., 2009; Wiegand et al., 2009; Alfouzan et al., 2017). In our study, we observed that *S.* Thompson strain JNQH950 isolated from the skin secretion displayed a remarkable capacity for robust biofilm formation. Notably, this strain persisted for three months in the toe secretion of a 58-year-old male patient with type 2 diabetes mellitus. Despite antibiotic treatment and undergoing three operations of toe amputation and skin grafting, the condition worsened, leading to the necessity of foot amputation due to progressive tissue necrosis. Phenotypic analysis showed the *S.* Thompson strain JNQH950 could form strong biofilm compared with other strains. It is suspected that bacteria are difficult to eradicate when protected within biofilms, thus acquire the enhanced ability to persist and spread in the human body or the environment (Lamas et al., 2018; Gual-De-Torrella et al., 2022).

Salmonella sp. has the capability to develop biofilms, and bacteria within these biofilms exhibit increased resistance to drugs, chemicals, physical and mechanical stresses, as well as evasion of host immune responses (Lamas et al., 2018). The primary constituents of *Salmonella* biofilms are curli fimbriae and cellulose (Lamas et al., 2018). Interestingly, genetic analysis revealed an intact *mrkABCDF* operon in strain JNQH950, which had been demonstrated associated with type 3 fimbriae expression, surface attachment, and biofilm formation in *K. pneumoniae* (Norman et al., 2008; Ong et al., 2009). The *mrkABCDF* operon harboring plasmid had highly conserved plasmid synteny and structure with a previously reported pOLA52 plasmid in *E.coli*, which also is an IncX1 plasmid and showed a high conjugative capability (Norman et al., 2008). In addition, the gene cluster had acquired mobility flanking by IS1 (Tn6011) compared to its original gene cluster (Norman et al., 2008). Further genetic analysis showed the *mrkABCDF* gene cluster has now spread among various enterobacterial species, but was not reported in *S. enterica* strains (Figure 7). In this study, although the conjugation was not performed due to the lack of selective marker, we can suspect the *mrkABCDF* loci could be mobilized through plasmid conjugation or genetic loci transposon. Taken together, to the best of our knowledge, this was the first report of *mrkABCDF* operon within *S. enterica* responsible for human infection. The emergence of such *Salmonella* strain emphasizes the urgent need for meticulous monitoring and surveillance to address potential public health implications. Nevertheless, the molecular mechanism responsible for the contribution of *mrkABCDF* to biofilm formation and enhanced antibiotic treatment resistance in *S. enterica* is yet to be elucidated.

The increasing prevalence of antibiotic resistance, particularly towards fluoroquinolones and third-generation cephalosporins, presents formidable challenges in clinical management (Fierer, 2022). Infections caused by antimicrobial-resistant *Salmonella*, especially those resistant to quinolones, pose a significant threat to human populations, leading to higher morbidity and mortality rates (Varma et al., 2005; Xia et al., 2009). Of particular concern is the emergence of nontyphoidal *Salmonella* strains that exhibit resistance to extended-spectrum cephalosporins, such as ceftazidime and ceftriaxone, which raises substantial public health concerns (Crump et al., 2015; Fakorede et al., 2023). These third-generation cephalosporins play a crucial role in managing invasive *Salmonella* infections, especially in vulnerable populations like children, for whom fluoroquinolones may not be the preferred treatment. Our study identified two MDR isolates that were resistant to AMP, CIP and TMP-SMZ, one of which exhibited resistance to third-generation cephalosporins. The presence of $bla_{\text{CTX-M-15}}$ gene, conferring cephalosporin resistance, was located on a transferable IncB/O/K/Z plasmid. The plasmid carried all essential elements necessary for conjugation and, importantly, also harbored the type IV pilus system, known to significantly enhance conjugation both *in vivo* and *in vitro* (Neil et al., 2020). Consequently, the combination of fluoroquinolone and cephalosporin resistance, carried on a highly transferable plasmid in these *Salmonella* isolates, raises serious concerns about the potential dissemination of these resistance traits. Vigilant monitoring and the implementation of comprehensive strategies are urgently needed to address this pressing public health issue.

Our data also showed that *S.* Enteritidis were the most common serovars detected in our hospital, which is consistent with the findings in other studies in China (Wang et al., 2015; Wang et al., 2023). In addition, the proportion of *S.* Mbandaka was reported to be 0.25% of the total NTS collection, most of which were from non-human origin (Wang et al., 2023). Genetic analysis revealed that the *S.* Enteritidis strains in this study displayed significant genetic diversity, in line with findings from an epidemiological study in China (Wang et al., 2015). On the other hand, our analysis of *S.* Mbandaka isolates revealed a different scenario. These isolates formed a single clonal lineage, indicating a common origin. A recent study in China had reported *S.* Mbandaka could be clonally transmitted between broiler farm and slaughterhouse (Wang et al., 2021b). Further comparison with a large-scale collection of *S.* Mbandaka in China identified one closely related strain, which was isolated from human feces in Zhejiang in 2017. Given previous studies suggesting *S.* Mbandaka's adaptation to survival in the farm environment (Hayward et al., 2016), our findings suggest that this clone in this study likely originated from a single source that persisted over 5 years in China.

In summary, our research provides the phenotypic and molecular overview of current serovar prevalence of NTS strains isolated from human origins in China. *S.* Enteritidis strains displayed significant genetic diversity while *S.* Mbandaka strains were suspected to derive from a single clonal expansion. The further spread of the $bla_{\text{CTX-M-15}}$ harboring IncB/O/K/Z plasmids and spread of virulent *mrkABCDF* operon into *Salmonella* in China and other global regions should be closely monitored.

Data availability statement

The datasets presented in this study can be found in online repositories. The names of the repository/repositories and accession number(s) can be found in the article/supplementary material.

Ethics statement

The studies involving humans were approved by The First Affiliated Hospital of Shandong First Medical University. The studies were conducted in accordance with the local legislation and institutional requirements. Written informed consent for participation in this study was provided by the participants' legal guardians/next of kin.

Author contributions

WM: Conceptualization, Methodology, Supervision, Writing – original draft. XC: Data curation, Methodology, Writing – original draft. XD: Writing – original draft. XL: Methodology, Writing – original draft. KL: Visualization, Writing – original draft. YW: Software, Writing – original draft. XS: Project administration, Writing – original draft. LC: Validation, Visualization, Writing – review & editing. MH: Conceptualization, Supervision, Writing – original draft, Writing – review & editing.

Funding

The author(s) declare financial support was received for the research, authorship, and/or publication of this article. This work was supported by the Natural Science Foundation of Shandong Province, China [grant number ZR2021MH078]; Clinical & Medical Science and Technology Innovation Program of Jinan, Shandong Province [grant number 202134040]; and Cultivate Fund from The First Affiliated Hospital of Shandong First Medical University & Shandong Provincial Qianfoshan Hospital [grant numbers QYPY2022NSFC0802].

Acknowledgments

We like to thank Bingqing Li for the gift of *S.* Typhimurium ATCC14028 strain.

Conflict of interest

The authors declare that the research was conducted in the absence of any commercial or financial relationships that could be construed as a potential conflict of interest.

Publisher's note

References

Akinyemi, K. O., Ajoseh, S. O., and Fakorede, C. O. (2021). A systemic review of literatures on human Salmonella enterica serovars in Nigeria, (1999-2018). *J. Infect. Dev. Ctries.* 15, 1222–1235. doi: 10.3855/jidc.12186

Akinyemi, K. O., Fakorede, C. O., Linde, J., Methner, U., Wareth, G., Tomaso, H., et al. (2023). Whole genome sequencing of Salmonella enterica serovars isolated from humans, animals, and the environment in Lagos, Nigeria. *BMC Microbiol.* 23, 164. doi: 10.1186/s12866-023-02901-1

Alcock, B. P., Raphenya, A. R., Lau, T. T. Y., Tsang, K. K., Bouchard, M., Edalatmand, A., et al. (2020). CARD 2020: antibiotic resistome surveillance with the comprehensive antibiotic resistance database. *Nucleic Acids Res.* 48, D517–D525. doi: 10.1093/nar/gkz935

Alfouzan, W., Bulach, D., Izumiya, H., Albassam, K., Sheikh, S., Alrubai'aan, N., et al. (2017). Carbuncle due to Salmonella Enteritidis: a novel presentation. *Gut Pathog.* 9, 51. doi: 10.1186/s13099-017-0200-2

Amuasi, J. H., and May, J. (2019). Non-typhoidal salmonella: invasive, lethal, and on the loose. *Lancet Infect. Dis.* 19, 1267–1269. doi: 10.1016/S1473-3099(19)30521-3

Branchu, P., Bawn, M., and Kingsley, R. A. (2018). Genome variation and molecular epidemiology of Salmonella enterica serovar typhimurium pathovariants. *Infect. Immun.* 86, e00079–18. doi: 10.1128/IAI.00079-18

Carattoli, A., Zankari, E., Garcia-Fernandez, A., Voldby Larsen, M., Lund, O., Villa, L., et al. (2014). In silico detection and typing of plasmids using PlasmidFinder and plasmid multilocus sequence typing. *Antimicrob. Agents Chemother.* 58, 3895–3903. doi: 10.1128/AAC.02412-14

CLSI (2021). *Performance Standards for Antimicrobial Susceptibility Testing, M100. 31st Edition* (Wayne, PA: Clinical and Laboratory Standards Institute).

Croucher, N. J., Page, A. J., Connor, T. R., Delaney, A. J., Keane, J. A., Bentley, S. D., et al. (2015). Rapid phylogenetic analysis of large samples of recombinant bacterial whole genome sequences using Gubbins. *Nucleic Acids Res.* 43, e15. doi: 10.1093/nar/gku1196

Crump, J. A., Medalla, F. M., Joyce, K. W., Krueger, A. L., Hoekstra, R. M., Whichard, J. M., et al. (2011). Antimicrobial resistance among invasive nontyphoidal Salmonella enterica isolates in the United States: National Antimicrobial Resistance Monitoring System 1996 to 2007. *Antimicrob. Agents Chemother.* 55, 1148–1154. doi: 10.1128/AAC.01333-10

Crump, J. A., Sjolund-Karlsson, M., Gordon, M. A., and Parry, C. M. (2015). Epidemiology, clinical presentation, laboratory diagnosis, antimicrobial resistance, and antimicrobial management of invasive Salmonella infections. *Clin. Microbiol. Rev.* 28, 901–937. doi: 10.1128/CMR.00002-15

Desikan, P., Kumar, Y., Pande, H. K., Jain, A., Panwalkar, N., Verma, M., et al. (2009). Isolated ulcerative skin lesion caused by Salmonella Weltevreden. *J. Infect. Dev. Ctries.* 3, 569–571. doi: 10.3855/jidc.477

Fakorede, C. O., Amisu, K. O., Saki, M., and Akinyemi, K. O. (2023). Co-existence of extended-spectrum beta-lactamases bla(CTX-M-9) and bla(CTX-M-15) genes in Salmonella species isolated from febrile and diarrhoeagenic patients in Lagos, Nigeria: a cross-sectional study. *Eur. J. Med. Res.* 28, 3. doi: 10.1186/s40001-022-00960-0

Fierer, J. (2022). Invasive non-typhoidal Salmonella (iNTS) infections. *Clin. Infect. Dis.* 75, 732–738. doi: 10.1093/cid/ciac035

Gebreyes, W. A., Thakur, S., Dorr, P., Tadesse, D. A., Post, K., and Wolf, L. (2009). Occurrence of spvA virulence gene and clinical significance for multidrug-resistant Salmonella strains. *J. Clin. Microbiol.* 47, 777–780. doi: 10.1128/JCM.01660-08

Graham, S. M., Molyneux, E. M., Walsh, A. L., Cheesbrough, J. S., Molyneux, M. E., and Hart, C. A. (2000). Nontyphoidal Salmonella infections of children in tropical Africa. *Pediatr. Infect. Dis. J.* 19, 1189–1196. doi: 10.1097/00006454-200012000-00016

Gual-De-Torrella, A., Delgado-Valverde, M., Perez-Palacios, P., Oteo-Iglesias, J., Rojo-Molinero, E., Macia, M. D., et al. (2022). Prevalence of the fimbrial operon mrkABCD, mrkA expression, biofilm formation and effect of biocides on biofilm formation in carbapenemase-producing Klebsiella pneumoniae isolates belonging or not belonging to high-risk clones. *Int. J. Antimicrob. Agents* 60, 106663. doi: 10.1016/j.ijantimicag.2022.106663

Hao, M., Ma, W., Dong, X., Li, X., Cheng, F., and Wang, Y. (2021a). Comparative genome analysis of multidrug-resistant Pseudomonas aeruginosa JNQH-PA57, a

clinically isolated mucoid strain with comprehensive carbapenem resistance mechanisms. *BMC Microbiol.* 21, 133. doi: 10.1186/s12866-021-02203-4

Hao, M., Schuyler, J., Zhang, H., Shashkina, E., Du, H., Fouts, D. E., et al. (2021b). Apramycin resistance in epidemic carbapenem-resistant Klebsiella pneumoniae ST258 strains. *J. Antimicrob. Chemother*. 76, 2017–2023. doi: 10.1093/jac/dkab131

Hayward, M. R., Petrovska, L., Jansen, V. A., and Woodward, M. J. (2016). Population structure and associated phenotypes of Salmonella enterica serovars Derby and Mbandaka overlap with host range. *BMC Microbiol.* 16, 15. doi: 10.1186/s12866-016-0628-4

Heras, J., Dominguez, C., Mata, E., Pascual, V., Lozano, C., Torres, C., et al. (2015). GelJ–a tool for analyzing DNA fingerprint gel images. *BMC Bioinf.* 16, 270. doi: 10.1186/s12859-015-0703-0

Katz, L. S., Griswold, T., Morrison, S. S., Caravas, J. A., Zhang, S., Den Bakker, H. C., et al. (2019). Mashtree: a rapid comparison of whole genome sequence files. *J. Open Source Softw.* 4, 1762. doi: 10.21105/joss.01762

Kurtz, S., Phillippy, A., Delcher, A. L., Smoot, M., Shumway, M., Antonescu, C., et al. (2004). Versatile and open software for comparing large genomes. *Genome Biol.* 5, R12. doi: 10.1186/gb-2004-5-2-r12

Lamas, A., Regal, P., Vazquez, B., Miranda, J. M., Cepeda, A., and Franco, C. M. (2018). Salmonella and Campylobacter biofilm formation: a comparative assessment from farm to fork. *J. Sci. Food Agric.* 98, 4014–4032. doi: 10.1002/jsfa.8945

Larsen, M. V., Cosentino, S., Rasmussen, S., Friis, C., Hasman, H., Marvig, R. L., et al. (2012). Multilocus sequence typing of total-genome-sequenced bacteria. *J. Clin. Microbiol.* 50, 1355–1361. doi: 10.1128/JCM.06094-11

Li, X., Xie, Y., Liu, M., Tai, C., Sun, J., Deng, Z., et al. (2018). oriTfinder: a web-based tool for the identification of origin of transfers in DNA sequences of bacterial mobile genetic elements. *Nucleic Acids Res.* 46, W229–W234. doi: 10.1093/nar/gky352

Liu, B., Zheng, D., Zhou, S., Chen, L., and Yang, J. (2022). VFDB 2022: a general classification scheme for bacterial virulence factors. *Nucleic Acids Res.* 50, D912–D917. doi: 10.1093/nar/gkab1107

Ma, W., Zhu, B., Wang, W., Wang, Q., Cui, X., Wang, Y., et al. (2023). Genetic and enzymatic characterization of two novel bla(NDM-36, -37) variants in Escherichia coli strains. *Eur. J. Clin. Microbiol. Infect. Dis.* 42, 471–480. doi: 10.1007/s10096-023-04576-y

Magiorakos, A. P., Srinivasan, A., Carey, R. B., Carmeli, Y., Falagas, M. E., Giske, C. G., et al. (2012). Multidrug-resistant, extensively drug-resistant and pandrug-resistant bacteria: an international expert proposal for interim standard definitions for acquired resistance. *Clin. Microbiol. Infect.* 18, 268–281. doi: 10.1111/j.1469-0691.2011.03570.x

Marchello, C. S., Birkhold, M., Crump, J. A., and Vacc-I, N.T.S.C.C. (2022). Complications and mortality of non-typhoidal salmonella invasive disease: a global systematic review and meta-analysis. *Lancet Infect. Dis.* 22, 692–705. doi: 10.1016/S1473-3099(21)00615-0

Marzano, A. V., Mercogliano, M., Borghi, A., Facchetti, M., and Caputo, R. (2003). Cutaneous infection caused by Salmonella typhi. *J. Eur. Acad. Dermatol. Venereol.* 17, 575–577. doi: 10.1046/j.1468-3083.2003.00797.x

Neil, K., Allard, N., Grenier, F., Burrus, V., and Rodrigue, S. (2020). Highly efficient gene transfer in the mouse gut microbiota is enabled by the Incl(2) conjugative plasmid TP114. *Commun. Biol.* 3, 523. doi: 10.1038/s42003-020-01253-0

Norman, A., Hansen, L. H., She, Q., and Sorensen, S. J. (2008). Nucleotide sequence of pOLA52: a conjugative IncX1 plasmid from Escherichia coli which enables biofilm formation and multidrug efflux. *Plasmid* 60, 59–74. doi: 10.1016/j.plasmid.2008.03.003

Ong, C. L., Beatson, S. A., Mcewan, A. G., and Schembri, M. A. (2009). Conjugative plasmid transfer and adhesion dynamics in an Escherichia coli biofilm. *Appl. Environ. Microbiol.* 75, 6783–6791. doi: 10.1128/AEM.00974-09

Page, A. J., Taylor, B., Delaney, A. J., Soares, J., Seemann, T., Keane, J. A., et al. (2016). SNP-sites: rapid efficient extraction of SNPs from multi-FASTA alignments. *Microb. Genom.* 2, e000056. doi: 10.1099/mgen.0.000056

Parry, C. M., Thomas, S., Aspinall, E. J., Cooke, R. P., Rogerson, S. J., Harries, A. D., et al. (2013). A retrospective study of secondary bacteraemia in hospitalised adults with community acquired non-typhoidal Salmonella gastroenteritis. *BMC Infect. Dis.* 13, 107. doi: 10.1186/1471-2334-13-107

Price, M. N., Dehal, P. S., and Arkin, A. P. (2009). FastTree: computing large minimum evolution trees with profiles instead of a distance matrix. *Mol. Biol. Evol.* 26, 1641–1650. doi: 10.1093/molbev/msp077

Schmartz, G. P., Hartung, A., Hirsch, P., Kern, F., Fehlmann, T., Muller, R., et al. (2022). PLSDB: advancing a comprehensive database of bacterial plasmids. *Nucleic Acids Res.* 50, D273–D278. doi: 10.1093/nar/gkab1111

Seemann, T. (2014). Prokka: rapid prokaryotic genome annotation. *Bioinformatics* 30, 2068–2069. doi: 10.1093/bioinformatics/btu153

Sullivan, M. J., Petty, N. K., and Beatson, S. A. (2011). Easyfig: a genome comparison visualizer. *Bioinformatics* 27, 1009–1010. doi: 10.1093/bioinformatics/btr039

Varma, J. K., Molbak, K., Barrett, T. J., Beebe, J. L., Jones, T. F., Rabatsky-Ehr, T., et al. (2005). Antimicrobial-resistant nontyphoidal Salmonella is associated with excess bloodstream infections and hospitalizations. *J. Infect. Dis.* 191, 554–561. doi: 10.1086/427263

Wang, Y. T., Lei, C. W., Liu, S. Y., Chen, X., Gao, Y. F., Zhang, Y., et al. (2021b). Tracking Salmonella enterica by whole genome sequencing of isolates recovered from broiler chickens in a poultry production system. *Int. J. Food Microbiol.* 350, 109246. doi: 10.1016/j.ijfoodmicro.2021.109246

Wang, Y., Liu, Y., Lyu, N., Li, Z., Ma, S., Cao, D., et al. (2023). The temporal dynamics of antimicrobial-resistant Salmonella enterica and predominant serovars in China. *Natl. Sci. Rev.* 10, nwac269. doi: 10.1093/nsr/nwac269

Wang, Y., Yang, B., Wu, Y., Zhang, Z., Meng, X., Xi, M., et al. (2015). Molecular characterization of Salmonella enterica serovar Enteritidis on retail raw poultry in six provinces and two National cities in China. *Food Microbiol.* 46, 74–80. doi: 10.1016/j.fm.2014.07.012

Wang, Y., Zhu, B., Liu, M., Dong, X., Ma, J., Li, X., et al. (2021a). Characterization of IncHI1B Plasmids Encoding Efflux Pump TmexCD2-ToprJ2 in Carbapenem-Resistant Klebsiella variicola, Klebsiella quasipneumoniae, and Klebsiella michiganensis Strains. *Front. Microbiol.* 12. doi: 10.3389/fmicb.2021.759208

Wen, S. C., Best, E., and Nourse, C. (2017). Non-typhoidal Salmonella infections in children: Review of literature and recommendations for management. *J. Paediatr. Child Health* 53, 936–941. doi: 10.1111/jpc.13585

Wick, R. R., Judd, L. M., Gorrie, C. L., and Holt, K. E. (2017). Unicycler: Resolving bacterial genome assemblies from short and long sequencing reads. *PloS Comput. Biol.* 13, e1005595. doi: 10.1371/journal.pcbi.1005595

Wiegand, G., Rauch, R., Hermann, M., Apitz, C., Hofbeck, M., and Heininger, U. (2009). [Salmonella enteritidis infection presenting with septic shock, renal failure and cutaneous manifestations]. *Klin. Padiatr.* 221, 41–43. doi: 10.1055/s-2007-984366

Xia, S., Hendriksen, R. S., Xie, Z., Huang, L., Zhang, J., Guo, W., et al. (2009). Molecular characterization and antimicrobial susceptibility of Salmonella isolates from infections in humans in Henan Province, China. *J. Clin. Microbiol.* 47, 401–409. doi: 10.1128/JCM.01099-08

Yu, G., Smith, D. K., Zhu, H., Guan, Y., and Lam, T. T. Y. (2017). ggtree: an R package for visualization and annotation of phylogenetic trees with their covariates and other associated data. *Methods Ecol. Evol.* 8, 28–36. doi: 10.1111/2041-210X.12628

Zhang, S., Den Bakker, H. C., Li, S., Chen, J., Dinsmore, B. A., Lane, C., et al. (2019). SeqSero2: rapid and improved Salmonella serotype determination using whole-genome sequencing data. *Appl. Environ. Microbiol.* 85, e01746–19. doi: 10.1128/AEM.01746-19

Zhao, S., Qaiyumi, S., Friedman, S., Singh, R., Foley, S. L., White, D. G., et al. (2003). Characterization of Salmonella enterica serotype newport isolated from humans and food animals. *J. Clin. Microbiol.* 41, 5366–5371. doi: 10.1128/JCM.41.12.5366-5371.2003

frontiers | Frontiers in Cellular and Infection Microbiology

TYPE Original Research
PUBLISHED 19 January 2024
DOI 10.3389/fcimb.2023.1322874

OPEN ACCESS

EDITED BY
Manuel Gerardo Ballesteros Monrreal,
University of Sonora, Mexico

REVIEWED BY
Maritza Alvarez-Ainza,
Universidad de Sonora, Mexico
Mehreen Arshad,
Ann & Robert H. Lurie Children's Hospital of Chicago, United States

*CORRESPONDENCE
María Dolores Alcántar-Curiel
alcantar@unam.mx
Verónica Jiménez-Rojas
verozenemij@hotmail.com

RECEIVED 17 October 2023
ACCEPTED 22 December 2023
PUBLISHED 19 January 2024

CITATION
Jiménez-Rojas V, Villanueva-García D, Miranda-Vega AL, Aldana-Vergara R, Aguilar-Rodea P, López-Marceliano B, Reyes-López A and Alcántar-Curiel MD (2024) Gut colonization and subsequent infection of neonates caused by extended-spectrum beta-lactamase-producing *Escherichia coli* and *Klebsiella pneumoniae*. *Front. Cell. Infect. Microbiol.* 13:1322874. doi: 10.3389/fcimb.2023.1322874

Gut colonization and subsequent infection of neonates caused by extended-spectrum beta-lactamase-producing *Escherichia coli* and *Klebsiella pneumoniae*

Verónica Jiménez-Rojas[1*], Dina Villanueva-García[2], Ana Luisa Miranda-Vega[2], Rubén Aldana-Vergara[1], Pamela Aguilar-Rodea[1], Beatriz López-Marceliano[1], Alfonso Reyes-López[3] and María Dolores Alcántar-Curiel[4*]

[1]Unidad de Investigación en Enfermedades Infecciosas, Hospital Infantil de México Federico Gómez, Ciudad de México, Mexico, [2]Departamento de Neonatología, Hospital Infantil de México Federico Gómez, Ciudad de México, Mexico, [3]Centro de Estudios Económicos y Sociales en Salud, Hospital Infantil de México Federico Gómez, Ciudad de México, Mexico, [4]Laboratorio de Infectología, Microbiología e Inmunología Clínica. Unidad de Investigación en Medicina Experimental, Facultad de Medicina, Universidad Nacional Autónoma de México, Ciudad de México, Mexico

The gut microbiota harbors diverse bacteria considered reservoirs for antimicrobial resistance genes. The global emergence of extended-spectrum beta-lactamase (ESBL)-producing Enterobacterales (ESBL-PE) significantly contributes to healthcare-associated infections (HAIs). We investigated the presence of ESBL-producing *Escherichia coli* (ESBL-PEco) and ESBL-producing *Klebsiella pneumoniae* (ESBL-PKpn) in neonatal patients' guts. Furthermore, we identified the factors contributing to the transition towards ESBL-PEco and ESBL-PKpn-associated healthcare-associated infections (HAIs). The study was conducted from August 2019 to February 2020, in a Neonatal Intensive Care Unit of the Hospital Infantil de México Federico Gómez. Rectal samples were obtained upon admission, on a weekly basis for a month, and then biweekly until discharge from the neonatology ward. Clinical data, culture results, and infection information were gathered. We conducted antimicrobial tests, multiplex PCR assay, and pulsed-field gel electrophoresis (PFGE) to determine the antimicrobial resistance profile and genetic relationships. A comparison between the group's controls and cases was performed using the Wilcoxon and Student t-tests. Of the 61 patients enrolled, 47 were included, and 203 rectal samples were collected, identifying 242 isolates. In 41/47 (87%) patients, colonization was due to ESBL-PEco or ESBL-PKpn. And nine of them developed HAIs (22%, 9/41). ESBL-PEco resistance to cephalosporins ranged from 25.4% to 100%, while ESBL-PKpn resistance varied from 3% to 99%, and both bacteria were susceptible to carbapenems, tigecillin, and colistin. The prevalent $bla_{\text{CTX-M-group-1}}$ gene accounted for 77.2% in ESBL-PEco and 82.2% in ESBL-PKpn, followed by bla_{TEM} 50% and $bla_{\text{OXA-1}}$ 43.8% in ESBL-PEco and bla_{TEM} 80.2% and bla_{SHV} 76.2% in ESBL-PKpn. Analysis of clonality revealed identical colonizing and

infection isolates in only seven patients. Significant risk factors included hospital stay duration, duration of antibiotic treatment, and invasive device usage. Our findings suggest high ESBL-PEco and ESBL-PKpn rates of colonization often lead to infection in neonates. Attention should be paid to patients with ESBL-PE.

KEYWORDS

Escherichia coli, *Klebsiella pneumoniae*, ESBL - extended-spectrum beta-lactamase, gut colonization, HAI - healthcare-associated infection, neonates

Introduction

Immediately following birth, the establishment of microorganisms begins, shaping the microbiota of newborns (Groer et al., 2014). The composition of this microbiota is influenced by various factors, including the mode of delivery, gestational age, birth weight, among others (Collado et al., 2012; Groer et al., 2014; Prince et al., 2014).

Unfortunately, hospitalized newborns are exposed and vulnerable to acquiring an altered microbiome due to the atypical care environment they experience in a Neonatal Intensive Care Unit (NICU) (Hartz et al., 2015). Coupled with their nascent immune system and multiple invasive procedures, they become susceptible to healthcare-associated infections (HAIs) (Calva et al., 1996; Groer et al., 2014). A significant influencing factor is medical treatment, particularly antibiotics, which have led to the emergence of bacteria capable of evading their action through various resistance mechanisms (Bäckhed et al., 2012; Vangay et al., 2015). Notably, among these resistant strains are ESBL-producing *Escherichia coli* (ESBL-PEco) and ESBL-producing *Klebsiella pneumoniae* (ESBL-PKpn), these Gram-negative rod-shaped bacteria are classified within the Enterobacteriaceae family of the order Enterobacterales. They are responsible for a wide array of infections that exacerbate healthcare challenges due to their remarkable ability to develop resistance against multiple drugs, severely limiting available treatment options. Consequently, the World Health Organization (WHO) has categorized them as "pathogens with critical priority" due to their escalating prevalence as causative agents of HAIs, underscoring the urgent need for research and the development of novel antibiotics (Tacconelli et al., 2018; CDC, 2019).

The presence of ESBL-PE in the gut microbiota could be a risk to both colonized patients and those who share the hospital environment (Armand-Lefèvre et al., 2018; Souverein et al., 2019; Denkel et al., 2020; Campos-Madueno et al., 2023).

The aim of this study was to prospectively investigate the incidence of neonates intestinally colonized with ESBL-PEco or ESBL-PKpn and the factors enabling the progression from colonization to infectious disease. Furthermore, we sought to characterize the ESBL genes and the clonality of the isolates.

Materials and methods

Study design, period, and area

A prospective case-control study was conducted between August 1, 2019, and February 28, 2020, in patients of both genders admitted to the NICU of the Federico Gómez Children's Hospital (HIMFG), a tertiary pediatric hospital in Mexico City, Mexico. The hospital has 229 beds across various specialties, with 30 beds specifically located in the neonatology hospitalization area. The Research, Ethics, and Biosafety Committees evaluated the study design and data sources for the HIM/2018/073, SSA 1522 study protocol, which involved a review of medical records generated during routine patient care. This study did not involve the performance of medical intervention or intentional modification of physiological variables by their searcher on patients or their legal guardians. Therefore, this project was classified as risk-free research for the study subjects. The informed consent emphasized the researchers' obligation to protect the identity and privacy of the patients included in the study.

Population, sample size, and data collection

After informed consent was obtained, rectal swabs were collected from all newborns admitted to the NICU for active surveillance and purposeful search of colonizing extended-spectrum beta-lactamases-producing ESBL-PEco and ESBL-PKpn. Demographic and clinical information of the patients was collected. Subsequently, rectal samples were collected weekly until the patients completed one month of hospitalization. Afterward, samples were collected every two weeks until discharge from the neonatology ward. All patient-related healthcare-associated infections (HAIs) were prospectively followed. HAIs were classified if the isolate was obtained after 48 h of NICU admission. When a patient presented an infectious event, the cultures identified as causing HAIs and the clinical data were collected.

Sample processing, bacterial isolation, and ESBL-PEco and ESBL-PKpn detection

Rectal samples were obtained using cotton swabs soaked in Cary-Blair transport medium, followed by inoculation and overnight culturing on MacConkey and 5% sheep blood agar plates. Subsequently, distinctive colonies of *E. coli* and *K. pneumoniae* were chosen and transferred to the VITEK 2 AST automated system (bioMérieux, Marcy-l'Étoile, France) for bacterial identification (with an accuracy range of 98-99% for *E. coli* and 95-97% for *K. pneumoniae*) and antimicrobial susceptibility testing. Strains from infectious processes were subculture on 5% sheep blood agar and incubated at 37°C for 18-24 h. The antibiotics evaluated included amikacin (AN), ampicillin-sulbactam (AMS), cefepime (FEP), cefoxitin (FOX), ceftazidime (CAZ), ceftriaxone (CRO), ciprofloxacin (CIP), colistin (COL), doripenem (DOR), ertapenem (ETP), gentamicin (GM), imipenem (IPM), meropenem (MEM), piperacillin/tazobactam (TZP), and tigecycline (TGC). Antibiotic susceptibility was interpreted using the Clinical and Laboratory Standards Institute (CLSI) guidelines (CLSI, 2023), and ESBL categorization was determined based on the susceptibility pattern to different cephalosporins.

The confirmation of ESBL-producing isolates was conducted using the combination disc method. A comparison of the zone of inhibition was made between ceftazidime (30 µg) and cefotaxime (30 µg) discs alone versus those of ceftazidime and cefotaxime discs containing clavulanic acid (10 µg). Following the incubation period, isolates displaying an increase in the zone diameter of ≥5 mm around either of the clavulanate combined discs compared to that of the disc alone were considered ESBL producers, according the criteria recommended by CLSI (CLSI, 2023). *E. coli* ATCC 25922 and *K. pneumoniae* ATCC 700603 strains were used as negative and positive controls for ESBL production, respectively.

ESBL gene detection

The total genomic DNA was extracted from an isolated colony of the strains using the Wizard Genomic DNA Purification kit (Promega, Madison, WI) following the manufacturer's instructions. The ESBL genes were detected using specific primer sets in PCR assays as previously described (Dallenne et al., 2010). The first assay involved a multiplex PCR targeting bla_{TEM}, bla_{SHV}, and $bla_{\text{OXA-1-like}}$ genes, while the second assay focused on $bla_{\text{CTX-M}}$ genes, covering phylogenetic groups 1, 2, and 9. Within these groups, specific variants were probed, including CTX-M-1, CTX-M-3, and CTX-M-15 from CTX-M group 1, CTX-M-2 from CTX-M group 2, and CTX-M-9, CTX-M-14 from CTX-M group 9. The third assay utilized simplex PCR for $bla_{\text{CTX-M-8/25}}$ groups, detecting CTX-M-8, CTX-M-25, CTX-M-26, and CTX-M-39 to CTX-M-41. Lastly, the fourth assay was conducted to detect minor ESBLs (VEB, PER, GES, ACC, MOX, and DHA). Additionally, we identified OXA β-lactamases (Groups OXA 1, 2, 51, and 58) using the primers previously described (Voets et al., 2011). For all samples, PCR was performed using Multiplex PCR Master containing Hot Start Taq polymerase (Jena Bioscience, Jena Germany) and 100 ng of DNA extracted from the samples, in a final volume of 25 µL. Amplification was carried out in a Cetus Thermal Cycler (Perkin-Elmer, Ueberlingen, Germany) under the specific conditions for each resistance gene to be detected. Amplified DNA fragments were separated on 1.5% agarose gels with 0.5X TBE (Tris-Borate-EDTA) buffer containing ethidium bromide (1 mg/ml). Gels were visualized using an iBright CL1000 imaging system (Invitrogen, Thermo Fisher Scientific). As a reference, DNA samples of previously reported isolates of *K. pneumoniae* carrying $bla_{\text{CTX-M-15}}$ (GenBank ID: AGE61862.1) and $bla_{\text{TEM-1}}$ (GenBank ID: ALJ57215.1) were utilized (Alcántar-Curiel et al., 2023). A clinical isolate of *E. coli* was employed as a positive control for $bla_{\text{OXA-1}}$ (GenBank ID: CP13738.1), while a clinical isolate of *K. pneumoniae* was utilized as a positive control for bla_{SHV} (GenBank ID: AWD75419.1). *E. coli* ATCC 25922 was employed as the negative control.

Clonal relationship between colonizing and invasive strains

Genetic relationships were determined by pulsed-field gel electrophoresis (PFGE) (Swaminathan et al., 2001). Genomic DNA was prepared in 1.2% agarose blocks and enzymatically digested with *Xba*I at 37°C for 2.5 h. DNA fragments were separated using the CHEF-DR II system (Bio-Rad Laboratories) with 1.1% agarose (SeaKem Gold®) at 5.5 V/cm, an initial pulse of 3.5 s, a final pulse of 30 s, and 14°C for 22 h. After staining and washing, the gel was visualized using an iBright CL1000 imaging system (Invitrogen, Thermo Fisher Scientific). Generated electrophoretic patterns were analyzed through visual inspection, detecting the position and number of bands. A dendrogram was constructed using simple matching and the unweighted pair-group method with arithmetic mean (UPGMA) clustering method using NTSYSpc. 2.1 software (Rohlf, 1998).

Prevalence and risk factors for ESBL-PEco and ESBL-PKpn colonization and occurrence

The prevalence of fecal colonization and invasive HAIs caused by ESBL-PEco or ESBL-PKpn was determined. To identify the risk factors for HAIs due to ESBL-PEco or ESBL-PKpn in patients colonized by these bacteria, the characteristics of colonized patients who developed HAIs (cases) were compared with those of colonized patients who did not develop HAIs due to ESBL-PEco or ESBL-PKpn (controls). Variables related to gestational weeks, birth weight, admission weight, previous hospitalization, prior antibiotic use, repeated antibiotic use, duration of antimicrobial treatment, early sepsis, invasive device use, and nutrition type were recorded. The comparison between groups in the case of variables on a continuous scale was carried out either using the Wilcoxon test for a distribution other than normal or the Student t-test for a

10.3389/fcimb.2023.1322874

normal distribution (McElduff et al., 2010). In the case of categorical variables, the chi-square and Fisher's exact tests were used (Nowacki, 2017). The alpha significance level used in all statistical tests was 5%.

Results

Study population, identification of the bacterial isolates, incidence of ESBL-PEco and ESBL-PKpn carriage

During the study period, 61 patients were enrolled. However, 14 patients were excluded from the study as they provide only a single rectal sample and could not continue with the follow-up. Among the remaining 47 patients, a total of 203 rectal samples were collected. In 45 of these patients (95.7%) and in 166 samples (81.7%), we identified 126 *E. coli* isolates and 111 *K. pneumoniae*. Specifically, 99 (78.6%) were categorized as ESBL-PEco, and 97 (87.4%) as ESBL-PKpn originating from a total of 41 patients (38 patients with ESBL-PEco, 39 patients with ESBL-PKpn, and 35 patients with both bacteria).

Nine out of these 41 patients experienced HAIs (22%) during their hospitalization, with six cases attributed to ESBL-PEco and three to ESBL-PKpn. These infectious events resulted in the isolation of 15 and 4 strains of each species (respectively), derived from different culture samples.

The peak colonization by ESBL-PEco and/or ESBL-PKpn was detected during the second week of hospitalization with a total of 18/41 (44%) patients, and the highest number of HAIs was also observed during the second week of hospitalization, with 6/12 (50%) cases (Supplementary Figure 1).

Demographical and clinical characteristics

Slightly more of the colonized patients with ESBL-PEco and/or ESBL-PKpn were male 24/41 (58.5%), born by cesarean section 25 (60.9%), and premature born before 37 weeks of gestation 21/41 (51.2%), with an average weight at hospital admission of 2,076 g (SD ± 835.4, minimum 648 g, maximum 3,490 g). The use of antibiotics prior to admission was reported in 28 patients (68.2%), same as hospital unit, 28 patients (68.2%) required antibiotics, with an average duration of treatment of 7.5 days (SD± 8.7, minimum 5, maximum 45 days) (Table 1). The relationship between the admission diagnosis of patients colonized with ESBL-PEco and/or ESBL-PKpn and the progression of ESBL-PEco or ESBL-PKpn-HAIs is shown in Figure 1A.

Upon admission of the newborns to the NICU, clinical data indicated suspicion of early sepsis in 16/47 (34%) cases, but none was corroborated by cultures. Throughout the follow-up period, after 48 hours of admission, 12 HAIs were clinically diagnosed in 41 of the patients included in the study, representing a prevalence of 29.3%. The types and frequency of HAIs are shown in Figure 1B, the most common infectious diagnosis was nosocomial sepsis with 6 cases (50%).

TABLE 1 Descriptive statistics of the risk factors for the development of HAIs in colonized patients by ESBL-producing *Escherichia coli* or ESBL-producing *Klebsiella pneumoniae*.

Risk factors	Colonized patients with ESBL-producing *Escherichia coli* or ESBL-producing *Klebsiella pneumoniae* *n* = 41		
	Patients without HAIs Control group *n*= 32	Patients with HAIs Case group *n* = 9	*p*
Sex			
Male *n* (%)	19 (59.4)	5 (55.6)	0.84
Female *n* (%)	13 (40.6)	4 (44.4)	
Delivery practice			
Cesarean *n* (%)	19 (59.4)	6 (66.7)	0.69
Vaginal *n* (%)	13 (40.6)	3 (33.3)	
Gestational age (weeks), mean (SD)	35.2 (4.6)	34 (4.8)	0.33
< 37 *n* (%)	16 (50)	5 (55.6)	0.77
≥ 37 *n* (%)	16 (50)	4 (44.4)	
Birth weight (g), mean (SD)	2,196.5 (860.3)	2,083.3 (1,157.4)	0.75
Weight at hospital admission (g), mean (SD)	2,097 (788.1)	2,001.2 (1,036.6)	0.72
Previous hospitalization *n* (%)	22 (68.7)	8 (21.4)	0.40
Use of antibiotics in the hospital unit *n* (%)	20 (62.5)	8 (88.9)	0.23
Hospital stay (days), mean ± SD	30.7 ± 21	50.7 ± 29	0.03
Repeated use of antibiotics *n* (%)	3 (9.4)	3 (33.3)	0.11
Duration of antibiotic treatment (days), mean (SD)	4.8 (5.7)	17 (10.9)	<0.001
Use of invasive devices (days), mean (SD)			
Catheter	9.2 (5.6)	23.8 (17.3)	0.002
Orotracheal tube	11.8 (7.3)	25.2 (19)	0.004
Chest tube	1.8 (5.8)	2.3 (3.7)	0.57
Urinary catheter	0.22 (0.49)	5.4 (9.5)	0.01
Type of nutrition (days), mean (SD)			
Fasting	4.8 (7.3)	6.5 (6.7)	0.15
Enteral nutrition	26.4 (20.6)	31.3 (23.5)	0.67
Parenteral nutrition	5.8 (7.6)	14.7 (24.3)	0.43

Antimicrobial resistance pattern of colonizing and infectious ESBL-PEco and ESBL-PKpn

All colonizing and infectious strains of ESBL-PEco (114 strains; 99 colonization strains and 15 HAIs strains) and ESBL-PKpn (101 strains; 97 colonization strains and 4 HAIs strains) were analyzed. One hundred percent of these strains were sensitive to carbapenems, tigecycline, and colistin. ESBL-PEco strains showed

10.3389/fcimb.2023.1322874

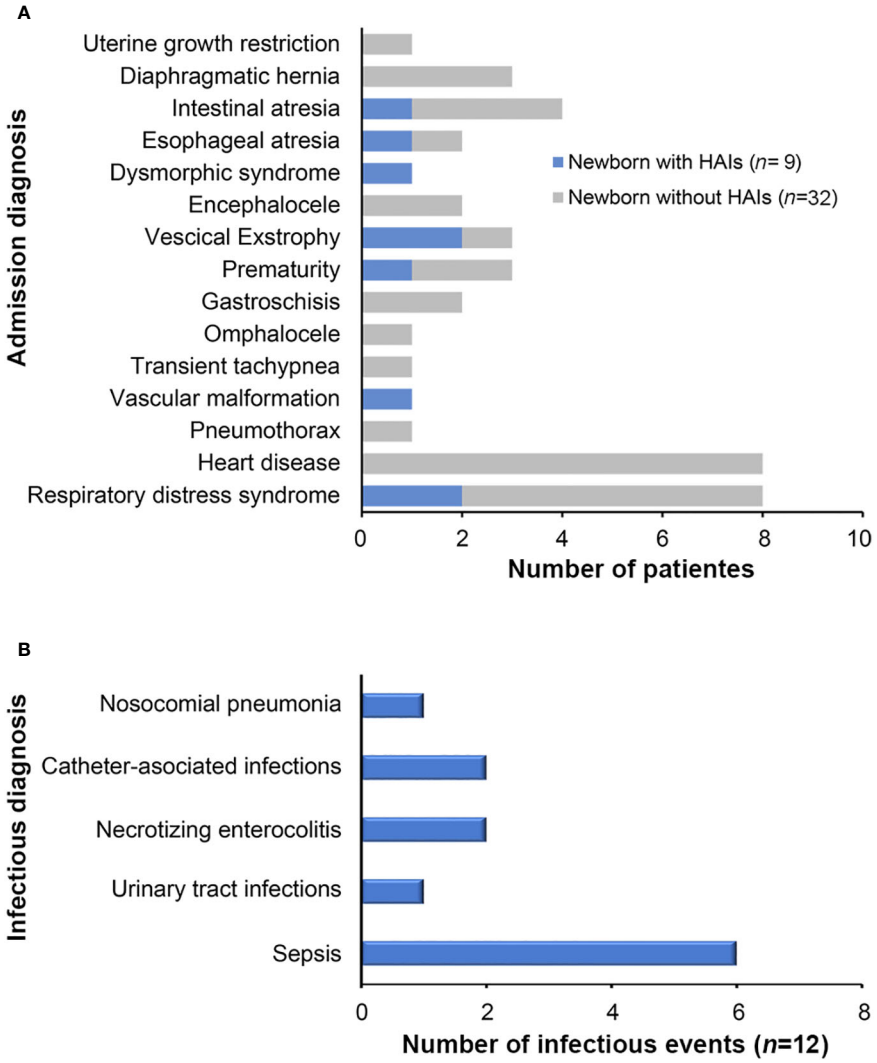

FIGURE 1
Diagnoses of neonatal patients colonized by ESBL-producing *Escherichia coli* and *Klebsiella pneumoniae*. **(A)** Admission diagnoses of patients colonized by ESBL-producing *Escherichia coli* and *Klebsiella pneumoniae* isolates who presented HAIs during hospitalization at the NICU. **(B)** HAIs diagnosed during the study period.

resistance rates of 25.4%, 100%, 65.7%, and 57.1% to cefoxitin, ceftriaxone, ceftazidime, and cefepime, respectively (Figure 2A), while in ESBL-PKpn strains, the resistance to the same cephalosporins was 2.9%, 99%, 45.5% and 23.7% (Figure 2B).

Occurrence of ESBL genes

The $bla_{\text{CTX-M-1 group}}$ gene was the most prevalent for both species, with 88/114 (77.2%) in ESBL-PEco and 83/101 (82.2%) in ESBL-PKpn, followed by bla_{TEM} 57/114 (50%) and $bla_{\text{OXA-1}}$ 50/114 (43.86%) in ESBL-PEco, and bla_{TEM} 81/101 (80.2%) and bla_{SHV} 77/101 (76.2%) in ESBL-PKpn (Table 2). The majority of isolates, 203/215 (94.4%), showed the coexistence of at least two of the analyzed genes. In total, 11 different profiles were detected in ESBL-PEco and 19 in ESBL-PKpn, with TEM+CTX-M-1 group being the most frequent profile in the ESBL-PEco strains (35/114, 30.7%). Meanwhile, the TEM + SHV + CTX-M-1 group + OXA-1 profile was the most common profile in ESBL-PKpn (46/101, 45.5%). The maximum number of different types of ESBL-encoding genes detected in a single strain was five, observed in one strain of ESBL-PKpn (Tables 3A, B).

Clonality between colonizing and infecting ESBL-PEco and ESBL-PKpn isolates

The determination of the genomic fingerprint of the 114 ESBL-PEco isolates detected 35 different pulse types, named in numerical order preceded by the initials PT (Figure 3A). Meanwhile, in the 101 ESBL-PKpn isolates, 30 different pulse types were detected, also named in numerical order preceded by the initials PT (Figure 3B).

We identified that 23 of 35 (65.7%) pulse types were detected once in ESBL-PEco strains, while the rest were found at least twice in the same or different patients. Is distinguished PT6 because was

10.3389/fcimb.2023.1322874

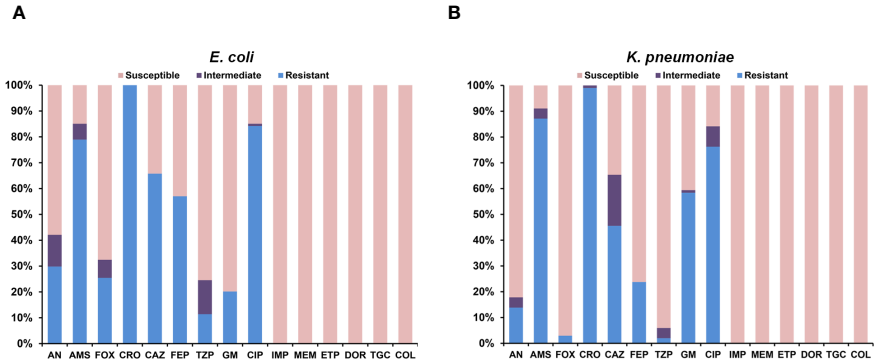

FIGURE 2
Antimicrobial susceptibility of colonizing and infectious ESBL-producing *Escherichia coli* and *Klebsiella pneumoniae*. **(A)** Isolates of *Escherichia coli*. **(B)** Isolates of *Klebsiella pneumoniae*.

detected in 37 isolates from colonization samples out of ten patients, and five of them (N29, N39, N45, N57, and N58) progressed to HAIs, while PT3 was identified in 19 strains from 10 patients, and none of them developed an HAI related to this pulse type. Week 13 of the study stands out, during which 11 different pulse types were isolated in the NICU (Figure 4A).

In relation to ESBL-PKpn, we observed that PT3 was the most prevalent in the NICU. This pulse type 3 was detected sequentially in patients N5, N1, N8, N2, N16, N19, N25, N27, N29, N42, N43, and N48. None of them developed HAI. Once again, week 13 of the study stands out, where eight different ESBL-PKpn pulse types were detected in the NICU neonatology hospitalization area (Figure 4B).

The analysis of the pulse types identified for each newborn is depicted in Figure 5. Our findings revealed that out of the 32 patients with ESBL-PEco present at least in two study time points, 21 (65.6%) demonstrated the same pulse types, suggesting a colonization event. Conversely, 11 out of 32 patients (34.4%) showed different ESBL-PEco pulse types at different time points, suggesting a transient acquisition of these clones. Similarly, among the 26 patients with ESBL-PKpn present at least in two study time points, 23 (88.5%) exhibited the same pulse types, suggesting a colonization event. In contrast, 3 out of 26 patients (11.5%) displayed unique ESBL-PKpn pulse types at different time points, suggesting a transient acquisition of these clones. Finally, clonality analysis revealed that five of seven patients colonized with ESBL-PEco (71.4%) and two of three patients colonized with ESBL-PKpn (66%) progressed to HAIs with the same colonizing isolate.

Risk factors for the occurrence of ESBL-PEco and ESBL-PKpn-HAIs

The analysis of clinical characteristics in the group of patients colonized by ESBL-PEco or ESBL-PKpn who did not develop HAIs (controls) and those who did progress to ESBL-PEco or ESBL-PKpn -HAIs (cases), revealed that variables associated with a higher risk of progression to ESBL-PEco and ESBL-PKpn-HAIs were hospital-length of stay (p = 0.03), duration of antibiotic treatment (p= <0.001) (Table 1), and the use of invasive devices such as catheters, (p= 0.002), orotracheal (p=0.004), and urinary catheters (p=0.01) (Table 1). There were two deaths in the group of ESBL-PEco and ESBL-PKpn-HAIs, representing 0.17% of the total patients in that group, and no differences were found between the groups with and without ESBL-PEco or ESBL-PKpn-HAIs.

Discussion

In this prospective study, it was revealed that upon admission to the HIMFG NICU, 27.6% (13/47) of patients were already colonized by ESBL-PEco and ESBL-PKpn. The percentage increased to 87% (41/47) by the end of the follow-up period, exceeding the reporting range, which typically ranged from 8% to 83% (Huerta-García et al., 2015; Folgori et al., 2018; Hagel et al., 2019; Edwards et al., 2023). Notably, the study by Huerta-García et al. carried out in our country reported that during the second

TABLE 2 Frequency of genes encoding resistance mechanisms in ESBL-producing *Escherichia coli* and *Klebsiella pneumoniae* isolated from neonates in the HIMFG NICU.

Gene	ESBL-PEco *n* = 114	%	ESBL-PKpn *n* = 101	%
$bla_{\text{CTX-M-1 group}}$	88	77.19	83	82.19
bla_{TEM}	57	50.00	81	80.19
bla_{SHV}	3	2.63	77	76.24
$bla_{\text{OXA-1}}$	50	43.86	58	57.43
$bla_{\text{CTX-M-9 group}}$	2	1.75	7	6.93

10.3389/fcimb.2023.1322874

TABLE 3A Distribution of ESBL gene profiles among ESBL-producing *Escherichia coli* from neonates in the HIMFG NICU.

ESBL profile (n = 114)	No isolates (%)	Number of genes in co-existence
TEM + CTX-M-1 group	35 (30.7)	2
CTX-M-1 group + OXA-1	24 (21)	2
CTX-M-1 group	19 (16.6)	1
OXA-1	11 (9.6)	3
TEM + CTX-M-1 group + OXA-1	7 (6.1)	2
TEM + OXA-1	7 (6.1)	1
TEM	4 (3.5)	1
TEM + CTX-M-9 group	2 (1.8)	2
TEM + SHV + CTX-M-1 group + OXA-1	1 (0.87)	4
TEM + SHV + CTX-M-1 group	1 (0.87)	3
TEM	1 (0.87)	1
No gene detected	2 (1.8)	0

TABLE 3B Distribution of ESBL gene profiles among ESBL-producing *Klebsiella pneumoniae* from neonates in the HIMFG NICU.

ESBL profile (n = 101)	No isolates (%)	Number of genes in co-existence
TEM + SHV + CTX-M-1 group + OXA-1	46 (45.54)	4
TEM + SHV + CTX-M-1 group	10 (9.9)	3
SHV + CTX-M-1 group	6 (5.94)	2
TEM + CTX-M-1 group	6 (5.94)	2
TEM + SHV + OXA-1	6 (5.94)	3
CTX-M-1 group	5 (4.95)	1
SHV	4 (3.96)	1
TEM + CTX-M-1 group + OXA-1	3 (2.97)	3
SHV + CTX-M-1 group + OXA-1	2 (1.98)	3
TEM	2 (1.98)	1
TEM + CTX-M-9 group	2 (1.98)	2
TEM + SHV	2 (1.98)	2
OXA-1	1 (0.99)	1
CTX-M-1 group + OXA-1	1 (0.99)	2
SHV + CTX-M-1 group + CTX-M-9 group	1 (0.99)	3
TEM + CTX-M-1 group + CTX-M-9 group	1 (0.99)	3
TEM + SHV + CTX-M-1 group + CTX-M-9 group	1 (0.99)	4
TEM + SHV + CTX-M-9 group	1 (0.99)	3
TEM + SHV + CTX-M-1 group + CTX-M-9 group + OXA-1	1 (0.99)	5

week of hospital stay, 81% of neonates were intestinally colonized by ESBL-PEco and ESBL-PKpn, while our study revealed 78.7% (37/47) colonization during the same week of hospitalization (Huerta-García et al., 2015). This demonstrates the rapid and dynamic nature of the colonization process, which could be influenced by various previously reported factors (Martin and Bachman, 2018; Yin et al., 2021). These factors encompass prolonged hospital stays, often resulting in increased utilization of invasive techniques. Additionally, a significant majority of these patients receive antimicrobial treatments, exerting selective pressure on these pathogens. Horizontal colonization via objects used in patient care, combined with inadequate hand hygiene practices among healthcare workers responsible for their care, represents another potential contributing factor. Moreover, insufficient nursing staff levels might hinder the delivery of adequate care to these patients.

As observed in this study, of the 41 patients colonized with ESBL- ESBL-PEco or ESBL-PKpn, 9 (22%) developed HAIs during their hospital stay in the NICU, representing a high infection rate compared to a previous report conducted in 2020 by Denkel et al., (Denkel et al., 2020) where they observed that ICUs exhibited the highest infection rate (17.2%), with 5.6% of HAIs attributed to ESBL-EP colonization. They also found that in 98% of patients with HAIs, the colonizing isolate and the pathogenic agent responsible for the HAI exhibited genetic identity (Denkel et al., 2020). Our results demonstrated that in some of the patients, colonization, and infection occurred with a bacterial strain of the same pulse type. Although the number of patients in this study is small, it supports the hypothesis that many infections, including bacteremia, originate from an intestinal reservoir (Denkel et al., 2014; Zerr et al., 2014; Platteel et al., 2015; Gorrie et al., 2017; Armand-Lefèvre et al., 2018; Souverein et al., 2019; Campos-Madueno et al., 2023).

The main risk factors observed development of HAIs include the duration of hospitalization, prior antibiotic use in the NICU, the length of antibiotic treatment, and the extended use of invasive devices such as orotracheal tubes and venous catheters. Our findings align with a study conducted by Smith et al., in 2010 (Smith et al., 2010), which identified increased use of central venous catheters and mechanical ventilation as risk factors for colonization and bloodstream infections by gram-negative bacilli, reflecting our study's observation regarding the duration of orotracheal tube use (Smith et al., 2010). Other risk factors identified in previous studies, such as mode of delivery, did not yield significant values as risk factors in our study (Reyman et al., 2019; Pirr and Viemann, 2020).

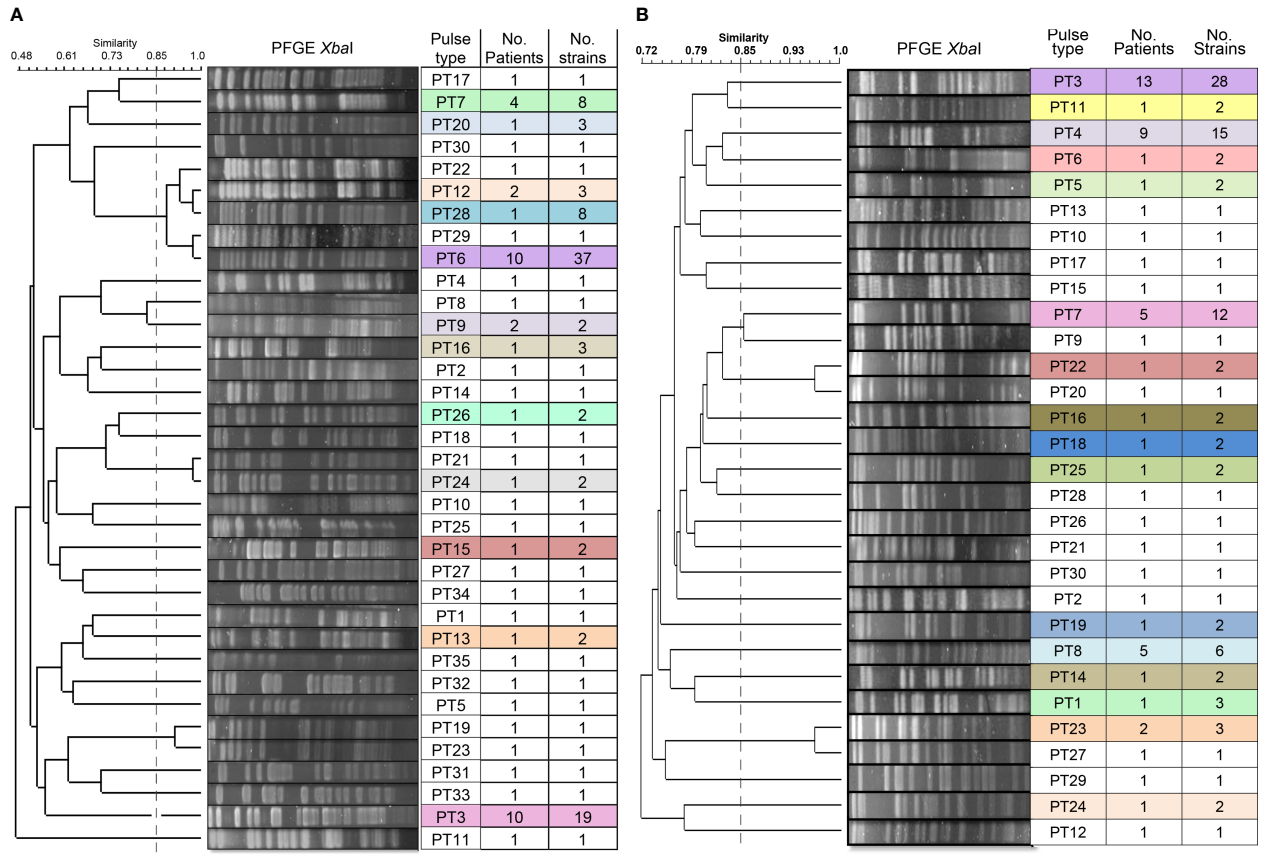

FIGURE 3
Dendrogram of the PFGE profiles of ESBL-producing *Escherichia coli* and *Klebsiella pneumoniae* isolates for colonization and HAIs in neonates hospitalized at the NICU. **(A)** A total of 114 isolates of *Escherichia coli* were grouped into 35 pulse types. **(B)** A total of 101 isolates of *Klebsiella pneumoniae* were grouped into 30 pulse types. The dashed line represents the 85% similarity level used in the cluster designation.

In the current study, we found that ESBL-PEco and ESBL-PKpn isolates, both colonizers and causative agents of HAIs, exhibited 100% susceptibility to carbapenems, tigecycline, and colistin. This keeps them within the appropriate therapeutic options for HAIs. Of concern is the resistance observed with cefepime (ESBL-PEco: 57.1%, ESBL-PKpn: 29.8%), which is the first-line empirical antibiotic choice for HAI treatment at our institution. As our results demonstrate, in the case of ESBL-PEco, there is less than a 50% possibility that treatment will be adequate before de-escalation therapy.

Currently, the rapid spread of ESBL-producing bacteria has led to their widespread distribution throughout the world. Several studies identify *E. coli* and *K. pneumoniae* as the main ESBL producers (Obeng-Nkrumah et al., 2013; Ouedraogo et al., 2016; Siriphap et al., 2022).

Although SHV and TEM were the first beta-lactamases to spread, they have gradually been replaced by CTX-M types. This phenomenon has been associated with the high mobilization of the genes encoding them (Shahid et al., 2011). The present study identified the CTX-M-1 group as the most common beta-lactamase gene in ESBL-PEco strains (77%) and in ESBL-PKpn (82.19%). These results are consistent with those reported in Germany (Schmiedel et al., 2014) and Ethiopia (Tufa et al., 2020), where the prevalence of CTX-M in both species was 50% and 82.7% respectively, while in India (Shahid et al., 2011), Romania (Ghenea et al., 2022), and Nepal (Koirala et al., 2021), ESBL-PEco strains showed 4.5%, 92.8 and 93.8% respectively and ESBL-PKpn strains, 39.2%, 71.8%, and 78.9%. Among our strains, CTX-M-9 showed a low prevalence (1.75% and 6.93% for ESBL-PEco and ESBL-PKpn, respectively). The low frequency of this beta-lactamase in Mexico can be attributed to its geographical origin so far our country, since it emerged in Lithuania, between 2012 and 2014. The authors reported its presence in 90.6% of bloodstream isolates of ESBL-PEco (Kirtikliene et al., 2022). This geographical origin affects its distribution, and the limited frequency suggests it may have difficulty spreading among different bacteria in the Mexican environment, possibly due to unique genetic traits or limited opportunities for dissemination.

The simultaneous occurrence of genes encoding distinct beta-lactamases has garnered attention in contemporary research, with numerous studies highlighting a progressive increase in prevalence over time (Munday et al., 2004; Oteo et al., 2010; Shahid et al., 2011; Schmiedel et al., 2014). Our investigation revealed an overwhelming 98% of isolates exhibited the coexistence of at least two distinct beta-lactamase genes. This percentage surpasses the reported frequencies in Iran (Rezai et al., 2015), Malaysia (Mahdi Yahya Mohsen et al., 2016), India (Bora et al., 2014), and Germany (Schmiedel et al., 2014), standing at 32%, 78%, 57%, and 78%,

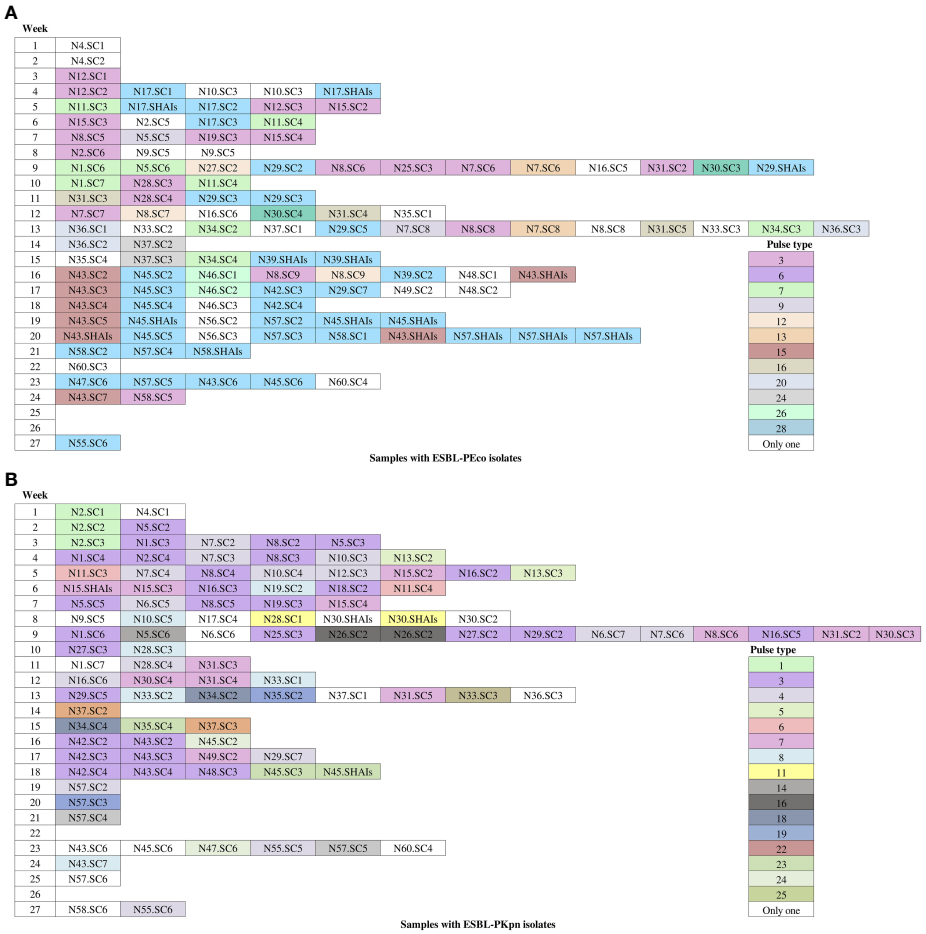

FIGURE 4
Occurrence of pulse types of ESBL-producing *Escherichia coli* and *Klebsiella pneumoniae* observed during the follow-up period. White-colored boxes represent different pulse types, each containing a single isolate for colonization and HAIs throughout the follow-up time. **(A)** *Escherichia coli* isolates. **(B)** *Klebsiella pneumoniae* isolates. N, neonate; SC, sample colonization; SHAIs, samples of HAIs.

respectively. In this intricate landscape, a study conducted in a Bosnian and Herzegovinian hospital unveiled that a substantial 77.3% of isolates from hospitalized patients harbored more than two distinct ESBL types (Ibrahimagić et al., 2017). Notably, the TEM + SHV + CTX-M-1 group + OXA-1 profile dominated, prevailing in ESBL-PKpn strains (63%, 28/44) and ESBL-PEco strains (10%, 1/10). Surprisingly, this specific ESBL profile is the same predominant pattern we identified in our research, manifesting in ESBL-PKpn strains (45.54%, 46/101) and an isolated ESBL-PEco strain (0.88%, 1/114). This compelling discovery underscores the successful coexistence of these resistance genes in ESBL-PKpn and alludes to the possibility of their dissemination via a plasmid, consistent with previous research (Cantón et al., 2012).

The clonality analysis performed highlighted the dissemination of clonal strains to other patients during the follow-up period. For instance, PT6 of ESBL-PEco was isolated in the initial rectal sample from patient N17.SC1. Three days later, due to symptoms, blood and urine samples were collected, and PT6 was found in both samples. Subsequently, PT6 was detected in colonization samples from nine patients, and in five of them (N29, N39, N45, N57, and N58), this pulse type progressed to HAIs. It is worth noting that in the subsequent rectal samplings of these patients, PT6 continued to be detected. At the end of the study, 37 PT6 strains were isolated in these 10 patients, one of whom (patient N43) developed HAIs related to PT28 (which was not detected in any other patient) and also showed colonization by PT6 in the sixth rectal sample. Another example was PT3 was detected upon admission (first rectal sample) in patient N12.SC1. Subsequently, in the fifth week of the study, it was identified in patient N15. Two weeks later, it was found in two other patients (patients N19 and N8), and it continued to disseminate until the end of the study. In total, we identified 19 PT3 strains in 10 patients, and none of them developed an HAI related to this pulse type. The 13th week of the study stands out, during which 11 different pulse types were isolated in the NICU (Figure 4A).

About ESBL-PKpn, we observed that PT3 was prevalent in the NICU. This pulse type was initially identified during the second week of patient´s N5 admission. Subsequently, it was sequentially spread to patients N1, N8, N2, N16, N19, N25, N27, N29, N42, N43,

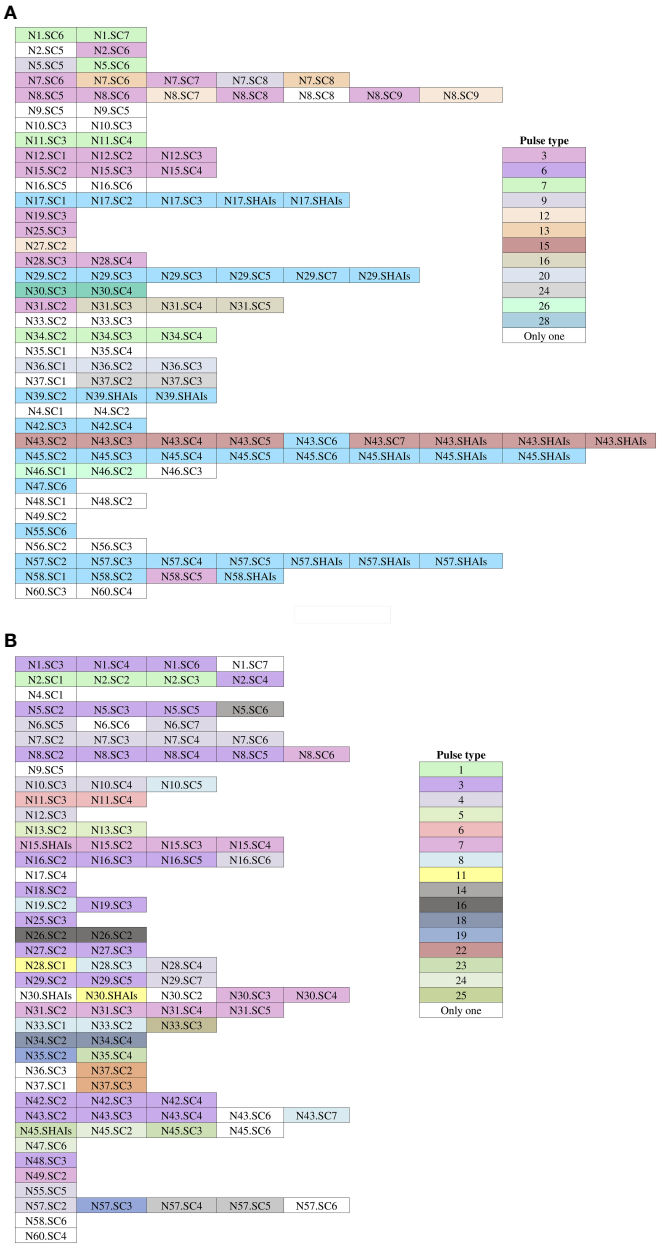

FIGURE 5
Pulse types of ESBL-producing *Escherichia coli* and *Klebsiella pneumoniae* from rectal samples collected from neonates during the follow-up time. **(A)** Isolates of *Escherichia coli*. **(B)** Isolates of *Klebsiella pneumoniae*. White-colored boxes represent different pulse types, each containing a single isolate. N, neonate; SC, sample colonization; SHAIs, sample of HAIs.

and N48. None of the 12 patients developed HAIs. Notably, patient N15, in whom PT7 was identified upon admission and during the first week of hospitalization, subsequently developed an HAI caused by the same clone. In contrast, patient N30 experienced a HAI that was not related to the previously isolated pulse types in their rectal samples. A particular case was patient N45, who was colonized with ESBL-PEco PT6 (associated with HAIs in other patients) starting from the second week with ESBL-PKpn PT24 and in the fourth week for ESBL-PKpn PT23. After six days, this patient developed HAIs in which ESBL-PEco PT6 and ESBL-PKpn PT23 were identified. Once again, week 13 of the study stands out, where eight different *K. pneumoniae* pulse types were detected in the NICU (Figure 4B).

We did not consider the progression to infection in patient N43 because *E. coli* P28 was detected both in the admission rectal sample and in the HAIs samples taken on the same day. We also excluded patient 39, whose initial rectal sample showed no bacterial growth, but on the following day of hospitalization, they were diagnosed with HAIs, confirmed by a positive culture for *E. coli* PT6. Their second colonization sample also belonged to the same pulse type.

The clonality analysis carried out on both colonization and infection isolates from the same patients showed that colonization preceded infection in 70% of cases. These findings underscore the frequent occurrence of cross-transmission events within our hospital's NICU. Consequently, continuous surveillance in this clinical setting is imperative, with particular emphasis on optimizing patient management to mitigate the substantial clonal dissemination and, subsequently, reduce the risk of HAIs.

Over the past decade, there has been a growing body of research aimed at elucidating the relationship between microbial colonization and the development of HAIs. As a result, we now better understand several factors that can disrupt the composition of the microbiome. These factors encompass variables such as the mode of birth, antibiotic prophylaxis administered to mothers undergoing cesarean sections, and antibiotic treatments (Vandenplas et al., 2020; Socha-Banasiak et al., 2021). Additionally, several hypotheses have emerged, including one suggesting that infections in colonized neonates may be attributed to the translocation of bacteria from the gastrointestinal tract to the bloodstream, facilitated by an immature or compromised intestinal barrier. Furthermore, indirect transmission through alternative routes due to the immaturity of defense mechanisms has been postulated (Basu, 2015). Collectively, these factors underscore the vulnerability of this neonatal population and emphasize the need for comprehensive research and intervention efforts.

One of the limitations encountered in this study was the relatively modest sample size of patients included, a consequence of the SARS-CoV-2 pandemic, which imposed restrictions on patient enrollment. Additionally, the confinement of the study to a single hospital setting is another limitation to consider. Consequently, it is important to acknowledge that the results obtained may not be fully representative of patients in the broader community or in other urban regions of Mexico. Nevertheless, despite these limitations, the study findings offer valuable insights and support the recommendation for the implementation of early ESBL-PEco and ESBL-PKpn identification strategies, and appropriate infection control and practices. These proactive measures have the potential to reduce the notable rates of bacterial colonization observed, consequently mitigating the risk of bacterial dissemination and HAIs.

Conclusions

This investigation has revealed that intestinal colonization by ESBL-PEco and ESBL-PKpn is a prevalent occurrence in hospitalized newborns, indicating that a considerable portion of them are susceptible to progressing to HAIs. Furthermore, patients colonized by ESBL-PEco and ESBL-PKpn strains producing CTX-M and TEM, deserve further attention due to the observed association between the development of HAIs and factors such as prolonged hospitalization and the use of invasive medical devices. The genetic similarity observed between colonizing and infecting ESBL-PEco and ESBL-PKpn strains underscores the importance of endogenous infection and clonal dissemination as predominant contributors to HAIs, predominantly attributed to *E. coli*. This study provides valuable insights that improve our understanding of the epidemiology of ESBL-producing *Escherichia coli* and *Klebsiella pneumoniae* and intestinal colonization in neonatal patients.

Data availability statement

The raw data supporting the conclusions of this article will be made available by the authors, without undue reservation.

Ethics statement

The studies involving humans were approved by the Research, Ethics, and Biosafety Committees. Hospital Infantil de México Federico Gómez. HIM/2018/073. The studies were conducted in accordance with the local legislation and institutional requirements. Written informed consent for participation in this study was provided by the participants' legal guardians/next of kin.

Author contributions

VJ-R: Writing – review & editing, Conceptualization, Funding acquisition, Investigation, Supervision, Writing – original draft. DV-G: Conceptualization, Writing – review & editing. AM-V: Investigation, Writing – original draft. RA-V: Writing – original draft, Methodology. PA-R: Methodology, Writing – original draft. BL-M: Methodology, Writing – original draft. AR-L: Methodology, Writing – original draft. MA-C: Conceptualization, Writing – review & editing.

Funding

The author(s) declare financial support was received for the research, authorship, and/or publication of this article. This work was supported by Federal Resources of the Hospital Infantil de México Federico Gómez (HIM/2018/073) of the Secretaría de Salud (SSA 1522), México.

Acknowledgments

The authors are grateful to José Luis Fernández-Vázquez from the Universidad Nacional Autónoma de México, Ciudad de México, for his technical assistance on the PCR assays and to Marco Elias Gudiño Zayas from the Universidad Nacional Autónoma de México, Ciudad de México, for his assistance with the graphic design. MA-C acknowledges the grant from Consejo Nacional de Humanidades, Ciencias y Tecnologías (CONAHCyT México) Ciencia de Frontera 2019-171880 project for supporting this study.

Conflict of interest

The authors declare that the research was conducted in the absence of any commercial or financial relationships that could be construed as a potential conflict of interest.

Publisher's note

All claims expressed in this article are solely those of the authors and do not necessarily represent those of their affiliated organizations, or those of the publisher, the editors and the reviewers. Any product that may be evaluated in this article, or claim that may be made by its manufacturer, is not guaranteed or endorsed by the publisher.

Supplementary material

The Supplementary Material for this article can be found online at: https://www.frontiersin.org/articles/10.3389/fcimb.2023.1322874/full#supplementary-material

SUPPLEMENTARY FIGURE 1
Frequency of colonization of ESBL-producing *Escherichia coli* and *Klebsiella pneumoniae* isolates for colonization and HAIs during the weeks of hospitalization of neonates admitted at the NICU.

References

Alcántar-Curiel, M. D., Huerta-Cedeño, M., Jarillo-Quijada, M. D., Gayosso-Vázquez, C., Fernández-Vázquez, J. L., Hernández-Medel, M. L., et al. (2023). Gram-negative ESKAPE bacteria bloodstream infections in patients during the COVID-19 pandemic. *PeerJ* 1, 1–21. doi: 10.7717/peerj.15007

Armand-Lefèvre, L., Andremont, A., and Ruppé, E. (2018). Travel and acquisition of multidrug-resistant Enterobacteriaceae. *Med. Mal Infect.* 48, 431–441. doi: 10.1016/j.medmal.2018.02.005

Bäckhed, F., Fraser, C. M., Ringel, Y., Sanders, M. E., Sartor, R. B., Sherman, P. M., et al. (2012). Defining a healthy human gut microbiome: Current concepts, future directions, and clinical applications. *Cell Host Microbe.* 12, 611–622. doi: 10.1016/j.chom.2012.10.012

Basu, S. (2015). Neonatal sepsis: the gut connection. *Eur. J. Clin. Microbiol. Infect. Dis.* 34, 215–222. doi: 10.1007/s10096-014-2232-6

Bora, A., Hazarika, N. K., Shukla, S. K., Prasad, K. N., Sarma, J. B., and Ahmed, G. (2014). Prevalence of blaTEM, blaSHV and blaCTX-M genes in clinical isolates of *Escherichia coli* and *Klebsiella pneumoniae* from Northeast India. *Indian J. Pathol. Microbiol.* 57, 249–254. doi: 10.4103/0377-4929.134698

Calva, J. J., Sifuentes-Osornio, J., and Cerón, C. (1996). Antimicrobial resistance in fecal flora: longitudinal community-based surveillance of children from urban Mexico. *Antimicrob. Agents Chemother.* 40, 1699–1702. doi: 10.1128/AAC.40.7.1699

Campos-Madueno, E. I., Moradi, M., Eddoubaji, Y., Shahi, F., Moradi, S., Bernasconi, O. J., et al. (2023). Intestinal colonization with multidrug-resistant Enterobacterales: screening, epidemiology, clinical impact, and strategies to decolonize carriers. *Eur. J. Clin. Microbiol. Infect. Dis.* 42, 229–254. doi: 10.1007/s10096-023-04548-2

Cantón, R., Akóva, M., Carmeli, Y., Giske, C. G., Glupczynski, Y., Gniadkowski, M., et al. (2012). Rapid evolution and spread of carbapenemases among Enterobacteriaceae. *Europe Clin. Microbiol. Infect.* 18, 413–431. doi: 10.1111/j.1469-0691.2012.03821.x

CDC (2019). "Antibiotic resistance threats in the United States," in *Center for Disease Control and Prevention*. (Atlanta, GA: U.S. Department of Health and Human Services).

CLSI (2023). "M100 Performance Standards for Antimicrobial Susceptibility Testing," in *Clinical Laboratory Standard Institute, 33nd Edition*. (United States).

Collado, M. C., Cernada, M., Baüerl, C., Vento, M., and Pérez-Martínez, G. (2012). Microbial ecology and host-microbiota interactions during early life stages. *Gut Microbes* 3, 352–365. doi: 10.4161/gmic.21215

Dallenne, C., da Costa, A., Decré, D., Favier, C., and Arlet, G. (2010). Development of a set of multiplex PCR assays for the detection of genes encoding important β-lactamases in Enterobacteriaceae. *J. Antimicrob. Chemother.* 65, 490–495. doi: 10.1093/jac/dkp498

Denkel, L. A., Maechler, F., Schwab, F., Kola, A., Weber, A., Gastmeier, P., et al. (2020). Infections caused by extended-spectrum β-lactamase-producing Enterobacterales after rectal colonization with ESBL-producing *Escherichia coli* or *Klebsiella pneumoniae*. *Clin. Microbiol. Infect.* 26, 1046–1051. doi: 10.1016/j.cmi.2019.11.025

Denkel, L. A., Schwab, F., Kola, A., Leistner, R., Garten, L., von Weizsäcker, K., et al. (2014). The mother as most important risk factor for colonization of very low birth weight (VLBW) infants with extended-spectrum β-lactamase-producing Enterobacteriaceae (ESBL-E). *J. Antimicrob. Chemother.* 69, 2230–2237. doi: 10.1093/jac/dku097

Edwards, T., Williams, C. T., Olwala, M., Andang'o, P., Otieno, W., Nalwa, G. N., et al. (2023). Molecular surveillance reveals widespread colonisation by carbapenemase and extended spectrum beta-lactamase-producing organisms in neonatal units in Kenya and Nigeria. *Antimicrob. Resist. Infect. Control.* 12 (1), 14. doi: 10.1186/s13756-023-01216-0

Folgori, L., Tersigni, C., Hsia, Y., Kortsalioudaki, C., Heath, P., Sharland, M., et al. (2018). The relationship between Gram-negative colonization and bloodstream infections in neonates: a systematic review and meta-analysis. *Clin. Microbiol. Infect.* 24, 251–257. doi: 10.1016/j.cmi.2017.08.008

Ghenea, A. E., Zlatian, O. M., Cristea, O. M., Ungureanu, A., Mititelu, R. R., Balasoiu, A. T., et al. (2022). TEM, CTX-M, SHV Genes in ESBL-Producing *Escherichia coli* and *Klebsiella pneumoniae* Isolated from Clinical Samples in a County Clinical Emergency Hospital Romania-Predominance of CTX-M-15. *Antibiotics* 11, 503. doi: 10.3390/antibiotics11040503

Gorrie, C. L., Mirc Eta, M., Wick, R. R., Edwards, D. J., Thomson, N. R., Strugnell, R. A., et al. (2017). Gastrointestinal carriage is a major reservoir of *Klebsiella pneumoniae* infection in intensive care patients. *Clin. Infect. Dis.* 65, 208–215. doi: 10.1093/cid/cix270

Groer, M. W., Luciano, A. A., Dishaw, L. J., Ashmeade, T. L., Miller, E., and Gilbert, J. A. (2014). Development of the preterm infant gut microbiome: A research priority. *Microbiome* 2, 38. doi: 10.1186/2049-2618-2-38

Hagel, S., Makarewicz, O., Hartung, A., Weiß, D., Stein, C., Brandt, C., et al. (2019). ESBL colonization and acquisition in a hospital population: The molecular epidemiology and transmission of resistance genes. *PloS One* 14. doi: 10.1371/journal.pone.0208505

Hartz, L. E., Bradshaw, W., and Brandon, D. H. (2015). Potential NICU environmental influences on the neonate's microbiome: A systematic review. *Adv. Neonatal Care* 15, 324–335. doi: 10.1097/ANC.0000000000000220

Huerta-García, G. C., Miranda-Novales, G., Díaz-Ramos, R., Vázquez-Rosales, G., and Solórzano-Santos, F. (2015). Intestinal colonization by Extended-spectrum beta-lactamase-producing Enterobacteriaceae in infants. *Rev. Invest. Clin.* 67, 313–317.

Ibrahimagić, A., Uzunović, S., and Bedenić, B. (2017). Prevalence of co-existence genes and clonal spread of ESBL-producing isolates causing hospital and community-acquired infections in Zenica-Doboj Canton, Bosnia and Herzegovina. *J. Health Sci.* 7, 80–90. doi: 10.17532/jhsci.2017.449

Kirtikliene, T., Mierauskaitė, A., Razmienė, I., and Kuisiene, N. (2022). Genetic characterization of multidrug-resistant *E. coli* isolates from bloodstream infections in Lithuania. *Microorganisms* 10, 449. doi: 10.3390/microorganisms10020449

Koirala, S., Khadka, S., Sapkota, S., Sharma, S., Khanal, S., Thapa, A., et al. (2021). Prevalence of CTX-M β -Lactamases Producing Multidrug Resistant *Escherichia coli* and *Klebsiella pneumoniae* among Patients Attending Bir Hospital, Nepal. *BioMed. Res. Int.* 2021, 9958294. doi: 10.1155/2021/9958294

Mahdi Yahya Mohsen, S., Hamzah, H. A., Muhammad Imad Al-Deen, M., and Baharudin, R. (2016). Antimicrobial susceptibility of *Klebsiella pneumoniae* and *Escherichia coli* with extended-spectrum β-lactamase associated genes in hospital Tengku Ampuan Afzan, Kuantan, Pahang. *Malays J. Med. Sci.* 23, 14–20.

Martin, R. M., and Bachman, M. A. (2018). Colonization, infection, and the accessory genome of *Klebsiella pneumoniae*. *Front. Cell Infect. Microbiol.* 8, 4. doi: 10.3389/fcimb.2018.00004

McElduff, F., Cortina-Borja, M., Chan, S. K., and Wade, A. (2010). When t-tests or Wilcoxon-Mann-Whitney tests won't do. *Adv. Physiol. Educ.* 34, 128–133. doi: 10.1152/advan.00017.2010

Munday, C. J., Xiong, J., Li, C., Shen, D., and Hawkey, P. M. (2004). Dissemination of CTX-M type β-lactamases in Enterobacteriaceae isolates in the People's Republic of China. *Int. J. Antimicrob. Agents.* 23, 175–180. doi: 10.1016/j.ijantimicag.2003.07.004

Nowacki, A. (2017). Chi-square and Fisher's exact tests. *Cleve Clin. J. Med.* 84, e20–e25. doi: 10.3949/CCJM.84.S2.04

Obeng-Nkrumah, N., Twum-Danso, K., Krogfelt, K. A., and Newman, M. J. (2013). High levels of extended-spectrum beta-lactamases in a major teaching hospital in Ghana: The need for regular monitoring and evaluation of antibiotic resistance. *Am. J. Trop. Med. Hyg.* 89, 960–964. doi: 10.4269/ajtmh.12-0642

Oteo, J., Pérez-Vázquez, M., and Campos, J. (2010). Extended-spectrum β-lactamase producing *Escherichia coli*: Changing epidemiology and clinical impact. *Curr. Opin. Infect. Dis.* 23, 320–326. doi: 10.1097/QCO.0b013e3283398dc1

Ouedraogo, A. S., Sanou, M., Kissou, A., Sanou, S., Solaré, H., Kaboré, F., et al. (2016). High prevalence of extended-spectrum ß-lactamase producing Enterobacteriaceae among clinical isolates in Burkina Faso. *BMC Infect. Dis.* 16, 326. doi: 10.1186/s12879-016-1655-3

Pirr, S., and Viemann, D. (2020). Host factors of favorable intestinal microbial colonization. *Front. Immunol.* 7. doi: 10.3389/fimmu.2020.584288

Platteel, T. N., Leverstein-van Hall, M. A., Cohen Stuart, J. W., Thijsen, S. F. T., Mascini, E. M., van Hees, B. C., et al. (2015). Predicting carriage with extended-spectrum beta-lactamase-producing bacteria at hospital admission: A cross-sectional study. *Clin. Microbiol. Infect.* 21, 141–146. doi: 10.1016/j.cmi.2014.09.014

Prince, A. L., Antony, K. M., Ma, J., and Aagaard, K. M. (2014). The microbiome and development: A mother's perspective. *Semin. Reprod. Med.* 32, 14–22. doi: 10.1055/s-0033-1361818

Reyman, M., van Houten, M. A., van Baarle, D., Bosch, A. A. T. M., Man, W. H., Chu, M. L. J. N., et al. (2019). Impact of delivery mode-associated gut microbiota dynamics on health in the first year of life. *Nat. Commun.* 10, 4997. doi: 10.1038/s41467-019-13014-7

Rezai, M. S., Salehifar, E., Rafiei, A., Langaee, T., Rafati, M., Shafahi, K., et al. (2015). Characterization of Multidrug Resistant Extended-Spectrum Beta-Lactamase-Producing *Escherichia coli* among Uropathogens of Pediatrics in North of Iran. *BioMed. Res. Int.* 309478. doi: 10.1155/2015/309478

Rohlf, J. F. (1998). "NTSYSpc, Numerical Taxonomy and Multivariate Analysis System Version 2.0 User Guide," in *Natural History*. (Department of Ecology and Evolution, State University of New York).

Schmiedel, J., Falgenhauer, L., Domann, E., Bauerfeind, R., Prenger-Berninghoff, E., Imirzalioglu, C., et al. (2014). Multiresistant extended-spectrum β-lactamase-producing Enterobacteriaceae from humans, companion animals, and horses in central Hesse, Germany. *BMC Microbiol.* 14, 187. doi: 10.1186/1471-2180-14-187

Shahid, M., Singh, A., Sobia, F., Rashid, M., Malik, A., Shukla, I., et al. (2011). bla_{CTX-M}, bla_{TEM}, and bla_{SHV} in Enterobacteriaceae from North-Indian tertiary hospital: High occurrence of combination genes. *Asian Pac J. Trop. Med.* 4, 101–105. doi: 10.1016/S1995-7645(11)60046-1

Siriphap, A., Kitti, T., Khuekankaew, A., Boonlao, C., Thephinlap, C., Thepmalee, C., et al. (2022). High prevalence of extended-spectrum beta-lactamase-producing *Escherichia coli* and *Klebsiella pneumoniae* isolates: A 5-year retrospective study at a Tertiary Hospital in Northern Thailand. *Front. Cell Infect. Microbiol.* 12, 955774. doi: 10.3389/fcimb.2022.955774

Smith, A., Saiman, L., Zhou, J., Della-Latta, P., Jia, H., and Graham, P. L. (2010). Concordance of gastrointestinal tract colonization and subsequent bloodstream infections with gram-negative bacilli in very low birth weight infants in the neonatal intensive care unit. *Pediatr. Infect. Dis. J.* 29, 831–835. doi: 10.1097/INF.0b013e3181e7884f

Socha-Banasiak, A., Pawłowska, M., Czkwianianc, E., and Pierzynowska, K. (2021). From intrauterine to extrauterine life—The role of endogenous and exogenous factors in the regulation of the intestinal microbiota community and gut maturation in early life. *Front. Nutr.* 8. doi: 10.3389/fnut.2021.696966

Souverein, D., Euser, S. M., Herpers, B. L., Kluytmans, J., Rossen, J. W. A., and Den Boer, J. W. (2019). Association between rectal colonization with highly resistant gram-negative rods (HR-GNRs) and subsequent infection with HR-GNRs in clinical patients: A one year historical cohort study. *PloS One* 14, e0211016. doi: 10.1371/journal.pone.0211016

Swaminathan, B., Barrett, T. J., Hunter, S. B., and Tauxe, R. V. (2001). PulseNet: the molecular subtyping network for foodborne bacterial disease surveillance, United States. *Emerg. Infect. Dis.* 7, 382–389. doi: 10.3201/eid0703.017303

Tacconelli, E., Carrara, E., Savoldi, A., Harbarth, S., Mendelson, M., Monnet, D. L., et al. (2018). Discovery, research, and development of new antibiotics: the WHO priority list of antibiotic-resistant bacteria and tuberculosis. *Lancet Infect. Dis.* 18, 318–327. doi: 10.1016/S1473-3099(17)30753-3

Tufa, T. B., Fuchs, A., Tufa, T. B., Stötter, L., Kaasch, A. J., Feldt, T., et al. (2020). High rate of extended-spectrum beta-lactamase-producing gram-negative infections and associated mortality in Ethiopia: a systematic review and meta-analysis. *Antimicrob. Resist. Infect. Control.* 9, 128. doi: 10.1186/s13756-020-00806-6

Vandenplas, Y., Carnielli, V. P., Ksiazyk, J., Luna, M. S., Migacheva, N., Mosselmans, J. M., et al. (2020). Factors affecting early-life intestinal microbiota development. *Nutrition* 78, 110812. doi: 10.1016/j.nut.2020.110812

Vangay, P., Ward, T., Gerber, J. S., and Knights, D. (2015). Cell host & Microbe perspective antibiotics, pediatric dysbiosis, and disease. *Cell Host Microbe* 17, 553–564. doi: 10.1016/j.chom.2015.04.006

Voets, G. M., Fluit, A. C., Scharringa, J., Cohen Stuart, J., and Leverstein-van Hall, M. A. (2011). A set of multiplex PCRs for genotypic detection of extended-spectrum β-lactamases, carbapenemases, plasmid-mediated AmpC β-lactamases and OXA β-lactamases. *Int. J. Antimicrob. Agents.* 37, 356–359. doi: 10.1016/j.ijantimicag.2011.01.005

Yin, L., He, L., Miao, J., Yang, W., Wang, X., Ma, J., et al. (2021). Carbapenem-resistant Enterobacterales colonization and subsequent infection in a neonatal intensive care unit in Shanghai, China. *Infect. Prev. Pract.* 3 (3), 100147. doi: 10.1016/j.infpip.2021.100147

Zerr, D. M., Qin, X., Oron, A. P., Adler, A. L., Wolter, D. J., Berry, J. E., et al. (2014). Pediatric infection and intestinal carriage due to extended-spectrum- cephalosporin-resistant Enterobacteriaceae. *Antimicrob. Agents Chemother.* 58, 3997–4004. doi: 10.1128/AAC.02558-14

frontiers | Frontiers in Public Health

TYPE Systematic Review
PUBLISHED 22 January 2024
DOI 10.3389/fpubh.2024.1337276

OPEN ACCESS

EDITED BY
Manuel Gerardo Ballesteros Monrreal,
University of Sonora, Mexico

REVIEWED BY
Srinivasan Velusamy,
Centers for Disease Control and Prevention (CDC), United States
Sergey Sidorenko,
Pediatric Research and Clinical Center for Infectious Diseases, Russia

*CORRESPONDENCE
María Macarena Sandoval
✉ macarena_sandoval@yahoo.com.ar

†These authors have contributed equally to this work

RECEIVED 12 November 2023
ACCEPTED 04 January 2024
PUBLISHED 22 January 2024

CITATION
Sandoval MM, Ruvinsky S, Palermo MC, Alconada T, Brizuela ME, Wierzbicki ER, Cantos J, Bardach A, Ciapponi A and Gagetti P (2024) Antimicrobial resistance of *Streptococcus pneumoniae* from invasive pneumococcal diseases in Latin American countries: a systematic review and meta-analysis.
Front. Public Health 12:1337276.
doi: 10.3389/fpubh.2024.1337276

Antimicrobial resistance of *Streptococcus pneumoniae* from invasive pneumococcal diseases in Latin American countries: a systematic review and meta-analysis

María Macarena Sandoval[1*†], Silvina Ruvinsky[1,2†], María Carolina Palermo[1†], Tomás Alconada[1†], Martín Eduardo Brizuela[1,3†], Eugenia Ramirez Wierzbicki[1†], Joaquín Cantos[1†], Ariel Bardach[1,4†], Agustín Ciapponi[1,4†] and Paula Gagetti[1,5†]

[1]Instituto de Efectividad Clínica y Sanitaria (IECS-CONICET), Buenos Aires, Argentina, [2]Coordinación de Investigación, Hospital de Pediatría "Dr. Juan P. Garrahan", Buenos Aires, Argentina, [3]Unidad de Pediatría, Hospital General de Agudos Vélez Sarsfield, Buenos Aires, Argentina, [4]Centro de Investigaciones Epidemiológicas y Salud Pública (CIESP-IECS), CONICET, Buenos Aires, Argentina, [5]Servicio Antimicrobianos, National Reference Laboratory (NRL), Instituto Nacional de Enfermedades Infecciosas (INEI)-ANLIS "Dr. Carlos G. Malbrán", Buenos Aires, Argentina

Background: Invasive pneumococcal disease has declined since pneumococcal conjugate vaccine introduction in Latin America and the Caribbean (LAC). However, serotype distribution and antimicrobial resistance patterns have changed.

Methods: We conducted a systematic review to evaluate the frequency of antimicrobial resistance of *Streptococcus pneumoniae* from invasive disease in LAC. Articles published between 1 January 2000, and 27 December 2022, with no language restriction, were searched in major databases and gray literature. Pairs of reviewers independently selected extracted data and assessed the risk of bias in the studies. The quality of antimicrobial resistance (AMR) studies was evaluated according to WHO recommendations (PROSPERO CRD42023392097).

Results: From 8,600 records identified, 103 studies were included, with 49,660 positive samples of *S. pneumoniae* for AMR analysis processed. Most studies were from Brazil (29.1%) and Argentina (18.4%), were cross-sectional (57.3%), reported data on AMR from IPD cases (52.4%), and were classified as moderate risk of bias (50.5%). Resistance to penicillin was 21.7% (95%IC 18.7–25.0, I^2: 95.9), and for ceftriaxone/cefotaxime it was 4.7% (95%IC 3.2–6.9, I^2: 96.1). The highest resistance for both penicillin and ceftriaxone/cefotaxime was in the age group of 0 to 5 years (32.1% [95%IC 28.2–36.4, I^2: 87.7], and 9.7% [95%IC 5.9–15.6, I^2: 96.9] respectively). The most frequent serotypes associated with resistance were 14 for penicillin and 19A for ceftriaxone/cefotaxime.

Conclusion: Approximately one-quarter of invasive pneumococcal disease isolates in Latin America and the Caribbean displayed penicillin resistance, with higher rates in young children. Ongoing surveillance is essential to monitor serotype evolution and antimicrobial resistance patterns following pneumococcal conjugate vaccine introduction.

KEYWORDS

Streptococcus pneumoniae, invasive pneumococcal disease, antimicrobial resistance, serotypes, Latin America

1 Introduction

Invasive disease caused by *Streptococcus pneumoniae* (IPD) is one of the leading causes of morbidity and mortality in children and older adults worldwide (1). IPD included mainly meningitis, bacteremia, and bacteremic pneumonia (2).

The invasiveness and pathogenesis of *S. pneumoniae* are defined by capsular composition; currently, one hundred serotypes have been identified (3).

In Latin America and the Caribbean, it is estimated that every year, IPD is responsible for up to 28,000 deaths, 182,000 hospitalizations, and 1.4 million outpatient consults (4).

To prevent IPD, different vaccines were developed, 23-valent pneumococcal polysaccharide vaccine (PPV23) and pneumococcal conjugate vaccines (PCVs) (5). In 2009 PCVs were introduced in Latin American countries, and since May 2016, 29 countries have incorporated PCV-10 or PCV-13 s in their national immunization programs (6).

Serotype distribution in IPD changes over time by age group, clinical manifestation, and regional location (7). SIREVA is an official regional laboratory surveillance program (SIREVA) that reports information about serotype distribution and antimicrobial resistance (AMR) in IPD in the pediatric and adult populations.

S. pneumoniae infections are frequently associated with inappropriate antimicrobial prescriptions both in the community and in the hospital. IPD rates have decreased since the implementation of national immunization programs. However, serotype distribution and resistance patterns have been modified (8).

Antimicrobial resistance has emerged in *S. pneumoniae* during the last years with a high impact on global health. Worldwide the highest rates of resistance to penicillin and erythromycin were found in serotypes 6B, 6A, 9 V, 14, 15A, 19F, 19A, and 23F (9). However, information about serotype distribution and antimicrobials in IPD is scarce.

This systematic review aimed to describe reported data about antimicrobial resistance and associated serotypes in IPD from Latin American and Caribbean countries.

2 Methods

The analysis presented here was part of a broader systematic review that included epidemiological data on the burden of pneumococcal disease in LAC. The findings on AMR are presented in this article. We conducted a systematic literature review and meta-analysis of AMR in IPD in LAC during the last 20 years following Cochrane methods (10), the MOOSE guidelines for observational studies (11), and the PRISMA statement for reporting systematic reviews and meta-analyses (12). The protocol is registered in PROSPERO CRD UK (registration number: CRD42023392097).

2.1 Inclusion criteria

Studies from any LAC countries, regardless of age or sex, risk groups, with at least 20 culture-confirmed cases from sterile sites (e.g., blood, cerebrospinal fluid, pleural fluid) were eligible for inclusion. IPD clinical presentations included sepsis/bacteremia, meningitis, bacteremic pneumonia, empyema, peritonitis, osteoarticular infection/septic arthritis, and endocarditis.

Cohort studies, case–control studies, cross-sectional studies, case series, epidemiological surveillance reports, hospital-based surveillance studies, interrupted time series (ITS), and controlled ITS (CITS) studies were included. Systematic reviews and meta-analyses were only considered as sources for primary studies. When data or data subsets reported in more than one publication were found, the one with the larger sample size or the most recent were selected.

2.2 Search strategy for identification of studies and data sources

Records published between 1 January 2000, and 27 December 2022, in the following databases: PubMed, Embase, CINAHL (Cumulative Index of Nursing and Allied Health Literature), LILACS (Latin American and Caribbean Health Science Literature)/ScieLO, EconLIT, Global Health, and Web of Science, with no language restriction, were searched. Strategies search, and terms for each database are presented in Supplementary Appendix A. The reference lists of the articles were hand-searched for additional information. We contacted the original authors to obtain any missing information or clarification, but for this analysis it was not necessary.

SIREVA, other regional or national surveillance databases, including antimicrobial resistance databases, and relevant sources like regional MoH, PAHO, and reports from referral hospitals were searched. Databases containing regional proceedings, congresses' annals, doctoral theses, websites from regional scientific meetings, experts, and related associations were also conducted.

2.3 Outcomes of interest

We explored outcomes by type of IPD, serotype distribution, and antimicrobial resistance reported during the same period.

2.4 Selection of articles and data extraction

Publications were screened by two reviewers using title and abstract according to the eligibility criteria. Discrepancies were solved by consensus of the entire work team. Potentially eligible articles were

retrieved in full text for further analysis. All screening phases of the study used COVIDENCE® software (13), a web-based platform designed to process systematic reviews.

One reviewer performed data extraction and verified by a second one using a pre-specified extraction online form previously piloted in 10 studies. From eligible articles, the research team extracted the following study information: publication and study characteristics (type of publication, year published, authors, geographic location, study design including domains for risk of bias assessment), study population characteristics (age, sex, sample size, population risk, inclusion and exclusion criteria), and outcomes (frequency of AMR and frequency of serotypes associated with AMR).

2.5 Risk of bias assessment

Included studies were assessed for risk of bias by two independent reviewers, with discrepancies resolved by consensus with the whole team. The risk of bias in observational studies and the control arm of trials was assessed using the checklists developed by the U. S. National Heart, Lung, and Blood Institute, which classify studies as high risk of bias (POOR), moderate risk of bias (FAIR), and low risk of bias (GOOD). For the assessment of cohort studies and cross-sectional studies, the tool comprises 14 items, while nine items apply to the case series studies (14).

2.6 Quality assessment of AMR studies

The quality of AMR studies was evaluated according to WHO recommendations (15).

2.7 Statistical analysis

2.7.1 Primary analysis

To analyze the data, descriptive statistics and performed a proportion meta-analysis, using metaprop {meta} package with R software version 4.2.2. were used (16, 17). We applied an arcsine transformation to stabilize the variance of proportions (Freeman-Tukey variant of the arcsine square root of transformed proportions method) (18). We applied DerSimonian-Laird weights for the random effects model where heterogeneity between studies was found. We calculated the I^2 statistics as a measure of the proportion of the overall variation in the proportion that was attributable to between-study heterogeneity. An $I^2 > 60–70\%$ was considered as substantial heterogeneity, and below 30% as low level of heterogeneity (19). Selective reporting within studies was assessed by comparing available protocols with the reports.

2.7.2 Subgroup analysis, sensitivity analysis, and investigation of heterogeneity

We conducted subgroup analyses classifying the studies by five-year calendar period, country, age group (0–5 years, 6–64 years, 65 or more years old), and by antibiotic resistance. Both types of analyses could contribute to the investigation of heterogeneity causes.

3 Results

3.1 Literature search and study selection

We identified 8,600 records in seven different databases. After eliminating duplicates, we screened the remaining 4,533 by title and abstract. We made a full-text assessment of 414 considered relevant to determine eligibility. Finally, 103 studies met the inclusion criteria (Figure 1).

3.2 Characteristics of included studies

The characteristics of the included studies are summarized in Supplementary Table 3 in Appendix A. There were 98 full texts, four abstracts, and one thesis; 59 (57.3%) were cross-sectional studies, 42 (40.9%) case series, one (0.9%) prospective cohort, and one (0.9%) non-comparative cohort.

The studies provided data on AMR in the following countries: Brazil ($n = 30$, 29.1%) between 1990 to 2019, Argentina ($n = 19$, 18.4%) between 1993 to 2019, Uruguay ($n = 12$, 11.8%) between 1987 to 2018, Colombia ($n = 8$, 7.9%) between 1994 to 2019, Chile ($n = 7$, 6.9%) between 1994 to 2014, Peru ($n = 5$, 4.9%) between 2000 to 2018, Mexico ($n = 4$, 3.9%) between 1994 to 2015, Paraguay ($n = 4$, 3.9%) between 1993 to 2018, Costa Rica ($n = 3$, 2.9%) between 1995 to 2015, Cuba ($n = 2$, 1.9%) between 2007 to 2016, French Guiana ($n = 1$, 0.9%) between 2000 to 2010, Jamaica ($n = 1$, 0.9%) between 1995 to 1999, Panama ($n = 1$, 0.9%) from 2010 and 2011, Puerto Rico ($n = 1$, 0.9%) during 2001 only, and Trinidad and Tobago ($n = 1$, 0.9%) between 1997 to 2013. There were also four studies reporting on AMR in various LAC countries (including Argentina, Bolivia, Brazil, Chile, Colombia, Costa Rica, Dominican Republic, Ecuador, El Salvador, Guatemala, Mexico, Nicaragua, Panama, Paraguay, Peru and Uruguay) between 1993 to 2015.

These studies were published between 2001 and 2022, with 38.8% ($n = 40$) published between 2000 and 2009 and 50.5% ($n = 52$) between 2010 and 2019. Only 10.7% ($n = 11$) were published in the last 3 years (2020 to 2022). The inclusion period of participants was from 1987 to 2019, with 41.7% ($n = 43$) of the studies that included participants before 2000, 47.6% ($n = 49$), which included participants between 2000 and 2009, and 10.5% ($n = 11$) included participants from 2010 onwards. Only two (1%) studies did not report the inclusion period. The reported duration of the studies ranged from 12 to 299 months.

Of the 103 studies, 54 (52.4%) reported data on AMR from IPD, 23 (22.3%) from meningitis (including two studies from IPD that only reported AMR from meningitis cases), 22 (21.4%) from pneumonia, and four (3.9%) from bacteremia. A total of 49,660 positive samples of *S. pneumoniae* for AMR analysis were processed, with a range of samples evaluated between 6 to 11,377, including 40,889 samples from IPD (range 17–11,377), 4,743 samples from pneumonia (range 11–2,629), 3,633 samples from meningitis (range 6–854), and 395 samples from bacteremia (range 56–167). In one study, the total number of samples processed was not reported.

AMR was tested for three or more antibiotics in 54.4% ($n = 56$) of the studies, two antibiotics in 23 studies (22.3%), and in the

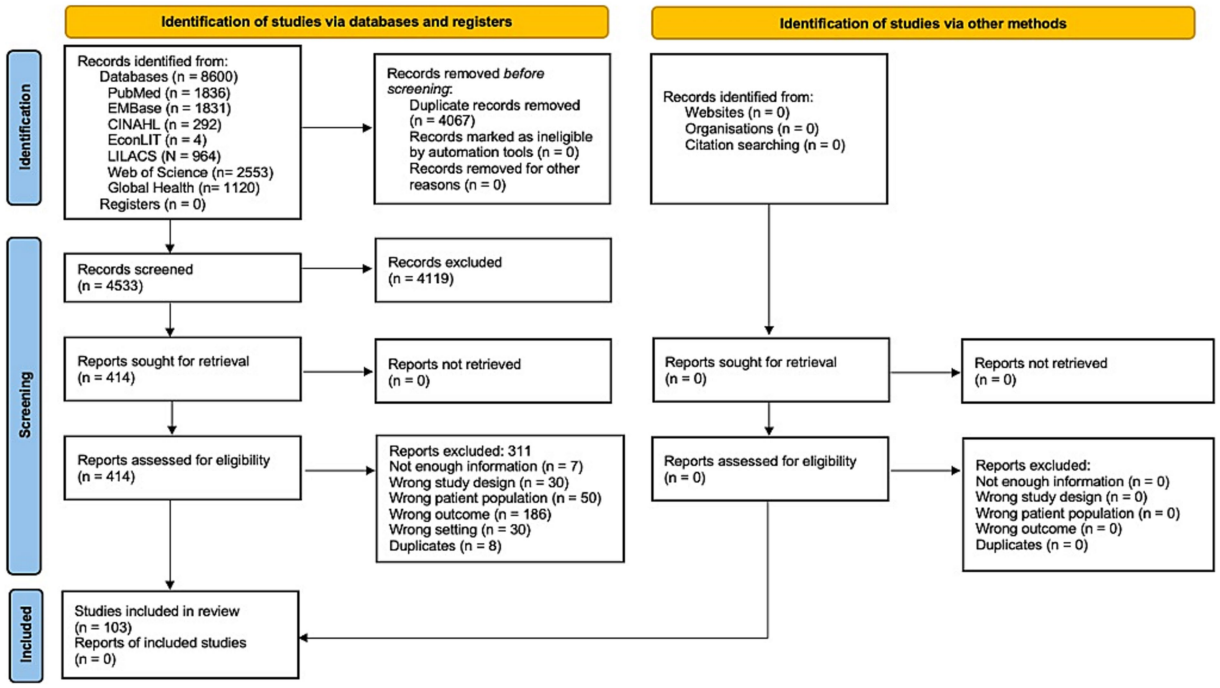

FIGURE 1
Study flowchart.

remaining 24 studies (23.3%) only for penicillin. Studies evaluating several antimicrobial resistance in IPD included principally: penicillin ($n = 53$), ceftriaxone/cefotaxime ($n = 44$), trimethoprim-sulfamethoxazole ($n = 44$) and erythromycin ($n = 44$). The methods reported in studies analyzed were epsilometric (E-test) in 26.2% ($n = 27$), broth dilution in 19.4% (n = 20), disk diffusion in 5.8% ($n = 6$), agar dilution in 3.9% ($n = 4$), automatized systems in 2.9% ($n = 3$). Only in a single study (0.9%) molecular techniques (WGS-based assessment) were used to predict antibiotic resistance from genomic data by detecting resistance genes. Also, in 25.3% ($n = 26$), combined methods were used. The method used was not reported in 15.6% ($n = 16$) of the studies.

The references of the included studies are in Supplementary Appendix A.

3.3 Risk of bias assessment

For cross-sectional and cohort studies, 40 (65.6%) were assessed as being at moderate (fair) risk, 15 (24.6%) were assessed as low (good) risk, and only six (9.8%) as high (poor) risk. The most frequent domains that did not meet the evaluation objectives were related to sample size justification, the evaluation of exposures more than once or different levels of exposure, and the blinding of the evaluators. For case series studies, 29 (69%) were rated as low risk, 12 (28.6%) as moderate risk, and only one (2.4%) as high risk. The domains that did not meet the objectives more frequently were whether the cases were consecutive and the description of the statistical methods. The complete evaluation of risk bias assessment by study design is in Supplementary Tables 4, 5 in Appendix A.

3.4 Quality assessment of AMR studies

The results of the quality assessment of AMR studies are summarized in Supplementary Table 6 in Appendix A. The quality was scored as high in 87.4% ($n = 90$) of the studies and moderate in the remaining 12.6% ($n = 13$). The most frequently missed items were not specifying whether a reference/control strain was included when assessing antimicrobial susceptibility (64.7%, $n = 66$), including less than 100 isolates, or not reporting the number of isolates evaluated (43.7%, $n = 45$).

3.5 Results of AMR of *Streptococcus pneumoniae* of included studies

Antimicrobial susceptibility results were interpreted according to the Clinical and Laboratory Standards Institutes (CLSI), meningitis breakpoints were used for penicillin and ceftriaxone/cefotaxime (Supplementary Table 7 in Appendix A). The percentage of resistance to penicillin from IPD cases ranged from 0% (Panama; s80) to 51.7% (Mexico; s74). In 29/50 (58%) studies, penicillin resistance was less than 25%, in 16/50 (32%) it was from 25 to 50%; and in 5/50 (10%) was more than 50%. The percentage of resistance to ceftriaxone/cefotaxime from IPD cases ranged between 0% (seven studies reported 0% of resistance; s4, s41, s50, s63, s85, s89, s92) to 26.1% (Uruguay; s74). In 36 (95%) studies, out of 38 studies analyzed, the percentage of resistance was less than 25%; in 30 (79%) the resistance was less than 10%. Only two (5%) studies reported a percentage of resistance of more than 25% (s74, s78). For trimethoprim-sulfamethoxazole, the percentage of resistance ranged from 6.1% (Brazil; s32) to 69% (Peru;

s85). In eight (25%) studies, out of 32, the percentage of resistance was less than 25%, in 13 (40.6%) the resistance ranged between 25 and 50%, and in 11 (34.4%) it was more than 50%. For erythromycin, the percentage of resistance ranged from 0% (Brazil and Colombia; s35, s63) to 50% (Cuba; s68). In 23 (79.3%) studies, out of 29, the resistance was less than 25%, and in six (20.7%) it was more than 25% (Supplementary Table 8 in Appendix A).

In 23 studies from meningitis cases, 22 reported resistance to penicillin, 16 to ceftriaxone/cefotaxime, eight to trimethoprim-sulfamethoxazole, and seven to erythromycin. The percentage of resistance to penicillin ranged from 0% (Costa Rica; s65) to 64.5% (Mexico; s79). In 14/22 studies (63.6%), the resistance reported was less than 25%; in seven (31.8%), between 25 and 50%, and in one study (4.6%) more than 50%. For ceftriaxone/cefotaxime, the resistance ranged from 0% (s21, s36, s43, s48, s71, s77, s79) to 16.7% (Argentina; s13). The percentage of resistance to trimethoprim-sulfamethoxazole ranged from 9.9% (s43) to 75% (both in Brazil; s33). In three (37.5%), the resistance reported was less than 25%; in two (25%), it was from 25 to 50%, and in the remaining three (37.5%) it was more than 50%. For erythromycin, the resistance ranged from 0% (Brazil; s43) to 41.9% (Cuba; s69). In six (85.7%) studies, the resistance reported was less than 25% (Supplementary Table 9 in Appendix A).

From pneumonia cases, 24 studies were analyzed; all of them reported resistance to penicillin, 14 to ceftriaxone/cefotaxime, five to trimethoprim-sulfamethoxazole, and seven to erythromycin. Penicillin resistance ranged from 0% (s11, s55, s56, s98, s99) to 62.7% (Uruguay; s97). In 14 (58.3%) studies, the resistance was less than 25%, in nine (37.5%) it was from 25 to 50%, and only one study reported a resistance of more than 50% (s97). Resistance to ceftriaxone/cefotaxime ranged from 0% (s9, s53, s54, s55, s73, s99) to 20.3% (Mexico; s73). Trimethoprim-sulfamethoxazole resistance ranged from 33.9% (Colombia; s73) to 67.3% (Argentina; s9). In 80% of the studies, resistance was more than 50%. Erythromycin resistance was less than 25%, ranging between 2.6% (Argentina; s73) to 24.5% (Mexico; s73; Supplementary Table 10 in Appendix A).

Only four studies reported antimicrobial susceptibility from bacteremia cases, with 395 isolates evaluated for penicillin, 163 for ceftriaxone/cefotaxime, and 56 for both trimethoprim-sulfamethoxazole and erythromycin. The percentage of resistance to penicillin ranged from 0% (Argentina; s17) to 20.6% (Argentina; s2). Two studies reported the resistance to ceftriaxone/cefotaxime, it was 0% in both (Argentina and Chile; s2, s51). One study reported the percentage of resistance to trimethoprim-sulfamethoxazole and erythromycin, with 17.9% of resistance each (s51; Supplementary Table 11 in Appendix A).

The full assessment of susceptibility of *S. pneumoniae* is in the Supplementary Tables 12–15 in Appendix B.

3.6 Serotypes associated with antimicrobial resistance

Forty-two studies (40.7%) reported the serotypes associated with antimicrobial resistance. All studies analyzed penicillin resistance, in 11 ceftriaxone/cefotaxime and the remaining seven erythromycin resistance. The most frequent serotype associated with penicillin resistance was serotype 14 (53.11%, $n = 2{,}808$), followed by serotypes 6B (10.93%, $n = 578$), 23F (10.63%, $n = 562$), and 19A (9.85%, $n = 521$). 5/42 (12%) studies only include serotype 19A isolates for analysis. The majority of serotypes related to AMR found are included in 518 the PVC13 vaccine. Additional serotypes included in the PVC20 519 vaccine were found much less frequently, with only 10 resistant 520 isolates serotyped as 15B (0.11%), 11A (0.04%), 12F and 8 (0.02% 521 each), resistant serotypes 10A, 22F and 33F were not reported 522 (Figure 2A).

For ceftriaxone/cefotaxime and erythromycin, the most frequent serotypes associated with resistance was 19A (58.48%, $n = 193$ and 46.27%, $n = 397$ respectively). In the case of ceftriaxone/cefotaxime, another five serotypes were reported associated with resistance but with a lower frequency, all included in the PVC10 vaccine (Figure 2B). Regarding erythromycin, except for serotypes 1, 4, 18C, and 22F, all the other serotypes included in the PVC10, PVC13, 529 and PVC20 vaccines were associated with resistance, with a frequency less than 5% (Figure 2C).

The complete assessment of serotypes associated with resistance is in Supplementary Tables 16–18 are in Appendix B.

3.7 Proportion meta-analysis for resistance to penicillin and ceftriaxone/cefotaxime

A proportion meta-analysis for resistance to penicillin and ceftriaxone/cefotaxime was performed. Subgroup analyses were conducted by five-year calendar period, country, and age range (0–5 years, 6–64 years, and 65 or more years; Table 1).

The resistance to penicillin was 21.7% (95%IC 18.7–25.0, I^2: 95.9; Supplementary Figure 1 in Appendix A). The highest resistance was observed between 2000 and 2004 with 35.8% (95%IC 27.1–45.5, I^2: 93.4), and the lowest between 2010 and 2014 with 5.9% (95%IC 1.2–24.5, I^2: 94.8; Supplementary Figure 2 in Appendix A). Regarding age, the highest resistance was in the age group of 0 to 5 years with 32.1% (95%IC 28.2–36.4, I^2: 87.7; Supplementary Figure 3 in Appendix A). When we analyzed by country we observed the highest resistance in Puerto Rico: 49.7% (95%IC 42.4–57.0, I^2: NA), Mexico: 45.5% (95%IC 33.3–58.3, I^2: 88.1), and Cuba: 44.7% (95%IC 35.5–54.3, I^2: NA), while in Chile the lowest resistance was observed with 11.6% (95%IC 4.0–29.2, I^2: 83.5; Figure 3).

The resistance to ceftriaxone/cefotaxime was 4.7% (95%IC 3.2–6.9, I^2: 96.1; Supplementary Figure 4 in Appendix A). Between 1995 and 1999 we observed the highest resistance with 11.2% (95%IC 6.2–19.3, I^2: 79.9; Supplementary Figure 5 in Appendix A). As with penicillin, the highest resistance was in the age group of 0 to 5 years with 9.7% (95%IC 5.9–15.6, I^2: 96.9; Supplementary Figure 6 in Appendix A). Analyzed by country the resistance in all was less than 10%, except in Mexico where we observed the highest with 17.3% of resistance (95%IC 9.5–29.4, I^2: 84.6; Figure 4).

3.8 Data analysis from regional laboratory surveillance database reports (SIREVA)

Among the countries of the region of the Americas most represented in SIREVA reports were Argentina, Brazil, Chile, and Colombia, which between 2013 and 2018 reported more than 600

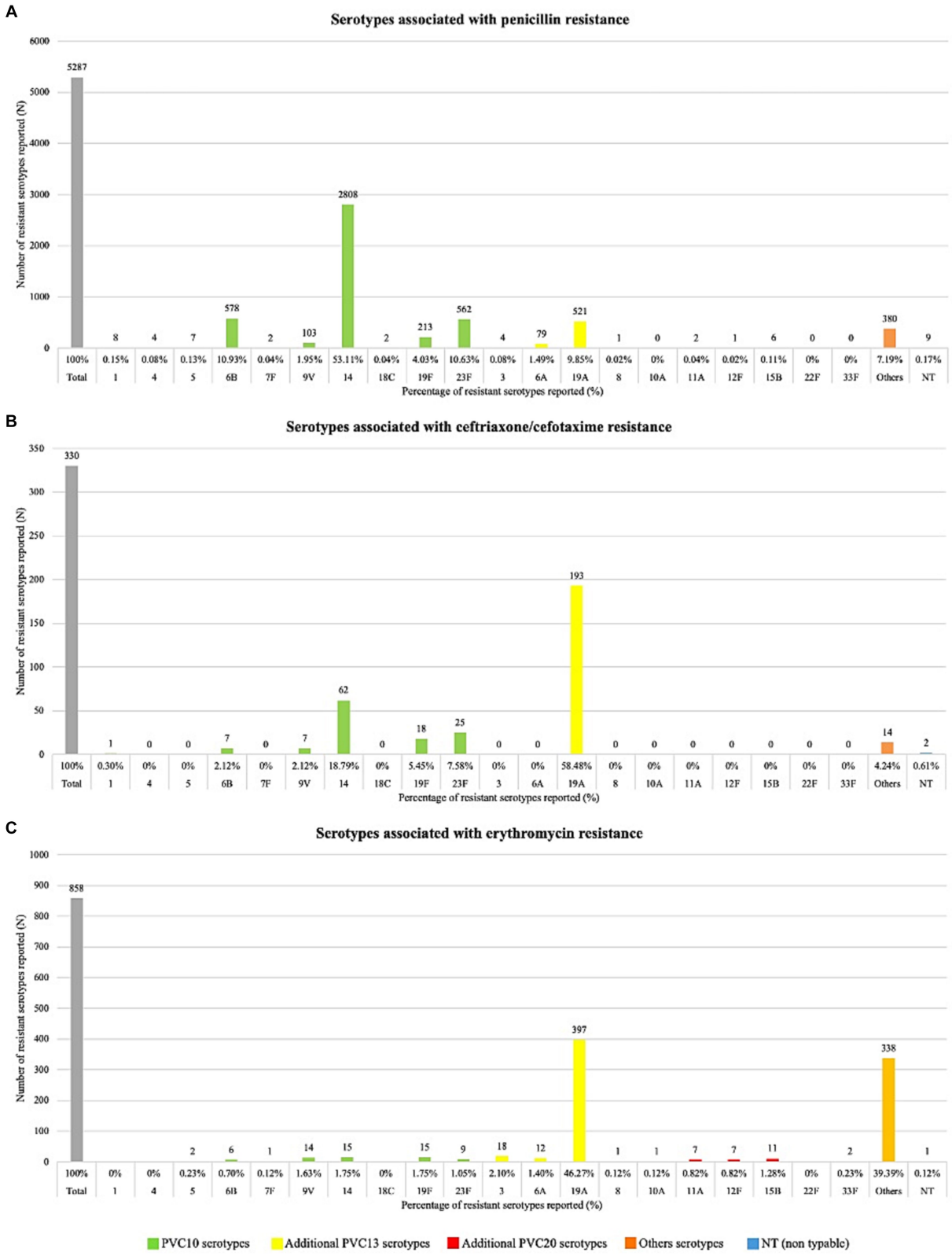

FIGURE 2
Serotypes associated with resistance. Serotypes associated with resistance to: (panel **A**) penicillin, (panel **B**) ceftriaxone/cefotaxime, (panel **C**) erythromycin.

results from children under 5 years old. Before 2013, non-PCV13 serotypes were not listed. Resistance to penicillin and cefotaxime did not present significant differences between 2013 and 2018 in any of the countries analyzed. Regarding erythromycin resistance, in Argentina, a significant increase ($p < 0.05$) was observed between 2013 and 2018. Analyzing the main serotypes related to antimicrobial

TABLE 1 Summary of proportion meta-analyses results for resistance to penicillin and ceftriaxone/cefotaxime, by five-year calendar period, age categories and country.

	Resistance to penicillin			Resistance to ceftriaxone/cefotaxime		
	Studies (N)	Proportion (95%IC)	I^2	Studies (N)	Proportion (95%IC)	I^2
Overall	92	21.71% (18.70–25.07)	95.9%	47	4.74% (3.21–6.94)	96.1%
By 5-years period						
1990–1994	2	24.99% (16.55–35.89)	27.5%	–	–	–
1995–1999	22	28.44% (23.69–33.71)	93.4%	8	11.28% (6.29–19.39)	79.9%
2000–2004	14	35.82% (27.14–45.55)	93.4%	12	7.03% (2.16–20.53)	93.5%
2005–2009	6	8.09% (3.66–16.93)	70.2%	9	8.03% (2.85–20.60)	92.9%
2010–2014	4	5.96% (1.22–24.53)	94.8%	10	5.34% (3.01–9.29)	59.1%
2015–2019	–	–	–	4	6.52% (3.58–11.58)	76.0%
By age						
0–5 years	35	32.17% (28.23–36.40)	87.7%	20	9.78% (5.98–15.61)	96.9%
6–64 years	2	15.66% (12.91–18.87)	80.3%	1	6.20% (5.55–6.93)	NA
≥65 years	3	18.25% (9.75–31.56)	92.9%	2	5.13% (4.47–5.87)	0%
By country						
Argentina	18	19.54% (13.00–28.31)	94.0%	9	6.74% (3.30–13.29)	97.2%
Brazil	31	20.09% (16.30–24.50)	94.0%	12	2.48% (0.97–6.18)	95.8%
Chile	6	11.69% (4.06–29.27)	83.5%	2	5.76% (1.74–17.41)	68.7%
Colombia	9	19.72% (15.34–24.97)	94.7%	8	4.14% (1.75–9.49)	96.3%
Costa Rica	2	27.77% (6.90–66.62)	92.6%	1	3.03% (0.76–11.32)	NA
Cuba	1	44.76% (35.55–54.35)	NA	1	7.62% (3.86–14.50)	NA
French Guiana	1	35.71% (20.41–54.62)	NA	–	–	–
Mexico	6	45.56% (33.31–58.37)	88.1%	4	17.30% (9.50–29.42)	84.6%
Paraguay	4	16.34% (8.66–28.68)	89.3%	4	1.64% (0.41–6.39)	72.7%
Peru	3	18.17% (13.51–24.00)	0%	2	3.10% (1.56–6.08)	0%
Puerto Rico	1	49.72% (42.41–57.04)	NA	1	3.39% (1.53–7.34)	NA
Uruguay	10	22.75% (9.13–46.30)	92.8%	4	6.69% (1.92–20.79)	96.3%

NA, Not Applicable.

resistance, when comparing 2013 with 2018, a significant increase in 19A was observed in Chile, as well as 24A in Argentina and Chile (Figure 5).

4 Discussion

This study analyzed mainly antimicrobial resistance and associated serotypes in IPD previous and post-introduction of PCVs in pediatric, adult, and mixed populations in healthcare facilities from 15 countries across the LAC region.

Antimicrobial resistance in *S. pneumoniae* changes over time depending on PCV implementation, serotype distribution, antimicrobial consumption, and other factors showed differences between countries (7, 20).

Since the introduction of PCVs in national immunization programs in LAC, a decrease in IPD and changes in serotype distribution and antimicrobial resistance patterns have been observed. We focus on antibiotics useful to treat pneumococcal diseases in children and adults (21, 22). In our study, we observed a global penicillin antimicrobial resistance rate was less than 50% in IPD in the LAC region; similar data was reported in other regions (23).

Over the years, penicillin resistance increased until it reached its highest level in 2000–2004, followed by a decline that, despite some fluctuations, coincided with the introduction of PCVs in the different countries of the region between 2008 and 2015 (6, 24). The highest rates of resistance were observed in children under 5 years, followed by adults older than 65. Resistance rates between 40 and 50% were reported in the majority before the introduction of PCVs in these countries. In countries from the region, penicillin rates higher than 50% were reported mainly in studies that include only 19A isolates. Despite the introduction of PCVs, serotype 19A remains among the most frequently associated with antimicrobial resistance and multidrug resistance (25). In the pre-PCV period, the studies that reported resistance to penicillin found it mainly associated with serotype 14.

Analysis of serotypes associated with penicillin resistance revealed a prevalence of serotypes 14, 23F, 6B, and other PCV10 serotypes in all studies conducted before the introduction of PCVs, and was

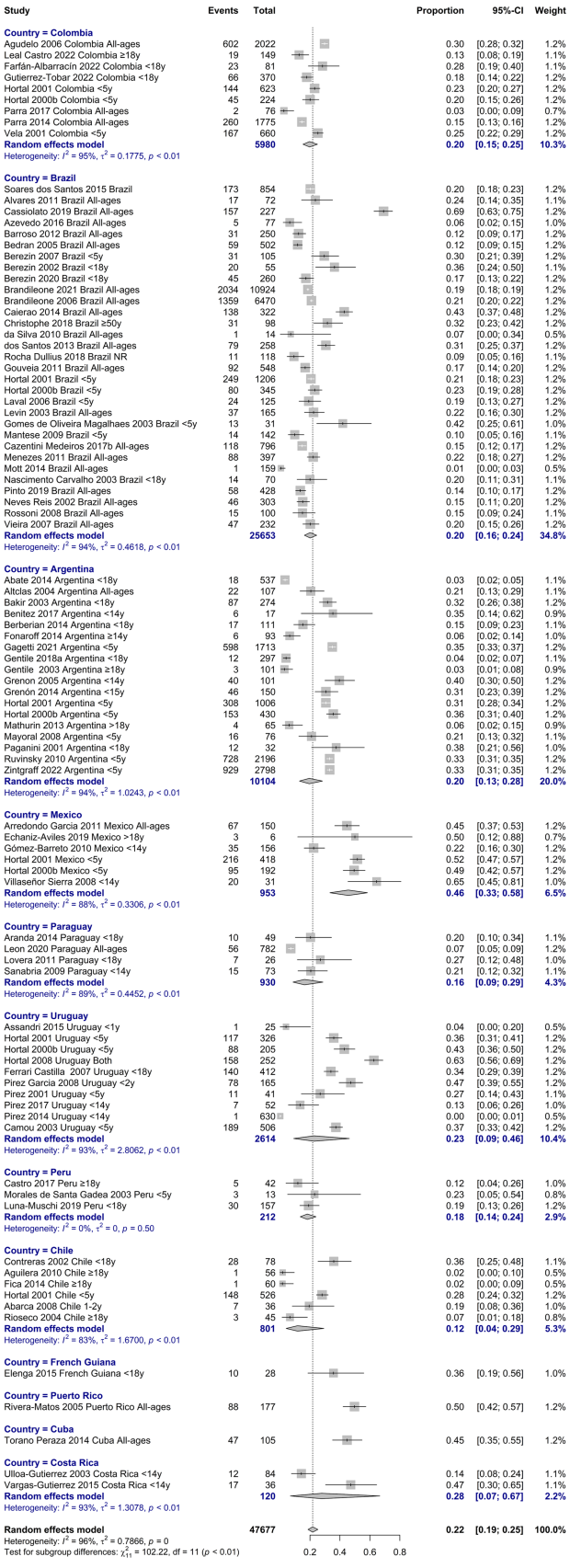

FIGURE 3
Proportion meta-analysis of resistance to penicillin by country.

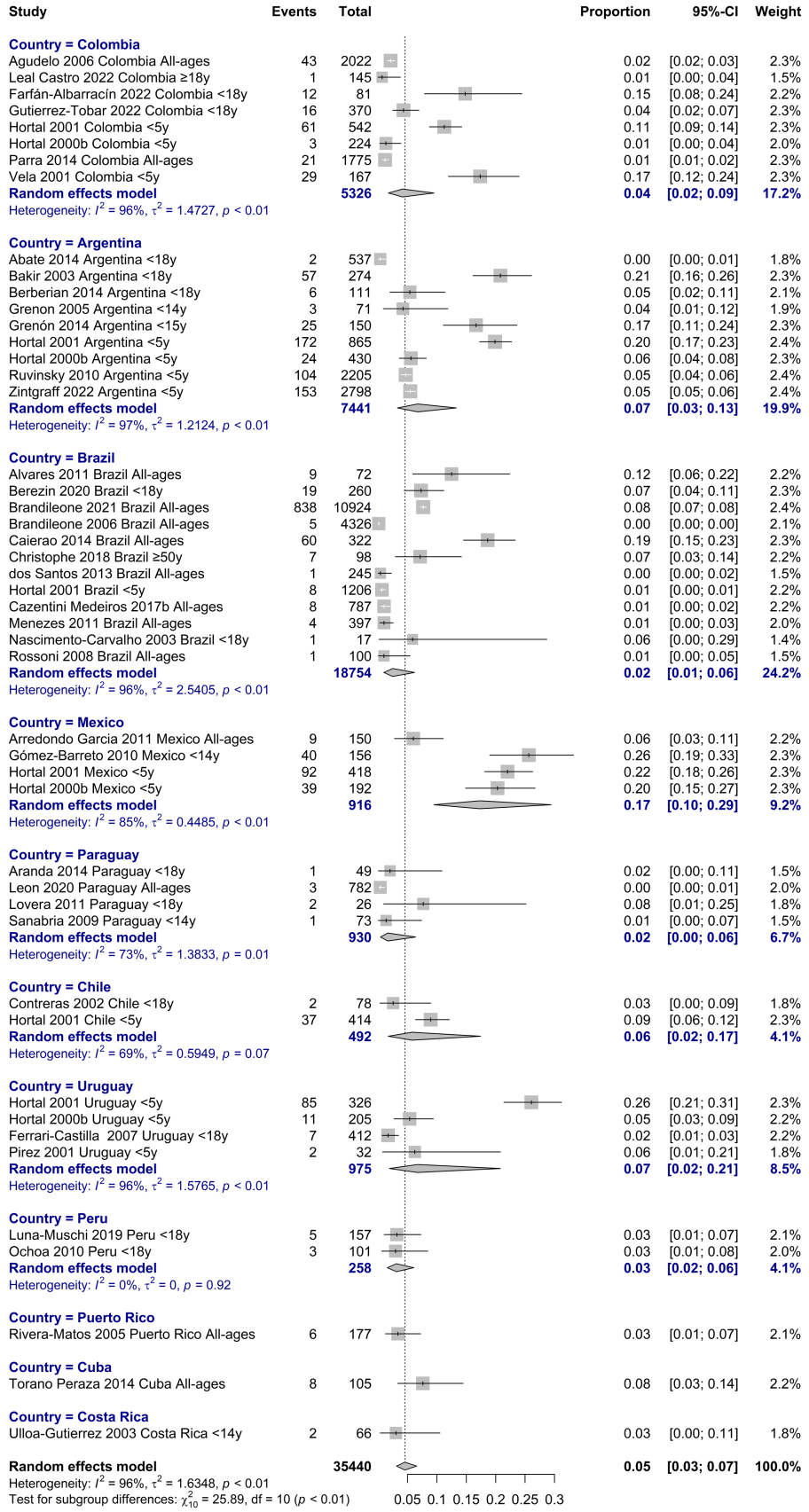

FIGURE 4
Proportion meta-analysis of resistance to ceftriaxone/cefotaxime by country.

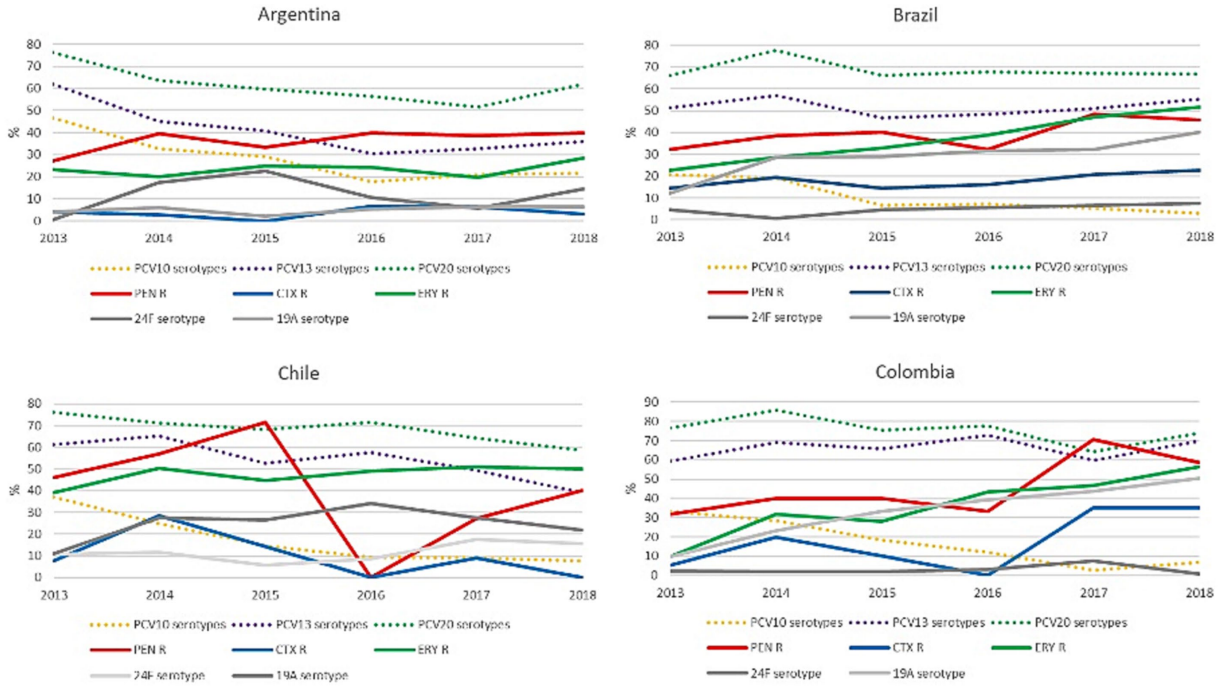

FIGURE 5
Variation over time of resistance to penicillin, ceftriaxone/cefotaxime and erythromycin, and the percentage of serotypes included in the different PCVs. Figure 4 shows the percentage of resistance to penicillin, ceftriaxone/cefotaxime and erythromycin, and the percentage of serotype 19A and 24F isolates between 2013 and 2018, as well as the percentage of serotypes included in PCV10, PCV13 and PCV20 (dotted lines). PEN: penicillin; CTX: ceftriaxone/cefotaxime; ERY: erythromycin; R: resistance. PCV10 was implemented in Brazil in March 2010 and in Chile in January 2011. PCV13 was implemented in Argentina in January 2012. In Colombia PCV13 was implemented in July 2011 and replaced by PCV10 in January 2012.

consistent with the global pattern and previous reports from LAC countries (26).

In a study conducted in Brazil, the emergence of non-PCV10 serotypes 19A and 6A penicillin-resistant isolates was observed in the post-PCV period (20). As a consequence the study describes an increase of antimicrobial non-susceptibility in a long-term post-PCV10 introduction.

A similar scenario was observed for ceftriaxone/cefotaxime-resistant strains, which were associated mainly with serotypes 14, 23F, and 19F in pre-vaccination studies and associated with serotype 19A and other new serotypes in post-vaccination studies.

Interestingly, outcomes from our study showed an increase in erythromycin resistance during the study period mainly related to serotype 19A and other non-vaccine serotypes. No changes in penicillin resistance, increased resistance to erythromycin, tetracycline, and multidrug resistance in the post-PCVs period were observed. In line with our results, the proportion of pneumococci showing resistance to first-line antimicrobials has decreased after vaccination. However, higher rates of resistance to other antimicrobials, mainly macrolides, have been observed in several countries, despite overall reductions in IPD attributable to vaccines, frequently associated with non-vaccine serotypes (27–29). Serotype 24F appears as an emergent serotype related to multidrug resistance and is characterized by its high invasiveness and probably influenced by antibiotic consumption (30).

One of the primary limitations of the study was the risk of bias of the included studies, which was mainly due to low sample sizes, selection bias, and information bias in the outcome measurement. Although, the risk assessment for cross-sectional and cohort studies showed that the majority were classified as moderate risk, and case series studies were mostly rated as low risk. Most of the studies included were case series and cross-sectional, which did not provide the best disease estimations. We try to exclude, as far as possible, those articles whose data seemed to be published in more than one article, but it is possible that some AMR data found have been reported by several studies. In Latin American and Caribbean countries (excluding pneumococcal meningitis), it is not mandatory to report to laboratory-based systems like SIREVA, and passive surveillance may not accurately reflect the prevalence of diseases.

According to this study, the treatment of choice for pneumonia remains penicillin or ampicillin and cefotaxime or ceftriaxone for meningitis and bacteremia.

The study provides data on AMR and associated serotypes throughout the LAC counties during pre- and post-vaccine periods, including the late post-vaccination period, which is very important to assess the changes produced by incorporating PCVs in the region. Our results highlight continuous surveillance's importance in assessing the dynamic of serotype distribution and antimicrobial resistance in pediatric and adult IPD from LAC.

5 Conclusion

The introduction of PCVs in LAC countries has led to changes in pneumococcal serotype distribution and antimicrobial resistance patterns in IPD. There was an overall decline in antibiotic resistance,

particularly to penicillin, after PCV implementation. However, concerning trends of increased erythromycin resistance and the emergence of non-vaccine serotypes associated with antibiotic resistance highlight the need for ongoing surveillance. Continuous monitoring of serotype evolution and antimicrobial resistance is essential to evaluate PCV impact and guide treatment recommendations for pneumococcal disease in Latin America and the Caribbean.

Data availability statement

The original contributions presented in the study are included in the article/Supplementary material, further inquiries can be directed to the corresponding author.

Author contributions

MS: Data curation, Investigation, Writing – original draft, Writing – review & editing. SR: Conceptualization, Formal analysis, Investigation, Methodology, Resources, Supervision, Writing – original draft, Writing – review & editing. MP: Data curation, Investigation, Writing – original draft, Writing – review & editing. TA: Data curation, Investigation, Writing – original draft, Writing – review & editing. MB: Data curation, Investigation, Writing – original draft, Writing – review & editing. EW: Investigation, Writing – review & editing. JC: Formal analysis, Investigation, Writing – review & editing. AB: Conceptualization, Funding acquisition, Investigation, Methodology, Project administration, Resources, Supervision, Writing – original draft, Writing – review & editing. AC: Conceptualization, Formal analysis, Funding acquisition, Investigation, Methodology, Project administration, Resources, Supervision, Writing – original draft, Writing – review & editing. PG: Formal analysis, Investigation, Methodology, Supervision, Writing – original draft, Writing – review & editing.

Funding

The author(s) declare financial support was received for the research, authorship, and/or publication of this article. This work was supported, in whole, by Pfizer Global Medical Grants (GMG), grant number: 76436251. The sponsor had no role in study design, data collection, data analysis, data interpretation, or report writing.

Acknowledgments

The authors would like to thank Daniel Comande, the librarian at the Institute for Clinical Effectiveness and Health Policy, for his contribution to the bibliographic searches.

Conflict of interest

The authors declare that the research was conducted in the absence of any commercial or financial relationships that could be construed as a potential conflict of interest.

Publisher's note

Supplementary material

The Supplementary material for this article can be found online at: https://www.frontiersin.org/articles/10.3389/fpubh.2024.1337276/full#supplementary-material

References

1. Wahl B, O'Brien KL, Greenbaum A, Majumder A, Liu L, Chu Y, et al. Burden of Streptococcus pneumoniae and *Haemophilus influenzae* type b disease in children in the era of conjugate vaccines: global, regional, and national estimates for 2000-15. *Lancet Glob Health*. (2018) 6:e744–57. doi: 10.1016/S2214-109X(18)30247-X

2. Malene BM, Oyvind H, Tor M, David NM, Jens O, Nanna VK, et al. Cost-effectiveness of 20-valent pneumococcal conjugate vaccine compared with 23-valent pneumococcal polysaccharide vaccine among adults in a Norwegian setting. *Cost Eff Resour Alloc*. (2023) 21:52. doi: 10.1186/s12962-023-00458-4

3. Drijkoningen JJC, Rohde GGU. Pneumococcal infection in adults: burden of disease. *Clin Microbiol Infect*. (2014) 20:45–51. doi: 10.1111/1469-0691.12461

4. Narváez PO, Gomez-Duque S, Alarcon JE, Ramirez-Valbuena PC, Serrano-Mayorga CC, Lozada-Arcinegas J, et al. Invasive pneumococcal disease burden in hospitalized adults in Bogota, Colombia. *BMC Infect Dis*. (2021) 21:1059. doi: 10.1186/s12879-021-06769-2

5. Golos M, Eliakim-Raz N, Stern A, Leibovici L, Paul M. Conjugated pneumococcal vaccine versus polysaccharide pneumococcal vaccine for prevention of pneumonia and invasive pneumococcal disease in immunocompetent and immunocompromised adults and children. *Cochrane Libr*. (2019) 2. doi: 10.1002/14651858.CD012306.pub2

6. de Oliveira LH, Camacho LAB, Coutinho ESF, Martinez-Silveira MS, Carvalho AF, Ruiz-Matus C, et al. Impact and effectiveness of 10 and 13-valent pneumococcal conjugate vaccines on hospitalization and mortality in children aged less than 5 years in Latin American countries: a systematic review. *PloS One*. (2016) 11:e0166736. doi: 10.1371/journal.pone.0166736

7. Grant LR, Slack MPE, Theilacker C, Vojicic J, Dion S, Reinert RR, et al. Distribution of serotypes causing invasive pneumococcal disease in children from high-income countries and the impact of pediatric pneumococcal vaccination. *Clin Infect Dis*. (2023) 76:e1062–70. doi: 10.1093/cid/ciac475

8. Reyburn R, Maher J, von Mollendorf C, Gwee A, Mulholland K, Russell F, et al. The impact of the introduction of ten- or thirteen-valent pneumococcal conjugate vaccines on antimicrobial-resistant pneumococcal disease and carriage: a systematic literature review. *J Glob Health*. (2023) 13:05001. doi: 10.7189/jogh.13.05001

9. Liñares J, Ardanuy C, Pallares R, Fenoll A. Changes in antimicrobial resistance, serotypes and genotypes in *Streptococcus pneumoniae* over a 30-year period. *Clin Microbiol Infect*. (2010) 16:402–10. doi: 10.1111/j.1469-0691.2010.03182.x

10. Higgins J, Welch V. Cochrane handbook for systematic reviews of interventions. Available from: http://www.training.cochrane.org/handbook

11. Stroup DF, Berlin JA, Morton SC, Olkin I, Williamson GD, Rennie D, et al. Meta-analysis of observational studies in epidemiology: a proposal for reporting. Meta-analysis of observational studies in epidemiology (MOOSE) group. *JAMA*. (2000) 283:2008–12. doi: 10.1001/jama.283.15.2008

12. Page MJ, McKenzie JE, Bossuyt PM, Boutron I, Hoffmann TC, Mulrow CD, et al. The PRISMA 2020 statement: an updated guideline for reporting systematic reviews. *BMJ*. (2021) 372:n71. doi: 10.1136/bmj.n71

13. Babineau J. Product review: Covidence (systematic review software). *J Can Health Libr Assoc*. (2014) 35:68–71. doi: 10.5596/c14-016

14. NHLBI, NIH. Study quality assessment tools. Available from: https://www.nhlbi.nih.gov/health-topics/study-quality-assessment-tools

15. Perilla MJ. *Manual for the laboratory identification and antimicrobial susceptibility testing of bacterial pathogens of public health importance in the developing world: Haemophilus influenzae, Neisseria meningitidis, Streptococcus pneumoniae, Neisseria gonorrhoea, Salmonella serotype Typhi, Shigella, and Vibrio cholerae*. Geneva: World Health Organization (2003).

16. Ripley BD. The R project in statistical computing. *MSOR Connections*. (2001) 1:23–5. doi: 10.11120/msor.2001.01010023

17. Balduzzi S, Rücker G, Schwarzer G. How to perform a meta-analysis with R: a practical tutorial. *Evid Based Ment Health*. (2019) 22:153–60. doi: 10.1136/ebmental-2019-300117

18. Freeman MF, Tukey JW. Transformations related to the angular and the square root. *AOMS*. (1950) 21:607–11.

19. DerSimonian R, Laird N. Meta-analysis in clinical trials. *Control Clin Trials*. (1986) 7:177–88. doi: 10.1016/0197-2456(86)90046-2

20. Brandileone MCC, Almeida SCG, Bokermann S, Minamisava R, Berezin EN, Harrison LH, et al. Dynamics of antimicrobial resistance of *Streptococcus pneumoniae* following PCV10 introduction in Brazil: Nationwide surveillance from 2007 to 2019. *Vaccine*. (2021) 39:3207–15. doi: 10.1016/j.vaccine.2021.02.063

21. Tunkel AR, Hartman BJ, Kaplan SL, Kaufman BA, Roos KL, Scheld WM, et al. Practice guidelines for the management of bacterial meningitis. *Clin Infect Dis*. (2004) 39:1267–84. doi: 10.1086/425368

22. Bradley JS, Byington CL, Shah SS, Alverson B, Carter ER, Harrison C, et al. The management of community-acquired pneumonia in infants and children older than 3 months of age: clinical practice guidelines by the Pediatric Infectious Diseases Society and the Infectious Diseases Society of America. *Clin Infect Dis*. (2011) 53:e25–76. doi: 10.1093/cid/cir531

23. Sader HS, Mendes RE, Le J, Denys G, Flamm RK, Jones RN. Antimicrobial susceptibility of *Streptococcus pneumoniae* from North America, Europe, Latin America, and the Asia-Pacific region: results from 20 years of the SENTRY antimicrobial surveillance program (1997-2016). *Open Forum Infect Dis*. (2019) 6:S14–23. doi: 10.1093/ofid/ofy263

24. Agudelo CI, Castañeda-Orjuela C, Brandileone MCC, Echániz-Aviles G, Almeida SCG, Carnalla-Barajas MN, et al. The direct effect of pneumococcal conjugate vaccines on invasive pneumococcal disease in children in the Latin American and Caribbean region (SIREVA 2006-17): a multicentre, retrospective observational study. *Lancet Infect Dis*. (2021) 21:405–17. doi: 10.1016/S1473-3099(20)30489-8

25. Desmet S, Theeten H, Laenen L, Cuypers L, Maes P, Bossuyt W, et al. Characterization of emerging serotype 19A pneumococcal strains in invasive disease and carriage, Belgium. *Emerg Infect Dis*. (2022) 28:1606–14. doi: 10.3201/eid2808.212440

26. Di Fabio JL, Castañeda E, Agudelo CI, De La Hoz F, Hortal M, Camou T, et al. Evolution of S treptococcus pneumoniae serotypes and penicillin susceptibility in Latin America, Sireva-Vigía group, 1993 to 1999. *Pediatr Infect Dis J*. (2001) 20:959–67. doi: 10.1097/00006454-200110000-00009

27. Kawaguchiya M, Urushibara N, Aung MS, Shinagawa M, Takahashi S, Kobayashi N. Serotype distribution, antimicrobial resistance and prevalence of pilus islets in pneumococci following the use of conjugate vaccines. *J Med Microbiol*. (2017) 66:643–50. doi: 10.1099/jmm.0.000479

28. Watkins ER, Kalizang'Oma A, Gori A, Gupta S, Heyderman RS. Factors affecting antimicrobial resistance in *Streptococcus pneumoniae* following vaccination introduction. *Trends Microbiol*. (2022) 30:1135–45. doi: 10.1016/j.tim.2022.06.001

29. Mohanty S, Feemster K, Yu KC, Watts JA, Gupta V. Trends in *Streptococcus pneumoniae* antimicrobial resistance in US children: a multicenter evaluation. *Open Forum Infect Dis*. (2023) 10. doi: 10.1093/ofid/ofad098

30. Lo SW, Mellor K, Cohen R, Alonso AR, Belman S, Kumar N, et al. Emergence of a multidrug-resistant and virulent *Streptococcus pneumoniae* lineage mediates serotype replacement after PCV13: an international whole-genome sequencing study. *Lancet Microbe*. (2022) 3:e735–43. doi: 10.1016/S2666-5247(22)00158-6

frontiers | Frontiers in Cellular and Infection Microbiology

TYPE Original Research
PUBLISHED 02 February 2024
DOI 10.3389/fcimb.2024.1328390

OPEN ACCESS

EDITED BY
Manuel Gerardo Ballesteros Monrreal,
University of Sonora, Mexico

REVIEWED BY
Yosainix Gaerste-Diaz,
Cuauhtémoc University, Mexico
Michal Bukowski,
Jagiellonian University, Poland

*CORRESPONDENCE
Heba M. Amin
htmagdy@msa.edu.eg

RECEIVED 26 October 2023
ACCEPTED 10 January 2024
PUBLISHED 02 February 2024

CITATION
Amer MA, Darwish MM, Soliman NS and Amin HM (2024) Resistome, mobilome, and virulome explored in clinical isolates derived from acne patients in Egypt: unveiling unique traits of an emerging coagulase-negative *Staphylococcus* pathogen.
Front. Cell. Infect. Microbiol. 14:1328390.
doi: 10.3389/fcimb.2024.1328390

Resistome, mobilome, and virulome explored in clinical isolates derived from acne patients in Egypt: unveiling unique traits of an emerging coagulase-negative *Staphylococcus* pathogen

Mai A. Amer[1], Manal M. Darwish[1,2], Noha S. Soliman[3] and Heba M. Amin[1*]

[1]Department of Microbiology and Immunology, Faculty of Pharmacy, October University for Modern Sciences and Arts, Giza, Egypt, [2]Medical Microbiology and Immunology Department, Faculty of Medicine, Ain Shams University, Cairo, Egypt, [3]Clinical and Chemical Pathology Department, Faculty of Medicine, Cairo University, Cairo, Egypt

Coagulase-negative staphylococci (CoNS) are a group of gram-positive staphylococcal species that naturally inhabit the healthy human skin and mucosa. The clinical impact of CoNS-associated infections has recently been regarded as a challenge for diagnosis and therapeutic options. CoNS-associated infections are primarily caused by bacterial resistance to antibiotics and biofilm formation. As antibiotics are still the most used treatment, this problem will likely persist in the future. The present study aimed to investigate the resistance and virulence of CoNS recovered from various acne lesions and explore their genetic basis. Skin swab samples were collected from participants with acne and healthy skin. All samples underwent conventional culture for the isolation of CoNS, MALDI-TOF confirmation, antibiotic susceptibility, and biofilm formation testing. A total of 85 CoNS isolates were recovered from the samples and preliminarily identified as *Staphylococcus epidermidis*. Isolates from the acne group (n = 60) showed the highest rates of resistance to penicillin (73%), cefoxitin (63%), clindamycin (53.3%), and erythromycin (48%), followed by levofloxacin (36.7%) and gentamycin (31.7%). The lowest rates of resistance were observed against tetracycline (28.3%), doxycycline (11.7%), and minocycline (8.3%). CoNS isolated from mild, moderate acne and healthy isolates did not show strong biofilm formation, whereas the isolates from the severe cases of the acne group showed strong biofilm formation (76.6%). Four extensively drug-resistant and strong biofilm-forming staphylococcal isolates recovered from patients with severe acne were selected for whole-genome sequencing (WGS), and their genomes were investigated using bioinformatics tools. Three of the sequenced genomes were identified as *S. epidermidis*; however, isolate 29AM was identified as *Staphylococcus warneri*, which is a newly emerging pathogen that is not commonly associated with acne and was not detected by MALDI-TOF. All the sequenced strains were multidrug-resistant and carried multiple resistance genes, including *blaZ*, *mecA*, *tet(K)*, *erm(C)*, *lnuA*, *vgaA*, *dfrC*, *fusB*, *fosBx1*, *norA*,

and *vanT*, which were found to be located on plasmids and chromosomes. Virulence features were detected in all genomes in the presence of genes involved in adherence and biofilm formation (*icaA*, *icaB*, *icaC*, *sdrG*, *sdrH*, *atl*, *ebh*, and *ebp*). Only the *S. warneri* isolate 29AM contained immune evasion genes (*capB*, *capC*, *acpXL*, and *manA*), an anti-phagocytosis gene (*cdsA*), and other unique features. As a result of their potential pathogenicity and antibiotic resistance, CoNS must be monitored as an emerging pathogen associated with acne infections. To the best of our knowledge, this is the first report to isolate, identify, and correlate *S. warneri* with severe acne infections among Egyptian patients using WGS and bioinformatic analysis.

KEYWORDS

CoNS, acne, antibiotic resistance, virulence, genome analysis, mobilizable genetic elements, *Staphylococcus epidermidis*, *Staphylococcus warneri*

1 Introduction

Staphylococcus species frequently colonize the skin of birds and mammals. *Staphylococcus* species are distinguished by their ability to coagulate blood into two main groups: coagulase-positive staphylococci, *Staphylococcus aureus*, and coagulase-negative staphylococci (CoNS), which include most species, such as *Staphylococcus epidermidis* (Otto, 2010). CoNS is a common skin microbiome organism and can inhibit the adhesion of virulent *S. aureus* and other pathogens (Christensen and Brüggemann, 2014). *S. epidermidis* is the most commonly isolated staphylococcal species from the human skin (Becker et al., 2014). It primarily colonizes the head, nose, and axilla. *Staphylococcus hominis* and *Staphylococcus capitis* are two additional common human skin colonizers. The latter is more commonly detected in the head and is more prevalent in adolescence. *Staphylococcus haemolyticus* and *Staphylococcus warneri* are less frequently observed in the human skin. Additionally, species that typically reside on farms or domestic animals, such as *Staphylococcus sciuri* or *Staphylococcus intermedius*, may transiently colonize humans (Otto, 2010). CoNS frequently exhibit multiple drug resistance, have few effective therapeutic choices, result in incurable diseases, and accumulate resistant strains in communities and hospitals. Antimicrobial resistance has various major causes, ranging from a lack of infection control to the inappropriate use of antibiotics. Recent investigations have shown that CoNS are highly resistant to erythromycin, vancomycin, oxacillin, methicillin, and penicillin (França, 2023). Scientists are paying attention to the emergence of multidrug-resistant (MDR) strains among CoNS and *S. warneri*, which is considered an emerging pathogen that can cause serious infections (Alawad et al., 2022).

S. epidermidis is commonly regarded as a commensal microorganism because it is beneficial to the skin in healthy environments (Cogen et al., 2008; Yang et al., 2022). Commensal *S. epidermidis* undergoes mutualistic and symbiotic interaction with the cutaneous system (Brüggemann, 2010). The skin hosts and supplements *S. epidermidis* with nutrients; in exchange, bacteria participate in host defense, innate immunity, and skin homeostasis. Through their microbial surface components, these bacteria interact with extracellular matrix proteins in the human skin (Arrecubieta et al., 2007; Brüggemann, 2010), which subsequently permits the interaction pathways between skin cells and bacteria (Yang et al., 2022). *S. epidermidis* can prevent biofilm formation of pathogenic strains via the secretion of bacteriocins (Paluch et al., 2020). Additionally, during the healing process of wounds or skin diseases, *S. epidermidis* lipoteichoic acid (LTA) can reduce skin inflammation (Fournière et al., 2020).

Although *S. epidermidis* plays a physiological role in maintaining skin homeostasis, it can be linked to some skin pathologies such as acne vulgaris, a prevalent chronic inflammatory skin condition affecting the pilosebaceous unit, where *S. epidermidis* was found to be overrepresented (Fitz-Gibbon et al., 2013; O'Neill and Gallo, 2018). Acne is primarily caused by three factors: (1) bacterial strains (Downing et al., 1986; Aydemir, 2014; Kutlu et al., 2023), *C. acnes* and *S. epidermidis* are both present, with *C. acnes* making up less than 2% of the skin surface bacteria and *S. epidermidis* being overrepresented (Fitz-Gibbon et al., 2013; O'Neill and Gallo, 2018); (2) qualitative and quantitative excessive seborrhea in sebaceous glands in acne lesions; and (3) keratinocytes with hyperkeratinization of the pilosebaceous unit, which causes the production of comedones, papules, and pustules (Jahns et al., 2012). The role of biofilms in acne development is an active area of research. Biofilms are complex communities of microorganisms that adhere to surfaces and produce a protective extracellular matrix. The formation of microbial communities, notably *Propionibacterium acnes* (*P. acnes*), as biofilms, contributes to the obstruction of follicles and the accumulation of sebum, dead skin cells, and bacteria. In this structured matrix, *P. acnes* exhibits increased resistance to antimicrobial agents and host immune responses, fostering

inflammation and contributing to the characteristic inflammatory lesions seen in acne. The resilience of biofilms poses challenges in treatment because their protective nature makes bacteria less susceptible to conventional therapies, potentially leading to treatment resistance and recurrent lesions. The chronic nature of acne, characterized by periods of exacerbation and remission, may be linked to the persistence of biofilms, emphasizing the need for research on disrupting biofilm formation as a potential target for innovative acne management strategies (Chen et al., 2017; Coenye et al., 2022).

Notably, some phylogenetic sequence types (STs) of *S. epidermidis* (e.g., ST2, ST5, ST23, and ST215) are associated with nosocomial infections, raising the possibility of their pathogenicity owing to their virulence and multidrug resistance properties (Månsson et al., 2015; Lee et al., 2018). Several virulence genes play an essential role in adhesion, biofilm development, and phenol-soluble modulation, in addition to the presence of mobile genetic elements (MGEs) that are involved in the acquisition and transmission of virulence and resistance features that enhance the pathogenicity of *S. epidermidis* (Bouchami et al., 2016; Rolo et al., 2017). One of the most important virulence factors of *S. epidermidis* is biofilm formation, which is mediated by intercellular adhesin (*ica*) and accumulation-associated protein (*aap*) genetic determinants (Arciola et al., 2015; Schaeffer et al., 2016). Biofilms are recognized as a common form of microbial growth that confer protection against the host immune system and antibiotic challenges (França, 2023). In CoNS biofilms, especially in *S. epidermidis*, the polysaccharide poly-N-acetylglucosamine (PNAG) is one of the most dominant metabolites, and up to 60% of the recovered clinical isolates produce the proteins encoded by the *icaADBC* genes (Ahmed et al., 2019). The first staphylococcal component with a key role in biofilm accumulation was identified as polysaccharide intercellular adhesin (PIA). However, not all strains of *S. epidermidis* strains possess the icaADBC operon and are formed by the protein products of this gene (Formosa-Dague et al., 2016; Schaeffer et al., 2016). Horizontal gene transfer (HGT) is one of the most significant methods for CoNS to acquire exogenous DNA and, as a result, antibiotic resistance genes in biofilms (Águila-Arcos et al., 2017). In recent years, attention has been focused on the arginine catabolic mobile element (ACME) system, a pathogenicity island hypothesized to promote host colonization and immune evasion (O'Connor et al., 2018). ACME likely descends from *S. epidermidis* and spreads horizontally to *S. aureus* (Onishi et al., 2013; Planet et al., 2013).

Considering emerging evidence for the pathogenicity of some specific strains of CoNS, assuming that not all staphylococcal isolates behave similarly, it has been challenging to identify clinically significant strains. To this end, we aimed to characterize CoNS isolated from healthy skin and acne lesions phenotypically by testing antimicrobial susceptibility and biofilm production, and genetically characterized CoNS isolated from severe acne infections using whole genome sequence (WGS) technology in order to understand the genetic basis of bacterial virulence, antibiotic resistance, and phylogenetic background.

2 Materials and methods

2.1 Sample collection

The present study was conducted with a total of 140 participants, divided into two groups: i) the acne group (n = 100) with various levels of severity, including mild (n = 25), moderate (n = 45), and severe acne (n = 30), and ii) the healthy group with healthy skin (n = 40). All participants were university students in Egypt aged 18–24 years. The patients recruited in this study were all non-diabetic, not previously treated with topical antibiotics, did not previously receive acne treatment, and had no history of underlying medical illnesses. For the female participants, skin samples were not collected during the menstrual period.

The participant clinician classified the degree of acne based on the clinical features into mild, moderate, and severe acne. The mild level was *Acne comedonica* (comedones and congestion), moderate level was papulopustular acne (mild papules and pustules), and severe form was pustule-nodular acne (severe pustules and nodules).

All participants provided written informed consent, and the study was approved by the research ethics committee of the pharmacy faculty of the October University for Modern Sciences and Arts (MSA) (approval number (M1/Ec1/2022PD).

2.2 Isolation of bacteria and preliminary identification of CoNS

Skin swabs of acne lesions were collected from the participants. For the growth of bacterial colonies, skin swabs were cultured in tryptic soy broth (TSB) (Oxoid, UK) at 37°C for 3 days (Huang et al., 2022). Purification was performed by serial subcultivation on 5% sheep blood agar (SBA) (Oxoid, UK) and mannitol salt agar (MSA) (Oxoid, UK) at 37°C for 24 h to obtain single colonies in pure culture. Isolates obtained from the blood and MSA were preliminarily identified as CoNS based on colony morphology and conventional biochemical reactions. Microscopic characteristics were studied using Gram staining. Catalase, DNase, slide coagulase activity, motility, and blood agar hemolysis tests were conducted according to the method by Freney et al. (1999). Isolate identity was subsequently confirmed using Matrix-Assisted Laser Desorption/Ionization Time-of-Flight Mass Spectrometry (MALDI-TOF MS) (Dubois et al., 2010).

2.3 Antibiotic susceptibility tests

The Kirby–Bauer disc diffusion method was used to screen CoNS isolates for antibiotic susceptibility. The adjusted bacterial culture, equivalent to 0.5 McFarland standard, was inoculated onto Muller Hinton agar (Lab M, UK) and incubated at 37°C for 24 h. Commercial antibiotic discs (Oxoid, England) were tested: penicillin (10 U), cefoxitin (30 µg), erythromycin (15 µg), vancomycin (30 µg), clindamycin (2 µg), tetracycline (30 µg), trimethoprim/sulfamethoxazole (1.25/23.75 µg), gentamicin (10 µg), levofloxacin (5 µg), tetracycline (30 µg), rifampin (5 µg), minocycline (30 µg), and

doxycycline (30 µg). The interpretative results matched the Clinical and Laboratory Standards Institute standards (CLSI) (CLSI, 2022).

2.4 Phenotypic characterization of biofilm production of CoNS isolates

The crystal violet assay was used to evaluate the ability of the staphylococcal isolates to form biofilms (Amer et al., 2021). Briefly, overnight cultures were adjusted to 10^5 CFU/ml and inoculated in 200 µl of TSB supplemented with 1% (v/v) glucose (LOBA Chemie, India), in 96-flat bottom polystyrene microtiter plate (Greiner Bio-one®, Germany). The microtiter plates were incubated at 37°C without shaking for 24 h. After incubation, microbial growth was determined by measuring the turbidity at 600 nm, after which the cells were removed, washed twice with sterile phosphate buffered saline (PBS), and left to air dry. The dried biofilms were then stained with 0.1% crystal violet (CV) (LOBA Chemie, India) for 15 min, excess stain was removed, the wells were washed with 200 µl sterile distilled water, excess water was removed, and the plates were dried. Finally, the stain was solubilized in 33% glacial acetic acid (LOBA Chemie, India). Colorimetric analysis of the biofilm biomass was performed at 545 nm. Biofilm formation was evaluated using the biofilm formation index, [BFI]: (AB – CW)/(GB – GW), where AB is the OD_{545} of the CV-stained microorganisms, CW is the OD_{545} nm of the stained blank wells containing only media, GB is the OD_{600} of the cell culture, and GW is the OD_{600} of the blank well. Isolates were classified into four groups: nonadherent (0.35), mild (0.35 to 0.69), moderate (0.70 to 1.09), and strong (>1.10) biofilm forming according to the specified semi-quantitative biofilm production classification described by Lucero-Mejía et al. (2020).

2.5 DNA extraction and detection of *icaA*, *icaD*, and *mecA* genes

Bacterial pellets of CoNS strains were pretreated with 180 µl lysis buffer formulated with 20 mM Tris–HCl, pH 8.0, 2 mM EDTA (ADWIC, Egypt), 1.2% Triton X-100, and lysozyme that was added immediately before use, at a final concentration of 20 mg/ml. After pretreatment, genomic DNA was extracted using the QIAamp® DNA Mini Kit (QIAGEN, Germany) according to the manufacturer's recommendations for gram-positive bacteria.

The presence of *icaA*, *icaD*, and *mecA* in the extracted DNA was detected by polymerase chain reaction using forward and reverse primers, as shown in Table 1. The amplification reaction was performed according to the method described by Petrelli et al. (2006), using a Biometra DNA thermal cycler (Hamburg, Germany). Amplicons were analyzed by electrophoresis on 1% agarose gels (Lonza, USA), stained with ethidium bromide dye (Sigma-Aldrich, USA), and visualized under a UV light transilluminator (LTF Labortechnik, Germany). Ruler Gene 100 bp A DNA ladder served as a DNA size indicator (Zhou et al., 2013).

2.6 Genomic characterization of *S. epidermidis* using whole genome sequencing

2.6.1 Library preparation and sequencing

Following DNA extraction using the QIAamp® DNA Mini Kit (QIAGEN, Germany), sequencing libraries were prepared using the Nextera XT DNA Library Preparation Kit (Illumina, USA) according to the manufacturer's instructions. Quality control was performed using an Agilent DNA 1000 chip, prior to shotgun sequencing using MiSeq (Illumina, USA). Preassembly processing of the generated reads was performed using FastQC. Trimmomatic v0.32 was used to remove low-quality (mean quality less than 25) or low-complexity reads, reads mapping to the human genome or large and small ribosomal units of bacteria, fungi, and humans, and known contaminants (e.g., phiX174, Illumina spike-in) (Bolger et al., 2014). All genomes are available in the NCBI genome (BioProject accession number PRJNA993660).

2.6.2 Genome assembly and annotation

Pre-processed reads were assembled *de novo* using SPAdes version 3.6.1, with contigs shorter than 1,000 nucleotides discarded (Bankevich et al., 2012). The analysis was only selected for reconstructed genomes with an N50 >50,000. The assembled contiguous sequences were submitted via the National Center for Biotechnology Information (NCBI) Prokaryotic Genome Annotation Pipeline to GenBank for gene annotation. The generated contigs were further analyzed to investigate the genetic elements of interest. After that, the most similar sequences were identified and a phylogenetic tree was constructed using the

TABLE 1 List of primers used in PCR.

Primers	Sequence (5′-3′)	Target Gene	Tm (°C)	Length	References
icaA_F	TCT CTT GCA GGA GCA ATC AA	*icaA*	56.4	188	Zhou et al. (2013)
icaA_R	TCA GGC ACT AAC ATC CAG CA		58.4		
icaD_F	ATG GTC AAG CCC AGA CAG AG	*icaD*	60.5	198	Zhou et al. (2013)
icaD_R	CGT GTT TTC AAC ATT TAA TGC AA		55.5		
mecA_F	AAA ATC GAT GGT AAA GGT TG GC	*mecA*	58.4	244	Zhou et al. (2013)
mecA_R	AGT TCT GCA GTA CCG GAT TT GC		62.1		

Bacterial and Viral Bioinformatics Resource Center (BV-BRC) (https://www.bv-brc.org/) (Olson et al., 2023).

2.6.3 Pathogenicity, resistome, and virulome analysis

PathogenFinder was used to predict the pathogenicity of the isolates for human hosts (https://cge.cbs.dtu.dk/services/PathogenFinder/). The assembled genomes obtained from the WGS data were annotated to identify the predicted resistome using ResFinder 4.1 (with a minimum length and threshold of 60% and 90%, respectively) (https://cge.cbs.dtu.dk/services/ResFinder/), and the Comprehensive Antibiotic Resistance Database (CARD) available at (https://card.mcmaster.ca/analyze/rgi) (Alcock et al., 2020), using the default selection criteria "perfect and strict hits only." These platforms were employed in combination to avoid the drawbacks of each platform.

The genetic basis (chromosomal single-nucleotide polymorphism [SNP]) for fluoroquinolone and rifampicin resistance genes from the assembled genomes was studied (Altschul et al., 1990). Alignment of *gyrA*, *gyrB*, *parC*, *parE*, and *rpoB* genes to the reference strains of *S. epidermidis* (ATCC®12228 and ATCC®35984) with their corresponding genes from the assembled isolates in this study. Mutations were analyzed using multiple sequence alignment (MSA) and SNP analysis tool provided by the BV-BRC (https://www.bv-brc.org/). Clustal Omega (1.2.4) provided by EMBL's European Bioinformatics Institute (EMBL-EBI) (https://www.ebi.ac.uk/Tools/msa/clustalo/) was used to perform MSA alignments of the predicted amino acid sequences. Colored alignments were visualized using the multiple alignment viewer tool MView 1.63, available at (https://www.ebi.ac.uk/Tools/msa/mview/) and hosted by EMBL-EBI.

VirulenceFinder 2.0 (using a minimum length of 60% and a threshold of 90%) (https://cge.cbs.dtu.dk/services/VirulenceFinder/) (Joensen et al., 2014), virulence factor database (VFDB) (http://www.mgc.ac.cn/cgi-bin/VFs/v5/main.cgi?func=VFanalyzer) and BacWGSTdb (http://bacdb.cn/BacWGSTdb) were used for screening the presence of virulence genes. The virulence determinants related to *S. epidermidis* were examined including adhesion, enzymes, biofilm formation, secretion, immune evasion, toxins, anti-phagocytosis, and intracellular survival.

2.6.4 *In silico* multilocus sequence typing

Multilocus sequence typing (MLST) was performed *in silico* using MLST 2.0, which is available on the website of the Center for Genomic Epidemiology (https://cge.cbs.dtu.dk/services/MLST/) (Larsen et al., 2012) and the public molecular typing database PubMLST (https://pubmlst.org/).

Sequence types were assigned comparing the internal fragments of the seven housekeeping genes (*arcC*, *aroE*, *gtr*, *mutS*, *pyrR*, *tpiA*, and *yqiL*) from *S. epidermidis* to determine the MLST sequence types (STs) (Thomas et al., 2007).

2.6.5 Identification of mobile genetic elements

Mobile genetic elements (MGEs) related to ARGs and their genomic context were investigated using NCBI annotations. The web-based typing tool SCC*mec*Finder was used to determine the SCC*mec* types and their structural position in the *S. epidermidis* isolates *in silico* (https://cge.cbs.dtu.dk/services/SCCmecFinder/). Plasmid replicon types were detected *in silico* using PlasmidFinder 2.1, available at (https://cge.cbs.dtu.dk/services/PlasmidFinder/) (Carattoli et al., 2014).

Prophage sequences within the assembled genomes were detected and annotated using PHASTER tool (https://phaster.ca/) (Arndt et al., 2016). Only "intact" prophage regions discovered by PHASTER were considered. The sites of the prophage regions were BLASTED against CARD to determine whether they included resistance genes. MobileElementFinder v1.0.3 was used to identify ISs and transposons flanking the resistance genes (Johansson et al., 2021), available at https://cge.cbs.dtu.dk/services/MGE/. NCBI annotations were used to investigate the support environment for resistance genes. Insightful Science's SnapGene viewer software v5.1.3.1, was used to examine the context of resistance genes by visualizing annotated contigs software (http://www.snapgene.com). Insertion sequences (ISs) were identified using BLAST analysis against the NCBI nucleotide database. Resistance islands were predicted using the IslandViewer4 web tool (http://www.pathogenomics.sfu.ca/islandviewer/) (Li and Durbin, 2010).

2.6.6 Clustered regularly interspaced short palindromic repeats/CRISPR-associated system, arginine catabolic mobile element, and restriction–modification system

CRISPRCasFinder tool available at (https://crisprcas.i2bc.paris-saclay.fr/CrisprCasFinder/Index) utilizes the default advanced parameters for CRISPR and the clustering model "SubTyping" for Cas to search the genomes for clustered regularly interspaced short palindromic repeats (CRISPR) and cas genes.

The restriction–modification system (R–M system) was detected using a minimum length of 60% and %ID threshold of 95% using Restriction–ModificationFinder 1.1, available at (https://cge.cbs.dtu.dk/services/Restriction-ModificationFinder/) (Camacho et al., 2009). ACME genes were identified and mapped within the genomes. The arc, opp3, and kdp operons were used to align the ACME components, which were then classified as arc and opp3 operons (type I), arc operons alone (type II), opp3 operons alone (type III), arc and kdp operons (type IV), and arc, opp, and kdp operons (type V).

2.6.7 Phylogenetic analyses using WGS-SNP and WGS-MLST trees

CSIPhylogeny (https://cge.cbs.dtu.dk/services/CSIPhylogeny/) was used to construct phylogenetic trees based on the maximum likelihood method of concatenated alignment of high-quality SNPs, which uses assembled contigs to perform SNP calling, SNP filtering, and phylogeny inference (Kaas et al., 2014). The analysis was performed on a platform using default parameters. The assembled genomes have been uploaded for comparison. To compare our isolates to *S. epidermidis* and *S. warneri* genomes available on the BV-BRC website, we searched and downloaded the *S. epidermidis*

and *S. warneri* genomes and included them in the analysis. Figtree program was used to edit and visualize the phylogenetic tree (http://tree.bio.ed.ac.uk/software/figtree/).

The core genome single nucleotide polymorphism (cgSNP)-based phylogenetic tree was visualized using the interactive tree of life (iTOL) web tool v6.7 (https://itol.embl.de/itol.cgi) associated with the isolates, and other genomic information, and antibiotic resistance determinants. A phylogenetic tree was also constructed using the isolates and closely related genomes derived from BV-BRC (https://www.bv-brc.org/).

2.6.8 Accession numbers

The assembled draft genomes from the Whole Genome Shotgun project were uploaded to the GenBank database under BioProject number PRJNA993660.

2.7 Statistical analysis

GraphPad Prism 8.0.0 for Windows (GraphPad Software Inc., CA, USA) was used for the statistical analysis. The independent samples t-test and two-way analysis of variance (ANOVA) were used to compare the antibiotic resistance determinants, biofilm-forming ability, and prevalence of biofilm-associated genes among CoNS isolates, with a *P*-value of 0.05 regarded as statistically significant.

3 Results

3.1 Clinical data and bacterial isolates

A total of 140 participants were enrolled in this study and divided into two groups: i) the acne group (n = 100) with various levels of severity, including mild (n = 25), moderate (n = 45), and severe acne (n = 30), and ii) the healthy group with healthy skin (n = 40). Sex distribution was represented in the form of 60 (60%) males and 40 (40%) females in the acne group, and 25 (62.5%) males and 15 (37.5%) females in the healthy group.

The culture of skin swabs yielded a total of 85 staphyloccal isolates that were preliminarily identified based on conventional biochemical reactions, all of which were gram-positive arranged in grape-like clusters, catalase-positive, DNase-negative, coagulase-negative, non-motile, and non-hemolytic on blood agar. All isolates were identified as *S. epidermidis* by MALDI-TOF MS. Sixty isolates were obtained from the acne group (60%), and 25 isolates (62.5%) were obtained from the healthy group.

3.2 Antibiotic susceptibility testing

The results of antimicrobial susceptibility testing of CoNS isolates from the acne and healthy groups are displayed in Supplementary Table 1, where isolates from the acne group (N = 60) showed the highest rates of resistance to penicillin (73%), cefoxitin (63%), clindamycin (53.3%), and erythromycin (48%), followed by levofloxacin (36.7%) and gentamycin (31.7%), while least rates of resistance were observed for tetracycline (28.3%), doxycycline (11.7%), and minocycline (8.3%). The antimicrobials with the highest rates of resistance among the healthy group isolates were clindamycin (56%), erythromycin (44%), penicillin (40%), and cefoxitin (40%), followed by levofloxacin (32%) and tetracycline (32%), whereas those with the lowest rates of resistance were gentamycin (20%), doxycycline (8%), and minocycline (0%). Comparing the resistance prevalence between the two groups of isolates showed a statistically significant difference (*P*-value <0.05) for penicillin and cefoxitin, however, no significant difference was observed for the other antimicrobials (Supplementary Table 1) (Figure 1). Out of the acne group, 15 isolates (25%) demonstrated multidrug resistance (MDR) to antibiotics, four of which were extensively drug resistant (XDR), whereas in the control group, two isolates exhibited resistance to multiple drugs (8%), and none were XDR. Statistical analysis revealed a significant difference between the two groups (*P*-value <0.05).

3.3 Phenotypic characteristics of biofilm production of CoNS isolates

Biofilm formation ability of CoNS isolates was tested using crystal violet biofilm assay method. Forty-four isolates recovered from the acne group (73.3%) and 11 isolates recovered from the healthy group (44%) were able to form biofilm. Biofilm-producers demonstrated strong, moderate, and weak biofilm production at rates of 38.3%, 28.3%, and 6.6% among CoNS isolates of the acne group (n=60), while rates of 0%, 8%, and 36% among CoNS isolates of healthy group (n=25), respectively (Supplementary Table 2). The utilization of an unpaired t-test in statistical analysis indicated a significant contrast between the acne and healthy groups. Notably, only isolates retrieved from the severe acne group exhibited the ability to form strong biofilms (76.6%). All MDR isolates recovered from the acne group formed strong biofilms. (Supplementary Table 2) (Figure 2).

3.4 Molecularly detected *icaA*, *icaD*, and *mecA* genes

Biofilm-associated gene carriage was assessed in the isolates recovered from acne and healthy samples. The distribution of the biofilm-associated genes is shown (Figure 3). Two-way ANOVA in statistical analysis revealed a significant difference in the prevalence of biofilm-associated genes among CoNS isolates obtained from individuals with moderate and severe acne compared to those from mild acne and healthy individuals (*P*-value <0.05). Four XDR and strong biofilm-forming CoNS isolates were coded as 29AM, 36AM, 48AF, and 54AF were selected for further study using WGS. The antibiotic resistance characteristics of the four isolates are presented in Table 2.

The CLSI breakpoints for CoNS were used to interpret antibiotic susceptibility tests. R, resistant; I, intermediate; S, susceptible; M, male; F, female. FOX, cefoxitin; PEN, penicillin;

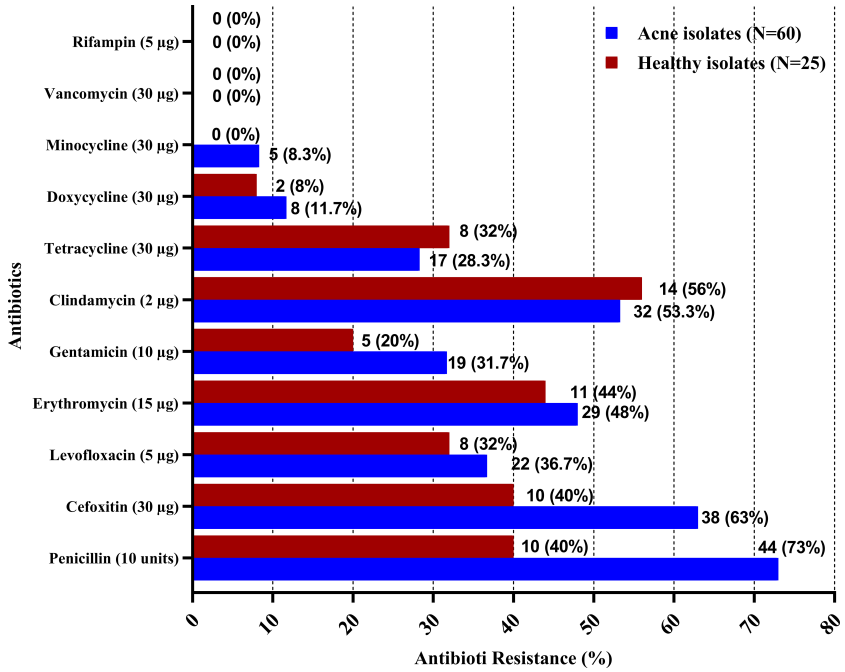

FIGURE 1
Antibiotic resistance among CoNS isolates from acne and healthy groups. Antibiotic susceptibility testing was performed for CoNS isolates using the Kirby–Bauer disk diffusion method, in accordance with the Clinical and Laboratory Standards Institute (CLSI).

LEV, levofloxacin; ERY, erythromycin; CHL, chloramphenicol; TET, tetracycline; DOX, doxycycline; MIN minocycline; CLI, clindamycin; RIF, rifampin; SXT, sulfamethoxazole/trimethoprim; VAN, vancomycin.

3.5 Genomic characterization of the selected CoNS isolates using WGS

3.5.1 Genome and assembly features, as well as resistome characterization

Based on the short-read sequences, draft genomes comprising 65–294 contigs were assembled with a mean N50 of 80,333 bp, covering approximately 81%–86% of the reference genome. Supplementary Table 3 displays the genome sequences and assembly parameters, such as size, number of contigs, number of RNAs, guanine–cytosine (GC) content (%), number of coding sequences, N50, and L50.

The isolates' draft genome size ranged from 2.3 Mb to 2.6 Mb, with a GC content of 31.88% to 32.44%. Three isolates coded as 36AM, 48AF, and 54AF were confirmed to be *S. epidermidis* using WGS, while the isolate coded as 29AM was identified as *S. warneri*, another multidrug-resistant CoNS.

Antibiotic resistance genes (ARGs) conferring resistance to β-lactams (*blaZ*), methicillin/oxacillin (*mecA*), glycopeptides (*vanT*, *vanY*), fluoroquinolone [*norA*, *norC*, *sdrM*], tetracyclines [*tet(K)*], macrolide–lincosamide–streptogramin B antibiotic (MLSB) [*erm(C)*, *vgaA*, and *InuA*], trimethoprim-sulfamethoxazole (*dfrC*), aminocoumarin (*gyrB*), fosfomycin (*fosBx1*), and fusidic acid (*fusB*) were detected in the isolated genomes (Table 3). All staphylococcal isolates except isolate 54AF possessed the *blaZ* gene, while all isolates except *S. warneri* 29AM possessed the *mecA* gene. ARGs related to trimethoprim-sulfamethoxazole-, tetracycline-, doxycycline-, and erythromycin-resistance followed resistance phenotypes. Isolates phenotypically resistant to these antibiotics and their corresponding ARGs were detected in the genomic context.

The four isolates showed agreement between the cefoxitin-resistant phenotype and either *mecA* or *blaZ* gene. The tetracycline-resistance gene *tet(K)* was only found in isolate 29AM, although all the tested isolates were phenotypically resistant to tetracycline.

Aminoglycoside resistance mechanisms were absent in all isolates, and none of the isolates were phenotypically resistant to gentamicin or amikacin. Furthermore, the MLSB resistance mechanism *erm (C)* was only detected in isolate 29AM, *vga (A)* was detected in all isolates except 54AF, *lnu (A)* was also detected in 36AM and 54AF isolates, and *dfrC* was detected in all isolates except 36AM. Antibiotic efflux pump genes (*norA*, *norC*, *sdrM*, *mdeA*, and *qacC*) were detected, which can also provide fluoroquinolone and macrolide resistance.

Mutations in *gyrA*, *gyrB*, *parC*, *pare*, and *rpoB* in *S. epidermidis* isolates compared to *S. epidermidis* ATCC®12228 were manually curated (Table 4). MSA of the predicted amino acid sequences of the genes carried by *S. epidermidis* isolates and close genomes retrieved from the BV-BRC database (Supplementary Table 5) compared to that of *S. epidermidis* strain ATCC®12228 was performed and visualized using M.View (Supplementary Figures 1–5). Moreover, MSA of *S. warneri* 29AM with the closely related *S. warneri* strains retrieved from the BV-BRC database (Supplementary Table 6) was also performed (Supplementary Figures 6–10), and there was no standard strain of *S. warneri*, so the gene mutation could not be detected. The

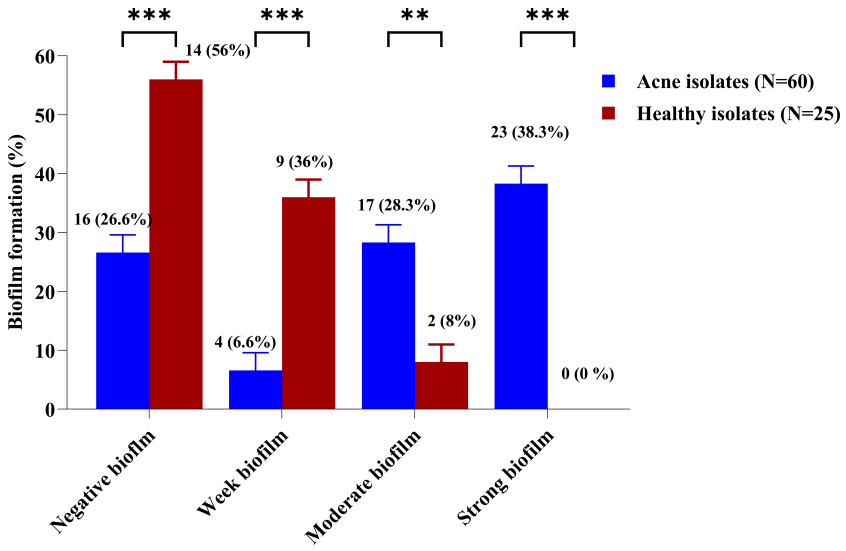

FIGURE 2
Biofilm formation percentage among CoNS isolates from the acne and healthy groups. The biofilm-forming ability of the CoNS isolates was assessed using a crystal violet assay. Adjusted overnight cultures were inoculated in 200 µl of TSB supplemented with 1% (v/v) glucose, in a 96-flat bottom polystyrene microtiter plate. The biofilms were then washed and stained with 0.1% crystal violet. The biofilm biomass was measured colorimetrically at 545 nm and evaluated using the biofilm formation index. Statistical analysis using two-way ANOVA, which was followed by multiple comparisons test with a significance level at ** $p < 0.01$; *** $p < 0.001$.

genome of isolate 36AM possessed eight mutations in *gyrA*, two mutations in *gyrB*, seven mutations in *parC*, and two mutations in *pare*, but no mutations were detected in *rpoB*. The gemome of isolate 48AF did not harbor any mutations. Isolate 54AF contained eight mutations in *gyrA*, one in *gyrB*, seven in *parC*, four in *parE*, and one in *rpoB*.

3.5.2 Detected pathogenicity and virulome in the *Staphylococcus* genomes

PathogenFinder estimated that the mean chance of isolates being pathogenic to humans ranged from 0.909 to 0.955 and matched numerous pathogenic families. Virulome analysis showed probable virulence genes encoding proteins from

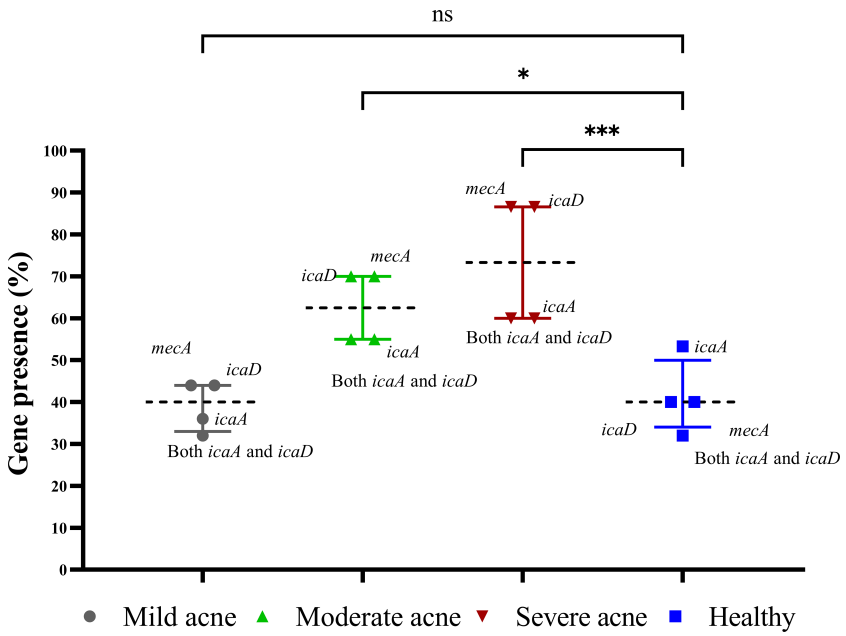

FIGURE 3
Prevalence of biofilm genes among CoNS isolates. The presence of *icaA*, *icaD*, and *mecA* in the extracted DNA was detected by polymerase chain reaction. The presence of the gene was represented as a percentage of the different acne and healthy groups, and the results are shown as medians with interquartile ranges. Statistical analysis using two-way ANOVA, which was followed by multiple comparisons test with a significance level at * $p < 0.05$; *** $p < 0.001$. ns, non-significant.

TABLE 2 The antibiotic susceptibility profile and accompanying metadata for the four staphylococcal isolates.

Isolate	Sex	Source Sample	Biofilm formation	FOX	PEN	LEV	ERY	CHL	TET	DOX	MIN	CLI	RIF	SXT	VAN
36AM	M	Acne	Strong	R	R	R	R	R	R	R	R	R	S	R	S
29AM	M	Acne	Strong	R	R	R	R	R	R	R	R	I	S	R	S
48AF	F	Acne	Strong	R	R	R	R	R	R	R	R	R	S	R	S
54AF	F	Acne	Strong	R	R	R	R	R	R	R	R	R	S	R	S

numerous *S. epidermidis* virulence categories, including adherence/biofilm production, enzymes, immune evasion, invasion, toxin, anti-phagocytosis, intracellular survival, and stress adaptability (Figure 4). Interestingly, the *S. warneri* isolate 29AM exclusively exhibited a higher number of virulence genes associated with acid resistance (*ureB*, *ureG*), anaerobic respiration (*narH*), antiphagocytosis (*cspA*), immune evasion (*capB*, *capC*, *acpXL*, *manA*), intracellular survival (*lplA1*), invasion (*lpeA*), iron uptake (*fagC*, *hemL*, *vctC*), lipid and fatty acid metabolism (*panD*), phagosome arresting (*ndK*), regulation (*lisR*, *sigA/rpoV*), stress adaptation (*katA*), and surface protein anchoring (*lgt*).

3.5.3 WGS-based multilocus-sequence typing

In silico MLST analyses identified three different MLST types: sequence type (ST) isolate 36AM: ST39, isolate 48AF: ST87, and isolate 54AF: ST719. Isolate 29AM was not identified by MLST. The most resistant isolate belonged to ST87 and contained 16 ARGs encoding for resistance to multiple antibiotic drug classes (Table 3).

3.5.4 Mobilome and the genetic support environment

In silico SCC*mec* typing/subtyping revealed three SCC*mec* types/subtypes, isolate 36AM belongs to SCC*mec* type V(5C2), isolate 48AF belongs to SCC*mec* type II (A2), and isolate 54AF belongs to SCC*mec* type V(2B),

PlasmidFinder and BacWGSTdb plasmid analysis showed ten distinct plasmid replicon types. Rep13 (3), rep7a (4), rep5a (3), and rep20 (3) were the most common types of plasmid replicons. Replicon types repUS35, rep10, rep5d, rep10b, rep21, repUS9 were only found in *S. warneri* 29AM.

ISs were detected in all tested isolates, except for isolate 48HF. Three distinct IS types from three distinct IS families were identified. IS families were IS256, 1S110, and IS200/IS605. IS256, family is well known to be associated with biofilm formation and virulence. IS256 family was found in *S. warneri* 29AM only. Furthermore, the resistance gene *erm(C)* was discovered exclusively in conjunction with transposon Tn554 in one isolate (29AM). The NCBI annotation of

TABLE 3 Genotypic characteristics of *Staphylococcus* isolates.

Isolates	Resistance genes (plasmid/chromoso-mal- mediated)	Plasmid replicon type	R–M system	*SCC*mec* type	ACME type	MLST	Insertion sequences	CRISPR-Cas elements	Pathogenicity score (no. of pathogenic families)
29AM	*blaZ*, *erm(C)*, *fusB*, *vanT vanY*, *vanW*, *dfrC*, *tet(k)*, *vgaA*, *sdrM*, *FosBx1*, *mdeA*, *sepA*, *gyrB*	rep13, rep7a, repUS35, rep10, rep5b, rep5d, rep10b, rep20, rep21, repUS9	–	–	–	Unknown[#]	IS256, ISSEP2	4 (2)	0.909 (31)
36AM	*mecA*, *blaZ*, *norA*, *norC*, *vanT vanY*, *dfrC*, *rpoC*,	rep13, rep5b, rep20, rep21, rep7a	–	SCC*mec* type V (5C2)	–	ST39	ISSep3, ISSep2	5 (3)	0.955 (86)
	sdrM, *FosBx1*, *mdeA*, *qacJ*, *lnuA*, *gyrB*, *sav1866*, *vgaA*								
48AF	*mecA*, *blaZ*, *norA*, *fusB*, *norC*, *sepA*, *sdrM*, *vanT*, *dfrC*, *mdeA*, *qacJ*, *gyrB* *blaZ*, *fosB*, *fusB*, *vga (A)*, *qacC*	rep13, rep7a, rep5b	–	SCC*mec* type II (A2)	–	ST87	–	5 (1)	0.945 (488)
54AF	*mecA*, *sepA*, *sdrM norA*, *norC*, *dfrC*, *vanT FosBx1*, *vanY*, *InuA*, *fosB*	rep7a, rep20	–	SCC*mec* type V (2B)	Present IVa	ST719	ISSep3, ISSep2	5 (3)	0.946 (150)

ACME, arginine catabolic mobile element; R–M system, restriction-modification system. ACME types I and II (arc and opp3 operons), III (opp3 operons only), IV (arc and kdp operons), and V (arc, opp, and kdp operons). Pathogenicity score: PathogenFinder predicts a bacteria's pathogenicity to human hosts. Closet pathogenic family strain linkage: MLST, multilocus sequence typing; CRISPR-Cas, clustered regularly interspaced short palindromic repeats/CRISPR-associated; S. epidermidis ATCC®12228. The SCCmecFinder was used to predict SCCmec type.
The table represents the resistome and mobilome determinants detected by the bioinformatics analysis to the sequenced genomes.
*SCCmec typing was determined with the SCCmecFinder.
[#]Unknown indicates that a sequence type could not be determined for the isolate due to the absence of alleles in the draft genomes.

10.3389/fcimb.2024.1328390

TABLE 4 *S. epidermidis* isolates mutations in *gyrA*, *gyrB*, *parC*, *parE*, and *rpoB* genes.

Isolate	*gyrA*	*gyrB*	*parC*	*parE*	*rpoB*
36AM	T700N, N811K, A820V, S826T,T828N, T829A, T831K, M854T	V7OI, V221I,	K236R, K272R, K639N, E641K, S650T, I761V, N772K	N404S, K568N	–
48HF	–	–	–	–	–
54HM	N811K, A820V, S826T,T828N, T829A, T831K, M854T, E862K	V7OI	K236R, K272R, K639N, E641K, S650T, I761V, N772K	L373I*, N404S, K568N, I575T	Y737S

*Putatively novel mutations.

isolates 29AM, 36AM, and 48AF identified the presence of the *blaZ* gene flanked by the regulatory genes *blaR1* and *blaI*; however, this configuration was absent in isolate 54AF. The genetic context of the specific resistance genes investigated in this study was analyzed with a focus on illustrating the interplay between Mobile Genetic Elements (MGEs), ARGs, and virulence genes (Table 5).

The PHASTER tool discovered intact prophages incorporated into the genomes of isolates 29AM and 54AF; no phages were detected in isolates 36AM and 48AF. The most common prophage was PHAGE_Staphy_StB12 (n = 4). No resistance genes were found in any of the prophages. The characteristics of the prophages, such as GC content and the number of coding sequences, are shown in Supplementary Table 4.

3.6 Identification and classification of clustered regularly interspaced short palindromic

Repeats/CRISPR-Associated Elements, Arginine Catabolic Mobile Element (ACME), and Restriction–Modification (RM) systems. CRISPRCasFinder detects CRISPR sequences. Each isolate contained at least one CRISPR sequence. CRISPR-associated (Cas) genes were found in all isolates. None of the isolates contained an R–M system. ACME was identified in *S. epidermidis* isolates 48AF and 54AF and was classified as type IV (Table 3).

3.7 Phylogenetic relatedness of the study isolates with their closely related *Staphylococcus* strains in genomic database

The phylogenetic relationships between the study isolates and their closely related genomes were determined for *S. epidermidis* isolates 36AM, 48AF, and 54AF core genomes and for *S. warneri* 29AM and were compared to the similar genomes detected by the BV-BRC database (Supplementary Tables 5, 6). A phylogenetic tree illustrating their genomic relatedness is shown in (Figures 5, 6). An SNP-based phylogenetic tree was generated using the tested genomes and *S. epidermidis* ATCC®12228, *S. epidermidis* ATCC®35984, *S. epidermidis* strain 785SEPI, and *S. warneri* strain SG1 (Figure 7).

4 Discussion

Acne is a common inflammatory skin disorder that affects the sebaceous glands. Although acne develops through the interaction of several factors, the exact cause of acne remains unknown. The interaction between skin bacteria and host immunity is increasingly thought to play an essential role in this condition, with variable microbial composition and activity detected in patients with acne (Lee et al., 2018).

Our research explored the microbial dynamics within acne, studied the CoNS recovered from acne, and compared them to healthy skins. While the recovery rates of CoNS isolates from acne-diseased individuals closely paralleled those from their healthy skin counterparts, a significant contrast emerged in the phenotypic characterization of antibiotic resistance and biofilm production. Antibiotic susceptibility testing revealed a landscape of antibiotic resistance patterns. Although the antibiotic resistance profiles showed no substantial differences between the two groups, except for penicillin and cefoxitin, it is noteworthy that isolates from individuals with acne displayed significantly increased biofilm production compared to those from individuals with healthy skin. In the acne group, isolates exhibited the ability to form moderate (28.3%) and strong biofilms (38.3%), in marked contrast to the healthy isolates, where only 8% demonstrated moderate biofilm

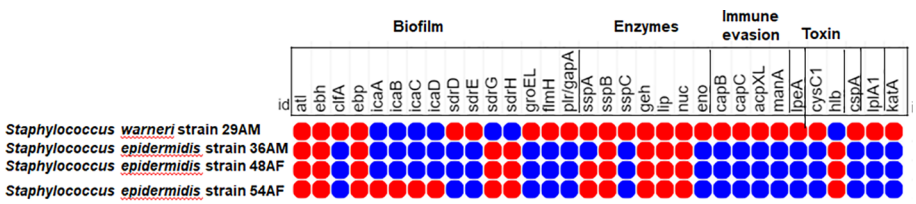

FIGURE 4
Heatmap showing the distribution of different virulence determinants among the sequenced isolates in the current study. The red circles denote the presence of virulence genes, whereas the lack of virulence genes is denoted by blue circles. The figure was created using the MORPHEUS online tool (https://software.broadinstitute.org/morpheus).

TABLE 5 MGEs in *Staphylococcus* strains linked to antibiotic resistance genes.

Isolate	Contig	MGEs	Closest nucleotide homology between a plasmid/ chromosome sequence (accession number)
29AM	14	*fusB*	*S. aureus* plasmid pUB101 (AY373761)
	20	IS256	*S. aureus* transposon 4001 *aacA-aphD* aminoglycoside resistance gene, complete cds, and right and left IS256 transposase gene (M18086)
	24	*bla(Z)*	*Streptococcus pneumoniae* genome assembly (CVLS01000543)
	29	rep5b	*S. epidermidis* plasmid SAP106B (GQ900455)
	31	repUS35	*S. warneri* SG1 plasmid clone pvSw2 genomic sequence (CP003671)
	34	rep5d	*S. aureus plasmid pJE1 remnant of replication protein Rep (rep), trimethoprim resistance protein* DfrA *(dfrA), thymidylate synthetase* ThyE *(thyE), and putative transposase* Tnp *(tnp) genes* (AF051916)
	36	rep5d	*S. aureus* plasmid pJE1 remnant of replication protein Rep (*rep*), trimethoprim resistance protein DfrA (*dfrA*), thymidylate synthetase ThyE (*thyE*), and putative transposase Tnp (*tnp*) genes, complete cds; and unknown gene (AF051916)
	37	*vga(A) rep7a*	*S. aureus* plasmid ATP-binding protein (*vga*) gene (M90056) *S. aureus* DNA, type-III staphylococcal cassette chromosome *mec* and SCCmercury: strain 85/2082 (AB037671)
	46	*tet(K)*	*S. aureus* tetracycline resistance plasmid pKH1, *tet* gene (U38656)
	48	repUS22	*S. aureus* plasmid SAP015B fragment (GQ900502)
	59	ISSep2	*S. epidermidis* ATCC *12228* (NC_004461)
	60	rep21	*S. aureus* plasmid pWBG754 (GQ900396)
	62	*erm(C) rep10*	*Bacillus subtilis* plasmid pIM13 (M13761) *S. aureus* strain E14 plasmid pDLK1 (GU562624)
	73	rep13	*S. aureus* plasmid pSK41 (AF051917)
	74	rep10b	*S. aureus* plasmid pSK6 (U96610)
	82	rep13	*S. aureus* strain WBG4364 plasmid pWBG1773 (EF537646)
36AM	48	ISSep3	*S. epidermidis* ATCC 12228 (NC_004461)
	78	*rep20 blaZ*	*S. saprophyticus* subsp. *saprophyticus* MS1146 plasmid pSSAP2 (HE616681) *S. haemolyticus* plasmid NVH96 plasmid (AJ302698)
	87	*fosB*	*S. epidermidis* RP62A (CP000029)
	90	ISSep2	*S.epidermidis* ATCC 12228 (NC_004461)
	205	*rep5b*	*S. epidermidis* ATCC 12228 plasmid pSE-12228-06 (AE015935)
	206	*rep13 qacC*	*S. epidermidis* CH plasmid pSepCH (AY092027) *S. aureus* replication (*rep*), control of replication (*cop*), and resistance protein (*QacC*) genes (M37889)
	223	*rep21 lnu(A)*	*S. aureus* plasmid pWBG754 (GQ900396) *S. haemolyticus linA* gene encoding lincosamide resistance (M14039)
	276	*rep7a*	*Staphylococcus hyicus* plasmid pSTE1 (HE662694)
	376	*Tet (K):TPA*	*S. warneri* strain 16A plasmid (CP031268.1)
	60	rep21	*S. aureus* plasmid pWBG754 (GQ900396)
	73	rep13	*S. aureus* plasmid pSK41 (AF051917)
	74	rep10b	*S. aureus* plasmid pSK6 (U96610)
	82	rep13	*S. aureus* strain WBG4364 plasmid pWBG1773 (EF537646)
48AF	7	*fusB*	*S. aureus* plasmid pUB101 (AY373761)
	15	blaZ	*S.epidermidis* strain Mt1p16 Mt1p16_contig_78 (MAJJ01000071)
	16	*fosB*	*S. epidermidis* RP62A (CP000029)
	27	*ACME*	*S. aureus* strain USA300_R114 SCC*mec* IVa and ACME genetic islands (KF175393)
	37	rep7a	Glutathione S-transferase%2C unnamed subgroup 2 *[Klebsiella pneumoniae]* (SAU83488)
	38	rep5b	*S. epidermidis* plasmid SAP108B (GQ900459)
	39	rep7a	Glutathione S-transferase%2C unnamed subgroup 2 *[K. pneumoniae]* (SAU83488)
	46	rep13 *qacC*	*S. epidermidis* CH plasmid pSepCH (AY092027) *S. aureus* replication (rep), control of replication (cop), and resistance protein (QacC) genes (M37889)
	49	*vga (A)LC*	*S. haemolyticus* lincosamide-streptogramin A resistance protein (*vga (A)*LC) gene (DQ823382)
	73	rep7a	Glutathione S-transferase%2C unnamed subgroup 2 *[K. pneumoniae]* (SAU83488)
54AF	8	ISSEP2	*S. epidermidis* ATCC 12228 (NC_004461)
	10	*fosB*	*S. epidermidis* RP62A (CP000029)

(Continued)

TABLE 5 Continued

Isolate	Contig	MGEs	Closest nucleotide homology between a plasmid/chromosome sequence (accession number)
	15	*ACME* ISSEP3	*S. aureus* strain USA300_R114 SCC*mec* IVa and ACME genetic islands (KF175393) *S. epidermidis* ATCC 12228 (NC_004461)
	16	rep20	*S. saprophyticus* subsp. *saprophyticus* MS1146 plasmid pSSAP2 (HE616681)
	35	*lnu (A)*	*S. haemolyticus linA* gene encoding lincosamide resistance (M14039)
	45	rep7a	*S. hyicus* plasmid pSTE1 (HE662694)

MGEs, mobile genetic elements.

formation, and none exhibited strong biofilm production. This highlights the significance of going beyond the bacterial existence to comprehend the functional distinctions that contribute to the development and pathogenesis of acne. The present study explored the biofilm-associated genes (*icaA*, *icaD*, and *mecA*), which were particularly prevalent in clinical isolates from participants with moderate to severe acne. Co-expression of *icaA* and *icaD* significantly augmented biofilm formation, with *icaD* exhibiting a higher positive detection rate. The correlation between drug resistance and biofilm formation was significant. Bacteria in biofilms exhibit increased resistance to antibiotics because of the surrounding protective matrix. This enhanced resistance may contribute to the development of MDR and XDR strains. In our study, all the strong biofilm-forming CoNS were MDR. Strong biofilm formation may serve as a mechanism by which bacteria evade the effects of antimicrobial agents, allowing them to persist and proliferate. A protective biofilm matrix can shield bacteria from the action of antibiotics, making it more difficult to eradicate the infection. Additionally, the coexistence of drug resistance and strong biofilm formation may contribute to the persistence of bacterial infections leading to chronic and recurrent conditions (Coenye et al., 2022).

Four XDR and strong biofilm-forming CoNS isolates, recovered from severe acne infections, were selected for genomic analysis. We investigated the genomic features using WGS, including MGEs, genetic contexts of the identified resistance genes, and virulence factors. Upon analyzing the genomes of the four strains, three isolates (36AM, 48AF, and 54AF) were confirmed to be *S. epidermidis*, whereas isolate 29AM was identified as *S. warneri*, a common CoNS that is regularly found in human mucous membranes and various sites, including the eye, peritoneum, wounds, and urethra. While constituting approximately 1% of skin staphylococci and prevalent in 50% of healthy adults, *S. warneri* is typically non-pathogenic. However, recent studies have highlighted its emergence as a potential pathogen, particularly associated with implanted materials, even in the absence of foreign bodies, and in immunocompromised individuals. This shift challenged previous perceptions of its limited pathogenicity (Otto, 2010; França,

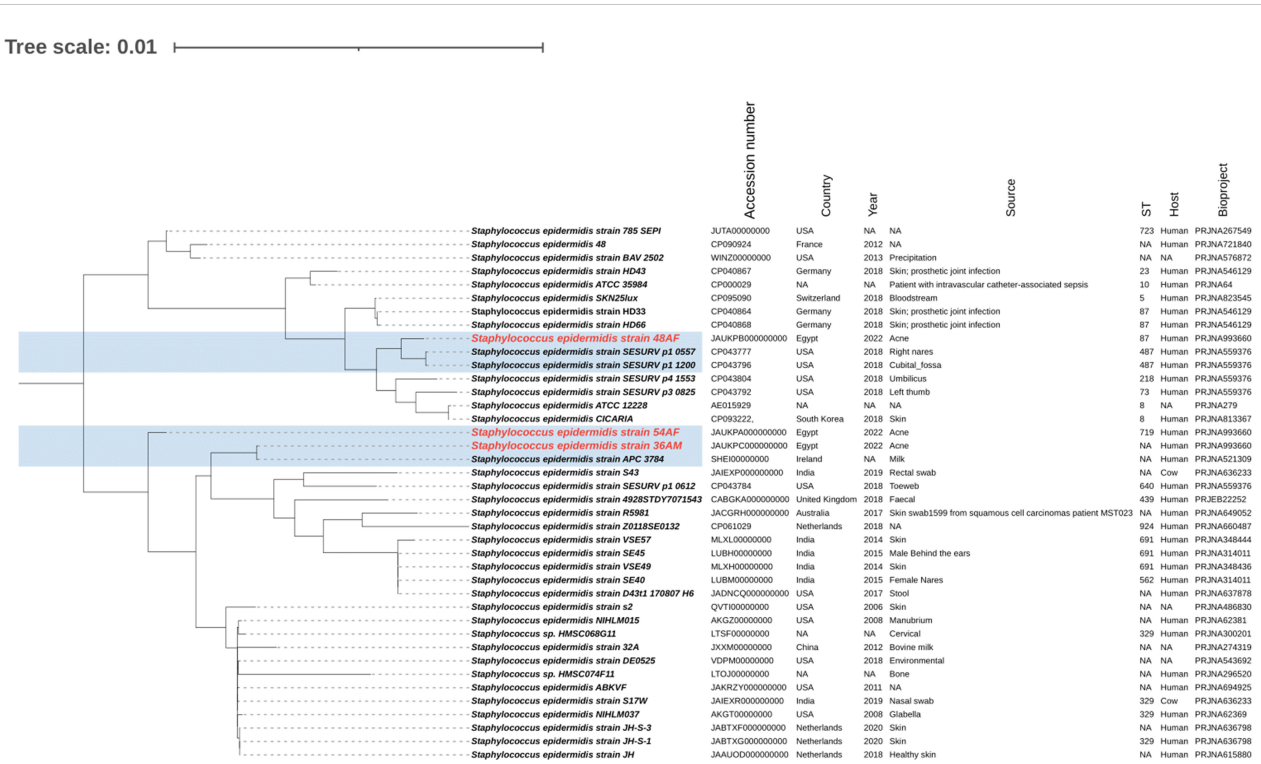

FIGURE 5
Whole genome-based phylogenetic tree of *S. epidermidis* isolates. The *S. epidermidis* genome sequenced in the current study was compared to the closely related genomes, highlighted in blue. The labels of the *S. epidermidis* strains sequenced in the current study are shown in red. The figure was created using the iTOL online tool v6.7 (https://itol.embl.de/).

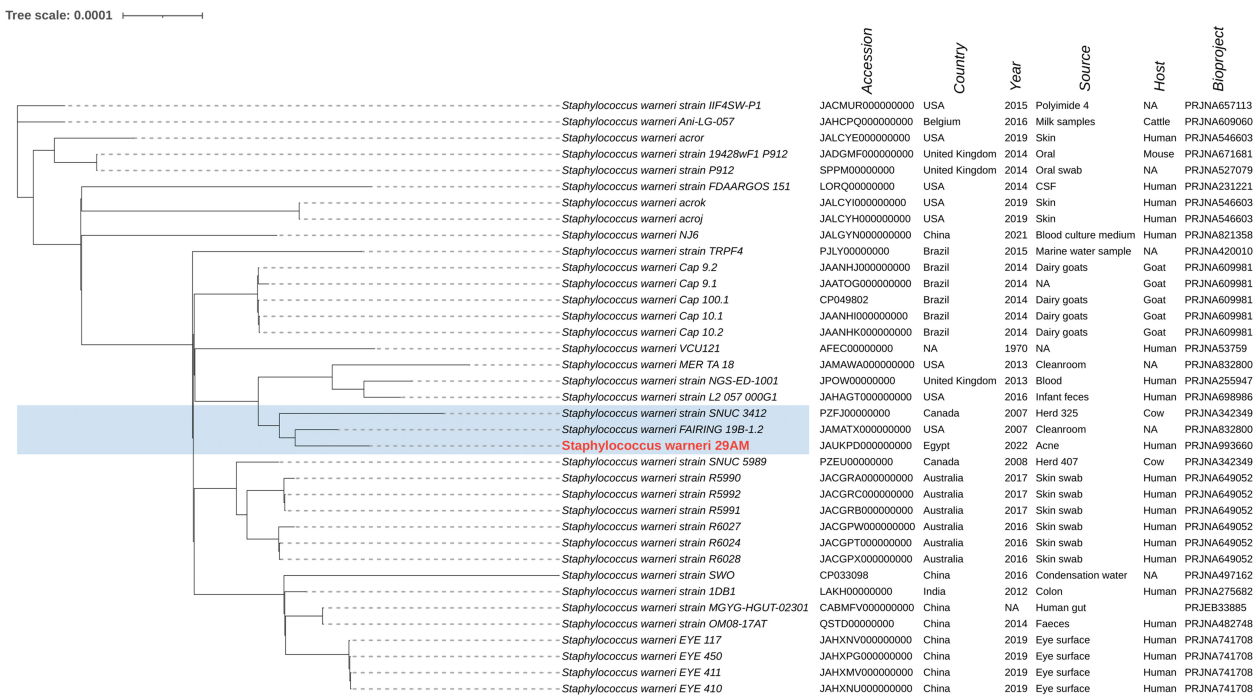

FIGURE 6
Whole genome-based phylogenetic tree of the *S. warneri* isolate 29AM. The *S. warneri* 29AM genome sequenced in the current study was compared to the closely related genomes, highlighted in blue. The label of the *S. warneri* strain sequenced in this study is shown in red. The figure was created using the iTOL online tool v6.7 (https://itol.embl.de/).

2023). The pathophysiology and epidemiology of this species are not well understood. Furthermore, methods used to distinguish *S. warneri* from *S. epidermidis*, such as conventional culturing techniques and MALDI-TOF MS, are not sufficiently sensitive (Dubois et al., 2010; Rosa et al., 2022). *S. epidermidis*, a common commensal on human epithelia, displays significant genetic diversity with over 400 recognized sequence types (STs), primarily clustering in CC2. The prevalent ST2, associated with invasiveness due to IS256 insertion sequences and *ica* genes, dominates in clinical isolates (Méric et al., 2015). The tested genomes were investigated for their ST types, and isolates 36AM, 48AF, and 54AF were identified as ST39, ST87, and ST719, respectively. Understanding the distribution of these STs in acne isolates could be relevant for investigating the genetic diversity and potential virulence factors associated with *S. epidermidis* in individuals with acne. Further analysis and comparison with STs from other contexts may provide insights into the role of specific genetic variants in the pathogenesis of acne or in the skin microbiome of patients with acne.

Genomic analysis of the isolates revealed a diverse and extensive drug resistance pattern involving various mechanisms, such as enzyme inactivation, target modification, and efflux pumps. Specific resistance genes (*dfrC*, *vanT*, *erm*©, *FOSBx1*, *blaZ*, and *norA*) and mutations in key genes (*gyrA*, *gyrB*, *parC*, *parE*, and *rpoB*) were identified. These findings align with those of previous studies and emphasize the adaptability of CoNS in acquiring resistance. The observed genetic diversity underscores the complexity of antibiotic resistance profiles (Xu et al., 2018; Cabrera-Contreras et al., 2019; Raue et al., 2020). The detection of *blaZ* in the isolates, along with their regulatory genes *blaR* and *blaI* in addition to the presence of the *mecA* gene, may explain the resistance to penicillin and cephalosporins observed in phenotypic antibiotic susceptibility testing, as reported by a previous study by Cabrera-Contreras et al. (2019). Despite the correlation between genotypic and phenotypic resistance to penicillin and cephalosporins, potential inconsistencies highlight the importance of considering factors such as sequencing quality.

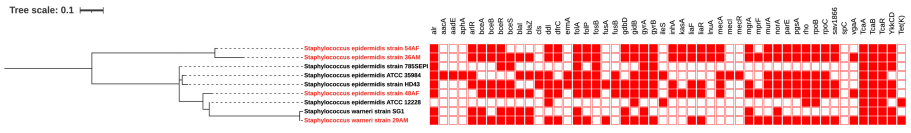

FIGURE 7
SNP-based phylogenetic tree of *Staphylococcus* isolates. SNP base phylogeny and heat map displaying the antimicrobial resistance genetic determinants among the sequenced isolates generated and selected genomes: *S. epidermidis* ATCC®12228, *S. epidermidis* ATCC®35984, *S. epidermidis* strain 785SEPI, and *S. warneri* strain SG1. Red and white indicate the presence and absence of ARGs, respectively. The labels of the strains sequenced in this study is shown in red. The figure was created using the iTOL online tool v6.7 (https://itol.embl.de/).

Both pathogenic and commensal *S. epidermidis* strains share many virulence genes (Otto, 2009). Adherence/biofilm-forming genes and multidrug resistance were found in the sequenced isolates and confirmed by the identification of adherence-related genes. The *ica* operon and IS256, both of which have been linked to the pathogenicity of *S. epidermidis*, were not detected in any of the isolates (Murugesan et al., 2018). This is comparable to the results of a study in Mexico, where 50% of *S. epidermidis* isolates were negative for the *ica* operon (Cabrera-Contreras et al., 2019).

All sequenced genomes contained several virulence genes encoding proteins associated with the pathogenesis of acne. Several genes such as *atl*, *ebh*, *epb*, *sdrG*, and *sdrH* are involved in adhesion and biofilm formation. Enzymes implicated in acne production, including proteases (*sspA*, *sspB*) and lipases (*geh*, *lip*, *nuc*), were produced by all isolates. The presence of the *hlb* gene encoding β-hemolysin toxin was supported by Kumar et al. (2016), suggesting a role in tissue damage and pathogen spread into deeper tissues (O'Neill et al., 2020). Similar virulence determinants were detected in many studies on *S. epidermidis*, including the elastin binding protein gene *ebp*, the serine protease gene *sspA*, the autolysin gene *atlE*, the lipase gene *geh*, the cell wall-associated fibronectin-binding protein gene *ebh*, the nuclease gene *nuc*, and the *ica* genes (Salgueiro et al., 2017; Xu et al., 2018; Raue et al., 2020).

Compared to *S. epidermidis*, *S. warneri* strain 29AM exhibited additional virulence factors related to the production of toxins, resistance to acidic conditions, evasion of the immune system, intracellular survival capabilities, invasion mechanisms, iron uptake processes, lipid metabolism modulation, phagosome arresting ability, stress adaptation strategies, and surface protein anchoring. All of these virulence factors play integral roles in shaping the course of acne development. These findings provide insights into the diverse virulence profiles contributing to acne pathophysiology, with *S. warneri* strain 29AM displaying enhanced virulence factors that are not commonly associated with acne pathogens.

These antibiotic resistance and virulence genes are part of the accessory genome, which is organized both within and between species. The prediction of pathogenicity of isolates towards human hosts produced a high average likelihood score (P_{score} 0.937), close to 1.00. This pathogenicity score is attributed to the presence of numerous virulence genes in the isolates, which supports their pathogenic potential in humans.

MGEs play a significant role in acne pathophysiology, contributing to the genetic diversity and adaptability of bacteria involved in acne, such as *S. epidermidis* and *S. warneri*. MGEs, including SCC*mec* and ACME, serve as repositories for both resistance and virulence genes. Their mobility allows the transfer of genetic material within and across bacterial species through horizontal gene transfer, contributing to the exchange of traits within the bacterial population (Sheppard et al., 2016; Foster, 2017).

In the context of acne, the presence of MGEs is associated with the acquisition of virulence and resistance genes. For instance, the study identified IS256, an insertion sequence linked to virulence and biofilm development, in a strong biofilm-forming *S. warneri* 29AM isolate. This suggests that MGEs may enhance the genomic organization of bacteria involved in acne, potentially influencing their pathogenicity and ability to form biofilms, which is a key factor in acne development (Murugesan et al., 2018). IS256 has been shown in previous investigations to enhance the genomic organization of pathogenic *S. epidermidis* isolates (Cabrera-Contreras et al., 2019). The discovery of the IS families IS110 and IS200/IS605 coincides with the findings of Raue et al. (2020). Moreover, this study identified resistance genes frequently carried on plasmids, demonstrating how MGEs can facilitate the spread of antibiotic resistance. Plasmid-borne genes, such as *erm*©, *lnu(A)*, *tet (K)*, *qacC*, and *blaZ*, can be easily transferred between bacterial cells through conjugation, contributing to the dissemination of resistance traits within the bacterial population associated with acne (Cabrera-Contreras et al., 2019).

In this study, the prophages were found to be incapable of carrying resistance genes through transduction. However, transposons identified in two isolates, 36AM and 48AF, including Tn554 flanking *erm (A)*, may facilitate the movement of beneficial genes, particularly those linked to antibiotic resistance, in the context of acne-associated bacteria (Mbelle et al., 2019).

The CRISPR-Cas system, a bacterial defense mechanism against phage infection, was identified in all isolates, providing a memory of the viral genetic code to prevent future infections. Each isolate also contained at least one intact prophage (Makarova et al., 2020). In a recent study by Raue et al. (2020), four CRISPR elements were discovered in the genome of biofilm-positive and methicillin-susceptible *S. epidermidis* O47 strain. The restriction–modification (R–M) system was not detected in any of the isolates in this study. The R–M system, similar to the CRISPR-Cas system, is a bacterial defense system against bacteriophage invasion (Vasu and Nagaraja, 2013). These defense systems are crucial for protecting bacteria from viral infections, contributing to our understanding of their role in the complex pathogenesis of acne.

The ACME system, recognized as a pathogenicity island, was found in two isolates (48AF and 54AF), raising interest because of its potential role in host colonization, immune evasion, and the transfer of virulence or survival genes (O'Connor et al., 2018). Studies have evaluated the resistance and virulence profiles of *S. epidermidis* isolates from bloodstream infections and neonatal nares, and an ACME carriage rate of 16% was found (Salgueiro et al., 2017). ACME have a greater prevalence and variety in *S. epidermidis* than in *S. aureus*. ACME is present in bacterial chromosomes adjacent to the *SCCmec* type IV element in *S. aureus* (Diep et al., 2006; Ellington et al., 2008). The present study demonstrated an association between ACME and SCC*mec* type IV, which is consistent with the findings of Du et al. (2013). Most resistance genes are flanked by transposases, ISs, or both, and these can transmit resistance genes within and between plasmids and chromosomes, potentially within and between bacterial strains (Mbelle et al., 2019).

These findings provide insights into the genetic factors influencing acne pathogenesis, particularly in the context of bacterial defense mechanisms and the interplay of virulence and resistance genes. The diversity of MGEs observed in the *Staphylococcus* genomes indicates an active process of gene exchange, suggesting that MGEs contribute to the evolution and adaptation of bacteria involved in acne pathophysiology.

This study diverges from the previous focus on pathogenic *S. aureus* by emphasizing the potential pathogenicity of CoNS, which are

typically considered commensals. To the best of our knowledge, this is the first report in Egypt that offers insights into the diversity, distribution, virulence, and resistance profiles of *S. epidermidis* and *S. warneri* isolates recovered from acne, establishing their relatedness to global strains through WGS. Despite the limited number of isolates, our research establishes a foundational understanding for future investigations, contributing to the comprehension of the potential role of CoNS in acne vulgaris. In conclusion, this study highlights the complex nature of acne, which explains its microbial interactions, biofilm formation, and virulence factors. This comprehensive insight is vital for developing targeted and personalized therapeutic strategies and advancing the understanding of acne pathophysiology for more effective treatment approaches.

5 Conclusion

CoNS is as a significant contributor to acne development and pathogenesis by releasing virulence factors, which are more abundant in acne patients than in normal skin. The diverse combinations of ARGs, virulence genes, and MGEs found in *S. epidermidis* and *S. warneri* isolates recovered from acne highlight the enriched content of mobilized antibiotic resistance and pathogenic features. This study emphasizes the importance of tracking CoNS genomes as emerging infectious agents and shedding light on their pathogenicity. Notably, our findings suggest that *S. warneri* is an emerging pathogen implicated in acne pathogenesis, urging reconsideration of its role in infectious processes. This study sheds light on the complex interplay between microbial elements and acne and offers valuable insights for future research and targeted interventions in acne management.

Data availability statement

The datasets presented in this study can be found in online repositories. The names of the repository/repositories and accession number(s) can be found in the article/Supplementary Material.

Ethics statement

The studies involving humans were approved by MSA University-Ethics Committee. The studies were conducted in accordance with the local legislation and institutional requirements. The participants provided their written informed consent to participate in this study.

Author contributions

MA: Data curation, Formal analysis, Methodology, Resources, Software, Validation, Visualization, Writing – original draft, Writing – review & editing. MD: Data curation, Formal analysis, Methodology, Writing – original draft. NS: Investigation, Methodology, Project administration, Resources, Writing – original draft. HA: Conceptualization, Formal analysis, Investigation, Methodology, Project administration, Supervision, Validation, Writing – original draft, Writing – review & editing.

Funding

The author(s) declare that no financial support was received for the research, authorship, and/or publication of this article.

Conflict of interest

The authors declare that the research was conducted in the absence of any commercial or financial relationships that could be construed as a potential conflict of interest.

Publisher's note

Supplementary material

The Supplementary Material for this article can be found online at: https://www.frontiersin.org/articles/10.3389/fcimb.2024.1328390/full#supplementary-material

References

Águila-Arcos, S., Álvarez-Rodríguez, I., Garaiyurrebaso, O., Garbisu, C., Grohmann, E., and Alkorta, I. (2017). Biofilm-forming clinical staphylococcus isolates harbor horizontal transfer and antibiotic resistance genes. *Front. Microbiol.* 8. doi: 10.3389/fmicb.2017.02018

Ahmed, D. M., Messih, M., Ibrahim, N. H., Meabed, M. H., and Abdel-Salam, S. M. (2019). Frequency of icaA and icaD determinants and biofilm formation among coagulase-negative staphylococci associated with nasal carriage in neonatal intensive care units. *Germs* 9 (2), 61–70. doi: 10.18683/germs.2019.1159

Alawad, M. J., Ali, G. A., and Goravey, W. (2022). Underrecognized pathogen; Staphylococcus warneri-associated native mitral valve endocarditis in an immunocompetent host: A case report and literature review. *Clin. Case Rep.* 10 (4), e05591. doi: 10.1002/ccr3.5591

Alcock, B. P., Raphenya, A. R., Lau, T. T. Y., Tsang, K. K., Bouchard, M., Edalatmand, A., et al. (2020). CARD 2020: antibiotic resistome surveillance with the comprehensive antibiotic resistance database. *Nucleic Acids Res.* 48 (D1), D517–d525. doi: 10.1093/nar/gkz935

Altschul, S. F., Gish, W., Miller, W., Myers, E. W., and Lipman, D. J. (1990). Basic local alignment search tool. *J. Mol. Biol.* 215 (3), 403–410. doi: 10.1016/S0022-2836(05)80360-2

Amer, M. A., Wasfi, R., Attia, A. S., and Ramadan, M. A. (2021). Indole derivatives obtained from Egyptian enterobacter sp. soil isolates exhibit antivirulence activities against Uropathogen. Proteus mirabilis. *Antibiotics (Basel)* 10 (4), 363. doi: 10.3390/antibiotics10040363.

Arciola, C. R., Campoccia, D., Ravaioli, S., and Montanaro, L. (2015). Polysaccharide intercellular adhesin in biofilm: structural and regulatory aspects. *Front. Cell Infect. Microbiol.* 5, 7. doi: 10.3389/fcimb.2015.00007

Arndt, D., Grant, J. R., Marcu, A., Sajed, T., Pon, A., Liang, Y., et al. (2016). PHASTER: a better, faster version of the PHAST phage search tool. *Nucleic Acids Res.* 44 (W1), W16–W21. doi: 10.1093/nar/gkw387

Arrecubieta, C., Lee, M. H., Macey, A., Foster, T. J., and Lowy, F. D. (2007). SdrF, a Staphylococcus epidermidis surface protein, binds type I collagen. *J. Biol. Chem.* 282 (26), 18767–18776. doi: 10.1074/jbc.M610940200

Aydemir, E. H. (2014). Acne vulgaris. *Turk. Pediatri. Ars.* 49 (1), 13–16. doi: 10.5152/tpa.2014.1943

Bankevich, A., Nurk, S., Antipov, D., Gurevich, A. A., Dvorkin, M., Kulikov, A. S., et al. (2012). SPAdes: a new genome assembly algorithm and its applications to single-cell sequencing. *J. Comput. Biol.* 19 (5), 455–477. doi: 10.1089/cmb.2012.0021

Becker, K., Heilmann, C., and Peters, G. (2014). Coagulase-negative staphylococci. *Clin. Microbiol. Rev.* 27 (4), 870–926. doi: 10.1128/CMR.00109-13

Bolger, A. M., Lohse, M., and Usadel, B. (2014). Trimmomatic: a flexible trimmer for Illumina sequence data. *Bioinformatics* 30 (15), 2114–2120. doi: 10.1093/bioinformatics/btu170

Bouchami, O., De Lencastre, H., and Miragaia, M. (2016). Impact of insertion sequences and recombination on the population structure of staphylococcus haemolyticus. *PLoS One* 11 (6), e0156653. doi: 10.1371/journal.pone.0156653

Brüggemann, H. (2010). "Skin: Acne and *Propionibacterium acnes Genomics*", in *Handbook of Hydrocarbon and Lipid Microbiolog*. Eds. K. N. Timmis (Berlin, Heidelberg: Springer). doi: 10.1007/978-3-540-77587-4_244

Cabrera-Contreras, R., Santamaría, R. I., Bustos, P., Martínez-Flores, I., Meléndez-Herrada, E., Morelos-Ramírez, R., et al. (2019). Genomic diversity of prevalent Staphylococcus epidermidis multidrug-resistant strains isolated from a Children's Hospital in México City in an eight-years survey. *PeerJ* 7, e8068. doi: 10.7717/peerj.8068

Camacho, C., Coulouris, G., Avagyan, V., Ma, N., Papadopoulos, J., Bealer, K., et al. (2009). BLAST+: architecture and applications. *BMC Bioinf.* 10, 421. doi: 10.1186/1471-2105-10-421

Carattoli, A., Zankari, E., García-Fernández, A., Voldby Larsen, M., Lund, O., Villa, L., et al. (2014). In silico detection and typing of plasmids using PlasmidFinder and plasmid multilocus sequence typing. *Antimicrob. Agents Chemother.* 58 (7), 3895–3903. doi: 10.1128/AAC.02412-14

Chen, X.-P., Li, W.-G., Zheng, H., Du, H.-Y., Zhang, L., Zhang, L., et al. (2017). Extreme diversity and multiple SCCmec elements in coagulase-negative Staphylococcus found in the Clinic and Community in Beijing, China. *Ann. Clin. Microbiol. Antimicrobials* 16 (1), 57. doi: 10.1186/s12941-017-0231-z

Christensen, G. J., and Brüggemann, H. (2014). Bacterial skin commensals and their role as host guardians. *Benef Microbes* 5 (2), 201–215. doi: 10.3920/BM2012.0062

CLSI (2022). *Performance Standards for Antimicrobial Susceptibility Testing; Twenty-First Informational Supplement. CLSI Document M100-S21* (Wayne, PA: Clinical and Laboratory Standards Institute).

Coenye, T., Spittaels, K.-J., and Achermann, Y. (2022). The role of biofilm formation in the pathogenesis and antimicrobial susceptibility of Cutibacterium acnes. *Biofilm* 4, 100063. doi: 10.1016/j.bioflm.2021.100063

Cogen, A. L., Nizet, V., and Gallo, R. L. (2008). Skin microbiota: a source of disease or defence? *Br. J. Dermatol.* 158 (3), 442–455. doi: 10.1111/j.1365-2133.2008.08437.x

Diep, B. A., Gill, S. R., Chang, R. F., Phan, T. H., Chen, J. H., Davidson, M. G., et al. (2006). Complete genome sequence of USA300, an epidemic clone of community-acquired meticillin-resistant Staphylococcus aureus. *Lancet* 367 (9512), 731–739. doi: 10.1016/S0140-6736(06)68231-7

Downing, D. T., Stewart, M. E., Wertz, P. W., and Strauss, J. S. (1986). Essential fatty acids and acne. *J. Am. Acad. Dermatol.* 14 (2 Pt 1), 221–225. doi: 10.1016/S0190-9622(86)70025-X

Du, X., Zhu, Y., Song, Y., Li, T., Luo, T., Sun, G., et al. (2013). Molecular analysis of Staphylococcus epidermidis strains isolated from community and hospital environments in China. *PLoS One* 8 (5), e62742. doi: 10.1371/journal.pone.0062742

Dubois, D., Leyssene, D., Chacornac, J. P., Kostrzewa, M., Schmit, P. O., Talon, R., et al. (2010). Identification of a variety of Staphylococcus species by matrix-assisted laser desorption ionization-time of flight mass spectrometry. *J. Clin. Microbiol.* 48 (3), 941–945. doi: 10.1128/JCM.00413-09

Ellington, M. J., Yearwood, L., Ganner, M., East, C., and Kearns, A. M. (2008). Distribution of the ACME-arcA gene among methicillin-resistant Staphylococcus aureus from England and Wales. *J. Antimicrob. Chemother.* 61 (1), 73–77. doi: 10.1093/jac/dkm422

Fitz-Gibbon, S., Tomida, S., Chiu, B. H., Nguyen, L., Du, C., Liu, M., et al. (2013). Propionibacterium acnes strain populations in the human skin microbiome associated with acne. *J. Invest. Dermatol.* 133 (9), 2152–2160. doi: 10.1038/jid.2013.21

Formosa-Dague, C., Feuillie, C., Beaussart, A., Derclaye, S., Kucharíková, S., Lasa, I., et al. (2016). Sticky matrix: adhesion mechanism of the staphylococcal polysaccharide intercellular adhesin. *ACS Nano* 10 (3), 3443–3452. doi: 10.1021/acsnano.5b07515

Foster, T. J. (2017). Antibiotic resistance in Staphylococcus aureus. Current status and future prospects. *FEMS Microbiol. Rev.* 41 (3), 430–449. doi: 10.1093/femsre/fux007

Fournière, M., Latire, T., Souak, D., Feuilloley, M. G. J., and Bedoux, G. (2020). Staphylococcus epidermidis and Cutibacterium acnes: Two Major Sentinels of Skin Microbiota and the Influence of Cosmetics. *Microorganisms* 8 (11), 1752. doi: 10.3390/microorganisms8111752

França, A. (2023). The role of coagulase-negative staphylococci biofilms on late-onset sepsis: current challenges and emerging diagnostics and therapies. *Antibiotics* 12 (3), 554. doi: 10.3390/antibiotics12030554

Freney, J., Kloos, W. E., Hajek, V., Webster, J. A., Bes, M., Brun, Y., et al. (1999). Recommended minimal standards for description of new staphylococcal species. Subcommittee on the taxonomy of staphylococci and streptococci of the International Committee on Systematic Bacteriology. *Int. J. Syst. Bacteriol.* 49 Pt 2, 489–502. doi: 10.1099/00207713-49-2-489

Huang, T. Y., Jiang, Y. E., and Scott, D. A. (2022). Culturable bacteria in the entire acne lesion and short-chain fatty acid metabolites of Cutibacterium acnes and Staphylococcus epidermidis isolates. *Biochem. Biophys. Res. Commun.* 622, 45–49. doi: 10.1016/j.bbrc.2022.06.068

Jahns, A. C., Lundskog, B., Ganceviciene, R., Palmer, R. H., Golovleva, I., Zouboulis, C. C., et al. (2012). An increased incidence of Propionibacterium acnes biofilms in acne vulgaris: a case-control study. *Br. J. Dermatol.* 167 (1), 50–58. doi: 10.1111/j.1365-2133.2012.10897.x

Joensen, K. G., Scheutz, F., Lund, O., Hasman, H., Kaas, R. S., Nielsen, E. M., et al. (2014). Real-time whole-genome sequencing for routine typing, surveillance, and outbreak detection of verotoxigenic Escherichia coli. *J. Clin. Microbiol.* 52 (5), 1501–1510. doi: 10.1128/JCM.03617-13

Johansson, M. H. K., Bortolaia, V., Tansirichaiya, S., Aarestrup, F. M., Roberts, A. P., and Petersen, T. N. (2021). Detection of mobile genetic elements associated with antibiotic resistance in Salmonella enterica using a newly developed web tool: MobileElementFinder. *J. Antimicrob. Chemother.* 76 (1), 101–109. doi: 10.1093/jac/dkaa390

Kaas, R. S., Leekitcharoenphon, P., Aarestrup, F. M., and Lund, O. (2014). Solving the problem of comparing whole bacterial genomes across different sequencing platforms. *PLoS One* 9 (8), e104984. doi: 10.1371/journal.pone.0104984

Kumar, B., Pathak, R., Mary, P. B., Jha, D., Sardana, K., and Gautam, H. K. (2016). New insights into acne pathogenesis: Exploring the role of acne-associated microbial populations. *Dermatol. Sin.* 34 (2), 67–73. doi: 10.1016/j.dsi.2015.12.004

Kutlu, Ö., Karadağ, A. S., and Wollina, U. (2023). Adult acne versus adolescent acne: a narrative review with a focus on epidemiology to treatment. *Anais Brasileiros Dermatol.* 98 (1), 75–83. doi: 10.1016/j.abd.2022.01.006

Larsen, M. V., Cosentino, S., Rasmussen, S., Friis, C., Hasman, H., Marvig, R. L., et al. (2012). Multilocus sequence typing of total-genome-sequenced bacteria. *J. Clin. Microbiol.* 50 (4), 1355–1361. doi: 10.1128/JCM.06094-11

Lee, J. Y. H., Monk, I. R., Gonçalves Da Silva, A., Seemann, T., Chua, K. Y. L., Kearns, A., et al. (2018). Global spread of three multidrug-resistant lineages of Staphylococcus epidermidis. *Nat. Microbiol.* 3 (10), 1175–1185. doi: 10.1038/s41564-018-0230-7

Li, H., and Durbin, R. (2010). Fast and accurate long-read alignment with Burrows-Wheeler transform. *Bioinformatics* 26 (5), 589–595. doi: 10.1093/bioinformatics/btp698

Lucero-Mejía, J. E., Romero-Gómez, S. D. J., and Hernández-Iturriaga, M. (2020). A new classification criterion for the biofilm formation index: A study of the biofilm dynamics of pathogenic Vibrio species isolated from seafood and food contact surfaces. *J. Food Sci.* 85 (8), 2491–2497. doi: 10.1111/1750-3841.15325

Makarova, K. S., Wolf, Y. I., Iranzo, J., Shmakov, S. A., Alkhnbashi, O. S., Brouns, S. J. J., et al. (2020). Evolutionary classification of CRISPR-Cas systems: a burst of class 2 and derived variants. *Nat. Rev. Microbiol.* 18 (2), 67–83. doi: 10.1038/s41579-019-0299-x

Månsson, E., Hellmark, B., Sundqvist, M., and Söderquist, B. (2015). Sequence types of Staphylococcus epidermidis associated with prosthetic joint infections are not present in the laminar airflow during prosthetic joint surgery. *Apmis* 123 (7), 589–595. doi: 10.1111/apm.12392

Mbelle, N. M., Feldman, C., Osei Sekyere, J., Maningi, N. E., Modipane, L., and Essack, S. Y. (2019). The resistome, mobilome, virulome and phylogenomics of multidrug-resistant escherichia coli clinical isolates from pretoria, South Africa. *Sci. Rep.* 9 (1), 16457. doi: 10.1038/s41598-019-52859-2

Méric, G., Miragaia, M., De Been, M., Yahara, K., Pascoe, B., Mageiros, L., et al. (2015). Ecological Overlap and Horizontal Gene Transfer in Staphylococcus aureus and Staphylococcus epidermidis. *Genome Biol. Evol.* 7 (5), 1313–1328. doi: 10.1093/gbe/evv066

Murugesan, S., Mani, S., Kuppusamy, I., and Krishnan, P. (2018). Role of insertion sequence element is256 as a virulence marker and its association with biofilm formation among methicillin-resistant Staphylococcus epidermidis from hospital and community settings in Chennai, South India. *Indian J. Med. Microbiol.* 36 (1), 124–126. doi: 10.4103/ijmm.IJMM_17_276

O'Connor, A. M., Mcmanus, B. A., Kinnevey, P. M., Brennan, G. I., Fleming, T. E., Cashin, P. J., et al. (2018). Significant enrichment and diversity of the staphylococcal arginine catabolic mobile element ACME in staphylococcus epidermidis isolates from

subgingival peri-implantitis sites and periodontal pockets. *Front. Microbiol.* 9, 1558. doi: 10.3389/fmicb.2018.01558

Olson, R. D., Assaf, R., Brettin, T., Conrad, N., Cucinell, C., Davis, J. J., et al. (2023). Introducing the Bacterial and Viral Bioinformatics Resource Center (BV-BRC): a resource combining PATRIC, IRD and ViPR. *Nucleic Acids Res* 51 (D1), D678–D689. doi: 10.1093/nar/gkac1003

O'Neill, A., and Gallo, R. (2018). Host-microbiome interactions and recent progress into understanding the biology of acne vulgaris. *Microbiome* 6 (1), 177. doi: 10.1186/s40168-018-0558-5

O'Neill, A. M., Nakatsuji, T., Hayachi, A., Williams, M. R., Mills, R. H., Gonzalez, D. J., et al. (2020). Identification of a human skin commensal bacterium that selectively kills cutibacterium acnes. *J. Invest. Dermatol.* 140 (8), 1619–1628.e1612. doi: 10.1016/j.jid.2019.12.026

Onishi, M., Urushibara, N., Kawaguchiya, M., Ghosh, S., Shinagawa, M., Watanabe, N., et al. (2013). Prevalence and genetic diversity of arginine catabolic mobile element (ACME) in clinical isolates of coagulase-negative staphylococci: identification of ACME type I variants in Staphylococcus epidermidis. *Infect. Genet. Evol.* 20, 381–388. doi: 10.1016/j.meegid.2013.09.018

Otto, M. (2009). Staphylococcus epidermidis–the A'ccidental' pathogen. *Nat. Rev. Microbiol.* 7 (8), 555–567. doi: 10.1038/nrmicro2182

Otto, M. (2010). Staphylococcus colonization of the skin and antimicrobial peptides. *Expert Rev. Dermatol.* 5 (2), 183–195. doi: 10.1586/edm.10.6

Paluch, E., Rewak-Soroczyńska, J., Jędrusik, I., Mazurkiewicz, E., and Jermakow, K. (2020). Prevention of biofilm formation by quorum quenching. *Appl. Microbiol. Biotechnol.* 104 (5), 1871–1881. doi: 10.1007/s00253-020-10349-w

Petrelli, D., Zampaloni, C., D'ercole, S., Prenna, M., Ballarini, P., Ripa, S., et al. (2006). Analysis of different genetic traits and their association with biofilm formation in Staphylococcus epidermidis isolates from central venous catheter infections. *Eur. J. Clin. Microbiol. Infect. Dis.* 25 (12), 773–781. doi: 10.1007/s10096-006-0226-8

Planet, P. J., Larussa, S. J., Dana, A., Smith, H., Xu, A., Ryan, C., et al. (2013). Emergence of the epidemic methicillin-resistant Staphylococcus aureus strain USA300 coincides with horizontal transfer of the arginine catabolic mobile element and speG-mediated adaptations for survival on skin. *mBio* 4 (6), e00889–e00813. doi: 10.1128/mBio.00889-13

Raue, S., Fan, S. H., Rosenstein, R., Zabel, S., Luqman, A., Nieselt, K., et al. (2020). The genome of staphylococcus epidermidis O47. *Front. Microbiol.* 11, 2061. doi: 10.3389/fmicb.2020.02061

Rolo, J., Worning, P., Nielsen, J. B., Bowden, R., Bouchami, O., Damborg, P., et al. (2017). Evolutionary origin of the staphylococcal cassette chromosome mec (SCCmec). *Antimicrob. Agents Chemother.* 61 (6), e02302-16. doi: 10.1128/AAC.02302-16

Rosa, N. M., Penati, M., Fusar-Poli, S., Addis, M. F., and Tola, S. (2022). Species identification by MALDI-TOF MS and gap PCR-RFLP of non-aureus Staphylococcus, Mammaliicoccus, and Streptococcus spp. associated with sheep and goat mastitis. *Vet. Res.* 53 (1), 84. doi: 10.1186/s13567-022-01102-4

Salgueiro, V. C., Iorio, N. L., Ferreira, M. C., Chamon, R. C., and Dos Santos, K. R. (2017). Methicillin resistance and virulence genes in invasive and nasal Staphylococcus epidermidis isolates from neonates. *BMC Microbiol.* 17 (1), 15. doi: 10.1186/s12866-017-0930-9

Schaeffer, C. R., Hoang, T.-M. N., Sudbeck, C. M., Alawi, M., Tolo, I. E., Robinson, D. A., et al. (2016). Versatility of Biofilm Matrix Molecules in Staphylococcus epidermidis Clinical Isolates and Importance of Polysaccharide Intercellular Adhesin Expression during High Shear Stress. *mSphere* 1 (5), e00165–e00116. doi: 10.1128/mSphere.00165-16

Sheppard, A. E., Stoesser, N., Wilson, D. J., Sebra, R., Kasarskis, A., Anson, L. W., et al. (2016). Nested Russian doll-like genetic mobility drives rapid dissemination of the carbapenem resistance gene blaKPC. *Antimicrob. Agents Chemother.* 60 (6), 3767–3778. doi: 10.1128/AAC.00464-16

Thomas, J. C., Vargas, M. R., Miragaia, M., Peacock, S. J., Archer, G. L., and Enright, M. C. (2007). Improved multilocus sequence typing scheme for Staphylococcus epidermidis. *J. Clin. Microbiol.* 45 (2), 616–619. doi: 10.1128/JCM.01934-06

Vasu, K., and Nagaraja, V. (2013). Diverse functions of restriction-modification systems in addition to cellular defense. *Microbiol. Mol. Biol. Rev.* 77 (1), 53–72. doi: 10.1128/MMBR.00044-12

Xu, Z., Misra, R., Jamrozy, D., Paterson, G. K., Cutler, R. R., Holmes, M. A., et al. (2018). Whole genome sequence and comparative genomics analysis of multi-drug resistant environmental staphylococcus epidermidis ST59. *G3 (Bethesda)* 8 (7), 2225–2230. doi: 10.1534/g3.118.200314

Yang, Y., Qu, L., Mijakovic, I., and Wei, Y. (2022). Advances in the human skin microbiota and its roles in cutaneous diseases. *Microbial. Cell Factories* 21 (1), 176. doi: 10.1186/s12934-022-01901-6

Zhou, S., Chao, X., Fei, M., Dai, Y., and Liu, B. (2013). Analysis of S. Epidermidis icaA and icaD genes by polymerase chain reaction and slime production: a case control study. *BMC Infect. Dis.* 13, 242. doi: 10.1186/1471-2334-13-242

frontiers | Frontiers in Public Health

TYPE Case Report
PUBLISHED 08 February 2024
DOI 10.3389/fpubh.2023.1307902

OPEN ACCESS

EDITED BY
Gerardo Cortés Cortés,
University of California, Santa Cruz,
United States

REVIEWED BY
Manuel Gerardo Ballesteros Monrreal,
University of Sonora, Mexico
Sahar Rostamian,
Harvard Medical School, United States

*CORRESPONDENCE
Jianbo Liu
✉ 13538759071@163.com

†These authors share first authorship

RECEIVED 05 October 2023
ACCEPTED 29 December 2023
PUBLISHED 08 February 2024

CITATION
Shao A, He Q, Jiao X and Liu J (2024) Hemoptysis caused by *Parvimonas micra*: case report and literature review. *Front. Public Health* 11:1307902. doi: 10.3389/fpubh.2023.1307902

Hemoptysis caused by *Parvimonas micra*: case report and literature review

Axue Shao[1,2†], Qingqing He[1,2†], Xin Jiao[1,2] and Jianbo Liu[1,2*]

[1]The First Clinical Medical School, Guangzhou University of Chinese Medicine, Guangzhou, China,
[2]The First Affiliated Hospital, Guangzhou University of Chinese Medicine, Guangzhou, China

Background: *Parvimonas micra* (*P. micra*), a Gram-positive anaerobic bacterium, exhibits colonization tendencies on oral mucosal and skin surfaces, potentially evolving into a pathogenic entity associated with diverse diseases. The diagnostic trajectory for *P. micra*-related diseases encounters delays, often with severe consequences, including fatality, attributed to the absence of symptom specificity and challenges in culture. The absence of a consensus on the diagnostic and therapeutic approaches to *P. micra* exacerbates the complexity of addressing associated conditions. This study aims to elucidate and scrutinize the clinical manifestations linked to *P. micra*, drawing insights from an extensive literature review of pertinent case reports.

Case presentation: A 53-year-old male sought medical attention at our institution presenting with recurrent hemoptysis. Empirical treatment was initiated while awaiting pathogen culture results; however, the patient's symptoms persisted. Subsequent metagenomic next-generation sequencing (mNGS) analysis revealed a pulmonary infection attributable to *P. micra*. Resolution of symptoms occurred following treatment with piperacillin sulbactam sodium and moxifloxacin hydrochloride. A comprehensive literature review, utilizing the PubMed database, was conducted to assess case reports over the last decade where *P. micra* was identified as the causative agent.

Conclusion: The literature analysis underscores the predilection of *P. micra* for immunocompromised populations afflicted by cardiovascular diseases, diabetes, orthopedic conditions, and tumors. Risk factors, including oral and periodontal hygiene, smoking, and alcohol consumption, were found to be associated with *P. micra* infections. Clinical manifestations encompassed fever, cough, sputum production, and back pain, potentially leading to severe outcomes such as Spondylodiscitis, septic arthritis, lung abscess, bacteremia, sepsis, and mortality. While conventional bacterial culture remains the primary diagnostic tool, emerging technologies like mNGS offer alternative considerations. In terms of treatment modalities, β-lactam antibiotics and nitroimidazoles predominated, exhibiting recovery rates of 56.10% (46/82) and 23.17% (19/82), respectively. This case report and literature review collectively aim to enhance awareness among clinicians and laboratory medicine professionals regarding the intricacies of *P. micra*-associated infections.

KEYWORDS

***Parvimonas micra*, hemoptysis, case report, literature review, MNGs**

Introduction

Parvimonas micra, referred to hereafter as *P. micra*, stands as a Gram-positive anaerobic coccobacillus (GPAC), exhibiting dimensions of approximately 0.3–0.7 µm. Its habitat encompasses the skin and mucosal surfaces of the oral cavity, upper respiratory tract, gastrointestinal tract, and the female genitourinary tract (1, 2). *Parvimonas micra* is implicated as the causative agent in a spectrum of ailments, ranging from sternum osteomyelitis (3), and femur osteomyelitis (4), to sepsis (5), endocarditis (5), hepatic abscesses (6, 7), and even fatal outcomes (1). Notably, *P. micra* predominantly affects immunocompromised hosts (8, 9) with infected individuals often presenting underlying risk factors such as oral infections, diabetes mellitus, and malignant tumors (9, 10). Manifestations of *P. micra* infections typically lack specificity, with reported symptoms encompassing fever, chills, low back pain, abdominal discomfort, gastrointestinal issues, body aches, impaired consciousness, and anorexia in 46 percent of cases (6, 10), as per reviews.

The diagnostic challenge associated with *P. micra* arises from its susceptibility to various pathogens, culture environments, and culture cycles. This often leads to delayed diagnosis, impeding clinicians' comprehension of the condition, appropriate antibiotic selection, and adversely impacting patient prognosis. To date, literature lacks any documented instances of hemoptysis resulting from *P. micra* infection. In this context, we present a case involving a 53-year-old male with *P. micra* lung infection, aiming to heighten clinicians' awareness of *P. micra*-induced extraoral infections and recurrent hemoptysis. Our objective is also to investigate the disease characteristics stemming from *P. micra* infection, achieved through a comprehensive literature review of pertinent case reports on *P. micra*. This endeavor seeks to augment awareness of *P. micra* among clinicians and laboratory medicine personnel.

Case presentation

The patient, a 53-year-old male, sought admission to the First Affiliated Hospital of Guangzhou University of Traditional Chinese Medicine (Guangzhou, China). Over the past year, he reported recurrent hemoptysis episodes, each comprising approximately 30 mL of dark red blood clots, occurring two or three times daily. Notably, the patient exhibited no fatigue or back pain. With a medical history encompassing diabetes mellitus and longstanding tuberculosis, under extended standardized treatment and follow-up for over 30 years, the patient disclosed a smoking history exceeding 10 years. He denied alcohol consumption and reported no family history of infectious or genetic diseases.

Upon admission, the patient presented with a temperature of 36.5°C, a pulse rate of 82 beats/min, a respiratory rate of 20 breaths/min, and a blood pressure reading of 160/95 mm Hg. Physical parameters included a height of 162.0 cm, body weight of 57.50 kg, and a body mass index (BMI) of 21.91 kg/m^2. Auscultation of respiratory sounds revealed rough sounds in both lungs, with diminished breath sounds in the left upper lung. Initial investigations involved routine cultures of respiratory specimens (sputum culture, *Mycobacterium tuberculosis* sputum smear, etc.), with Supplementary Table 1 displaying the preliminary laboratory results. Notably, the Galactomannan antigen test (GM) and D-glucan fungal antigen test (G test) returned negative results.

Chest CT enhancement images unveiled scattered multiple nodules and mass-like shadows in both lungs, featuring irregularly shaped cavities and necrotic areas (see Supplementary Figure 1). Given these findings and the overall clinical presentation, a high likelihood of pulmonary infection was considered. Consequently, empirical intravenous administration of ceftriaxone sodium (2 g, q12h) was initiated on the first day of admission, pending pathogen identification for tailored antibiotic therapy.

On the fourth day post-admission, sputum smear, routine common bacterial and fungal cultures, and *Mycobacterium tuberculosis* and TB-Dot tests yielded no pathogenic evidence. Fiberoptic bronchoscopy (Supplementary Figure 2) was subsequently performed, obtaining bronchoalveolar lavage fluid (BALF) for routine culture and metagenomic next-generation sequencing (mNGS) analysis at Guangzhou Genguji Laboratory Co (Guangzhou, China). Following standard nucleic acid extraction and library construction procedures, the [NextSeq CN500] platform generated high-quality sequencing data, subsequently compared with the Genghis Khan Pathogenic Microorganisms Database containing 31,000+ microorganism sequences to identify and characterize pathogenic microorganisms (Supplementary Figure 3). BALF yielded 255,421,15 clean sequence readings, of which 190,393 were identified as microorganisms at the genus level, with 583 matching Microcystis at the species level (Supplementary Table 2).

Extended routine culture testing of sputum specimens and BALF samples failed to yield positive results. A thorough patient reexamination, including oral examination, revealed halitosis, dark red, or dark black free gingiva and gingival papilla, easy bleeding on probing, localized tartar or calculus, and some loose and shifted teeth. These oral findings were attributed to the patient's prolonged site work, lack of dietary attention, poor personal hygiene habits, and chronic smoking. The oral environment corroborated the mNGS results. However, drug sensitivity testing was omitted for this pathogen, given that mNGS routinely tests for drug-resistance genes in anaerobic bacteria only under exceptional circumstances. Subsequent to literature review and consultation with specialists in the Department of Pharmacy, the treatment regimen transitioned to piperacillin sulbactam sodium (6 g, q12h, IV) and moxifloxacin hydrochloride tablets (0.4 g, qd, PO), supplemented with splenic amine oral lyophilized powder (2 mg, qd, PO) and gamma globulin (2.5 g, qd, IV) to modulate the body's immunity. Simultaneously, pulmonary function rehabilitation training, meridian flow injection, auricular acupuncture, acupoints paste, and other distinctive Chinese medicine treatments were employed to enhance the patient's disease resistance and promote recovery. Following 7 days of treatment, hemoptysis symptoms abated, leading to the patient's discharge. Subsequent outpatient follow-up over 2 months indicated an acceptable condition with no hemoptysis recurrence.

Literature review

Search strategy

A systematic exploration was conducted on the PubMed online databases employing the keywords: "*Parvimonas micra*,"

"Streptococcus micros," "*Peptostreptococcus micros*," "Streptococcus anaerobic micros," "Diplococcus glycinophilus," and "*Peptococcus glycinophilus*."

Inclusion and exclusion criteria

Inclusion criteria encompassed case report studies on *P. micra*-associated diseases (e.g., sepsis, abscesses, and spondylitis) written in English and published after 2013. Exclusion criteria comprised studies published before 2013 and those penned in languages other than English.

Data extraction and analysis

A meticulous review of all articles was undertaken to eliminate duplicate cases, ensuring comprehensive information for inclusion in the review. Data were meticulously extracted and presented as descriptive statistics in an Excel file.

Results

Search results

A total of 726 documents were retrieved using the designated keywords, yielding 84 case reports. Following a full-text review, 10 articles were excluded (six not published in English, and four not attributing *P. micra* as the primary causative organism), resulting in 74 studies meeting the inclusion criteria. A cumulative 82 patients were included, and the specific clinical characteristics of the 74 studies are detailed in Supplementary Table 3.

Demographics

The mean age of patients with *P. micra* was 62.51 years (age range: 23–94 years, excluding one case involving a 9-year-old child). Of the 82 patients, 53 were male (64.63%) and 29 were female (35.37%).

Symptom

Prominent complaints included fever ($n = 23$, 28.05%), cough and sputum ($n = 21$, 25.61%), and low back pain ($n = 18$, 21.95%). Conversely, less frequently observed symptoms encompassed sore throat (1, 1.22%) and tachycardia (1, 1.22%).

Risk factors/underlying disease

Cardiovascular disease history (e.g., atrial fibrillation, congestive heart failure, and cerebrovascular accident) was observed in 24 (29.27%) patients, hypertension in 19 (23.17%), orthopedic disease in 15 (18.29%), and diabetes mellitus in 14 (17.07%). Additionally, 7 (8.54%) patients had a history of tumors, 19 (23.17%) had oral and periodontal problems, 13 (15.85%) had smoking habits, and six (7.32%) had drinking habits.

Infection route

The infection route was reported in 28 (34.15%) cases of oral, 2 (2.44%) cases of the surgical site, 2 (2.44%) cases of mucosal, and 1 (1.22%) case of percutaneous infections. No details about the route of infection were recorded in 49 (59.76%) patients.

Diagnosis method

Among patients, 57 (69.51%) used routine bacterial cultures, 22 (26.83%) used blood cultures, and 35 (42.68%) used other tissue cultures such as pus and puncture biopsy tissues. Additionally, nine cases (10.96%) used mNGS testing, nine cases (10.96%) used MALDI-TOF mass spectrometry, and eight cases (9.56%) used 16S rRNA.

Organism(s)

Various pathogens associated with concomitant multimicrobial infections included *Streptococcus pyogenes*, *Stenotrophomonas maltophilia*, *Pasteurella multocida*, *Fusobacterium nucleatum*, odontolyticus, *Actinomyces meyeri*, *A. rimae*, and others. *Parvimonas micra* as an individual pathogen was found in 53 cases (64.63%).

Desease(s)

In 74 publications, *P. micra* often caused orthopedic-related diseases in 32 cases (39.02%), including spondylodiscitis (11/32, 34.38%), septic arthritis (8/32, 25%); respiratory diseases in 15 cases (18.29%), including lung abscess (7/15, 46.65%), pulmonary embolism (2/15, 13.33%), pneumonia (2/15, 13.33%); and bloodstream infections in 6 cases (7.32%), of which bacteremia (3/6, 50%), sepsis (3/6, 50%).

Antibacterial agents

Beta-lactam antibiotics, such as ceftriaxone, piperacillin/tazobactam, and ampicillin-sulbactam, were used in 50 patients; nitazole antibiotics were used in 20 cases; clindamycin was used in 12 cases; and carbapenem antibiotics were used in seven cases. Among them, 34 cases used two or more antibiotics.

Outcome

A majority of cases (72/82, 87.80%) were successfully treated, with eight cases (9.76%) admitted to the ICU, of which four cases (9.76%) required mechanical ventilation. Ten cases (12.20%) resulted in mortality due to multiple organ failure. Notably, the recovery rate of patients using β-lactam antibiotics was 56.10% (46/82), with a mortality rate of approximately 4.88%. The cure rate for ceftriaxone was 28% (14/50), piperacillin/tazobactam 14% (7/50), and ampicillin/sulbactam sodium 30% (15/50). For patients with nitroimidazoles, the cure rate was 23.17% (19/82); lincomycin 15.85% (13/82); and carbapenems 3.66% (3/82).

Discussion

In scrutinizing 82 case reports detailing *P. micra* infections from the past decade, gleaned from PubMed, our analysis reveals a predilection of *P. micra* for instigating orthopedic-related afflictions such as spondylodiscitis, septic arthritis, and post-surgical prosthetic joint infections. Additionally, respiratory disorders, including lung abscess, septic pulmonary embolism, and septic thorax, emerge as significant sequelae. The spectrum extends to rare occurrences of bacteremia and sepsis. This survey underscores intervertebral disks (11), large joints (12), lungs (13), liver (14), and brain (15) as primary sites of *P. micra* invasion, accentuating the imperative consideration of *P. micra* anaerobic

infections in tandem with conventional bacterial infections in clinical scenarios involving the aforementioned sites.

Based on the literature review, the initial manifestations of *P. micra* infection encompass fever, cough, sputum production, and lower back pain, alongside additional complaints such as malaise, shortness of breath, and weight loss. Predominantly, patients exhibit fever and pain, with the latter concentrated in the lower back, implicating a potential connection to inflammation induced by *P. micra*. Notably, lipoteichoic acid (LTA) is identified as the virulence factor of *P. micra*, a specialized anaerobic Gram-positive coccobacillus residing in the oral cavity. LTA, a membrane-bound polymer characteristic of Gram-positive bacteria, plays fundamental roles in regulating autolysin activity, scavenging divalent cations (e.g., magnesium ions), and altering the cell wall's charge properties, thereby influencing bacterial-host cell interactions (16–18).

Recent scholarship, both domestically and internationally, has delved into the biological activity of LTA in Gram-positive pathogenic bacteria within the oral cavity. Findings indicate that LTA elicits immune and inflammatory responses, inducing the release of inflammatory factors like TNF-α, IL-1β, and IL-6 from neutrophils and macrophages, thereby contributing to local inflammation and edema. Moreover, *P. micra* demonstrates robust protein hydrolase activity, generating various pathogenic substances such as protein hydrolase, collagenase, and hyaluronidase (19–21), fostering tissue lysis and inflammation expansion (20, 21).

Some studies reveal that *P. micra*, present in infected root canals of patients with chronic apical periodontitis, engages in metabolic processes utilizing amino acids and polypeptides, establishing trophic symbiosis with dominant pathogenic bacteria in dental pulp (22). This symbiotic relationship enhances mutual virulence and resistance, playing a pivotal role in pathogenic effects. Combining these insights with the literature review, it can be inferred that *P. micra* employs three primary routes to infect different human body parts: bloodstream transmission, direct external inoculation, and transmission from neighboring tissues. Among these, bloodstream dissemination resulting from oral infection emerges as the most prevalent transmission route. Periodontitis history, dental surgery, and poor oral hygiene strongly correlate with *P. micra* infection, as documented in literature (23, 24). Oral infections and compromised oral health facilitate the entry of *P. micra* or soluble toxins into the bloodstream, where they interact with circulating specific antibodies, causing immune damage and inflammation at distant sites (25). Hematogenous dissemination may reach the spine, affecting blood-rich vertebral endplates initially and subsequently leading to local spread to adjacent intervertebral disks or vertebral bodies, resulting in characteristic lesions of intervertebral space infection. Rarely, the infection may spread posteriorly, giving rise to epidural or subdural abscesses, or even meningitis. Lateral spread can lead to various abscess formations, including lumbar major, retroperitoneal, subphrenic, paravertebral, retropharyngeal, and mediastinal abscesses. Primary sites of infection encompass the oral cavity, skin mucosa and soft tissues, respiratory tract, and surgical incisions.

In this presented case, the predominant clinical manifestation was hemoptysis, a recognized symptom frequently associated with pulmonary, bronchial, and circulatory disorders, carrying a substantial risk of asphyxiation and mortality, with an estimated 15% fatality rate in cases of massive hemoptysis (26). Globally, tuberculosis stands as the primary association with hemoptysis; nonetheless, the etiological spectrum encompasses a broad array of pulmonary (e.g., infection, malignancy, airway injury, or trauma), cardiac (e.g., heart failure, cardiac valvular disease, and pulmonary hypertension), vascular (e.g., pulmonary embolism and arteriovenous malformations), vasculitides (e.g., granulomatous polyangiitis), and miscellaneous factors, including coagulation disorders (medical, acquired, and congenital), drug-induced complications, and alveolar protein deposition disorders (27). In the context of our reported case, the patient's history included remote tuberculosis with hemoptysis over 3 decades prior, which significantly predates the current episode. The patient reported resolution following standardized anti-tuberculosis treatment. Based on the hospitalization, tuberculosis-related test outcomes, and imaging findings, we excluded the recurrence of tuberculosis and bronchiectasis as contributing factors.

Conversely, hemoptysis attributed to *Parvimonas micra* is a clinical rarity. As posited by Dustin L. Higashi, *P. micra* displays characteristic features of an inflammatory organism, thriving in the milieu of active inflammation and the destruction of inflammatory tissue. It ranks among the most prevalent species in numerous studies of mucosal inflammatory diseases and systemic abscesses (28). Murphy's research further delineates *P. micra*'s induction of macrophages to secrete elevated levels of IL-6, IL-8, and RANTES, along with the stimulation of pro-inflammatory cytokines such as PKA, ERK2, JNK, and p38 from various intracellular signaling pathways. These mechanisms collectively potentiate endotoxin action, thereby influencing the onset of inflammatory responses (2). The hypothesis posits that *P. micra* may release diverse inflammatory mediators through these mechanisms, culminating in the compromise of capillaries within bronchial mucosa or lesions, ultimately resulting in the rupture of submucosal blood vessels and increased permeability, culminating in hemoptysis.

Regarding the diagnostic approaches for *P. micra*, the cases documented in the literature indicate that routine bacterial cultures, including blood culture (26.83%) and culture from puncture biopsy of pus and tissue (42.68%), were predominantly utilized for detection. In our presented case, conventional culture tests yielded negative results, prompting the adoption of metagenomic next-generation sequencing (mNGS) for a definitive diagnosis. This deviation from traditional diagnostic methods is underscored by the inherent limitations of conventional pathogen testing, such as susceptibility to the culture environment, prolonged culture duration, potential impact of prior antibiotic administration, and specific characteristics of the pathogen itself (29). These limitations contribute to the clinical plausibility of false-negative outcomes. Therefore, when conventional pathogen detection yields inconclusive results or when patients exhibit limited improvement despite extended treatment, innovative techniques like mNGS, MALDI-TOF mass spectrometry analysis, and 16S rRNA detection prove invaluable for rapid pathogen identification, guiding subsequent tailored treatments.

Regarding treatment, in this particular case with a clearly identified pathogen, the empirical use of ceftriaxone was replaced with piperacillin sulbactam sodium and moxifloxacin, resulting in alleviation of the patient's hemoptysis symptoms. It is noteworthy that there is currently no consensus on the antibiotic treatment of *P. micra*. Literature review indicates *P. micra*'s high sensitivity to various antibiotics, including penicillin, meropenem, clindamycin, piperacillin

sodium sulbactam sodium, vancomycin, and linezolid (30–32). However, some studies report varying degrees of resistance to penicillin, metronidazole, clindamycin, and vancomycin, while showing susceptibility to imipenem and piperacillin sodium sulbactam sodium (32–34). This aligns with the findings of our case. Notably, our literature review suggests that most cases exhibit favorable outcomes when treated with β-lactams and narrow-spectrum anti-anaerobic drugs like ceftriaxone, piperacillin/tazobactam, ampicillin-sulbactam, clindamycin, and metronidazole. However, our case deviated from this trend, with no improvement observed after ceftriaxone treatment, possibly indicating strain-specific variations in *P. micra*'s response to the same antibiotic (35).

A minority of reported cases (36–38) exhibited uncontrolled infections post-treatment: 8 (9.76%) required ICU admission, 4 (9.76%) underwent mechanical ventilation, and 10 (12.20%) succumbed to multi-organ failure. Consequently, we advocate for drug susceptibility testing specific to *P. micra* to inform antimicrobial usage when conditions permit. Additionally, attention should be directed toward defining the duration of antibiotic use for different sites of *P. micra* infections, and criteria for discontinuation should include symptomatic regression, improvement, and normalization of infection markers such as ESR or CRP. Our case collection underscores the significance of surgery, thorough debridement, and a combination of antimicrobial drugs in addressing *P. micra*-associated abscesses in bone, joints, muscles, lungs, and brain.

In terms of prognosis, 72 patients (87.80%) exhibited a gradual recovery from the infection, while 10 patients (12.20%) succumbed to multiorgan failure (14, 36, 39–44), the majority of whom presented severe comorbid underlying conditions such as cardiovascular diseases, neoplasms, and immune-related diseases. This underscores the imperative need for heightened vigilance regarding *P. micra* infection, particularly in individuals predisposed to compromised oral hygiene, diabetes mellitus, malignancy, and cardiovascular and cerebrovascular diseases. Furthermore, attention should be directed toward patients exhibiting nonspecific symptoms, including high fever of unknown origin, pain, and hemoptysis, with the aim of facilitating early detection and treatment of *P. micra*-induced infections.

In conclusion, we present a case of pulmonary infection attributed to *P. micra*, where hemoptysis serves as the primary symptom. Through a comprehensive review of pertinent literature, our intent is to direct clinicians' attention toward *P. micra*, offering insights for clinical diagnosis and treatment.

Written informed consent for the publication of this report, inclusive of lung CT images, was obtained from the patients. This study adhered to the principles of the Declaration of Helsinki and received approval from the Research Ethics Committee of the First Affiliated Hospital of Guangzhou University of Traditional Chinese Medicine (JY2022-264).

Limitation

Nevertheless, several limitations exist in this case report. Firstly, routine culture tests failed to detect *P. micra* and other microorganisms, potentially attributable to various factors such as sampling techniques, professional proficiency, and the purity of *P. micra*. Secondly, alternative diagnostic methods, including 16S rRNA gene sequencing, PCR nucleic acid sequencing, and lung tissue biopsy mNGS, were not employed. Additionally, post-treatment bronchoalveolar lavage fluids were not subjected to mNGS testing to confirm the complete eradication of *P. micra*. Lastly, the mechanism of hemoptysis induced by *P. micra* remains under investigation, and a consensus on the treatment of *P. micra* infection is yet to be established, necessitating further follow-up studies.

Data availability statement

The raw data has been uploaded and is available in the EBI Metagenomics database with the serial number: PRJEB72347. Further inquiries can be directed to the corresponding author.

Ethics statement

The studies involving human participants were reviewed and approved by Medicine Ethics Committee of First Affiliated Hospital of Guangzhou University of Chinese Medicine. Written informed consent was obtained from the individual for the publication of any potentially identifiable images or data included in this article.

Author contributions

AS: Writing – original draft. QH: Writing – original draft. XJ: Writing – review & editing. JL: Writing – review & editing.

Funding

The author(s) declare that no financial support was received for the research, authorship, and/or publication of this article.

Conflict of interest

The authors declare that the research was conducted in the absence of any commercial or financial relationships that could be construed as a potential conflict of interest.

Publisher's note

Supplementary material

The Supplementary material for this article can be found online at: https://www.frontiersin.org/articles/10.3389/fpubh.2023.1307902/full#supplementary-material

References

1. Jiang Y, Qin W, Li J, Gao Y, Zeng Y. A case report of Sepsis and death caused by *Parvimonas Micra*, a rare anaerobe. *Front Public Health*. (2022) 10:994279. doi: 10.3389/fpubh.2022.994279

2. Murphy EC, Frick IM. Gram-positive anaerobic cocci--commensals and opportunistic pathogens. *FEMS Microbiol Rev*. (2013) 37:520–53. doi: 10.1111/1574-6976.12005

3. Aranowicz A, van den Brandt SL, Slankamenac K, Keller DI. Destructive osteomyelitis involving Parvimonas Micra and *Campylobacter Rectus*. *BMJ Case Rep*. (2022) 15:e250886. doi: 10.1136/bcr-2022-250886

4. Itoh N, Akazawa N, Ishibana Y, Hamada S, Hagiwara S, Murakami H. Femoral osteomyelitis caused by Oral anaerobic Bacteria with mixed bacteremia of campylobacter rectus and *Parvimonas Micra* in a chronic periodontitis patient: a case report. *BMC Infect Dis*. (2022) 22:613. doi: 10.1186/s12879-022-07573-2

5. Suzuki T, Ishikawa K, Matsuo T, Kijima Y, Aoyagi H, Kawai F, et al. Pacemaker infection and endocarditis due to *Parvimonas Micra*: a case report and systematic review. *Anaerobe*. (2021) 72:102459. doi: 10.1016/j.anaerobe.2021.102459

6. Strobel S, Whitaker D, Choi E, Lindow J, Lago K. *P. micra* and *F. necrophorum*: hepatic abscesses in a healthy soldier. *Hepat Abscess Healthy Soldier*. (2022) 2022:5500365. doi: 10.1155/2022/5500365

7. Ho A, Duvapu B, Duong N, Samantara S. First case of splenic abscess Parvimonas Micra and bacteremia *Porphyromonas Gingivalis* coinfection. *Cureus*. (2022) 14:e28103. doi: 10.7759/cureus.28103

8. Tindall BJ, Euzéby JP. Proposal of Parvimonas gen. Nov. and Quatrionicoccus gen. Nov. as replacements for the illegitimate, prokaryotic, generic names Micromonas Murdoch and Shah 2000 and Quadricoccus Maszenan et Al. 2002, respectively. *Int J Syst Evol Microbiol*. (2006) 56:2711–3. doi: 10.1099/ijs.0.64338-0

9. Didilescu AC, Rusu D, Anghel A, Nica L, Iliescu A, Greabu M, et al. Investigation of six selected bacterial species in Endo-periodontal lesions. *Int Endod J*. (2012) 45:282–93. doi: 10.1111/j.1365-2591.2011.01974.x.

10. Shimizu K, Horinishi Y, Sano C, Ohta R. Infection route of Parvimonas Micra: A case report and systematic review. *Health*. (2022) 10. doi: 10.3390/healthcare10091727

11. Uemura H, Hayakawa K, Shimada K, Tojo M, Nagamatsu M, Miyoshi-Akiyama T, et al. *Parvimonas Micra* as a causative organism of spondylodiscitis: a report of two cases and a literature review. *Int J Infect Dis*. (2014) 23:53–5. doi: 10.1016/j.ijid.2014.02.007

12. Roy M, Roy AK, Ahmad S. Septic arthritis of knee joint due to *Parvimonas Micra*. *BMJ Case Rep*. (2017) 2017. doi: 10.1136/bcr-2017-221926

13. Zhang Y, Song P, Zhang R, Yao Y, Shen L, Ma Q, et al. Clinical characteristics of chronic lung abscess associated with *Parvimonas Micra* diagnosed using metagenomic next-generation sequencing. *Infect Drug Resis*. (2021) 14:1191–8. doi: 10.2147/idr.S304569

14. Kim EY, Baek YH, Jung DS, Woo KS. Concomitant liver and brain abscesses caused by *Parvimonas Micra*. *Kor J Gastroenterol*. (2019) 73:230–4. doi: 10.4166/kjg.2019.73.4.230

15. Vazquez Guillamet LJ, Malinis MF, Meyer JP. Emerging role of *Actinomyces Meyeri* in brain abscesses: a case report and literature review. *IDCases*. (2017) 10:26–9. doi: 10.1016/j.idcr.2017.07.007

16. Jin L, Zhu W, Xia D. Effect of *Streptococcus pyogenes* lipophosphatidic acid on the differentiation ability of human periodontal membrane stem cells. *Beijing Stomatol*. (2018) 26:1–4.

17. Wang L, Ye D, Wang J, Niu W. *Enterococcus faecalis* LTA activates NLRP3 inflammasome by promoting high ROS expression. *Oral Med Res*. (2018) 34:112–6.

18. Lin D, Chen Y, Peng Z, Gao Y. Effects of *Enterococcus faecalis* lipophosphatidic acid on macrophage autophagy. *Chin J Oral Med Res*. (2018) 12:69–75.

19. Uematsu H, Hossain MZ, Alam T, Ikeda T, Kuvatanasuchati J, Hoshino E Degradation of serinecontainning oligopeptides by Peptosteptcoccus micros ATCC 33270. *Oral Microbiol Immunol* (2007) 22: 381–383. doi: 10.1111/j.1399-302X.2007.00374.x

20. Ota-Tsuzuki C, Alves Mayer MP. Collagenase production and hemolytic activity related to 16S rRNA variability among *Parvimonas micra* oral isolates. *Anaerobe*. (2010) 16:38–42. doi: 10.1016/j.anaerobe.2009.03.008

21. Tam YC, Chan EC. Purification and characterization of hyaluronidase from oral Peptostreptococcus species. *Infect Immun*. (1985) 47:508–13. doi: 10.1128/iai.47.2.508-513.1985

22. Cobankara FK, Orucoglu H, Sengun A, Belli S. The quantitative evaluation of apical sealing of four endodontic sealers. *J Endodontics*. (2006) 32:66–8. doi: 10.1016/j.joen.2005.10.019

23. Gahier M, Cozic C, Bourdon S, Guimard T, Cormier G. Spinal infections caused by *Parvimonas micra*. *Med Mal Infect*. (2015) 45:397–8. doi: 10.1016/j.medmal.2015.07.006

24. Endo S, Nemoto T, Yano H, Kakuta R, Kanamori H, Inomata S, et al. First confirmed case of spondylodiscitis with epidural abscess caused by *Parvimonas micra*. *J Infect Chemother*. (2015) 21:828–30. doi: 10.1016/j.jiac.2015.06.002

25. van de Beek D, Farrar JJ, de Gans J, Mai NT, Molyneux EM, Peltola H, et al. Adjunctive dexamethasone in bacterial meningitis: a meta-analysis of individual patient data. *Lancet Neurol*. (2010) 9:254–63. doi: 10.1016/S1474-4422(10)70023-5

26. Wang Y, Wang X, Fu H, Kou S, Huang D, Shen Z, et al. Yunnan Baiyao adjuvant treatment for patients with hemoptysis: a systematic review and Meta-analysis. *eCAM*. (2022) 2022:1–14. doi: 10.1155/2022/4931284

27. O'Corragain OA, Gupta R. A 49-year-old man with Postcoital hemoptysis. *Chest*. (2021) 159:e81–5. doi: 10.1016/j.chest.2020.08.2095

28. Higashi DL, Krieger MC, Qin H, Zou Z, Palmer EA, Kreth J, et al. Who is in the Driver's seat? *Parvimonas Micra*: An understudied Pathobiont at the crossroads of Dysbiotic disease and Cancer. *Environ Microbiol Rep*. (2023) 15:254–64. doi: 10.1111/1758-2229.13153

29. Jin X, Li J, Shao M, Lv X, Ji N, Zhu Y, et al. Improving suspected pulmonary infection diagnosis by Bronchoalveolar lavage fluid metagenomic next-generation sequencing: a multicenter retrospective study. *Microbiol Spectr*. (2022) 10:e0247321. doi: 10.1128/spectrum.02473-21

30. Watanabe T, Hara Y, Yoshimi Y, Fujita Y, Yokoe M, Noguchi Y. Clinical characteristics of bloodstream infection by *Parvimonas micra*: retrospective case series and literature review. *BMC Infect Dis*. (2020) 20:578. doi: 10.1186/s12879-020-05305-y

31. Boattini M, Bianco G, Cavallo R, Costa C. *Parvimonas micra* bacteremia following endoscopic retrograde cholangiopancreatography: a new route of infection. *Anaerobe*. (2018) 54:136–9. doi: 10.1016/j.anaerobe.2018.09.003

32. Guérin F, Dejoies L, Degand N, Guet-Revillet H, Janvier F, Corvec S, et al. Vitro antimicrobial susceptibility profiles of gram-positive anaerobic cocci responsible for human invasive infections. *Microorganisms*. (2021) 9:1665. doi: 10.3390/microorganisms9081665

33. Badri M, Nilson B, Ragnarsson S, Senneby E, Rasmussen M. Clinical and microbiological features of bacteraemia with gram-positive anaerobic cocci: a population-based retrospective study. *Clin Microbiol Infect*. (2019) 25:760.e1–6. doi: 10.1016/j.cmi.2018.09.001

34. Rams TE, Sautter JD, van Winkelhoff AJ. Antibiotic resistance of human periodontal pathogen *Parvimonas micra* over 10 years. *Antibiotics*. (2020) 9:709. doi: 10.3390/antibiotics9100709

35. Shilnikova II, Dmitrieva NV. Evaluation of antibiotic susceptibility of gram-positive anaerobic cocci isolated from Cancer patients of the N. *N Blokhin Russian Cancer Res Center J Pathog*. (2015) 2015:648134. doi: 10.1155/2015/648134

36. Yu Q, Sun L, Xu Z, Fan L, Du Y. Severe pneumonia caused by *Parvimonas Micra*: a case report. *BMC Infect Dis*. (2021) 21:364. doi: 10.1186/s12879-021-06058-y

37. Cobo F, Borrego J, Rojo MD, Navarro-Marí JM. Polymicrobial anaerobic bacteremia due to Atopobium Rimae and *Parvimonas Micra* in a patient with Cancer. *Anaerobe*. (2018) 54:260–3. doi: 10.1016/j.anaerobe.2018.02.002

38. García Carretero R, Luna-Heredia E, Olid-Velilla M, Vazquez-Gomez O. Bacteraemia due to *Parvimonas Micra*, a commensal pathogen, in a patient with an Oesophageal tumour. *BMJ Case Rep*. (2016) 2016:bcr2016217740. doi: 10.1136/bcr-2016-217740

39. Orsini J, Frawley BJ, Gawlak H, Gooch R, Escovar J. Severe Sepsis with septic shock as a consequence of a severe community-acquired pneumonia resulting from a combined legionella Pneumophila and *Streptococcus Pneumoniae* infection. *Cureus*. (2020) 12:e10966. doi: 10.7759/cureus.10966

40. Cesta N, Foroghi Biland L, Neri B, Mossa M, Campogiani L, Caldara F, et al. Multiple hepatic and brain abscesses caused by *Parvimonas Micra*: a case report and literature review. *Anaerobe*. (2021) 69:102366. doi: 10.1016/j.anaerobe.2021.102366

41. Miyazaki M, Asaka T, Takemoto M, Nakano T. Severe Sepsis caused by *Parvimonas Micra* identified using 16s ribosomal Rna gene sequencing following patient death. *IDCases*. (2020) 19:e00687. doi: 10.1016/j.idcr.2019.e00687

42. Sawai T, Koga S, Ide S, Yoshioka S, Matsuo N, Mukae H. An iliopsoas abscess caused by *Parvimonas Micra*: a case report. *J Med Case Rep*. (2019) 13:47. doi: 10.1186/s13256-019-2004-0

43. Chaucer B, Smith N, Beatty D, Yadav M. Multiple hepatic abscess from *Parvimonas Micra*: an emerging gastrointestinal microbe. *ACG Case Rep J*. (2018) 5:e70. doi: 10.14309/crj.2018.70

44. Bangert E, Hofkirchner A, Towheed TE. Concomitant *Parvimonas Micra* septic arthritis and Pseudogout after Total knee arthroplasty. *J Clin Rheumatol*. (2019) 25:e47–50. doi: 10.1097/rhu.0000000000000728

frontiers | Frontiers in Cellular and Infection Microbiology

TYPE Original Research
PUBLISHED 07 January 2025
DOI 10.3389/fcimb.2023.1259764

OPEN ACCESS

EDITED BY
Margarita María De La Paz Arenas-Hernandez,
Benemérita Universidad Autónoma de Puebla, Mexico

REVIEWED BY
Edwin Barrios-Villa,
Universidad de Sonora, Sonora, Mexico
Tahereh Navidifar,
Shoushtar Faculty of Medical Sciences, Iran

*CORRESPONDENCE
Fernando A. Gonzales-Zubiate
fgonzales@yachaytech.edu.ec
Nilton Lincopan
lincopan@usp.br

RECEIVED 16 July 2023
ACCEPTED 10 October 2023
PUBLISHED 07 January 2025

CITATION
Gonzales-Zubiate FA, Tambor JHM, Valencia-Bacca J, Villota-Burbano MF, Cardenas-Arias A, Esposito F, Moura Q, Fuga B, Sano E, Pariona JGM, Jacome MPO and Lincopan N (2025) Pandemic one health clones of *Escherichia coli* and *Klebsiella pneumoniae* producing CTX-M-14, CTX-M-27, CTX-M-55 and CTX-M-65 ESβLs among companion animals in northern Ecuador. *Front. Cell. Infect. Microbiol.* 13:1259764. doi: 10.3389/fcimb.2023.1259764

Pandemic one health clones of *Escherichia coli* and *Klebsiella pneumoniae* producing CTX-M-14, CTX-M-27, CTX-M-55 and CTX-M-65 ESβLs among companion animals in northern Ecuador

Fernando A. Gonzales-Zubiate[1*], José Humberto M. Tambor[2,3], Juan Valencia-Bacca[4], María Fernanda Villota-Burbano[5], Adriana Cardenas-Arias[6,7], Fernanda Esposito[6,8], Quézia Moura[9], Bruna Fuga[6,7,8], Elder Sano[7], Jesus G. M. Pariona[8], Mishell Poleth Ortiz Jacome[1] and Nilton Lincopan[6,7,8*]

[1]School of Biological Sciences & Engineering, Yachay Tech University, San Miguel de Urcuquí, Ecuador, [2]Centro Universitário ENIAC, São Paulo, Brazil, [3]INTI International University, Persiaran Perdana BBN, Nilai, Negeri Sembilan, Malaysia, [4]Department of Microbiology and Immunology, Wake Forest School of Medicine, Winston Salem, NC, United States, [5]Dogs & Cats Hospital Veterinario, Ibarra, Imbabura, Ecuador, [6]One Health Brazilian Resistance Project (OneBR), São Paulo, Brazil, [7]Department of Microbiology, Institute of Biomedical Sciences, University of São Paulo, São Paulo, Brazil, [8]Department of Clinical Analysis, School of Pharmacy, University of São Paulo, São Paulo, Brazil, [9]Federal Institute of Espírito Santo, Vila Velha, Brazil

From a One Health perspective, dogs and cats have begun to be recognized as important reservoirs for clinically significant multidrug-resistant bacterial pathogens. In this study, we investigated the occurrence and genomic features of ESβL producing Enterobacterales isolated from dogs, in the province of Imbabura, Ecuador. We identified four isolates expressing ESβLs from healthy and diseased animals. In this regard, two *Escherichia coli* strains producing CTX-M-55-like or CTX-M-65 ESβLs belonged to the international ST10 and ST162, whereas two *Klebsiella pneumoniae* producing CTX-M-14 or CTX-M-27 belonged to ST35 and ST661. Phylogenomic analysis clustered (95-105 SNP differences) CTX-M-55/ST10 *E. coli* from companion animal with food and human *E. coli* strains of ST10 isolated in 2016, in Australia and Cambodia, respectively; whereas CTX-M-27-positive *K. pneumoniae* ST661 was clustered (201-216 SNP differences) with human strains identified in Italy, in 2013 and 2017, respectively. In summary, we report the presence and genomic data of global

human-associated clones of CTX-M-producing *E. coli* and *K. pneumoniae* in dogs, in Ecuador. The implementation of a national epidemiological surveillance program is necessary to establish future strategies to control the dissemination of antibiotic-resistant priority pathogens using a One Health approach.

KEYWORDS

ESβL, gram-negative bacteria, Enterobacterales, antimicrobial resistance, One Health, veterinary medicine, genomic data

1 Introduction

Although Enterobacterales are natural inhabitants of the intestinal tract of mammals, some genus and species can cause infections of the respiratory and urinary systems, skin, ear, and soft tissue of human and non-human hosts (Zogg et al., 2018). In this regard, *Escherichia coli* and *Klebsiella pneumoniae* are leading causes of healthcare-associated infections worldwide (Pesesky et al., 2015), with carbapenem- and broad-spectrum cephalosporin-resistant lineages being categorized as critical priority pathogens by the World Health Organization (Tacconelli et al., 2018). Certainly, and even more worrying is the fact that extended-spectrum β-lactamase (ESβL)-producing strains are no longer restricted to hospital locations but also represents a serious problem involving pets, wildlife, and environmental and food safety (Lopes et al., 2021; Salgado-Caxito et al., 2021).

CTX-M enzymes have become the most prevalent type of ESβLs globally (Cantón & Coque, 2006; Pitout and Laupland, 2008). It is remarkable that the first report on the emergence of a CTX-M enzyme was in 1988, from a laboratory dog used in β-lactams research in Japan (Matsumoto et al., 1988), whereas *E. coli* producing $bla_{\text{CTX-M-1}}$-type enzyme was first described in a healthy dog in Portugal. Since then, a significant occurrence of CTX-M-type ESβL-producing Enterobacterales has been documented in healthy and diseased dogs and cats from Asian, European and South American countries (Salgado-Caxito et al., 2021).

From a public health perspective, the rapid appearance of resistant bacterial populations among dogs and cats, and the close contact between household pets and people have favored the transmission of antibiotic-resistant bacteria from companion animals to humans (Damborg et al., 2016; Kawamura et al., 2017; Salgado-Caxito et al., 2021; Sellera et al., 2021). Transfer of resistant bacteria between humans and their dogs has been well documented (Albrechtova et al., 2012), as was illustrated by the identification of the same *E. coli* clone from a urinary tract infection in a dog, and from its household members (Johnson et al., 2008), although the direction of transfer is often difficult to prove (Pomba et al., 2017). In addition, the intensive use of antimicrobials in animals can be an important factor in the development of antimicrobial-resistant microorganisms (Caprioli et al., 2000; Umber and Bender, 2009; Marshall and Levy, 2011; Seiffert et al., 2013; Samanta et al., 2015). In this sense, companion animals might act as source of human contamination but may also be contaminated by human bacteria (Okubo et al., 2014; Fernandes et al., 2018; Melo et al., 2018). Furthermore, the role of companion animals as a source of AMR has, so far, been neglected (Ewers et al., 2012).

In South America, multidrug-resistant Enterobacterales are a major concern as the region exhibits some of the higher rates of antimicrobial resistance worldwide (Bonelli et al., 2014). The first report of ESβL in this region in companion animals was published in 2008 from *E. coli* isolates obtained from fecal samples of dogs and cats in Chile (Moreno et al., 2008). In that context, nosocomial infections caused by ESβL producing Enterobacterales have increased in the region more than others, since 2005 (Guzmán-Blanco et al., 2014). Several factors such living in crowded conditions, malnutrition, ineffective healthcare systems, deficient drug supply chain, massive use of antimicrobials in livestock and agriculture linked to lack of financial resources might be related to the greater prevalence of ESβLs in countries with lower economic resources (Villegas et al., 2008). In this study, we report the occurrence and genomic data of ESβL-producing *E. coli* and *K. pneumoniae* strains in dogs from Imbabura, Ecuador.

2 Materials and methods

2.1 Bacterial isolates and antibiotic susceptibility profile

During a microbiological and genomic surveillance study carried out in 2018, a total of 125 rectal swabs from dogs (64 healthy animals and 61 sick animals) were collected from the province of Imbabura in Ecuador, in order to monitor the presence of clinically significant drug-resistant Gram-negative bacteria in companion animals (Supplementary Table 1). Samples were collected between April and June and between October and December 2018; from a veterinary clinic located in Ibarra that attend the following counties in Imbabura: Antonio Ante, Cotacachi, Ibarra, Otavalo, Pimampiro, and San Miguel de Urcuquí (Figure S1).

The samples were cultured on blood and MacConkey agar plates supplemented with ceftriaxone (2 μg/mL) being incubated at 37°C overnight (Jacob et al., 2020). Bacteria were identified by conventional biochemical tests, whereas antimicrobial susceptibility testing was performed by the disk diffusion method on Mueller–

Hinton agar plates (Clinical and Laboratory Standards Institute, 2023a; Clinical and Laboratory Standards Institute, 2023b). In addition, human and veterinary antibiotics including amoxicillin-clavulanic acid, ceftazidime, cefotaxime, ceftriaxone, ceftiofur, cefepime, cefoxitin, aztreonam, ertapenem, meropenem, imipenem, nalidixic acid, enrofloxacin, ciprofloxacin, trimethoprim/sulfamethoxazole, gentamicin, amikacin, and chloramphenicol, were tested (Supplementary Table 2). Additionally, minimum inhibitory concentration (MIC) of cefotaxime was determined by using ETEST® strips (bioMérieux). The results were interpreted according to Clinical and Laboratory Standards Institute (Clinical and Laboratory Standards Institute, 2023a; Clinical and Laboratory Standards Institute, 2023b). ESβL production was screened by the double disk synergy test (DDST) (Jarlier et al., 1988).

2.2 Whole genome sequencing analysis

Whole genomic DNA was extracted (PureLinkTM; Invitrogen) and used to prepare a library that was sequenced using the NextSeq550 platform (2 x 75-bp paired-end) (Illumina), and the *de novo* assembly method was the Unicycler v.0.4.8 with Phred20 as minimum score quality of reads. The contigs generated for all genomes were submitted to NCBI using the WGS submission and automatic annotation was performed by PGAP (Prokaryotic Genome Annotation Pipeline v.3.2.); CDSs, RNAs and pseudo genes are shown in Tables 1, 2. The genomes were analyzed by MLST 2.0, ResFinder 4.1, and PlasmidFinder 2.1 tools from the Center for Genomic Epidemiology (CGE). Additionally, antibiotic resistance and virulence genes were predicted using the Comprehensive Antibiotic Resistance Database (CARD) and the Virulence Factor Database (VFDB), respectively, whereas genes related with mercury, arsenic and disinfectant resistance (quaternary ammonium compounds) were screened using an in-house and the BIGSdb database. For phylotyping *E. coli*, the *in silico* Clermont phylotyper tool was used (https://ezclermont.hutton.ac.uk/).

2.3 Phylogenetic analysis

A search for genomic data of isolates for each sequence type identified was performed, in order to recruit genomes for phylogenetic comparison. Assemblies with no metadata for country, year and source of isolation were ignored. For *E. coli* strains, genomes were downloaded from Enterobase (3,572 assemblies of *E. coli* ST10 and 442 assemblies of ST162), while for *K. pneumoniae* strains, a search for each ST were performed on bacWGSTdb (http://bacdb.cn/BacWGSTdb/), and genomes were downloaded from NCBI GenBank (*i.e.*, 60 assemblies of *K. pneumoniae* ST35 and 19 assemblies of ST661). With exception of ST661, which had only 19 assemblies downloaded, 30 genomes with highest average nucleotide identity (ANI) of each ST comparing with this work's assemblies were performed using

TABLE 1 Genomic characteristics of lineages of ESBL-producing *Escherichia coli* strains recovered from rectal swabs collected in dogs in Ecuador.

Characteristics	ECU3_SQ178	EE12_SQ154
Source	Dog rectal swab	Dog rectal swab
Year of isolation	2018	2018
Genome size (bp)	4,847,206	4,893,054
G + C content (%)	50,7	50,7
rRNA	2	2
tRNAs	45	39
ncRNAs	7	9
N° total of genes	4,784	4,727
No. of CDS[a]	4,595	4,549
ST	10	162
Clermont phylotype	A	B1
Resistome		
β-Lactams	$bla_{CTX\text{-}M\text{-}55}$-like	$bla_{CTX\text{-}M\text{-}65}$
Aminoglycosides	*aph(3")-Ib*, *aph(6)-Id*	*aadA1*, *aadA2b*
Phenicols	*florR*	*clmA1*
Sulfonamides	*sul2*	*sul3*
Tetracycline	*tetA*	–
Trimethoprim	–	*dfrA1*
Fosfomycin	*fosA3*	*fosA3*
Quinolones	*gyrA* (D87N), *parC* (S80I), *marA*	*marA*
Heavy metal		
Arsenic	*arsB*, *arsC*, *arsR*	*arsB*, *arsR*
Mercury	-	*merR*
Tellurium	*tehA*, *tehB*	*tehA*, *tehB*
Biocides and disinfectants	*mdtEFKN*, *emrDK*, *acrAEF*, *tolC*	*mdtEFK*, *emrDK*, *mvrC*, *acrAEF*, *tolC*, *qacF*
Herbicides (glyphosate)	*phnCDFGHIJKLMNOP*	*phnJ*
Virulome		
Common pilus	*yagZ/ecpA*, *yagY/ecpB*, *yagX/ecpC*, *yagW/ecpD*	*yagZ/ecpA*, *yagY/ecpB*, *yagX/ecpC*, *yagW/ecpD*
Fimbrial protein	-	*fimBCDEGI*
Enterobactin siderophore	*entB*	-
Salmochelin siderophore	*iroCDEN*	*iroCDEN*
Type II secretion system (T2SS)	*gspM*	*gspK*
Plasmids	IncFIA, IncFIB, IncFII	IncFIB
GenBank accession number	JACWHI000000000.1	JACWHK000000000.1

TABLE 2 Genomic characteristics of lineages of ESBL-producing *Klebsiella pneumoniae* strains recovered from rectal swabs collected in dogs in Ecuador.

Characteristics	ECUD12_SQ166	EE25K_SQ190
Source	Dog rectal swab	Dog rectal swab
Year of isolation	2018	2018
Genome size (bp)	5,342,763	5,560,571
G + C content (%)	57,4	57,2
rRNA	2	2
tRNAs	39	46
ncRNAs	7	8
N° total of genes	5,283	5,412
No. of CDS[a]	5,142	5,270
ST	661	35
K-locus/O-locus	KL28/O2v1	-/O1v1
wzi/ICE*Kp*/*ybt*	84/-/-	37/ICE*Kp3*/*ybt 9*
Resistome		
β-Lactams	$bla_{CTX-M-27}$, bla_{SHV-27}	$bla_{CTX-M-14}$, bla_{LAP-2}, bla_{SHV-33}
Aminoglycosides	*aac(3)IV*, *aac(6')-Ib-cr*, *aadA1*, *aadA16*, *aadA2b*, *aph (4)-la*	–
Phenicols	*clmA1*	–
Sulfonamides	*sul1*, *sul3*	*sul1*
Tetracycline	*tetD*	–
Trimethoprim	*dfrA27*	*dfrA1*
Fosfomycin	*fosA6*	*fosA6*
Quinolones	*qnrB52*, *aac(6')-Ib-cr*, *oqxA*, *oqxB*	*qnrS1*, *oqxA*, *oqxB*
Macrolides	*mphA*	–
Rifampicin	*arr-3*	–
Heavy metal		
Arsenic	–	*arsB, arsC, arsD, arsR*
Silver	*silABCEFRS*	*silABCEFRS*
Biocides and disinfectants	*qacF*	*smvR*
Virulome		
Yersiniabactin siderophore	–	*ybtSXQPAUTE*, *irp1*, *irp2*, *fyuA*
Plasmids	IncFIB	IncFIB
GenBank accession number	JACWHJ000000000.1	JACWHL000000000.1

FastANIv1.32 (https://github.com/ParBLiSS/FastANI/). ANI values between downloaded and query genomes were ≥99.7625% for *E. coli* ST10, ≥99.7807% for *E. coli* ST162, ≥99.7631% for *K. pneumoniae* ST35 and ≥99.575% for *K. pneumoniae* ST661. CSI Phylogeny (https://cge.food.dtu.dk/services/CSIPhylogeny/) was used with default settings to generate approximate maximum-likelihood SNP-based trees. Chromosome sequences of SCU-118 (NZ_CP051716.1) and LD91-1 (NZ_CP042585.1) *E. coli* strains, and RJY9645 (NZ_CP041353.1) and F13 (NZ_CP026162.1) of *K. pneumoniae* strains were used as reference for *E. coli* ST10 and ST162, and *K. pneumoniae* ST35 and ST661, respectively. ABRicatev1.0.1 (https://github.com/tseemann/abricate) was used with ResFinder and PlasmidFinder databases to screen antimicrobial resistance genes and plasmids on each recruited genome. Identity and coverage limits were set to 98% and 100%, respectively. iTOLv6 (https://itol.embl.de/) was used to annotate the tree with data from Enterobase, bacWGSTdb and ABRicate.

3 Results and discussion

Forty-tree cephalosporin-resistant Gram-negative bacteria were isolated from 23 healthy dogs and 16 sick dogs (Supplementary Tables 1, 2). From the latter, eight dogs presented with gastrointestinal complications, four with metabolic syndrome, two with dermatological disease, one with respiratory problems, and another with cerebrovascular accident. Based on confirmation of ESβL phenotype, four bacterial isolates exhibiting a MDR profile (Magiorakos et al., 2012) were sequenced: i) *E. coli* strain ECU3_SQ178 (GenBank accession number: JACWHI000000000.1) isolated from a 6-month-old healthy female dog mixed breed, with no previous treatments reported. This strain presented resistance to ceftazidime, cefotaxime (MIC > 32 μg/mL), ceftriaxone, cefepime, aztreonam, nalidixic-acid, enrofloxacin, ciprofloxacin, and chloramphenicol, being susceptible to amoxicillin-clavulanic acid, cefoxitin, ertapenem, meropenem, imipenem, gentamicin, amikacin, trimethoprim-sulfamethoxazole (Supplementary Table 2). In this regard, WGS analysis predicted the presence of genes associated with resistance to β-lactams ($bla_{CTX-M-55}$-like), phenicols (*floR*), tetracyclines (*tetA*), sulphonamides (*sul2*), aminoglycosides [*aph(3")-Ib*, *aph(6)-Id*], fosfomycin (*fosA3*), and quinolones (*gyrA*-D87N and *parC*-S80I point mutations, *marA*). On the other hand, genes conferring tolerance to heavy metals [arsenic (*arsBCR*) and tellurium (*tehAB*)], herbicide [glyphosate (*phnCDFGHIJKLMNOP*)], biocides and disinfectants (*mdtEFKN*, *emrDK*, *acrAEF* and *tolC*) were also predicted (Table 1); ii) *E. coli* strain EE12_SQ154 (GenBank accession number: JACWHK000000000.1) isolated from a 4-years-old female Yorkshire terrier dog with a history of physical decline, cerebrovascular accident and shock. It was not reported by the private veterinary clinic the treatment received prior to the sample collection. Antimicrobial susceptibility testing revealed resistance to ceftazidime, cefotaxime (MIC > 32 μg/mL), ceftriaxone, cefepime, aztreonam, nalidixic-acid, enrofloxacin, ciprofloxacin, trimethoprim-sulfamethoxazole, chloramphenicol, and gentamicin, and susceptibility to amoxicillin-clavulanic acid, cefoxitin, ertapenem, meropenem, imipenem and amikacin (Supplementary Table 2). The antimicrobial resistome included genes conferring resistance to β-lactams ($bla_{CTX-M-65}$), aminoglycosides (*aadA1*, *aadA2b*), fosfomycin (*fosA3*), phenicol (*cmlA1*), sulphonamides (*sul3*),

trimethoprim (*dfrA1*), quinolones (*marA*), heavy metals [arsenic (*arsBR*), tellurium (*tehAB*) and mercury (*merR*)], herbicide [glyphosate (*phnJ*)], biocides and disinfectants (*mdtEFK*, *emrDK*, *acrAEF*, *tolC*, *qacF* and *mvrC*) (Table 1); iii) *K. pneumoniae* strain ECU12_SQ166 (GenBank accession number: JACWHJ000000000.1), isolated from a 12-year-old male English Shepherd dog admitted to a private veterinary clinic with signs of diarrhea, melena, vomiting, septicemia, and chronic kidney failure leading to death. Based on the anamnesis and initial physical examination, fluid therapy was established, as a stabilization measure (lactated ringer solution), and a not specified β-lactam antibiotic was administered. The strain exhibited resistance to amoxicillin-clavulanic acid, ceftazidime, cefotaxime (MIC > 32 μg/mL), ceftriaxone, cefepime, aztreonam, ceftiofur, trimethoprim-sulfamethoxazole, nalidixic-acid, enrofloxacin, ciprofloxacin, and gentamicin, being susceptible to cefoxitin, ertapenem, meropenem, imipenem, and amikacin (Supplementary Table 2). The resistome analysis predicted resistance genes to β-lactams ($bla_{CTX-M-27}$, bla_{SHV-27}), fosfomycin (*fosA6*), trimethoprim (*dfrA27*), rifampicin (*arr-3*), sulfonamides (*sul1*, *sul3*), aminoglycosides [*aac(3)IV*, *aac(6')-Ib-cr*, *aadA1*, *aadA16*, *aadA2b*, *aph(4)-la*], macrolides (*mphA*), quinolones [*aac (6')-Ib-cr*, *oqxA*, *oqxB*, *qnrB52*], phenicols (*cmlA*), tetracyclines (*tetD*), silver (*silABCEFRS*) and ammonium quaternary compounds (*qacF*) (Table 2); (iv) *K. pneumoniae* strain EE25K_SQ190 (GenBank accession number: JACWHL000000000.1) isolated from an 8-year-old male German shepherd dog, presenting with discomfort, anorexia and foreign body gingivitis. After clinical examination, the foreign body was removed and a combination of amoxicillin/clavulanic acid plus a non-steroidal anti-inflammatory was prescribed. Antimicrobial susceptibility testing revealed resistance to cefotaxime (MIC > 32 μg/mL), ceftriaxone, cefepime, nalidixic-acid, enrofloxacin, ciprofloxacin, and trimethoprim-sulfamethoxazole. This strain showed to be susceptible to amoxicillin-clavulanic acid, ceftazidime, cefoxitin, aztreonam, ertapenem, meropenem, imipenem, amikacin and gentamicin (Supplementary Table 2). Resistome encompass genes resistant to β-lactams ($bla_{CTX-M-14}$, bla_{SHV-33}, bla_{LAP2}), fosfomycin (*fosA6*), trimethoprim (*dfrA1*), quinolones (*oqxA*, *oqxB*, *qnrS1*), and sulphonamides (*sul1*), silver (*silABCEFRS*), arsenic (*arsBCDR*) and chlorhexidine (*smvR*) (Table 2).

While CTX-M-55- and CTX-M-65-positive *E. coli* strains belonged to ST10 and ST162, *K. pneumoniae* producing CTX-M-27 and CTX-M-14 ESβLs belonged to ST661 and ST35, respectively. *E. coli* ST10 and ST162 have been previously associated with human infections (Coelho et al., 2011; Chen et al., 2014), being further identified in hospital sewage (Zhao et al., 2017), bovines (Umpiérrez et al., 2017), birds (Fuentes-Castillo et al., 2020), and dogs (Yasugi et al., 2021). The $bla_{CTX-M-55}$ gene has been widely identified globally in *E. coli* isolates from various animal species (Kiratisin et al., 2007; Zhang et al., 2014; Birgy et al., 2018; Lupo et al., 2018). The remarkable prevalence of this gene, accompanied by a high propensity for horizontal gene transfer has facilitated its rapid and wide spread (Yang et al., 2023). In Ecuador $bla_{CTX-M-55}$ has been the most prevalent allele of the bla_{CTX-M} family in *E. coli* from poultry settings, followed by $bla_{CTX-M-65}$ and $bla_{CTX-M-2}$ (Ortega-Paredes et al., 2020a). On the other hand, according to Enterobase (https://enterobase.warwick.ac.uk/), ST10 has been identified in dogs from Germany, United States of America (USA), United Kingdom, South Korea, Canada and New Zealand, whereas in Ecuador ST10 has been identified in humans, wild animals, and environmental samples; confirming the One Health importance of this global lineage in this country. In fact, phylogenomic analysis showed that strain ECU3_SQ178 (CTX-M-55/ST10) clustered (95-105 SNP differences) with food and human *E. coli* strains of ST10 isolated in 2016, in Australia and Cambodia, respectively, whereas CTX-M-65-positive *E. coli* ST162 (strain EE12_SQ154) showed ubiquity, being clustered (207-265 SNP differences) with other four drug-resistant *E. coli* strains of ST162 isolated from livestock (USA, 2016), poultry (USA, 2020), human (Australia, 2014) and companion animal (USA, 2007) (Figure 1, Supplementary Table 3). Moreover, data retrieved from Enterobase confirm occurrence of this *E. coli* clone in companion animals from Germany, USA, and Canada. Interestingly, this is the first report of *E. coli* ST162 found in companion animal, in South America.

In the case of *K. pneumoniae* ST661 and ST35 clones, they have been previously isolated from nosocomial pneumonia in humans (Zhao et al., 2019), rectal swabs from pigs and fecal human samples (Leangapichart et al., 2021). Moreover, ST661 has been recovered from aquatic environments (Furlan et al., 2020), hospitalized patients (Piazza et al., 2019), being recently reported as responsible for outbreaks in Europe (Martin et al., 2017); whereas ST35 has been identified among ESβL-producing *K. pneumoniae* strains in hospital settings (Marcade et al., 2013; Frenk et al., 2020), being lately recognized as a multidrug-resistant clone with worldwide distribution (Shen et al., 2020).

For CTX-M-27-positive *K. pneumoniae* ST661 (ECU12_SQ166), phylogenomic analysis revealed relationship (201-216 SNP differences) with human strains identified in Italy, in 2013 and 2017, respectively (Figure 2, Supplementary Table 3). Strikingly, all the three isolates within the clade carried an IncFIB-type plasmid. Moreover, ECU12_SQ166 and the human strain isolated in 2017 exhibited an identical MDR profile, sharing bla_{SHV-27}, *sul1* and *mph(A)* resistance genes. In brief, *K. pneumoniae* ST661 is other global clone identified in Italy, China, England, Brazil, Tunisia, Thailand, Uruguay, Mexico and Taiwan (Yan et al., 2015; Ku et al., 2017; Martin et al., 2017; Patil et al., 2019; Piazza et al., 2019; Sghaier et al., 2019; Furlan et al., 2020; Hassen et al., 2020; Ludden et al., 2020; Leangapichart et al., 2021; Papa-Ezdra et al., 2021; Toledano-Tableros et al., 2021).

In companion animals, ESβL production among *Klebsiella* isolates has been associated with CTX-M-14 and CTX-M-15 variants (Harada et al., 2016). In this study, CTX-M-14-positive *K. pneumoniae* EE25K_SQ190 belonged to ST35. Although this clone has been previously identified in China, Romania, Yemen, Israel, France, Spain and Thailand (Marcade et al., 2013; Cubero et al., 2016; Alsharapy et al., 2020; Frenk et al., 2020; Kong et al., 2020; Shen et al., 2020; Surleac et al., 2020; Zhong et al., 2020; Leangapichart et al., 2021), phylogenomic analysis clustered (353-354 SNP differences) EE25K_SQ190 with a human clone identified in Turkey in 2013 and 2014 (Figure 2, Supplementary Table 3).

Although, in Ecuador, occurrence of *E. coli* producing ESβL has been reported in pets, chicken, humans, food, vegetables, broiler

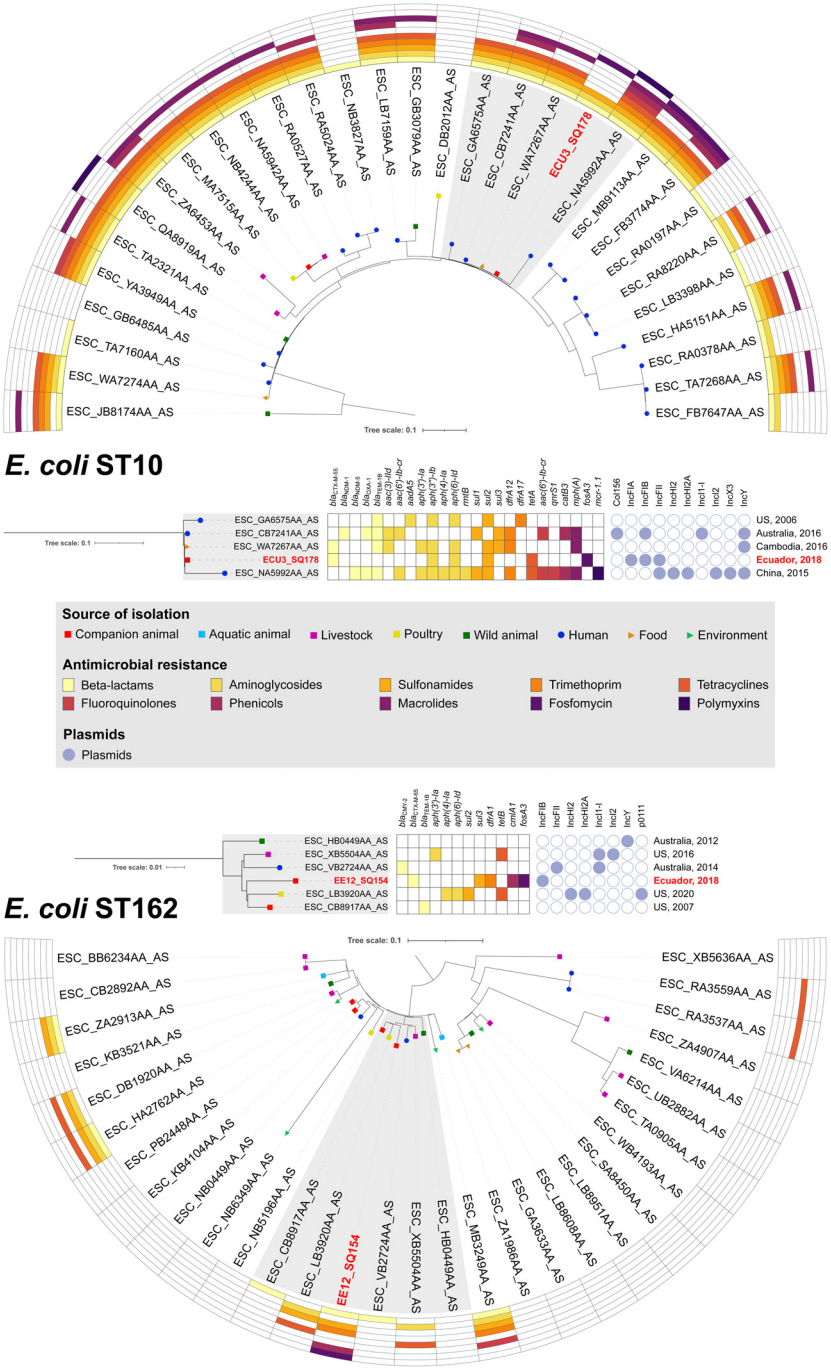

FIGURE 1
Phylogenetic trees of *E. coli* strains. SNP-based phylogenetic trees of *E. coli* ST10 and ST162, and heatmap showing presence/absence of antibiotic resistance genes for 10 antibiotics, and their source of isolation. Details on resistome, plasmidome and origin are showed for clusters formed with CTX-M-55-producing *E. coli* ECU3_SQ178 and CTX-M-65 *E. coli* EE12_SQ154 strains, isolated from dogs, in Ecuador.

farms, and river water samples, in Quito (Vinueza-Burgos et al., 2016; Chiluisa-Guacho et al., 2018; Ortega-Paredes et al., 2018; Ortega-Paredes et al., 2019; Vinueza-Burgos et al., 2019; Zurita et al., 2019; Ortega-Paredes et al., 2020a; Ortega-Paredes et al., 2020b; Zurita et al., 2020), and in other cities such as Guayaquil (Soria Segarra et al., 2018), Esmeraldas (Hedman et al., 2019), Loja (Delgado et al., 2016), and Cuenca (Zurita et al., 2013); as well as in the provinces of Tungurahua and Cotopaxi (Sánchez-Salazar et al., 2020), genomic data are scarce. Specifically, while CTX-M-55 and CTX-M-65-producing *E. coli* have been previously reported in dogs in central Ecuador, and in Quito (Ortega-Paredes et al., 2019; Albán et al., 2020; Salinas et al., 2021), CTX-M-producing *K. pneumoniae* have been isolated from human hosts in Cuenca (Nordberg et al., 2013), Quito, Guayaquil, and Azogues (Zurita et al., 2013), so far.

In summary, we report genomic data of global One Health-associated clones of CTX-M-55 and CTX-M-65-producing *E. coli*,

10.3389/fcimb.2023.1259764

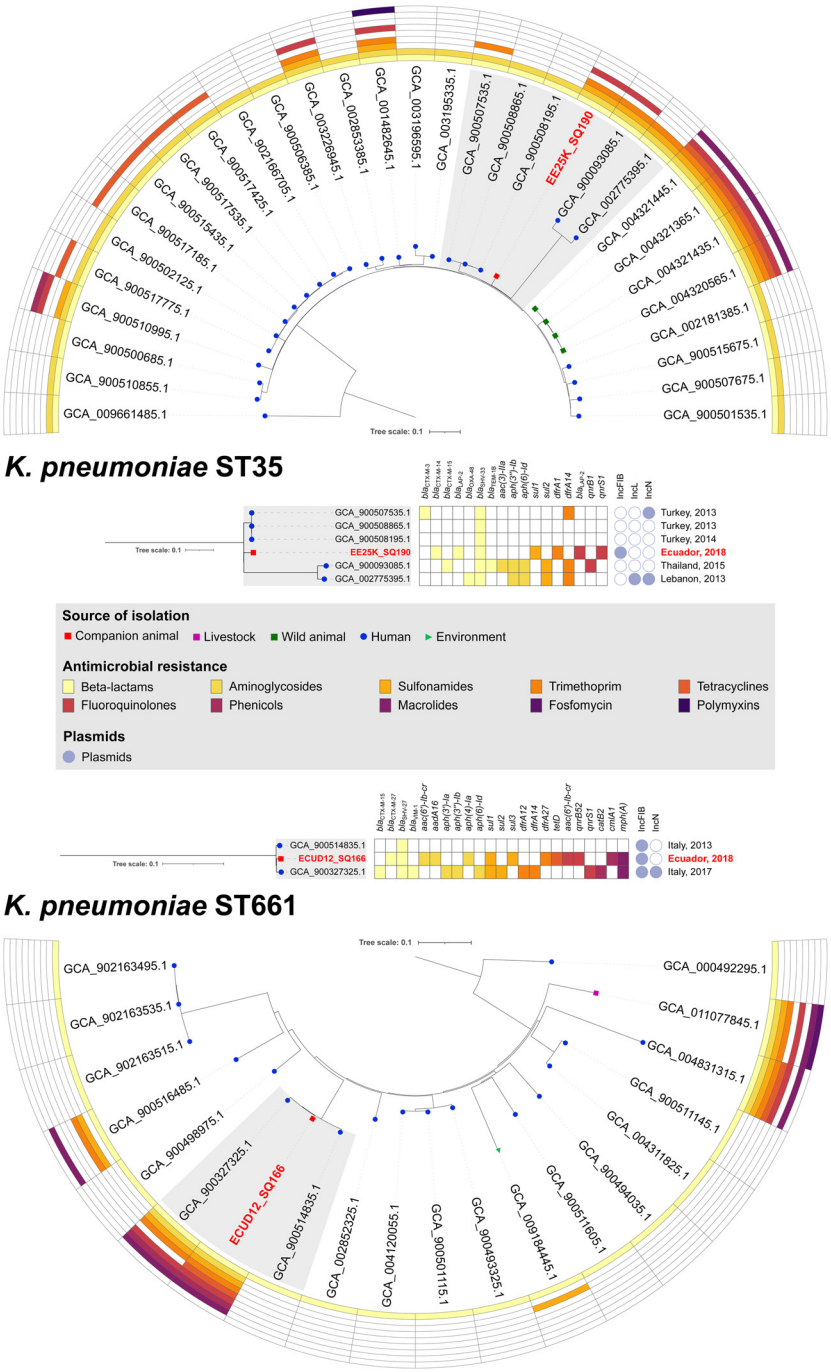

FIGURE 2
Phylogenetic trees of *K. pneumoniae* strains. SNP-based phylogenetic trees of *K. pneumoniae* ST35 and ST661, and heatmap showing presence/absence of antibiotic resistance genes for 10 antibiotics, and their source of isolation. Details on resistome, plasmidome and origin are showed for clusters formed with CTX-M-14-producing *K. pneumoniae* EE25K_SQ190 and CTX-M-27-producing *K. pneumoniae* ECUD12_SQ166 strains, isolated from dogs in Ecuador.

and CTX-M-14 and CTX-M-15-producing *K. pneumoniae* in dogs from the province of Imbabura, in Ecuador. The implementation of a national epidemiological surveillance program is necessary to establish future strategies to control the dissemination of antibiotic-resistant priority pathogens using a One Health approach.

Data availability statement

The datasets presented in this study can be found in online repositories. The names of the repository/repositories and accession number(s) can be found in the article/supplementary material.

Ethics statement

The animal studies were approved by MSc. Elena Dorothea Balarezo Cisneros President of the Ethics Committee for Research Processes Yachay Tech University. The studies were conducted in accordance with the local legislation and institutional requirements. Written informed consent was obtained from the owners for the participation of their animals in this study.

Author contributions

FAG-Z: Conceptualization, Formal analysis, Project administration, Supervision, Writing – original draft, Writing – review & editing. JT: Formal analysis, Writing – review & editing. JV-B: Formal analysis, Methodology, Writing – original draft, Writing – review & editing. MV-B: Investigation, Methodology, Writing – review & editing. AC-A: Methodology, Writing – review & editing. FE: Formal analysis, Methodology, Software, Writing – review & editing. QM: Formal analysis, Methodology, Writing – review & editing. BF: Methodology, Writing – review & editing. ES: Formal analysis, Methodology, Software, Writing – review & editing. JGMP: Formal analysis, Methodology, Validation, Writing – review & editing. MJ: Investigation, Writing – review & editing. NL: Conceptualization, resources, Formal analysis, Writing – original draft, Writing – review & editing.

Funding

The author(s) declare financial support was received for the research, authorship, and/or publication of this article. This study was supported by the Fundação de Amparo à Pesquisa do Estado de São Paulo (FAPESP, 2020/08224-9 and 2019/15778-4) and Conselho Nacional de Desenvolvimento Científico e Tecnológico (CNPq 422984/2021-3 and 314336/2021-4). NL is a research fellow of CNPq (314336/2021-4). FE was a research fellow of FAPESP (2019/15778-4).

Acknowledgments

We are grateful to FAPESP and CNPq. We also thank Cefar Diagnóstica Ltda. (São Paulo, Brazil) and CEFAP-GENIAL facility for kindly supplying antibiotic discs for susceptibility testing and Illumina sequencing, respectively.

Conflict of interest

The authors declare that the research was conducted in the absence of any commercial or financial relationships that could be construed as a potential conflict of interest.

Publisher's note

All claims expressed in this article are solely those of the authors and do not necessarily represent those of their affiliated organizations, or those of the publisher, the editors and the reviewers. Any product that may be evaluated in this article, or claim that may be made by its manufacturer, is not guaranteed or endorsed by the publisher.

Supplementary material

The Supplementary Material for this article can be found online at: https://www.frontiersin.org/articles/10.3389/fcimb.2023.1259764/full#supplementary-material

References

Albán, M. V., Núñez, E. J., Zurita, J., Villacís, J. E., Tamayo, R., Sevillano, G., et al. (2020). Canines with different pathologies as carriers of diverse lineages of *Escherichia coli* harbouring *mcr-1* and clinically relevant β-lactamases in central Ecuador. *J. Glob. Antimicrob. Resist.* 22, 182–183. doi: 10.1016/j.jgar.2020.05.017

Albrechtova, K., Dolejska, M., Cizek, A., Tausova, D., Klimes, J., Bebora, L., et al. (2012). Dogs of nomadic pastoralists in Northern Kenya are reservoirs of plasmid-mediated cephalosporin-and quinolone-resistant *Escherichia coli*, including pandemic clone B2-O25-ST131. *Antimicrob. Agents Chemother.* 56, 4013–4017. doi: 10.1128/AAC.05859-11

Alsharapy, S. A., Gharout-Sait, A., Muggeo, A., Guillard, T., Cholley, P., Brasme, L., et al. (2020). Characterization of carbapenem-resistant *Enterobacteriaceae* clinical isolates in Al Thawra University Hospital, Sana'a, Yemen. *Microb. Drug Resist.* 26, 211–217. doi: 10.1089/mdr.2018.0443

Birgy, A., Madhi, F., Hogan, J., Doit, C., Gaschignard, J., Caseris, M., et al. (2018). CTX-M-55-, MCR-1-, and FosA-producing multidrug-resistant *Escherichia coli* infection in a child in France. *Antimicrob. Agents Chemother.* 62, e00127–e00118. doi: 10.1128/aac.00127-18

Bonelli, R. R., Moreira, B. M., and Picão, R. C. (2014). Antimicrobial resistance among *Enterobacteriaceae* in South America: history, current dissemination status and associated socioeconomic factors. *Drug Resist. Updat.* 17, 24–36. doi: 10.1016/j.drup.2014.02.001

Cantón, R., and Coque, T. M. (2006). The CTX-M β-lactamase pandemic. *Curr. Opin. Microbiol.* 9, 466–475. doi: 10.1016/j.mib.2006.08.011

Caprioli, A., Busani, L., Martel, J. L., and Helmuth, R. (2000). Monitoring of antibiotic resistance in bacteria of animal origin: Epidemiological and microbiological methodologies. *Int. J. Antimicrob. Agents.* 14, 295–301. doi: 10.1016/S0924-8579(00)00140-0

Chen, Y., Chen, X., Zheng, S., Yu, F., Kong, H., Yang, Q., et al. (2014). Serotypes, genotypes and antimicrobial resistance patterns of human diarrhoeagenic *Escherichia coli* isolates circulating in southeastern China. *Clin. Microbiol. Infect.* 20, 52–58. doi: 10.1111/1469-0691.12188

Chiluisa-Guacho, C., Escobar-Perez, J., and Dutra-Asensi, M. (2018). First detection of the CTX-M-15 producing *Escherichia coli* O25-ST131 pandemic clone in Ecuador. *Pathogens.* 7, 42. doi: 10.3390/pathogens7020042

CLSI (2023a). *Performance standards for antimicrobial disk and dilution susceptibility tests for bacteria isolated from animals - 6th edition: VET01S* (Clinical and Laboratory Standards Institute).

CLSI (2023b). *Performance standards for antimicrobial susceptibility testing. 33rd* (CLSI supplement M100. Clinical and Laboratory Standards Institute).

Coelho, A., Mora, A., Mamani, R., López, C., González-López, J. J., Larrosa, M. N., et al. (2011). Spread of *Escherichia coli* O25b:H4-B2-ST131 producing CTX-M-15 and SHV-12 with high virulence gene content in Barcelona (Spain). *J. Antimicrob. Chemother.* 66, 517–526. doi: 10.1093/jac/dkq491

Cubero, M., Grau, I., Tubau, F., Pallarés, R., Dominguez, M. A., Liñares, J., et al. (2016). Hypervirulent *Klebsiella pneumoniae* clones causing bacteraemia in adults in a

teaching hospital in Barcelona, Spain, (2007-2013). *Clin. Microbiol. Infect.* 22, 154–160. doi: 10.1016/j.cmi.2015.09.025

Damborg, P., Broens, E. M., Chomel, B. B., Guenther, S., Pasmans, F., Wagenaar, J. A., et al. (2016). Bacterial zoonoses transmitted by household pets: state-of-the-art and future perspectives for targeted research and policy actions. *J. Comp. Pathol.* 155, S27–S40. doi: 10.1016/j.jcpa.2015.03.004

Delgado, D. Y. C., Barrigas, Z. P. T., Astutillo, S. G. O., Jaramillo, A. P. A., and Ausili, A. (2016). Detection and molecular characterization of β-lactamase genes in clinical isolates of Gram-negative bacteria in Southern Ecuador. *Braz. J. Infect. Dis.* 20, 627–630. doi: 10.1016/j.bjid.2016.07.001

Ewers, C., Bethe, A., Semmler, T., Guenther, S., and Wieler, L. H. (2012). Extended-spectrum β-lactamase-producing and AmpC-producing *Escherichia coli* from livestock and companion animals, and their putative impact on public health: A global perspective. *Clin. Microbiol. Infect.* 18, 646–655. doi: 10.1111/j.1469-0691.2012.03850.x

Fernandes, M. R., Sellera, F. P., Moura, Q., Carvalho, M. P. N., Rosato, P. N., Cerdeira, L., et al. (2018). Zooanthroponotic transmission of drug-resistant *Pseudomonas aeruginosa*, Brazil. *Emerg. Infect. Dis.* 24, 1160–1162. doi: 10.3201/eid2406.180335

Frenk, S., Rakovitsky, N., Temkin, E., Schechner, V., Cohen, R., Kloyzner, B. S., et al. (2020). Investigation of outbreaks of extended-spectrum beta-lactamase-producing *Klebsiella pneumoniae* in three neonatal intensive care units using whole genome sequencing. *Antibiotics.* 9, 1–10. doi: 10.3390/antibiotics9100705

Fuentes-Castillo, D., Esposito, F., Cardoso, B., Dalazen, G., Moura, Q., Fuga, B., et al. (2020). Genomic data reveal international lineages of critical priority *Escherichia coli* harbouring wide resistome in Andean condors (*Vulturgryphus* Linnaeus 1978). *Mol. Ecol.* 29, 1919–1935. doi: 10.1111/mec.15455

Furlan, J. P. R., Savazzi, E. A., and Stehling, E. G. (2020). Genomic insights into multidrug-resistant and hypervirulent *Klebsiella pneumoniae* co-harboring metal resistance genes in aquatic environments. *Ecotox. Environ. Saf.* 201, 110782. doi: 10.1016/j.ecoenv.2020.110782

Guzmán-Blanco, M., Labarca, J. A., Villegas, M. V., and Gotuzzo, E. (2014). Extended spectrum β-lactamase producers among nosocomial *Enterobacteriaceae* in Latin America. *Braz. J. Infect. Dis.* 18, 421–433. doi: 10.1016/j.bjid.2013.10.005

Harada, K., Shimizu, T., Mukai, Y., Kuwajima, K., Sato, T., Usui, M., et al. (2016). Phenotypic and molecular characterization of antimicrobial resistance in *Klebsiella* spp. isolates from companion animals in Japan: clonal dissemination of multidrug-resistant extended-spectrum β-lactamase-producing *Klebsiella pneumoniae*. *Front. Microbiol.* 7. doi: 10.3389/fmicb.2016.01021

Hassen, B., Abbassi, M. S., Benlabidi, S., Ruiz-Ripa, L., Mama, O. M., Ibrahim, C., et al. (2020). Genetic characterization of ESBL-producing *Escherichia coli* and *Klebsiella pneumoniae* isolated from wastewater and river water in Tunisia: predominance of CTX-M-15 and high genetic diversity. *Environ. Sci. pollut. Res.* 27, 44368–44377. doi: 10.1007/s11356-020-10326-w

Hedman, H. D., Eisenberg, J. N. S., Vasco, K. A., Blair, C. N., Trueba, G., Berrocal, V. J., et al. (2019). High prevalence of extended-spectrum beta-lactamase CTX-M-producing *Escherichia coli* in small-scale poultry farming in rural Ecuador. *Am. J. Trop. Med. Hyg.* 100, 374–376. doi: 10.4269/ajtmh.18-0173

Jacob, M. E., Keelara, S., Aidara-Kane, A., Matheu Alvarez, J. R., and Fedorka-Cray, P. J. (2020). Optimizing a screening protocol for potential extended-spectrum β-lactamase *Escherichia coli* on MacConkey agar for use in a global surveillance program. *J. Clin. Microbiol.* 58, e01039–e01019. doi: 10.1128/JCM.01039-19

Jarlier, V., Nicolas, M. H., Fournier, G., and Philippon, A. (1988). Extended broad-spectrum β-lactamases conferring transferable resistance to newer β-lactam agents in *Enterobacteriaceae*: hospital prevalence and susceptibility patterns. *Clin. Infect. Dis.* 10, 867–878. doi: 10.1093/clinids/10.4.867

Johnson, J. R., Clabots, C., and Kuskowski, M. A. (2008). Multiple-host sharing, long-term persistence, and virulence of *Escherichia coli* clones from human and animal household members. *J. Clin. Microbiol.* 46, 4078–4082. doi: 10.1128/JCM.00980-08

Kawamura, K., Sugawara, T., Matsuo, N., Hayashi, K., Norizuki, C., Tamai, K., et al. (2017). Spread of CTX-type extended-spectrum β-lactamase-producing *Escherichia coli* isolates of epidemic clone B2-O25-ST131 among dogs and cats in Japan. *Microb. Drug Resist.* 23, 1059–1066. doi: 10.1089/mdr.2016.0246

Kiratisin, P., Apisarnthanarak, A., Saifon, P., Laesripa, C., Kitphati, R., and Mundy, L. M. (2007). The emergence of a novel ceftazidime-resistant CTX-M extended-spectrum β-lactamase, CTX-M-55, in both community-onset and hospital-acquired infections in Thailand. *Diagn. Microbiol. Infect. Dis.* 58, 349–355. doi: 10.1016/j.diagmicrobio.2007.02.005

Kong, Z., Liu, X., Li, C., Cheng, S., Xu, F., and Gu, B. (2020). Clinical molecular epidemiology of carbapenem-resistant *Klebsiella pneumoniae* among pediatric patients in Jiangsu province, China. *Infect. Drug Resist.* 13, 4627–4635. doi: 10.2147/IDR.S293206

Ku, Y. H., Chuang, Y. C., Chen, C. C., Lee, M. F., Yang, Y. C., Tang, H. J., et al. (2017). *Klebsiella pneumoniae* isolates from meningitis: epidemiology, virulence and antibiotic resistance. *Sci. Rep.* 7, 1–10. doi: 10.1038/s41598-017-06878-6

Leangapichart, T., Lunha, K., Jiwakanon, J., Angkititrakul, S., Järhult, J. D., Magnusson, U., et al. (2021). Characterization of *Klebsiella pneumoniae* complex isolates from pigs and humans in farms in Thailand: population genomic structure, antibiotic resistance and virulence genes. *J. Antimicrob. Chemother.* 76, 2012–2016. doi: 10.1093/jac/dkab118

Lopes, R., Fuentes-Castillo, D., Fontana, H., Rodrigues, L., Dantas, K., Cerdeira, L., et al. (2021). Endophytic lifestyle of global clones of extended-spectrum β-lactamase-producing priority pathogens in fresh vegetables: a trojan horse strategy favoring human colonization? *MSystems.* 6, e01125–e01120. doi: 10.1128/msystems.01125-20

Ludden, C., Moradigaravand, D., Jamrozy, D., Gouliouris, T., Blane, B., Naydenova, P., et al. (2020). A one health study of the genetic relatedness of *Klebsiella pneumoniae* and their mobile elements in the east of England. *Clin. Infect. Dis.* 70, 219–226. doi: 10.1093/cid/ciz174

Lupo, A., Saras, E., Madec, J. Y., and Haenni, M. (2018). Emergence of $bla_{CTX\text{-}M\text{-}55}$ associated with *fosA*, *rmtB* and *mcr* gene variants in *Escherichia coli* from various animal species in France. *J. Antimicrob. Chemother.* 73, 867–872. doi: 10.1093/jac/dkx489

Magiorakos, A. P., Srinivasan, A., Carey, R. B., Carmeli, Y., Falagas, M. E., Giske, C. G., et al. (2012). Multidrug-resistant, extensively drug-resistant and pandrug-resistant bacteria: An international expert proposal for interim standard definitions for acquired resistance. *Clin. Microbiol. Infect.* 18, 268–281. doi: 10.1111/j.1469-0691.2011.03570.x

Marcade, G., Brisse, S., Bialek, S., Marcon, E., Leflon-Guibout, V., Passet, V., et al. (2013). The emergence of multidrug-resistant *Klebsiella pneumoniae* of international clones ST13, ST16, ST35, ST48 and ST101 in a teaching hospital in the Paris region. *Epidemiol. Infect.* 141, 1705–1712. doi: 10.1017/S0950268812002099

Marshall, B. M., and Levy, S. B. (2011). Food animals and antimicrobials: Impacts on human health. *Clin. Microbiol. Rev.* 24, 718–733. doi: 10.1128/CMR.00002-11

Martin, J., Phan, H. T. T., Findlay, J., Stoesser, N., Pankhurst, L., Navickaite, I., et al. (2017). Covert dissemination of carbapenemase-producing *Klebsiella pneumoniae* (KPC) in a successfully controlled outbreak: long- and short-read whole-genome sequencing demonstrate multiple genetic modes of transmission. *J. Antimicrob. Chemother.* 72, 3025–3034. doi: 10.1093/jac/dkx264

Matsumoto, Y., Ikeda, F., Kamimura, T., Yokota, Y., and Mine, Y. (1988). Novel plasmid-mediated β-lactamase from *Escherichia coli* that inactivates oxyimino-cephalosporins. *Antimicrob. Agents Chemother.* 32, 1243–1246. doi: 10.1128/AAC.32.8.1243

Melo, L. C., Oresco, C., Leigue, L., Netto, H. M., Melville, P. A., Benites, N. R., et al. (2018). Prevalence and molecular features of ESBL/pAmpC-producing *Enterobacteriaceae* in healthy and diseased companion animals in Brazil. *Vet. Microbiol.* 221, 59–66. doi: 10.1016/j.vetmic.2018.05.017

Moreno, A., Bello, H., Guggiana, D., Domínguez, M., and González, G. (2008). Extended-spectrum β-lactamases belonging to CTX-M group produced by *Escherichia coli* strains isolated from companion animals treated with enrofloxacin. *Vet. Microbiol.* 129, 203–208. doi: 10.1016/j.vetmic.2007.11.011

Nordberg, V., Quizhpe Peralta, A., Galindo, T., Turlej-Rogacka, A., Iversen, A., Giske, C. G., et al. (2013). High Proportion of intestinal colonization with successful epidemic clones of ESBL-producing *Enterobacteriaceae* in a neonatal intensive care unit in Ecuador. *PloS One* 8, e76597. doi: 10.1371/journal.pone.0076597

Okubo, T., Sato, T., Yokota, S. I., Usui, M., and Tamura, Y. (2014). Comparison of broad-spectrum cephalosporin-resistant *Escherichia coli* isolated from dogs and humans in Hokkaido, Japan. *J. Infect. Chemother.* 20, 243–249. doi: 10.1016/j.jiac.2013.12.003

Ortega-Paredes, D., Barba, P., Mena-López, S., Espinel, N., Crespo, V., and Zurita, J. (2020b). High quantities of multidrug-resistant *Escherichia coli* are present in the Machángara urban river in Quito, Ecuador. *J. Water Health* 18, 67–76. doi: 10.2166/wh.2019.195

Ortega-Paredes, D., Barba, P., Mena-López, S., Espinel, N., and Zurita, J. (2018). *Escherichia coli* hyperepidemic clone ST410-A harboring $bla_{CTX\text{-}M\text{-}15}$ isolated from fresh vegetables in a municipal market in Quito-Ecuador. *Int. J. Food Microbiol.* 280, 41–45. doi: 10.1016/j.ijfoodmicro.2018.04.037

Ortega-Paredes, D., de Janon, S., Villavicencio, F., Ruales, K. J., de la Torre, K., Villacís, J. E., et al. (2020a). Broiler farms and carcasses are an important reservoir of multi-drug resistant *Escherichia coli* in Ecuador. *Front. Vet. Sci.* 7. doi: 10.3389/fvets.2020.547843

Ortega-Paredes, D., Haro, M., Leoro-Garzón, P., Barba, P., Loaiza, K., Mora, F., et al. (2019). Multidrug-resistant *Escherichia coli* isolated from canine faeces in a public park in Quito, Ecuador. *J. Glob. Antimicrob. Resist.* 18, 263–268. doi: 10.1016/j.jgar.2019.04.002

Papa-Ezdra, R., Caiata, L., Palacio, R., Outeda, M., Cabezas, L., Bálsamo, A., et al. (2021). Prevalence and molecular characterisation of carbapenemase-producing *Enterobacterales* in an outbreak-free setting in a single hospital in Uruguay. *J. Glob. Antimicrob. Resist.* 24, 58–62. doi: 10.1016/j.jgar.2020.11.006

Patil, S., Chen, X., and Wen, F. (2019). Exploring the phenotype and genotype of multi-drug resistant *Klebsiella pneumoniae* harbouring $bla_{CTX\text{-}M}$ group extended-spectrum β-lactamases recovered from paediatric clinical cases in Shenzhen, China. *Ann. Clin. Microbiol. Antimicrob.* 18, 1–6. doi: 10.1186/s12941-019-0331-z

Pesesky, M. W., Hussain, T., Wallace, M., Wang, B., Andleeb, S., Burnham, C. D., et al. (2015). KPC and NDM-1 genes in related Enterobacteriaceae strains and plasmids from Pakistan and the United States. *Emerg. Infect. Dis.* 21, 1034–1037. doi: 10.3201/eid2106.141504

Piazza, A., Comandatore, F., Romeri, F., Brilli, M., Dichirico, B., Ridolfo, A., et al. (2019). Identification of $bla_{VIM\text{-}1}$ gene in ST307 and ST661 *Klebsiella pneumoniae* clones in Italy: old acquaintances for new combinations. *Microb. Drug Resist.* 25, 787–790. doi: 10.1089/mdr.2018.0327

Pitout, J. D., and Laupland, K. B. (2008). Extended-spectrum β-lactamase-producing *Enterobacteriaceae*: an emerging public-health concern. *Lancet Infect. Dis.* 8, 159–166. doi: 10.1016/S1473-3099(08)70041-0

Pomba, C., Rantala, M., Greko, C., Baptiste, K. E., Catry, B., van Duijkeren, E., et al. (2017). Public health risk of antimicrobial resistance transfer from companion animals. *J. Antimicrob. Chemother.* 72, 957–968. doi: 10.1093/jac/dkw481

Salgado-Caxito, M., Benavides, J. A., Adell, A. D., Paes, A. C., and Moreno-Switt, A. I. (2021). Global prevalence and molecular characterization of extended-spectrum β-lactamase producing-*Escherichia coli* in dogs and cats - a scoping review and meta-analysis. *One Health* 12, 100236. doi: 10.1016/j.onehlt.2021.100236

Salinas, L., Loayza, F., Cárdenas, P., Saraiva, C., Johnson, T. J., Amato, H., et al. (2021). Environmental spread of extended spectrum beta-lactamase (ESBL) producing *Escherichia coli* and ESBL genes among children and domestic animals in Ecuador. *Environ. Health Perspect.* 129, 27007. doi: 10.1289/EHP7729

Samanta, I., Joardar, S. N., Mahanti, A., Bandyopadhyay, S., Sar, T. K., and Dutta, T. K. (2015). Approaches to characterize extended spectrum beta-lactamase/beta-lactamase producing *Escherichia coli* in healthy organized vis-a-vis backyard farmed pigs in India. *Infect. Genet. Evol.* 36, 224–230. doi: 10.1016/j.meegid.2015.09.021

Sánchez-Salazar, E., Gudiño, M. E., Sevillano, G., Zurita, J., Guerrero-López, R., Jaramillo, K., et al. (2020). Antibiotic resistance of *Salmonella* strains from layer poultry farms in central Ecuador. *J. Appl. Microbiol.* 128, 1347–1354. doi: 10.1111/jam.14562

Seiffert, S. N., Hilty, M., Perreten, V., and Endimiani, A. (2013). Extended-spectrum cephalosporin-resistant gram-negative organisms in livestock: An emerging problem for human health? *Drug Resist. Updat.* 16, 22–45. doi: 10.1016/j.drup.2012.12.001

Sellera, F. P., Da Silva, L. C. B. A., and Lincopan, N. (2021). Rapid spread of critical priority carbapenemase-producing pathogens in companion animals: a One Health challenge for a post-pandemic world. *J. Antimicrob. Chemother.* 76, 2225–2229. doi: 10.1093/jac/dkab169

Sghaier, S., Abbassi, M. S., Pascual, A., Serrano, L., Díaz-De-Alba, P., Said, M., et al. (2019). Extended-spectrum β-lactamase-producing *Enterobacteriaceae* from animal origin and wastewater in Tunisia: first detection of O25b-$B2_3$-CTX-M-27-ST131 *Escherichia coli* and CTX-M-15/OXA-204-producing *Citrobacter freundii* from wastewater. *J. Glob. Antimicrob. Resist.* 17, 189–194. doi: 10.1016/j.jgar.2019.01.002

Shen, Z., Gao, Q., Qin, J., Liu, Y., and Li, M. (2020). Emergence of an NDM-5-producing hypervirulent *Klebsiella pneumoniae* sequence type 35 strain with chromosomal integration of an integrative and conjugative element, ICEKp1. *Antimicrob. Agents Chemother.* 64, e01675–e01619. doi: 10.1128/AAC.01675-19

Soria Segarra, C., Soria Baquero, E., and Cartelle Gestal, M. (2018). High prevalence of CTX-M-1-like enzymes in urinary isolates of *Escherichia coli* in Guayaquil, Ecuador. *Microb. Drug Resist.* 24, 393–402. doi: 10.1089/mdr.2017.0325

Surleac, M., Barbu, I. C., Paraschiv, S., Popa, L. I., Gheorghe, I., Marutescu, L., et al. (2020). Whole genome sequencing snapshot of multidrug resistant *Klebsiella pneumoniae* strains from hospitals and receiving wastewater treatment plants in Southern Romania. *PloS One* 15, 1–17. doi: 10.1371/journal.pone.0228079

Tacconelli, E., Carrara, E., Savoldi, A., Harbarth, S., Mendelson, M., Monnet, D. L., et al. (2018). Discovery, research, and development of new antibiotics: the WHO priority list of antibiotic-resistant bacteria and tuberculosis. *Lancet Infect. Dis.* 18, 318–327. doi: 10.1016/S1473-3099(17)30753-3.

Toledano-Tableros, J. E., Gayosso-Vázquez, C., Jarillo-Quijada, M. D., Fernández-Vázquez, J. L., Morfin-Otero, R., Rodríguez-Noriega, E., et al. (2021). Dissemination of bla_{NDM-1} gene among several *Klebsiella pneumoniae* sequence types in Mexico associated with horizontal transfer mediated by IncF-like plasmids. *Front. Microbiol.* 12. doi: 10.3389/fmicb.2021.611274

Umber, J. K., and Bender, J. B. (2009). Pets and antimicrobial resistance. *Vet. Clin. N. Am. - Small Anim. Pract.* 39, 279–292. doi: 10.1016/j.cvsm.2008.10.016

Umpiérrez, A., Bado, I., Oliver, M., Acquistapace, S., Etcheverría, A., Padola, N. L., et al. (2017). Zoonotic potential and antibiotic resistance of *Escherichia coli* in neonatal calves in Uruguay. *Microbes Environ.* 32, 275–282. doi: 10.1264/jsme2.ME17046

Villegas, M. V., Kattan, J. N., Quinteros, M. G., and Casellas, J. M. (2008). Prevalence of extended-spectrum β-lactamases in South America. *Clin. Microb. Infect.* 14, 154–158. doi: 10.1111/j.1469-0691.2007.01869.x

Vinueza-Burgos, C., Cevallos, M., Ron-Garrido, L., Bertrand, S., and De Zutter, L. (2016). Prevalence and diversity of *Salmonella* serotypes in Ecuadorian broilers at slaughter age. *PloS One* 11, 1–12. doi: 10.1371/journal.pone.0159567

Vinueza-Burgos, C., Ortega-Paredes, D., Narvaéz, C., De Zutter, L., and Zurita, J. (2019). Characterization of cefotaxime resistant *Escherichia coli* isolated from broiler farms in Ecuador. *PloS One* 14, 1–14. doi: 10.1371/journal.pone.0207567

Yan, J. J., Wang, M. C., Zheng, P. X., Tsai, L. H., and Wu, J. J. (2015). Associations of the major international high-risk resistant clones and virulent clones with specific ompK36 allele groups in *Klebsiella pneumoniae* in Taiwan. *New Microbes New Infect.* 5, 1–4. doi: 10.1016/j.nmni.2015.01.002

Yang, J.-T., Zhang, L.-J., Lu, Y., Zhang, R.-M., and Jiang, H.-X. (2023). Genomic insights into global $bla_{CTX-M-55}$-positive *Escherichia coli* epidemiology and transmission characteristics. *Microbiol. Spectr.* 11, e0108923. doi: 10.1128/spectrum.01089-23

Yasugi, M., Hatoya, S., Motooka, D., Matsumoto, Y., Shimamura, S., Tani, H., et al. (2021). Whole-genome analyses of extended-spectrum or AmpC β-lactamase-producing *Escherichia coli* isolates from companion dogs in Japan. *PLoSONE.* 16, e0246482. doi: 10.1371/journal.pone.0246482

Zhang, J., Zheng, B., Zhao, L., Wei, Z., Ji, J., Li, L., et al. (2014). Nationwide high prevalence of CTX-M and an increase of CTX-M-55 in *Escherichia coli* isolated from patients with community-onset infections in Chinese County Hospitals. *BMC Infect. Dis.* 14, 659. doi: 10.1186/s12879-014-0659-0

Zhao, F., Feng, Y., Lü, X., McNally, A., and Zong, Z. (2017). Remarkable diversity of *Escherichia coli* carrying *mcr-1* from hospital sewage with the identification of two new *mcr-1* variants. *Front. Microbiol.* 8. doi: 10.3389/fmicb.2017.02094

Zhao, D., Zuo, Y., Wang, Z., and Li, J. (2019). Characterize carbapenem-resistant *Klebsiella pneumoniae* isolates for nosocomial pneumonia and their Gram-negative bacteria neighbors in the respiratory tract. *Mol. Biol. Rep.* 46, 609–616. doi: 10.1007/s11033-018-4515-y

Zhong, X. S., Li, Y. Z., Ge, J., Xiao, G., Mo, Y., Wen, Y. Q., et al. (2020). Comparisons of microbiological characteristics and antibiotic resistance of *Klebsiella pneumoniae* isolates from urban rodents, shrews, and healthy people. *BMC Microbiol.* 20, 1–8. doi: 10.1186/s12866-020-1702-5

Zogg, A. L., Simmen, S., Zurfluh, K., Stephan, R., Schmitt, S. N., and Nüesch-Inderbinen, M. (2018). High prevalence of extended-spectrum β-Lactamase producing *Enterobacteriaceae* among clinical isolates from cats and dogs admitted to a veterinary hospital in Switzerland. *Front. Vet. Sci.* 5. doi: 10.3389/fvets.2018.00062

Zurita, J., Alcocer, I., Ortega-Paredes, D., Barba, P., Yauri, F., Iñiguez, D., et al. (2013). Carbapenem-hydrolysing β-lactamase KPC-2 in *Klebsiella pneumoniae* isolated in Ecuadorian hospitals. *J. Glob. Antimicrob. Resist.* 1, 229–230. doi: 10.1016/j.jgar.2013.06.001

Zurita, J., Solís, M. B., Ortega-Paredes, D., Barba, P., Paz y Miño, A., and Sevillano, G. (2019). High prevalence of B2-ST131 clonal group among extended-spectrum β-lactamase-producing *Escherichia coli* isolated from bloodstream infections in Quito, Ecuador. *J. Glob. Antimicrob. Resist.* 19, 216–221. doi: 10.1016/j.jgar.2019.04.019

Zurita, J., Yánez, F., Sevillano, G., Ortega-Paredes, D., and Paz y Miño, A. (2020). Ready-to-eat street food: a potential source for dissemination of multidrug-resistant *Escherichia coli* epidemic clones in Quito, Ecuador. *Lett. Appl. Microbiol.* 70, 203–209. doi: 10.1111/lam.13263

Frontiers in
Cellular and Infection Microbiology

Investigates how microorganisms interact with their hosts

Explores bacteria, fungi, parasites, viruses, endosymbionts, prions and all microbial pathogens as well as the microbiota and its effect on health and disease in various hosts.

Discover the latest Research Topics

See more →

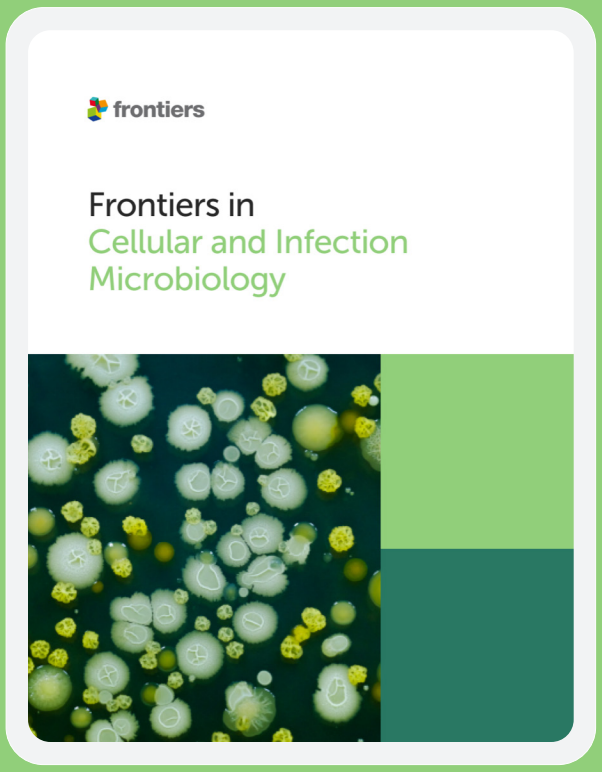

Frontiers

Avenue du Tribunal-Fédéral 34
1005 Lausanne, Switzerland
frontiersin.org

Contact us

+41 (0)21 510 17 00
frontiersin.org/about/contact